Design and investigation into a novel aerosol testing device

Hopkins, Rachel

Award date:
2002

Awarding institution:
University of Bath

Design and Investigation Into a Novel Aerosol Testing Device

Submitted by

Rachel Hopkins B.Pharm.(Hons.), M.R.Pharm.S.

for the degree of Doctor of Philosophy

of the University of Bath

2002

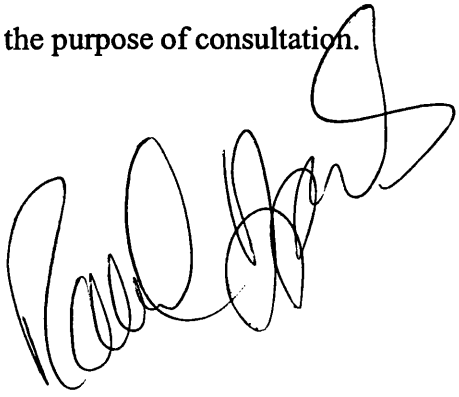

ProQuest LLC
789 East Eisenhower Parkway
P.O. Box 1346
Ann Arbor, MI 48106-1346

Acknowledgements

I would like to thank both my supervisors at the University of Bath, Mike Tobyn and John Staniforth for their help, support and encouragement. I would like to thank my industrial supervisors Ian Shrubb and Paul Wright from AstraZeneca who have been instrumental in my development throughout the course of my work.

Thanks also go to Nicola Ditchburn, David Lewis, Paul Young, David Morton, Jason McConville, Mo Aydin, Fraser Steele, Martyn Clarke, Rob Price and other members of the department of Pharmacy and Pharmacology for their help and assistance during my time as a postgraduate at the University of Bath.

I would also like to thank Jamie Ay-Yung and Daniel Clarke for their assistance during parts of this work, Ming Li and Stuart MacGregor from the department of Mechanical Engineering, University of Bath for their help and guidance in the field of engineering and fluid dynamics.

Lastly, but by no means least I would like to thank all of my friends and family for their constant support throughout the years. Thank-you Nia, Dad, Mum, Gareth and Di for your help, patience and encouragement and for allowing me the time to finish writing this thesis. I dedicate this work to all of you.

Abstract

A novel device for the testing of medicinal aerosols has been developed. Devices exist which can quantify the potentially respirable particles within an aerosol cloud, these generally have not been produced to mimic the physiological conditions of the lung or predict lung deposition patterns. The novel device, the Shell Model Lung (SML) has been developed as a novel *in vitro* device that aims to provide a correlation between the *in vitro* and *in vivo* analysis of medicinal aerosols intended for pulmonary administration.

The SML design was based on the hemispherical transformation of the human lung incorporating data taken from the Weibel model of the human lung. Data from the Weibel model was used to construct the interior network of holes representing the airways of the human lung in the five shells.

A two-dimensional physical model (2DSML) has been developed along with a computational fluid dynamics model. This has enabled pressure measurements to be taken throughout the 2DSML by encasing it within two Perspex sheets. Fluid visualisation studies of the device were performed to assess the flow response to streak and bolus injections of coloured dye into the model.

The model has undergone a calibration at AEA (Culham) using monodisperse particles. The calibration has demonstrated that the model collects particles by more than one mechanism. The results have shown that the SML is capable of separating an aerosol cloud. The theoretical cut point and the experimentally determined cut point at Shell1 are in good agreement. The model has been tested using commercially available metered dose and dry powder inhalers. Factors involved in the separation of aerosol clouds have been investigated such as altering the flow rate through the device. The commercially available inhalers used during the study have been assessed using an Andersen Cascade Impactor.

Recommendations for further work have been made including the overall improvement of the design, introducing an anatomical throat, improving flow conditions and increasing the surface for deposition.

Table of Contents

Appendices

Chapter 1 General Introduction

1.1 Lung Physiology

The total surface area of a human lung is in the order of 40 to 80m^2. The lung contains approximately 300 million alveoli, which make up around 90% of the total absorption surface available in the lung. The lungs are separated into lobes; the right lung is made up of three and the left two lobes. These lobes are further divided into bronchopulmonary segments; each segment receives its own segmental bronchus, which consists of lobules of around 1 cm in diameter these are generally pyramidal in shape (Weibel and Gomez, 1962). Within each lobule a terminal bronchus supplies an acinus, a complex of alveolated airways distal to the terminal bronchioles that is, beginning with the first order respiratory or 'transitional' bronchioles (Haefeli-Bleuer and Weibel, 1988). Within this structure further divisions of the bronchiole eventually give rise to the alveoli. The upper airways can be considered as conducting and conditioning ducts and the lower regions, especially the alveoli as tissues for the exchange of gasses. The lung is a complex structure its primary function is the exchange of gasses between air and blood. The huge surface area required for this purpose is achieved by the branching 'tree-like' structure. The branching generally occurs in a regular pattern (Weibel, 1991).

1.2 Local Treatments to the lung

Diseases of the lung can be targeted directly by the application of drugs onto the lung tissue thus avoiding first pass metabolism and reducing side effects in the patient.

Bronchodilators: act on the smooth muscle in the lung to reverse the constriction of the airway. Clinical effect is better when they are dispersed throughout the lower respiratory tract (Newhouse, 1998). Therefore aerosols of β receptor agonists containing small particles are more effective. The drug will act on the lung in the same way irrespective of the cause on constriction (Rang and Dale, 1994).
Examples: salbutamol, terbutaline. Salmeterol is a long acting drug of the same class.

Muscarinic receptor antagonists: are used to treat reflex muscle spasms caused by the parasympathetic nervous system receptors are located in the Bronchi (Newhouse, 1998).
Examples: Ipratropium Bromide, Oxitropium.

Glucocorticoids: inhibit inflammatory mediators.
Examples: Beclomethasone, Fluticasone, Budesonide

Sodium Cromoglycate / Nedocromil Sodium: the mechanism is unclear but it is thought to stabilise the cells, which release the inflammatory mediators, and suppresses other types of inflammatory cells.

Antibiotics and antiviral agents

In conditions where bacteria or viruses may easily colonise the lung to produce infections such as cystic fibrosis (CF) or acquired immunodeficiency syndrome (AIDS), it may be necessary to administer drugs directly to the lung tissue. *Pseudomonas aeruginosa* or *Staphylococcus aureus* commonly causes infections associated with CF. Aerosolised antibiotics deliver a large concentration directly to

the site of the infection. If the antibiotic is administered systemically very high doses are required to create a therapeutic level in the sputum. A high incidence of side effects associated with aminoglycosides when taken orally prevent their routine use however, when presented as an aerosol formulation they become more acceptable.

Pentamidine: used to treat infections caused by the protozoan *Pneumosystic carinii*, a cause of pneumonia to which AIDS patients are susceptible.

1.3 Protein delivery to the lung for systemic effects

The systemic pharmacological response by aerosolised insulin delivered to the lung was first reported in 1971 by Wigley (Wigley *et al.*, 1971). For aerosols to have a systemic effect, they must reach the alveoli and become absorbed into the bloodstream. It is difficult for proteins to be delivered orally as the enzymes present in the stomach break down and deactivate proteins.

For a macromolecule such as insulin to cross the air/ blood barrier that is the lung tissue it has to cross several layers. The first barrier is the lung surfactant, a single molecular monolayer lining the tissues of the pulmonary tract. Under the surfactant is a layer of surface lining fluid in the conducting airways it contains mucus and is moved by ciliary activity to the trachea. The surface lining fluid at the alveolar level is thinner and no cilia are present in these tissues. The macromolecule has to get through the surfactant layer and dissolve in the surface lining fluid before it can get to the epithelial cells. Macromolecular absorption occurs as a natural process. (Johnson, 1997)

- Absorptive transcytosis – through cell absorption,
- Paracellular transport – between cell absorption.

These routes through the epithelial layer lead the molecule to the interstitium and basement membrane of the lung tissue these structures hold the epithelium in its conformation. They appear to not hinder the progress of the macromolecule. Once through the cells of the lung the macromolecule diffuses through the vascular epithelium and into the blood stream (Patton, 1996).

It is thought that an insulin formulation must have a d_{ae} in the region of 1 - 3μm to reach its site of absorption (Patton, 1997). There are significant formulation problems when dealing with proteins and peptides. The complex structure of proteins makes them particularly unstable. Changes in their secondary, tertiary or quaternary structure can alter or destroy their potency. It is very easy to denature the physical structure of proteins; heating, cooling, pH changes and shear can change these physical characteristics. Various methods of incurring stability on proteins may be used during formulation. Excluding water from, adding excipients such as sugars, polyols, surfactants or polymers to the protein structure will enhance the physical stability of the molecule (Parkins and Lashmar, 2000).

1.4 Particle size

In order for the drug particles to reach their site of action they generally have a size in the range of 2 to 5μm. An ideal aerosol will contain particles of exactly the same shape and size this is termed a monodisperse aerosol. In reality, the particles in a typical pharmaceutical aerosol cloud are polydisperse, this means their aerodynamic diameter varies from around 0.5μm to more than 12μm. The size distribution of the

polydisperse particles in pulmonary aerosols generally approximate to a lognormal size function.

The geometric standard deviation σ_g is a measure of the aerosol size polydispersity. A monodisperse population would have a $\sigma_g = 1$. It is impossible to prepare a medicinal aerosol, which is monodisperse, so $\sigma_g \sim 1.2$ is conventionally set as the limit at which polydispersity starts.

The drug particles in an aerosol are not the same shape; the size of a particle is said to be a function of its aerodynamic diameter, d_{ae}.

The d_{ae} is defined as the diameter of a sphere of unit density, which has the same terminal settling velocity as the particle in question.

The mass median aerodynamic diameter (MMAD) is the aerodynamic size of the particles below or above which 50% of the drug particles reside. When any new drug and or formulation for pulmonary administration are assessed the aerosol is tested for its drug content and also the aerodynamic diameter of the particles present in the aerosol cloud. The d_{ae} of an aerosol is thought to influence the lung deposition pattern that will be seen.

1.5 Impactor Theory

Collection of particles by impaction exploits a particle's inability to follow a curved path. The principle of collecting particles by impaction is sound and used routinely. A vertical jet of a given diameter is directed at a horizontal plate as particles travel through the jet at a given velocity the inertia imparted on them will determine if they can negate the 90^0 'bend' and avoid a collision with the plate. Figure 1.1 is a schematic cross sectional diagram of an impactor, particles with high momentum will not follow the airflow and so impact on the collecting surface. It is possible for smaller particles to continue in the path of the airflow and move through the stage of the impaction device.

Figure 1.1 schematic diagram of impaction.

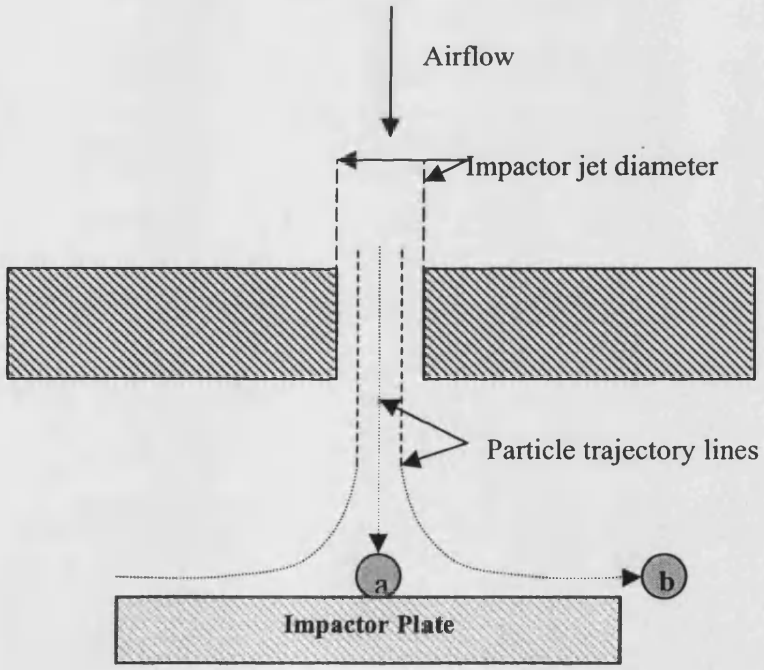

Particle 'a' has been collected on the impaction plate, as its momentum cannot be overcome by the direction of the airflow around the plate. Particle 'b' has less

momentum and so remains in the airflow and will be carried to the next impaction stage where the airflow will be increased and the particle given a higher momentum.

For a given plate there is said to be a cut point (units = metres) above which, particles will be collected i.e. impact on the plate or be collected on a previous collecting surface. A cut point should be as sharp as possible for the user to be confident of the results an impaction device produces. The measure of the 'sharpness' of a cut point is called the efficiency curve. An efficiency curve will be constructed for each plate or collecting surface using theoretical or calibration data.

The Stokes Number, Stk for an impactor is defined as the ratio of the particles stopping distance at the average jet exit velocity U to the jet radius (or half width for a rectangular nozzle) r.

Theoretical determinations of a cut point would involve solving the Navier-Stokes equation for each jet's geometry. For routine calibration of instruments an aerosol with monodisperse particles of known diameters is used and the results are plotted as collection efficiency (% of the total collection for the collecting surface in question of the whole impactor at the relevant particle size) against particle size. Figure 1.2 shows a collection efficiency curve examples of this type of graph can be seen in chapter 4.

Figure 1.2 Example of a collection efficiency curve

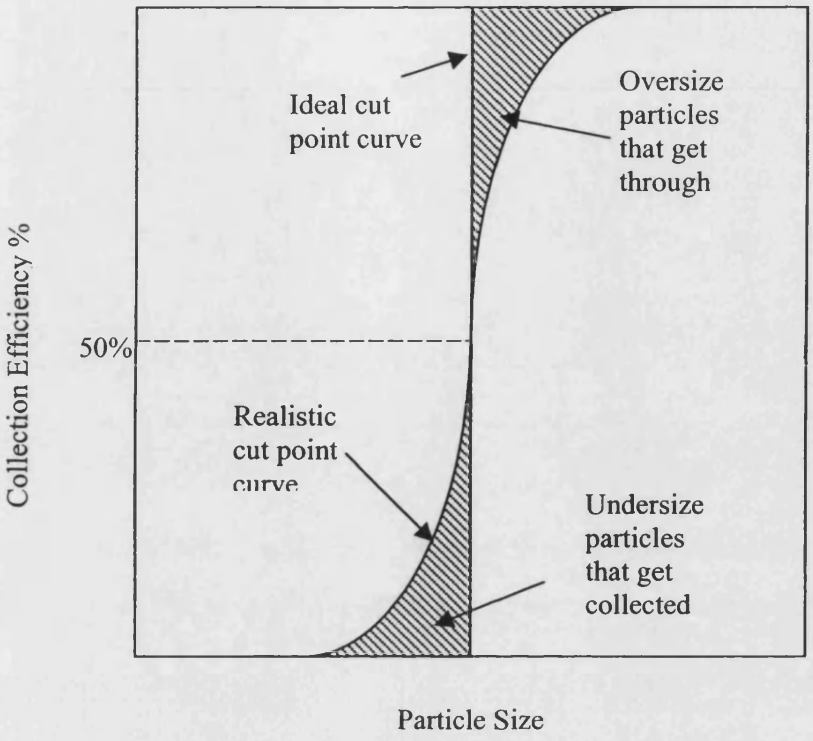

1.6 *In vitro* Testing of Medicinal Aerosols

It is generally accepted that a drug contained in a pharmaceutical aerosol must reach a specific area of the pulmonary environment to have its effect.

A number of *in vitro* test methods for medical aerosols have been developed. These devices are intended to aid the formulation development and quality control of such systems. The testing devices available to us are purely analytical and although they accurately describe the aerosol cloud sizing characteristics, they cannot predict the region of the lung in which the aerosol will deposit.

1.6.1 The Andersen Cascade Impactor

The Andersen Sampler was first designed for assessing microbiological particles in the air (Andersen, 1956). Andersen set out to produce a device, which could be used to collect, count and size viable airborne particles. The model was later developed into a cascade impactor for the aerodynamic sizing of both liquid and solid non-viable particles. The Mark I impactor was launched in 1970 and covers a range of 0.4μm to 11.0μm. The Mark II impactor most commonly used today was released in 1977 it had been redesigned to reduce particle bounce and minimise wall-losses. This device now appears as standard testing equipment for medical aerosols in the USP. The Andersen Cascade Impactor (ACI) is probably the most comprehensive aerosol separator available it fractionates the aerosol into 8 size ranges from 10 to 0.43μm. Particles larger than 10μm are retained in a preseparator, eight further stages providing 50% cut-off diameters of 9.0, 5.8, 4.7, 3.3, 2.1, 1.1, 0.7 and 0.4μm, and a final filter. This impactor operates at a flow rate of 28.3 L min^{-1} (Graseby-Andersen, 1985). A preseparator may be placed above stage 0 in order to remove any particles above 10.0μm from the aerosol cloud.

Using impactor theory, Stein (1999) describes how much individual ACI's vary in their cut-points. The jet diameters of three ACI's were measured and theoretical cut-points were determined based on the data. The ACI's used were well within the manufacturers size specification range. On testing three MDI formulations in the three pre-determined ACI's it was found that measurements for each MDI on a given ACI appeared very consistent. Variations between ACI's for the same MDI formulation were large. It is therefore important to use these instruments with care and it may be necessary to take into consideration any additional calibration data made available.

The jet dimensions (ideal) of an ACI range from 0.0994" to 0.00095". The process of making such small holes however well regulated will contain some error. When trying to distinguish between particle sizes of maybe less than 0.1μm this error may become significant in a characterisation of an aerosol cloud.

Impactors are generally used to test metered dose inhalers however, it is possible to make several modifications to the operation of the ACI for the testing of dry powder inhalers. The "new" ACI (Mark II, 8 stage ACI) has an extra stage inserted (stage -1) above stage 0 which allows the ACI to be operated at 60 l min^{-1} and retain the capability to achieve a cut-point at 9.0μm. Without this extra stage the first cut-point would be 8.6μm, thus reducing the range of fractionation. The operation of the ACI at a flow rate of 60 l min^{-1} is necessary if dry powder inhalers are to be tested using this apparatus (Nichols *et al.*) creating the necessary pressure drop of 4kPa over the device (Byron, 1997). A further modification of the ACI has been described by Nichols and Smurthwaite (1998), stage 7 has been removed as its cut-point is of little value and stage -0 added to allow stage -1 to be fitted. ACI plates are made of aluminium therefore it is sometimes necessary to coat the plates. When using dry particles (Rao and Whitby) or low numbers of liquid particles, "single puff" determinations (Nasr *et al.*) it has been advised to apply a sticky layer to the plate. Coating the plates prevents the bouncing of particles off the surface, wall loss, blow-off, de-agglomeration and re-entraining in the ACI. Coating of the plates may be achieved using for example, silicone, grease or glycerine.

The characterisation of an aerosol generated by nebulisation has caused some difficulty. After around 6 minutes of operation four nebulisers tested had an aerosol

output temperature of between 5°C and 14°C (Phipps and Gonda). Stapleton and Finlay (1998) reported a MMAD error between the operation of the ACI at ambient and cooled (10°C) temperature was 52%. It was suggested that the nebulisers could be heated to room temperature but this may change any one of the aerosols physical properties.

1.6.2 The Marple- Miller Impactor (MMI)

This impactor has five stages plus a final filter. The particle cut-off diameters are 10.0, 5.0, 2.5, 1.25 and 0.625μm. Calibration data for this impactor are available for operation at 30 or 60 l min^{-1}. There is no method of preseparation of the aerosol in this apparatus and it does not completely disassemble after each analysis, which is a disadvantage as there may be some loss of the drug within the impactor particularly with some DPI devices (Olsson, Asking and Johansson, 1998). The high cost of this instrument has also been cited as a reason for its relatively narrow use (Marple *et al.*, 1995). In 1998 Olson *et al* developed a low-flow version of the MMI. A low flow rate impactor would be particularly useful when investigating the deposition of an aerosol in a child or when a low-inhalation flow rate is recommended to a patient. The flow rates designated were 4.9 and 12 litre min^{-1}. To achieve a comprehensive range of cut-points the MMI was modified for use at the low flow rates. The jet nozzle diameter at each stage was altered according to impaction theory to provide the necessary cut-point. A reported <5% inter-stage drug loss within the impactor is in line with the USP recommendations.

1.6.3 Single Stage Impactor

The impactor described as Apparatus B, (BP) or Single stage Impactor no.2 (U.S.P.) is constructed from aluminium. The impactor has a cut-off diameter of 9.8μm (which is well outside the respirable range). Furthermore the particles impact onto a solid plate and thus, if they are solid and dry they may bounce off the plate unless the plate is sufficiently coated. The TSI and Apparatus B generally operate at a flow rate of 60 l min^{-1} unless otherwise calibrated at different flow rates.

1.6.4 The Twin Stage Impinger (TSI)

The TSI is also known as Apparatus A, B.P., or Single Stage Impactor no.3, U.S.P. A TSI is made of glass it divides the aerosol into two size fractions, particles above and below a cutpoint of 6.4μm, although jet modifications can be made which allow other size fractions to be analysed. The TSI does not give adequate data on the range of particle sizes present in the aerosol cloud but it is a quick method and good for screening.

1.6.5 The Multi-Stage Liquid Impinger (MSLI)

The MSLI is particularly suitable for testing dry powder inhalers. Drug particles are collected on a liquid surface that has a high capacity for powder retention (Asking and Olsson, 1997). There are four stages plus a filter stage; which can give an adequate analysis of an aerosol. The MSLI has been calibrated at various flow rates (30 to 100 l min^{-1}) and has a lower loss of drug on its walls than the Anderson or the Marple-Miller impactor (Olsson *et al.,* 1998) however; the analysis of the MSLI is difficult and time consuming.

These instruments generally characterise the aerosol cloud with reasonable accuracy and calibration data are available for all however, they do not accurately predict how the drug particles will be distributed in the lung. In general the guiding principles in their design have been ease and accuracy of analysis rather than an attempt to closely mimic the physiological situation pertaining in the healthy or diseased lung.

1.6.6 NGI – the Next Generation Impactor

The NGI was designed specifically for pharmaceutical aerosol testing. Its design was drawn from a series of requirements set in place by a consortium made up of European Industrial scientists (Wright and Shrubb, 1998). The NGI has many advantages over the devices described above.

As it was designed specifically to test particles for inhalation it operates and is calibrated over a wide range of flow rates (30 to 100 l min^{-1}). The cut points throughout the device over the flow rate range were designed to give suitable information around the region of interest.

The impactor uses a USP throat as an entry port. Each collection stage is a 'cup' rather than a flat plate this enables the collection stages to be coated if appropriate and allows larger quantities of drug to be deposited than a flat plate would. The collection cups and low wall losses allow for a quick turnaround as the cups may be removed for analysis and clean cups immediately replaced. The NGI has an absolute filter at the exit.

Although the NGI appears to have many advantages over the other devices described it still gives no information on *in vivo* performance of aerosols. The impactors by definition collect particles by impaction however this is not the only method of particle deposition in the lung.

The analytical instruments used for aerosols testing were briefly compared:

Figure 1.3 Comparison of impactors and impingers currently available.

Device	Quick?	Easy to analyse?	Good separation?	Good Preseparation?
Twin-stage Impinger	Yes	Yes	No	N/A
Andersen	No	Yes	Yes	Yes
Marple-Miller	No	Yes	Yes	No
Multi-stage Liquid Impinger	No	No	Yes	Yes
Next Generation Impactor	No	Yes	Yes	Yes

1.6.7 General discussion

In general the more stages a testing device possesses the better the resolution of the results. Unfortunately this means that the device will require lengthy analysis. As discovered by Stein and Olson (1997) the ACI although an excellent device is subject to large inter device variability, the calculations governing impaction are precise so if the jets in the device are not particularly well defined then the impactor will have varied cut points. It would therefore be advisable to calibrate any aerosol testing instrument before use in the lab.

As the MSLI contains fewer stages but still provides aerosol fractionation of the diameters of interest then it may be better to use the device for more routine work such as quality control procedures (Holzner and Müller, 1995).

Single stage impactors or impingers are useful tools for screening and initial development as they are quick, efficient and accurate once calibrated. Even though these devices are included in the BP more evidence of an aerosol performance is generally required for regulatory purposes.

1.7 *In vivo* Aerosol Testing Methods

1.7.1 Pharmacokinetic studies

The method can provide a useful comparison of bioavailability between formulations and devices (Chrystyn, 2000) but gives no information on lung deposition patterns in the subject's lung. Using the charcoal block method will stop any gastrointestinal absorption of the drug and so it can be said drug levels detected in the blood or urine are a results of pulmonary delivery of the drug. As drug delivery to the lung requires very small doses for clinical effects the method of testing blood and urine levels must be extremely sensitive and accurate. The pharmacology of many drugs means comparisons between them may be difficult as rates of absorption receptor binding time and drug metabolism can be markedly different (Snell and Ganderton, 1999).

1.7.2 Lung Casts

Cadaver casts have been made and investigated extensively for respiratory tract dimensions and geometry (Yeh and Schum, 1980) providing similar data to the Weibel model. The technique allows far more detailed lobar investigation and production of airway replicas up to generation 8 (Cheng *et al.*, 1997). Airway casts may be used to assess deposition of radiolabelled aerosol or undergo calibration tests (Zhou and Cheng, 2000) as with other *in vitro* testing methods.

Advances in microscopy techniques have allowed greater detail of lung surface structures to be analysed (Weibe and Laurensen, 1995 and Poinar *et al.*, 1996). These advanced techniques have focussed on respiratory healthy human subjects or animal models. To compliment the work into realistic models for aerosol testing it would be of interest to investigate the extent of obstruction to treatment in the lung and how this affects patients in specific disease states. It is unlikely that the methods outlined here could be used routinely for pharmaceutical aerosol assessment.

1.7.3 Planar (Two-dimensional) Imaging

Using radiolabelled aerosols allows the imaging of the drug *in vivo.* The technique is non invasive and observations can be made, as the drug is *in situ.* It is possible to incorporate the radiolabel molecule into the drug structure but this is rare. Therefore, a label may be associated with the drug molecule or simply added to the formulation (Zainudin *et al.,* 1989) in both cases it is essential that the process can be validated and it can be seen that the radiolabel is acting as a good marker for the drug (Snell and Ganderton, 1999). Validation of the association of the label with the drug and the unchanged properties of the aerosol cloud can be carried out using simple imaging using controls and *in vitro* analysis with Andersen cascade impactors (Biddiscombe *et al.*,1993) or MSLIs (Steed *et al.,* 1995).

A commonly used radiolabeling technique for salbutamol (Biddiscombe *et al.,* 1993) involved putting dry technetium pertecnetate ($^{99m}TcO_4^-$) in a vial with the required surfactant, propellant and micronised salbutamol. The mixture was then placed into a sonic bath for thorough mixing and then sealed into a canister. It was demonstrated that the radiolabel was adsorbed onto the salbutamol by allowing the drug to cream

out of suspension and then using simple imaging (with a control) checking the position of radioactivity emission. Substituting the drug for radiolabelled inert particles (e.g. Teflon) of a suitable size has also been used for such studies.

It has been shown that as well as labelling the drug the lactose carrier particles in a dry powder inhaler may also be radiolabelled (Karhu *et al.*, 2000). Only a small amount of the inhaled lactose deposits in the lung. Most lactose deposition takes place in the mouth as design suggests and is swallowed.

Once the radiolabelled drug is administered to the subject the process of imaging can begin. The raw data gathered (primary counts) must be corrected for background radioactivity, radioactive decay and the depth of the signal in the body. Once these are corrected for the data are termed 'secondary counts'. As the rays pass through the body they may become scattered or absorbed by the tissues of the body. Corrections for this type of loss of signal are termed 'attenuation correction factors' (ACF) (Pitcairn and Newman, 1997). They are ratios and are essential to avoid deposition underestimation. They take into account the density and type of tissues that the signal must pass through in particular the lung stomach and oropharynx (Snell and Ganderton, 1999), which obstruct the signal.

Planar imaging is an important technique aiding the understanding of drug deposition in the lung. Gamma scintigraphy studies allow imaging of a human lung after deposition of a radiolabelled aerosol has occurred. Gamma scintigraphy of course only detects and identifies the presence of the drug in the lung it does not indicate clinical effect (Newman, 1995). The oropharyngeal and respiratory tract may be

investigated (Steed *et al.*, 1995) and the lung system as a whole may be divided into discrete regions (Figure 1.4) of interest (Newman *et al.*, 1998).

Figure 1.4. Schematic diagram of the 'regions of interest' as applied to planar imaging. (Adapted from Newman *et al.*, 1998).

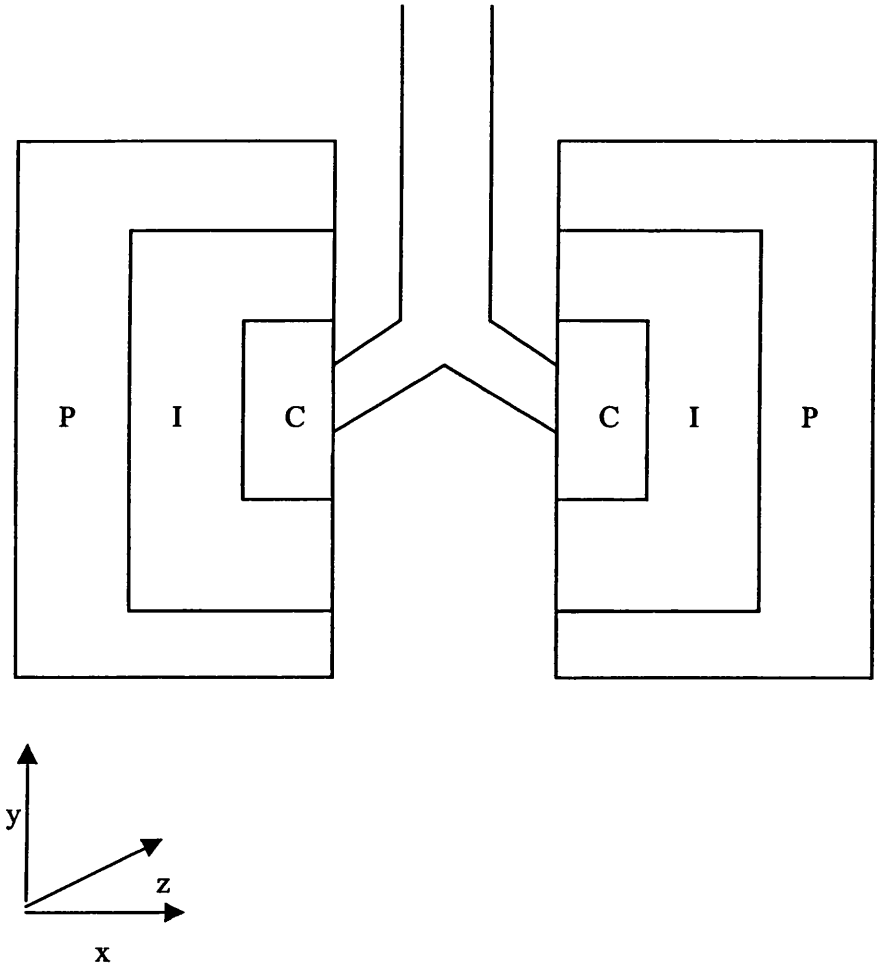

C = Central region

I = Intermediate region

P = Peripheral region

The regions may be analysed individually and the ratios between them assessed. This can be particularly useful for making comparisons between devices and formulations (see below).

The technique is two-dimensional so although the central region contains mostly conducting generations they will overlap with some alveolar airways (Snell and Ganderton, 1999) as the structure of the lung develops also in the 'z' direction. For each type of device planar imaging gives potential local bioavailability data (Newman and Wilding, 1998). It is therefore convenient to use the 'regions of interest' to compare between devices as outlined above.

Two-dimensional imaging has been used for the study of MDIs containing both CFC and HFA propellants (Richards *et al.*, 1998 and Laube *et al.*, 1998). The use of MDIs with spacer devices has also been attempted (Thorsson *et al.*, 1998) where appropriate. The devices can then be assessed *in vivo* and comparisons drawn between use of MDI and MDI with spacer. Of more use to clinicians maybe are studies involving asthmatic patients (Borgström *et al.*, 2000) even though this type of study makes experimental procedures more difficult to design. Patient usage variability when using a DPI (Turbuhaler™) was equivalent to that seen in healthy subjects. Variability when using MDIs was far greater highlighting the potential coordination and formulation problems that can be encountered. A comparison of solution and suspension MDIs in healthy and asthmatic subjects (Sanders *et al.*, 1997) has found lung doses of the solution MDI to be almost identical between the two subject groups (healthy 61.13% ±10.95 n = 11, asthmatics 58.59% ±17.75 n = 9). The total lung dose between the two groups when using a suspension MDI was found

to be significantly different (healthy 17.42% ±5.32 n = 11, asthmatics 9.92% ±4.41 n = 9).

The technique is now well established for all types of inhalation method and has been used to assess novel pharmaceutical aerosol generators (Farr *et al.*, 2000). The imaging process illustrates drug deposition in the lung which as has been discussed is more relevant than *in vitro* data. It has highlighted the overestimation of some (impinger) *in vitro* analyses giving a lower result for the <5μm (termed 'respirable') fraction *in vivo* (Newman, 1998).

It is important to be able to relate these studies to clinical responses; investigated by Smalldone (1996) and Laube (1996). Using both pharmacokinetic and gamma scintigraphy can yield different results (Borgström *et al.*, 1998 and Pauwels *et al.*, 1997), as all deposition in the lung would be observed even though some of it will be removed by mucocilliary clearance before absorption into the bloodstream. It is also important to take into account radioactive decay and drug clearance (Bondesson *et al.*, 2000). Pauwles and co workers (1997) found that due to intra-patient lung function variability the relationship between pharmacokinetic and gamma scintigraphy must be subject to a specified regimen for any useful data to be gained the technique must therefore be standardised (Newman, 2000).

1.7.4 Three-dimensional *in vivo* imaging

Single Photon Emission Computed Tomography (SPECT) is a technique utilising radiolabeling of aerosols and imaging them in three-dimensions. Using a combination

of SPECT and x-ray computed Tomography (CT), Perring and co workers (1994) developed a mathematical transformation of the lung into a series of hemispheres. A more detailed description of this may be found in section 2.3. After inhalation of a radiolabelled aerosol by a subject the model provides a framework for radiolabelled image signals to be assessed and quantified. The aerosol may be prepared in the same way as for 2D analysis and attenuation factors still have to be taken into account.

The model was used to assess the radioactivity signal after ^{99m}Tc labelled albumin microspheres (Fleming *et al.*, 1995) were inhaled by a subject. The results could then be expressed as total activity per shell as a percentage of the total activity detected. The hemispherical 'structure' was further improved after Martonen *et al.*, (1995) devised a 3D branching network so the data could be approximated to generation number. The interpretation of the data into 23 generations is felt to be a little ambitious considering the distance between each generation at generation 6 to 7 is just on the limit of the resolution of the SPECT technique (0.8cm, Perring *et al.*, 1994) and therefore the lower generation are well below the level. Generation 6 was found to be 0.9cm in the Weibel model and the length of generation 9 in each of the five lobes of the lung was found to be less than 0.9cm by Yeh and Schum (1980). This poses the question of validating the generation interpreting transformation.

Using the three-dimensional imaging technique outlined above nebulisers (Fleming, Hashish *et al.*, 1996 and Fleming, Halson *et al.*, 1996) and MDIs (Summers *et al.*, 1996) have been analysed in this way.

Two-dimensional imaging requires less radioactivity to be present in the subject than three-dimensional imaging. It is quicker and unlike three-dimensional imaging validated (Newman and Wilding, 1999). It has been suggested that Planar imaging fits in between *in vitro* analysis and clinical data (Newman *et al.*, 2000). The 2D technique does indeed give a better idea of deposition in the lung but it is felt that more advanced *in vitro* models would be more suitable if they could be validated using gamma scintigraphy both 2D and 3D and clinical data.

Another method of 3D imaging was described by Dolovich *et al.*, (2000). Positron Emission Tomography (PET) utilises labelling of an aerosol with a position emitting isotope (e.g. ^{11}C, ^{13}N, ^{15}O, ^{18}F). The signal was recorded from the subject after inhalation of the labelled aerosol by a ring of radiation detectors. This has an advantage over SPECT in that where a gamma camera takes images whilst rotating around the subject (64 projections around 360° each taking 30 seconds, Fleming *et al.*, 1996), taking a much longer time that PET (as short as three minutes). The length of time taken during SPECT means the researcher has to account for decay of radioactivity but clearance from the lung is not accounted for (mucocilliary clearance is approximately 0.2mm min^{-1} in the trachea) (Marriott, 1990). This puts many possibilities for errors into the method of SPECT.

PET offers better resolution (4 to 5 mm) than SPECT but it is necessary to derive the subjects physiology before special attribution of signals can begin which can be time consuming and is expensive. The results of PET imaging are therefore less 'universal' than SPECT and can be difficult to interpret.

1.7.5 Mathematical models

Mathematical models have been designed to correlate with *in vitro* devices (Martonen *et al.*, 1992) and more extensively lung geometry models in particular the Weibel model (Kim *et al.*, 1983 and Martonen, 1993). Deposition models have limited success because the geometries and flow parameters in the lung are extremely complex (Hofmann, 1996). Possible factors to incorporate into the design of such systems are hygroscopicity, particle coagulation and geometries of deformed or diseased airways (Gradón and Podgórski, 1996).

It has been demonstrated that some mathematical models including the ICRP (International Corporation for Radiological Protection) model differ significantly from regional deposition studies using radiolabelled drug (Finlay *et al.*, 1998). The advance of technology means more complex computations can be achieved and techniques in modelling physiological systems are constantly improving.

A general improvement of these models would be to include mucocilliary determinations. Mucus is present in the human body down to terminal bronchioles. If the body perceives formulation components to be 'toxic' hypersecretion and coughing may occur (Marriott, 1990).

1.8 Factors affecting deposition in the lung

The physical properties of the aerosol particles: particle size (d_{ae}), density of the particle material and the force of gravity, can all contribute to the deposition patterns of the aerosol particles in question. The breathing characteristics of a patient;

including inhalation and exhalation flow rates, tidal volume and the period of breath-holding pause, have a wide variability and determine the concentration of the drug which is deposited in the lung. Along with patient variability the presence and severity of disease in the lung will greatly affect the level of drug deposition.

Mechanisms of deposition for medical aerosols are thought to include (Hickey, 1992, Haefeli-Bleuer and Weibel, 1988)

1.8.1 Gravitational settling

The force of gravity acts on the fine particles. Under laminar flow conditions, they fall under the force of gravity, a distance equal to the terminal velocity multiplied by the time of travel. Assuming the particles were evenly distributed over the cross section of an airstream, it would be possible to calculate the probability of deposition in tubular airways and in spherical alveoli.

The force of gravity acts on fine particles. The particles fall through the air at a constant velocity.

$$\mu_t = Pgd^2/18\,\eta \qquad (1)$$

d = particle diameter

P = density

μ_t = terminal velocity

g = acceleration due to gravity

η = viscosity of air (1.9×10^6 $Nm^{-2}s$)

1.8.2 Deposition by diffusion

Deposition by diffusion increases as the particle size decreases. However the force of gravity acts on the particles, as their mass becomes less, the force with which they are pulled becomes less. The particle diameter at which both processes have a combined minimum value is approximately 0.5μm. Particles of this size have the least probability of respiratory deposition.

1.8.3 Impaction

When particles are inhaled they follow the air-stream, if the conducting bronchiole suddenly changes direction a drug particle may tend to continue in its original direction of flow, possibly impacting on an airway wall depending on its momentum. A particle in this way may deposit on the airway wall. The effective stopping distance h_s at right angles to the direction of travel in a curved tube is:

$$h_s = \mu_t \, \mu_{\sin \sigma} / g \qquad (2)$$

h_s = effective stopping distance

μ = velocity of the air-stream

σ = angle of the approaching bend

g = acceleration due to gravity

The probability of inertial deposition I, is proportional to the ratio of the stopping distance h_s to the radius R of the airway, that is:

$$I \propto h_s/R \propto \mu_t \sin\sigma / g\, R \qquad (3)$$

I = probability of inertial deposition

R = airway radius

Calculated inertial deposition shows a dependence on particle size as follows

10μm	50%
7μm	33%
5μm	20%
3μm	10%
1μm	1%

The relative humidity in the lung is believed to be over 99% therefore particles inhaled into the lung will almost certainly undergo hygroscopic growth, increasing their probability of impaction or gravitational settling.

Deposition by interception and electrostatic precipitation can be important mechanisms of deposition in other situations but are not thought to contribute significantly to the *in vivo* deposition of medical aerosols. They may however play a significant role during the *in vitro* analysis and processing of some pharmaceutical aerosol devices (Byron *et al.*, 1997, Peart *et al.*, 1998 and Eilbeck *et al.*, 2000).

1.9 Aims and objectives

The purpose of this work is to design and develop a novel aerosol testing device for analysing medicinal aerosols. The devices currently in use do not adequately demonstrate where deposition will occur in the human respiratory tract. Using the available methods gives accurate data on the size of the particles contained in an aerosol however they do not reflect how these particles will act within the lung environment.

The devices described in this chapter adequately analyse an aerosol cloud with respect to aerodynamic diameter. Mathematical models predict deposition; radiolabeling studies visually demonstrate particle deposition. This thesis aims to provide an *in vitro* testing device more closely resembling the lung in its particle collection characteristics. Current analytical testing methods are unable to be correlated reliably with either mathematical predictions or gamma scintigraphy studies. A requirement for such a device is apparent in the industry.

An analytical tool giving quick reliable data on deposition patterns would be of benefit to formulators, analysts and quality specialists working in the aerosol field. The cost and analysis time for such a model would be far less than running *in vivo* pharmacological or gamma scintigraphy tests on human subjects. The following work addresses the points made above.

Chapter 2 Design

2.1 Introduction

A novel aerosol testing device was required for use by the pharmaceutical industry. As previously discussed the current Pharmacopoeial standards are not necessarily the only or best methods to sufficiently demonstrate the *in vivo* deposition of a pharmaceutical inhaler. Many of the available devices were not designed with the intention of using them for these purposes. The new device was outlined by the Next Generation Impactor Group set up in 1996 (Wright and Shrubb, 1998). This consortium consisted of 12 companies working together to design a new impactor with input from selected experts in the field. To gain an understanding of why a new device was needed assessments of the available impactors, impingers and *in vivo* techniques were made. Production of aerosols was also investigated to understand the laws governing generation and deposition of the drug particle.

Pharmaceutical aerosols are sized in order to predict if they are capable of reaching and deposition in the intended area of the lung. An ideal aerosol will consist of particles of exactly the same size, as discussed previously this is not the case. To discover the characteristics of a particular formulation it is necessary to perform sizing experiments. The preferred choice in industry at the moment is the Anderson Cascade Impactor (ACI) this gives a good range of discrete size fractions. The data produced may be manipulated to calculate the mass median aerodynamic diameter and the geometric standard deviation.

This data was used to show how well your formulation performs and during quality control procedures.

2.2 Development of the Shell Model Lung

2.2.1 Purpose

When designing a novel device it was decided to look at the whole area of aerosol science with consideration to the issues above. It was thought that however precise, informative and practical the impactors currently in use are they tell the operator very little about how the aerosol will behave in the patient. The impactors we use give invaluable data required for the development, comparison and regulation of medicinal aerosols. Such aerosols cannot be tested *in vivo* for these purposes on a day-to-day basis.

The importance of γ-camera imaging of radiolabelled drug has been discussed in Chapter 1. This technique produces data showing exactly where in the patient's lungs the aerosol deposits. Using SPECT analysis in conjunction with pharmacokinetic studies produces a general profile of the activity of the drug in the patient. It would be extremely complicated to design a model to perform this function *in vitro*. It may be possible however, to combine aspects of the *in vivo* and *in vitro* studies to reflect the chance of the drug particles reaching the desired space in the patient's lung and producing an effect.

For the purpose of designing a useful analytical tool for laboratory use it was decided to base the design on the 3-dimensional studies of human lungs as described below and not the 2-dimensional situation as used by Newman *et al.*, (1998). The 3-dimensional aspect of an *in vitro* model would of course be closer to the *in vivo* situation.

If the *in vivo* dimensions of the human lung were included in the model it would be reasonable to assume the *in vitro* model would behave in a similar fashion. Keeping the model as simple as possible even though a compromise was crucial to its use as an analytical tool. The casting of human airways has been described in section 1.8.3. This work is important to our understanding of the effects of geometry on deposition profiles it would not be a good laboratory tool as it represents the situation of airway geometry of one deceased patient. The cast made were rigid and so do not accurately reflect the 'breathing' motion seen *in vivo*.

SPECT (as discussed in section 1.8.5) analysis gives three-dimensional information on the deposition patterns of radiolabelled aerosols in the lung. To analyse the information obtained a mathematical hemispherical transformation of the lung (figure 2.1) was developed by Perring *et al.*, (1994) and later used by Fleming *et al.*, (1995).

2.2.2 Details of SPECT mathematical transformation

The lung being modelled is the right lung and not the whole lung system. The lung 'space' was considered in relation to a three-dimensional matrix of cube volume elements

or voxels. Its x, y, and z co-ordinates described each voxel. The centre of the lung (x_c, y_c, z_c) was defined as the point where the main bronchus crosses the surface boundary of the lung space.

Figure 2.1. Hemispherical Transformation (adapted from Perring *et al.*, 1994)

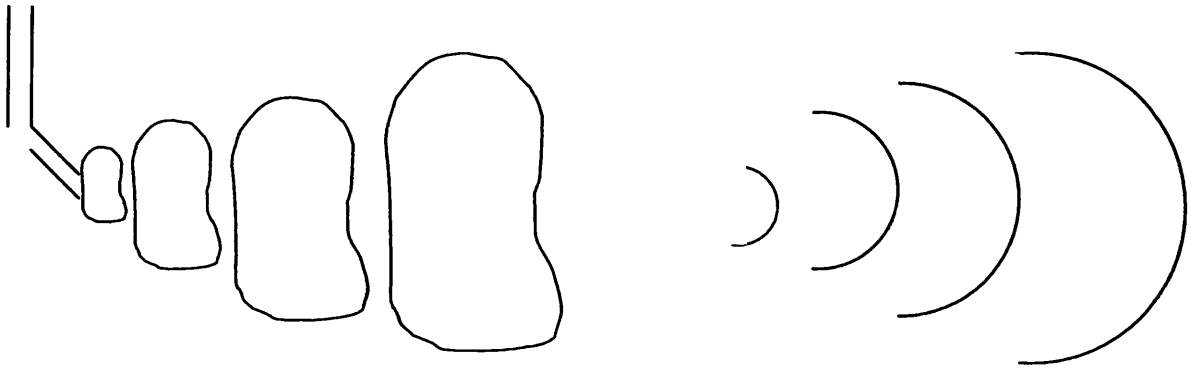

Generation 1.....23 Shell 1.....10

Using data obtained from gamma scintigraphy studies and anatomical dimensions of a subject from an MRI study allowed the relation of aerosol deposition to physical anatomy. Mathematically modifying the subject's lung into the hemispherical structure and 'superimposing' it onto the SPECT data allows 3-dimensional view of the spatial distribution pattern in the lung.

The analysis of the radionuclide distribution is limited by the resolution of the SPECT imaging process, which is in the order of 1 cm. Therefore, due to the effective radius of the lung being approximately 10 cm, ten shell divisions were used.

The Shell Model Lung was based on these hemispherical transformations. It was hoped that combining the model for computational assessment of real patient data with an internal structure representative of the *in vivo* situation a compromise between *in vitro* and *in vivo* aerosol testing could be reached. The model was designed as a shell structure. In order for the flow of air and particle separation to occur the shells had to contain holes. It was decided to try to replicate the dimensions of the human airways for the three-dimensional space that the shell occupied. This data collection is described below.

2.2.3 Details of the Weibel model of the airway tree

The model was based on data of airway dimensions from the Weibel model of the airway tree (Weibel and Gomez, 1962). The Weibel model of the airway tree is shown below for generations 0 to 14, data for the model was collected after many measurements taken during post mortem studies.

Figure 2.2. Typical path airway model of a human lung:

Generation	Number N(z)	Airway Segment Diameter (mm)	Length (cm)	Total airway cross Section (cm^2)
0	1	18	12	2.54
1	2	12.2	4.76	2.33
2	4	8.3	1.9	2.13
3	8	5.6	0.76	2
4	16	4.5	1.27	2.48
5	32	3.5	1.07	3.11
6	64	2.8	0.9	3.96
7	128	2.3	0.76	5.1
8	256	1.86	0.64	6.95
9	512	1.54	0.54	9.56
10	1024	1.3	0.46	13.4
11	2048	1.09	0.39	19.6
12	4096	0.95	0.33	28.8
13	8192	0.82	0.27	44.5
14	16384	0.74	0.16	69.4

Several assumptions were made:

1. The conducting airways (up to generation 14) were considered to consist of airway paths each of which branches outwards from the centre of the lung and around a radial path, terminating in a acinus
2. The acini fill the remaining volume uniformly

In this model there are equal numbers of airway paths in each of the generations 1 to 14, the Weibel model contains progressively fewer actual airways in the lower generations. In the hemispherical model the airway paths can be considered to be merging together to produce the smaller number of actual airways, each of which has a progressively larger cross-sectional area.

The path length distribution includes all the statistical extremes of variation in the Weibel model. The airways are described as a branching 'tree', which is divided into generations, the trachea being generation 0 and the alveoli generation 23. Many of the airways do not branch from generation 1 through to 23, as alveoli are present on the airways representing lower generations i.e. close to the bronchus. Generations 1 to 14 are considered to be the conducting airways and generations 15 to 23 the acinar airways. Acinar airways are the complex of alveolated airways connected to a first order respiratory bronchiole. The model is suggesting that the 'conducting' airways are divided into ten sets each of which ends in its given shell. The model described here does not take into account the sharp or subtle bending seen in the airways resulting in longer

path lengths and higher surface areas. To make the design and manufacturing processes of the SML easier and quicker, the model does not represent any irregularities in branching of the airways the model was designed to a symmetrical theory.

2.2.4 Transformation

To develop the Shell Model Lung, Weibel data for generation 1 to 14 was transformed into data representing 10 shells of the three-dimensional shell model.

As the model is based on the hemispherical transformation model it was decided to acknowledge the constraints placed on that model when designing the SML. The centre of the lung in relation to the Weibel model was taken to be around one third along the length of the main bronchus, generation 1. It was therefore necessary to begin the iterative transformations of the Weibel data with generation 1 even though this generation does not appear in the shell structure. This would enable a better fit when trying to interpret the results from the SML in relation to SPECT data. Figures 2.3 and 2.4 show the graphs drawn to complete the data transformation. The iterative transformation was therefore, began at generation 1.4 to represent shell 1 increasing in increments of 1.4 until 10 shells were accounted for.

Figure 2.3 Airway segment diameter for each lung generation (1-14)

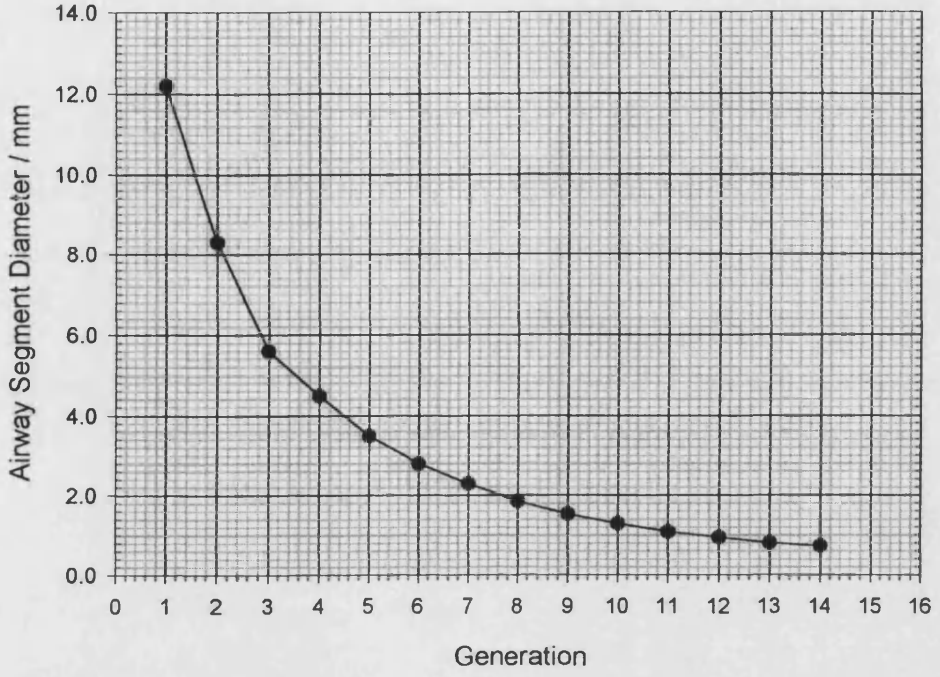

The values for the airway segment diameters at the point of each shell were read directly from the graph see figure 2.2

Figure 2.4 The total airway cross section in each generation (1-14)

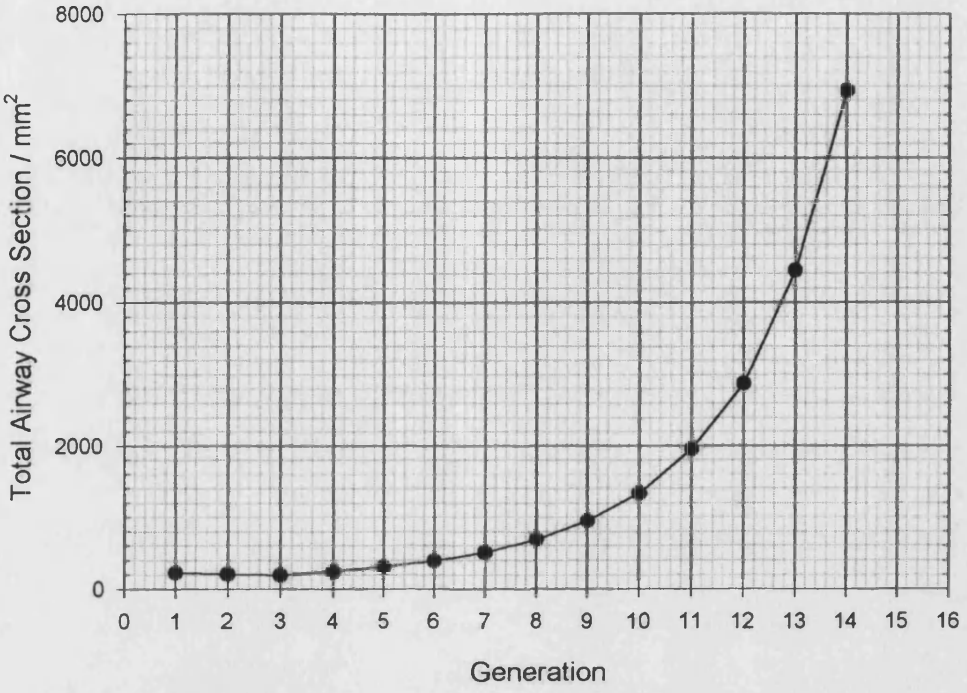

To fit total airway cross-section diameter (single, 3 parameter exponential growth).

$$f=y0+a*\exp(b*x) \qquad (4)$$

Sigma Plot (4.0) description of the equation:

fit f to y
[Constraints]
b>0
[Options]
tolerance=0.000100
stepsize=100
iterations=100

R = 0.99986460 Rsqr = 0.99972922 Adj Rsqr = 0.99967507

Standard Error of Estimate = 36.6890

	Coefficient	**Std. Error**	**t**	**P**

y0	**198.4697**	17.7048	11.2099	<0.0001
a	**12.5974**	0.9598	13.1255	<0.0001
b	**0.4484**	0.0055	81.7249	<0.0001
x	**generation**			

Analysis of Variance:

	DF	**SS**	**MS**	**F**	**P**
Regression	2	49697995.0167	24848997.5084	18460.2694	<0.0001
Residual	10	13460.7990	1346.0799		
Total	12	49711455.8157	4142621.3180		

Statistically equation 4 is satisfied and so it was used to calculate total airway cross section at each shell point.

2.2.5 Incorporating the transformation into the design

It was decided that the spacing of the holes over the shell surface should be equidistant. This makes the model symmetrical and makes the design and manufacture processes simpler.

Surface area of a hemisphere of radius r:

$$2\pi r^2 \qquad (5)$$

It is necessary to leave a small amount of surface area for the attachment of each shell to the back plate it was found that the area within a distance, δl, of 5mm from the shell edge was sufficient.

Surface area of space required for fitting:

$$\delta l * 2\pi r \qquad (6)$$

Therefore the length of the equivalent square:

$$(2\pi r^2 - \delta l * 2\pi r)^{0.5} \qquad (7)$$

Number of holes on one side of the equivalent square:

$$\sqrt{N} \tag{8}$$

Equation for the distance between each hole (D):

$$D = ((2\pi r^2 - \delta l * 2\pi r)/N)^{0.5} \tag{9}$$

2.2.6 Calculated dimensions

Using this equation, hole centre to hole centre distances were calculated. The number of holes in each of the 10 shells of the SML is given in figure 2.5

Figure 2.5 Calculated dimension for the SML

Shell	Generation	Airway Segment Diameter / mm	Total Airway Cross Section / mm^2	Number of holes / N
1	1.4	10.6	222	2.5
2	2.8	6.0	242	7
3	4.2	4.2	281	20
4	5.6	3.0	353	50
5	7.0	2.3	489	117
6	8.4	1.8	743	292
7	9.8	1.25	1218	993
8	11.2	1.0	2109	2686
9	12.6	0.9	3379	5940
10	14.0	0.7	6906	16059

It was decided for economical and analytical purposes to have only 5 shells in the model. The even numbers; 2,4,6,8,10 were chosen; this makes the model symmetrical and includes the final stage.

Each hole represents an airway in that particular three-dimensional space within the lung. The remaining volume was considered to be uniformly filled with acini even though the

shells would act as the collecting surfaces for particles in the model. The holes were drilled into each shell at 90° angles to the surface to replicate the varying angles achieved by airway branching and to reduce burring of the metal. The actual dimensions of the constructed SML are given in Figure 2.6 and 2.7.

2.2.7 Actual dimensions

Figure 2.6. Shell measurements (n = 3 in all cases)

Shell	Mean Internal Diameter / mm	Mean Shell Thickness / mm (St Dev)	Mean Shell External Height / mm
Shell 1	35.5	3.13 (0.03)	22
Shell 2	77.5	2.0 (0.05)	44
Shell 3	110.6	2.88 (0.07)	62
Shell 4	160	3.04 (0.01)	83
Shell 5	200	2.97 (0.03)	102
Outlet Pipe	10.12		

Figure 2.7. Hole Measurements for each shell (n = 9 in all cases)

Shell	Mean Hole Diameter / mm (St Dev)	Number of Holes (N)
Shell 1	5.43 (0.09)	7
Shell 2	3.02 (0.08)	43
Shell 3	1.82 (0.03)	298
Shell 4	0.99 (0.01)	2478

2.2.8 Material consideration

The structure of the model was required to be rigid and rugged enough for everyday use. Glass would have been too difficult to manufacture with the necessary holes in each shell. It would have been heavy and rather delicate. Another option was to form the structure in silicone this seemed too costly and time consuming after investigation.

Aluminium was chosen as the material for the SML, it is a cheap, light inert metal. The University of Bath Science Workshop had considerable experience of working with aluminium so the manufacturing process could begin as soon as the design was completed.

2.2.9 Problems encountered with manufacturing

Each shell had to be cut from a solid block of aluminium to create the hemispherical structure. Several production methods were investigated before this was chosen such as spinning or forming a mesh to create the shell structure. It was a costly and time consuming method but, proved to be the only one that could be carried out successfully on the premises and within the time constraints. Unfortunately the Workshop could manufacture only shells 1, 2 and 3. Shells 4 and 5 were too big to be milled in the same way. The machinery used at the Workshop was too small to manufacture the larger shells.

Until a manufacturer could be found to make the larger shells it was decided to press on with characterising the incomplete SML. A large cylinder was fitted over the shells to

create a final stage including an outlet pipe for a vacuum pump to be attached. The initial SML design is shown in Figure 2.8.

The initial data collection using the incomplete SML is presented in Chapter 5.

Figure 2.8 Line diagram of the initial Shell Model Lung.

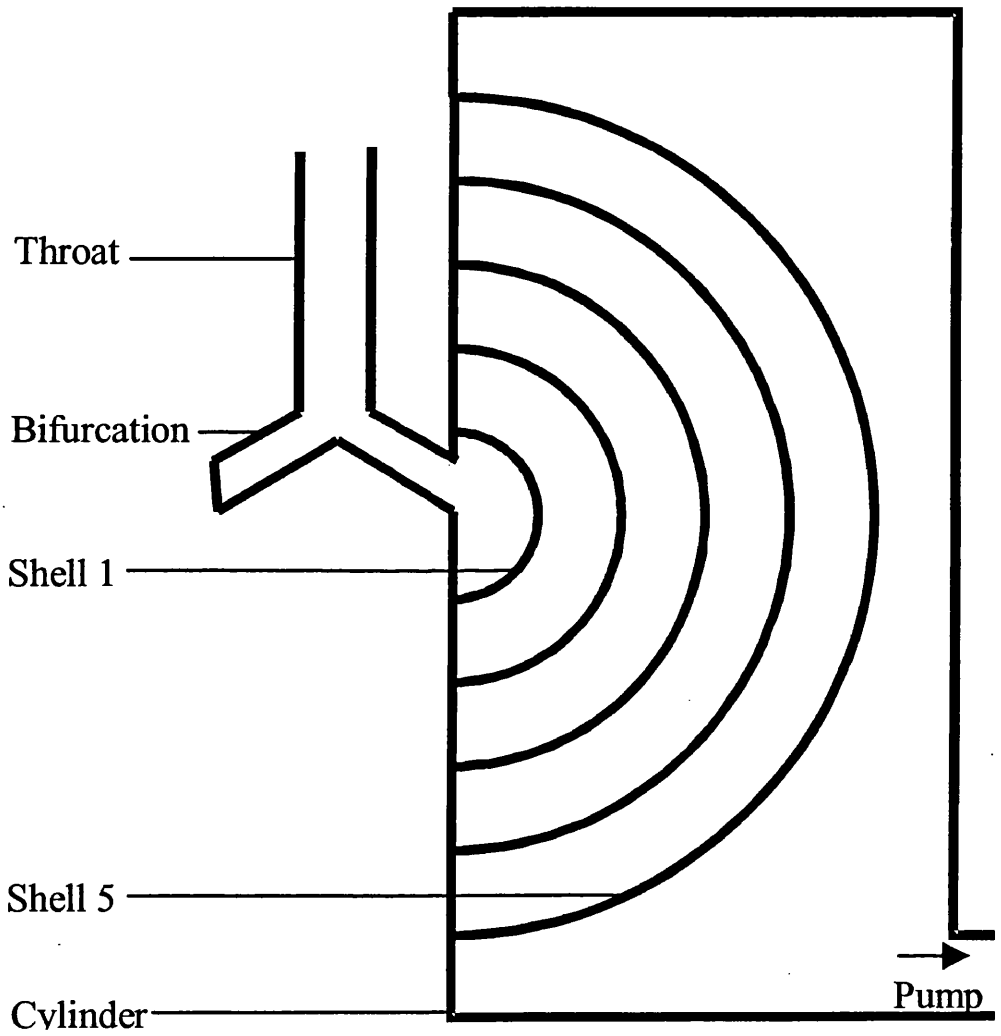

To complete the SML it was necessary to review the initial design configuration. Considering shell 5 and the large number of holes necessary in the shell, it was decided

this shell would be the final collecting stage. This resulted in the cylinder being discarded and the model becoming more compact. The hole content in shell 5 as designed would make it very time consuming and more importantly extremely expensive to manufacture.

The redesigned shell 5 contained no holes apart from an outlet pipe leading to the pump. The cost of the model was reduced by redesigning shell 5. The complete revised Shell Model Lung is shown in as a drawing in figure 2.12 and a photograph in figure 2.13. It took a few months to find an engineering company willing and able to undertake the manufacture of the final shells. Fortunately a company in Bath was found (Sayers Engineering) who had sufficiently large and advanced machinery to complete the job.

The manufacturing process of the larger shells took some time to complete, as they required more precision during manufacture than the smaller shells.

2.2.10 Bifurcation re-manufacture

The bifurcation entry port of the SML was manufactured to 20mm to allow the USP throat to be fitted directly to the SML. To represent the bronchiole, the original design of the bifurcation entry port had an internal diameter that decreased to 12mm (see figure 2.9). It is understood that the narrowing of the bifurcation entry port would have increased the flow velocity as the fluid moves through this area. Furthermore, the surface of the original bifurcation entry port was very rough and quite crude; this would have the effect of introducing turbulence into the flow as it passes this area. After some initial

measurements, it was decided to have the part remade in a more appropriate three-dimensional aspect to the specified dimensions. Sayers Engineering of Bath made the new bifurcation (figure 2.10).

Figure 2.9 Photograph of the old Bifurcation.

Figure 2.10 Photograph of the new Bifurcation.

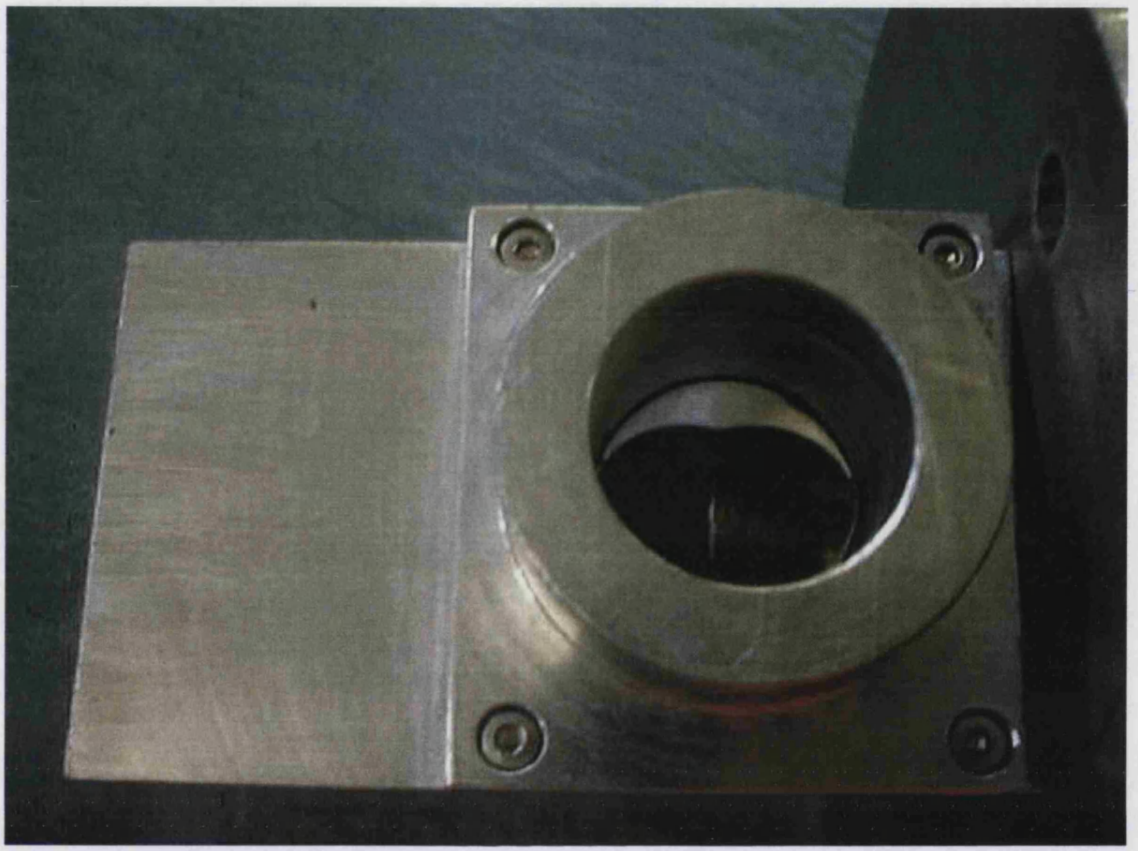

A series of experiments to show the improved three-dimensional SML are detailed in chapter 5. All calibration work was performed using the new bifurcation. Experimental work was carried out to show that the new bifurcation improved collection in the shells of the SML (section 5.11).

2.2.11 Theoretical cut point calculation for the SML bifurcation

It was first essential to calculate the theoretical Reynolds number at the bifurcation (Marple *et al.*, 1974):

$$Re = \frac{\rho V W}{\mu} \qquad (10)$$

Re = Reynolds Number

$\rho = 1.205$ kg m^{-3}

V = Velocity at the bifurcation (ms^{-1})

W = Diameter of bifurcation (m)

$\mu = 1.822 \times 10^{-5}$ Pa s

At a flow rate of 30 l min^{-1}:

$$V = \frac{Q}{A} \qquad (11)$$

$Q = 30$ l min^{-1} (equivalent to: 5×10^{-4} m^3 s^{-1})

$$A = \pi r^2 \qquad (12)$$

Where,

r = 0.005m

$$A = 7.854 \times 10^{-5} \text{ m}^3 \qquad (13)$$

Therefore:

$$V = \frac{5 \times 10^{-4}}{7.854 \times 10^{-5}} \qquad (14)$$

$$V = 6.37 \text{ m s}^{-1} \qquad (15)$$

Calculating the Reynolds number using (10):

$$Re = \frac{1.205 \times 6.37 \times 0.01}{1.822 \times 10^{-5}} \qquad (16)$$

$$Re = 4213 \qquad (17)$$

In consideration of the cut point at shell 1 it was necessary to assume very simplistic boundary conditions:

1. The velocity and flow field were in the direction of the bulk flow only
2. Velocity was zero at a solid surface

2.2.12 Geometric considerations

It was shown by Huang and Tsai (2001) that gravity considerations should be taken into account for accurate cut point calculations. It was shown that if Re were less than 1500 the gravitational force would reduce the Stokes number and thus affect the cut point diameter. At a Re of over 4000 as calculated in equation (17) it is reasonable to assume in theory no gravitational effect on the calculated cut point. As airflow exits the bifurcation it was assumed that the 'jet' was round.

2.2.13 d_{50} Calculation

In the simplest case for a circular 'jet' exit it can be said when designing a regular in-line impactor that the square root of the Stokes Number ($St_{50}^{1/2}$) may be assumed to be 0.5 (John, 1999). However the calculation depends on the impactor being vertical and the impaction plate being horizontal to the direction.

Using an assumed stokes number as suggested by Hinds (Hinds, 1999) of 0.49 in calculating the cutpoint of an impactor with a circular nozzle then:

$$d_{50}\,(C_c^{0.5}) = \left\{ \frac{9\,\pi\,\eta\,D_j^3\,St_{50}}{4\rho_p Q} \right\}^{1/2} \qquad (18)$$

Correcting for Cunningham slip correlation:

$$d_{50} = \left(\frac{9\pi\eta D_j^3 St_{50}}{4\rho_p Q} \right)^{0.5} - 0.78x10^{-6} \qquad (19)$$

Figure 2.11 Table of calculated cutpoints at specific flow rates the values calculated from equation 16 for the d50 cutoff diameters at 20, 30 and 60l/min assuming a 10mm bifurcation diameter.

Flow rate l min^{-1}	d_{50}
20	9.51
30	7.72
60	5.46

It is of course possible using these types of calculation to design an impactor giving desired cutpoints (Marple and Willeke, 1976). Using these calculations as an estimate of the cutpoint size and the recommendations for ensuring such an impactor gives the sharpest cutpoints it would be possible to devise specific instruments for the analysis of aerosols.

2.2.14 D_{50} calculation using measured dimensions

The actual diameter of the bifurcation at the exit was found to be 12mm. Performing the calculation again using this measurement gives:

Where, r = 0.006m

$$A = 1.13 \times 10^{-4}\ m^3 \qquad (20)$$

Therefore:

$$V = \frac{6 \times 10^{-4}}{1.13 \times 10^{-4}} \qquad (21)$$

$$V = 5.31\ m\ s^{-1} \qquad (22)$$

Calculating the Reynolds number using (10):

$$Re = \frac{1.205 \times 5.31 \times 0.01}{1.822 \times 10^{-5}} \qquad (23)$$

$$Re = 3511 \qquad (24)$$

Using equation 17 above:

$$d_{50} \square C_c = 10.3 \times 10^{-6} \text{ m} \qquad (25)$$

Correcting for Cunningham slip correlation, equation (18) gives:

$$d_{50} = 10.3 - 0.078 = 10.22 \ \mu\text{m} \qquad (26)$$

It is possible that the geometrical constraints on the model and gravitational effects on the particles (Re < 4000 in practice see equation (24)) reduce the cut point. Calculating the cut point using equation (17) (disregarding the Reynolds Number) gives an agreeable value. Due to the geometry and direction of flow it is difficult to accurately predict the Reynolds number at the many positions therefore an approximation has been made (a Computational Fluid Dynamics model in figure 3.6 shows that the pressure in shell 1 is uneven and figure 3.20 demonstrates that the area is subject to turbulence).

2.2.15 Line diagrams

Figure 2.12 Line diagram of the Shell Model Lung

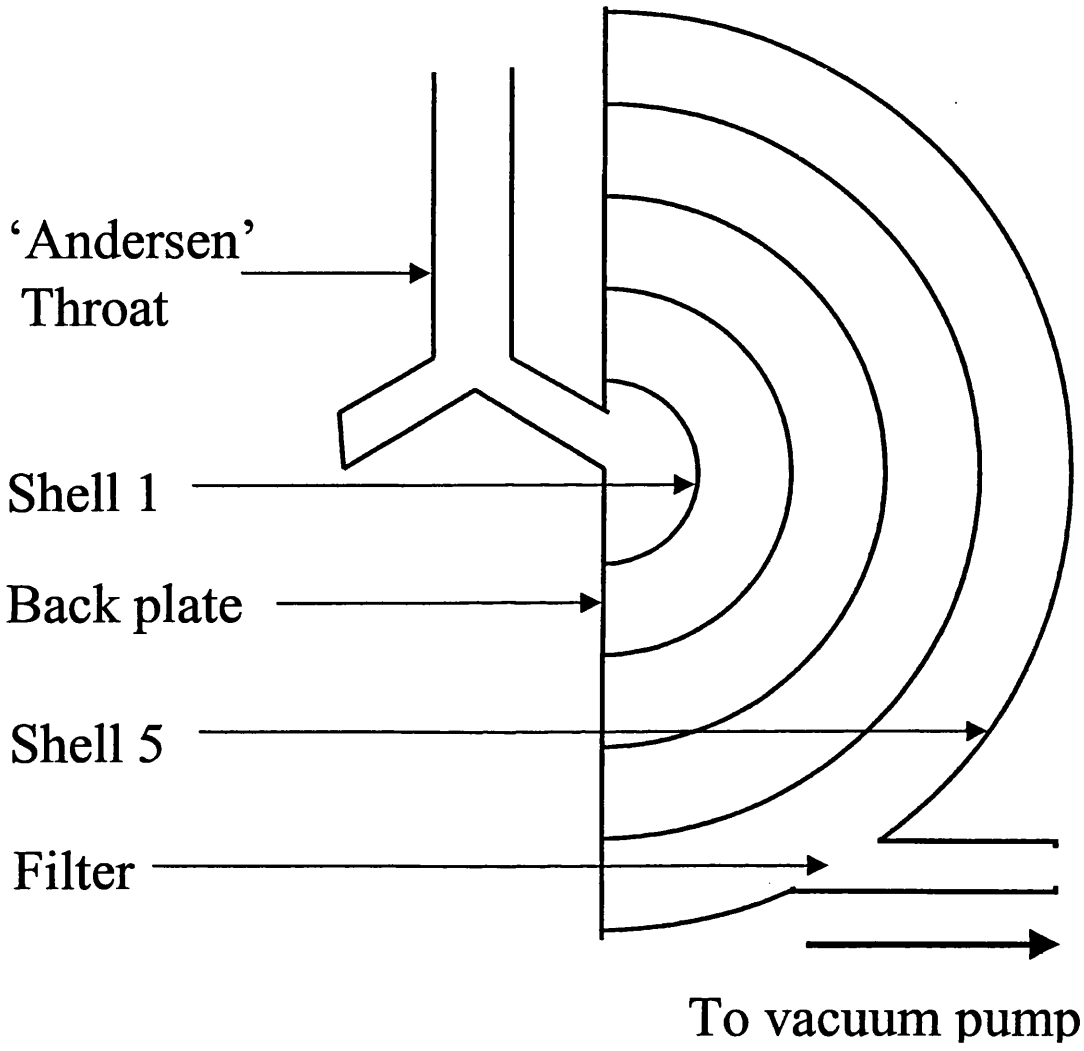

2.2.16 Pictures

Figure 2.13 Photograph of the Shell Model Lung.

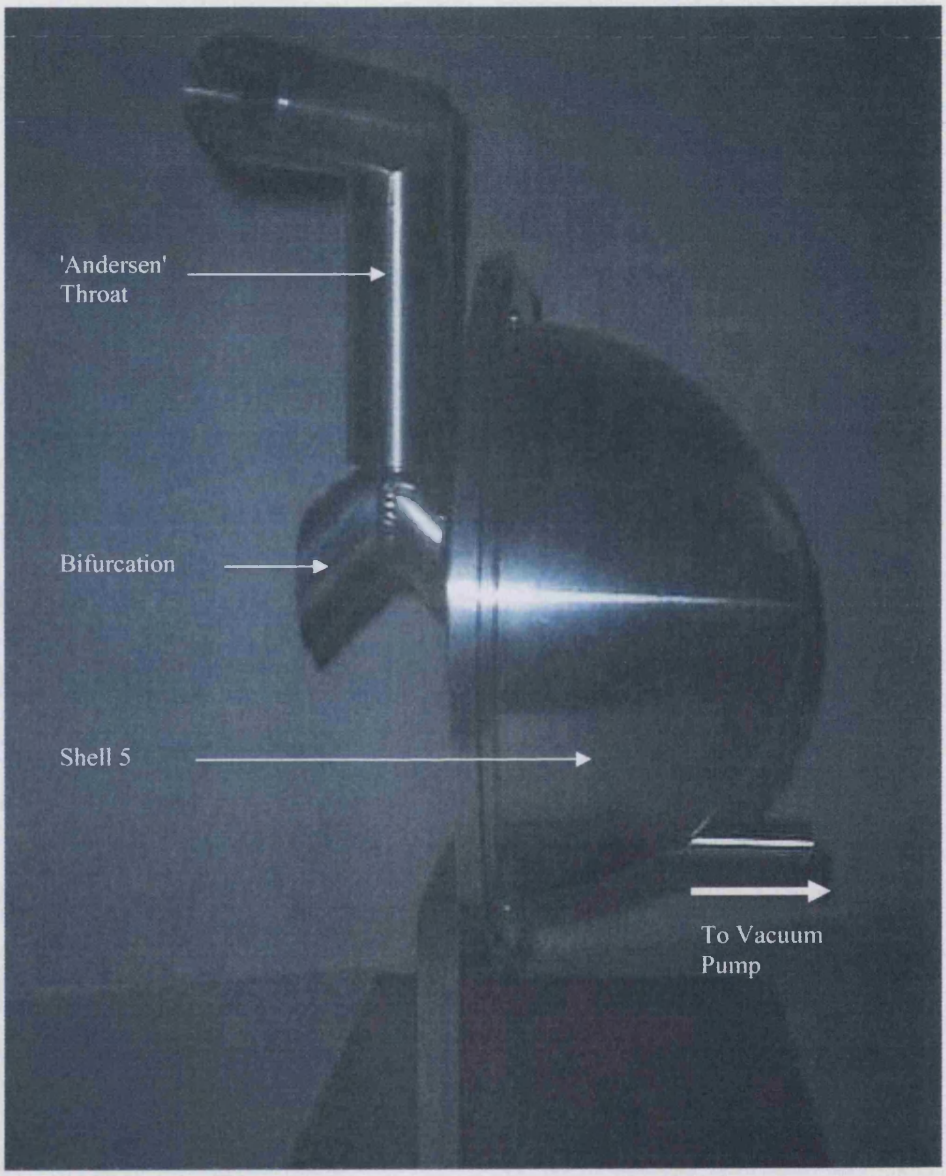

Figure 2.14 Photograph of Shells 1, 2, 3 and 4

Figure 2.15 photograph of Shells 1,2,3 and 4 (interior)

Chapter 3 Design and analysis of the 2-dimensional Shell Model Lung (2DSML)

3.1 Introduction

The 2DSML was devised to compare the CFD results with a physical model. If the 3D model was to be assessed for its fluid flow properties it would have been very complex to incorporate the necessary features into the model. It is necessary to sample the airflow in the cavities of the shells and throughout the model as a whole. This would mean extra holes would have had to be put into the model to allow this to happen. These extra holes would have to be blocked up when the model was in operation as an aerosol testing device. The difficulty arises due to the hemispherical structure of the design it would be rather difficult and costly to produce these extra sampling points in the model and very awkward to reassemble the model once the sampling line was inserted in the correct position. As the model is made of aluminium it would then be impossible to see if the sampling line remained correctly positioned after reassembly.

3.2 Design of the 2DSML

The potential solution to the problem was to design a 2-dimensional model. It would be quite impossible to manufacture a truly 2-dimensional physical model so a thickness of around 20mm in order for the required number of holes to be drilled into each shell was deemed to be satisfactory for the design brief and manufacturing requirements. The aim was to build a model incorporating as many of the three-dimensional models features as possible.

The model was turned from a complete plate of aluminium and then the parts were separated once the basic design structure had been formed. The work took a little time to complete but the two-dimensional model was far less costly than the three-dimensional model.

Each two-dimensional shell was designed as previously discussed in section 2.3 and figure 2.7 shows the line diagram used. The two-dimensional shells were designed as outline in figure 3.1 below.

Figure 3.1. Table of design shell dimensional data. Each shell to have fixed 3rd dimension of 20mm to account for the insertion of holes.

Shell	Distance from Back Plate mm	Surface Area mm^2
1	20	1256.6
2	40	2513.3
3	60	3769.9
4	80	5026.5
5	100	6283.2

To conserve the features of the three-dimensional model as much as possible the number of holes in each two-dimensional shell was based on the % hole content of each three-dimensional shell. Using data for the three-dimensional model the % Hole in each shell was calculated, figure 3.2 contains the data for these calculations.

Figure 3.2. Data from the 3DSML to calculate the % Hole in each shell.

Shell	Hole Diameter mm	Surface Area of Hole mm^2	Number of Holes	Surface Area of 3D shell mm^2	% Hole in shell
1	5.43	23.2	7	2513.3	6.5
2	3.02	7.2	43	10053.1	3.0
3	1.82	2.6	298	22619.5	3.4
4	0.99	0.7	2478	40212.4	4.7

The % Hole contained in each shell was then transformed into a number for hole content in the 2DSML. Figure 3.3 contains the data for these calculations.

Figure 3.3. Calculated data for the number of holes in each shell calculated from the % hole in each shell of the three-dimensional model. 'Number of holes' was rounded to the closest whole number.

Shell	Hole Diameter Mm	Surface Area of Hole mm^2	Surface Area of 2D shell mm^2	% Hole in shell	Number of Holes
1	6	28.3	1256.6	6.5	**3**
2	3	7.1	2513.3	3.0	**11**
3	1.8	2.5	3769.9	3.4	**51**
4	1	0.7	5026.5	4.7	**304**

Unfortunately the holes could not be manufactured to the exact specified diameters as stated however the actual diameters were a close alternative, figure 3.4 gives the data for the actual manufactured dimensions of the 2DSML.

3.3 Manufacture of the 2DSML

Figure 3.4. 2DSML dimensions (n=4, errors s.d. (0.03))

Shell	Hole Diameter mm	Surface Area of Hole mm^2	Surface Area of 2D shell mm^2	% Hole in shell	Number of Holes
1	5.74	25.8	1256.6	8.2	**4**
2	3.28	8.4	2513.3	3.3	**10**
3	1.74	2.4	3769.9	3.2	**51**
4	1.02	0.8	5026.5	4.9	**310**

As the hole diameter in Shell 1 was less than the 6mm designed diameter it was decided to have 4 holes in the shell instead giving a '% Hole in shell' value of 8.2%. Even though this seems a high value it was in fact closer to the original design specifications for the three-dimensional model as outlined in Section 2.3.3. Again with the second shell as the hole diameter was more than the specified value it was decided to round down the number of holes to 10 giving a '% Hole in shell' value of 3.3%.

Unfortunately a mistake was made in the two-dimensional Shell 4 and 310 holes were drilled instead of 304, the calculated distance between each holes was slightly wrong and the computer equipment drilled according to the programmed data. This gave a '% Hole in shell' value of 4.9% this was deemed satisfactory (+0.2%). It would have been too expensive to re-make the one shell as the whole model was formed from one piece of aluminium.

Once the drilling of the holes was completed the model could be mounted. Perspex was chosen as the material for enclosing the model. It was necessary to make a tight seal between the model and the case and the case had to be transparent. To make the measurement necessary it was also essential that the material could be worked with easily. For this reason glass was not chosen as Perspex is more pliable and lighter. The completed model is shown as a photograph in figure 3.5. The Perspex plates were bolted together to form a reliable seal. As it was not intended for the 2DSML to be used as an aerosol testing device the use of Perspex and the electrostatic considerations of this type of material on particles was irrelevant.

The design, manufacture and analysis of the 2DSML were personally directed at all times. The experimental work described below was carried out in the department of mechanical engineering at the University of Bath and was at all times personally supervised.

Figure 3.5. Photograph of the 2DSML

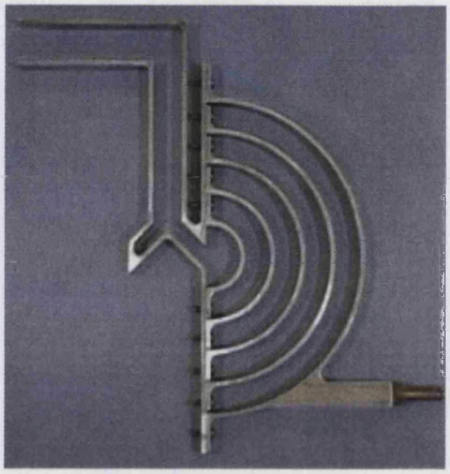

3.4. Computational Fluid Dynamics

Dr Ming Li at the Department of Mechanical Engineering, University of Bath, constructed a CFD model of the 2DSML. Data for the design were provided and the project directed in conjunction with the design and manufacture of the 2DSML. The software used was STAR-CD (Version 3 Computational Dynamics, London, UK) a finite volume based package. A brief summary of the qualities of CFD will be given followed by a summary of the work carried out on this particular project.

3.4.1 Basic Principles

The modelling of fluid flow begins by ensuring the conservation laws of physics are applied. These are:

1. Mass is conserved
2. Rate of change of momentum = sum of forces on a fluid particle (Newton's 2nd law)
3. Rate of change of energy = sum of the rate of heat addition to and the rate of work done on a fluid particle (1st law of thermodynamics)

The fluid can be attributed velocity, pressure, density and temperature if these conditions are adhered to and the operator has set conditions appropriately. The fluid is considered to consist of fluid 'particles' the smallest amounts of fluid able to be reliably modelled i.e. individual molecules have no effect on the qualities being investigated.

The conservation of mass in the fluid essentially requires the increase of mass within the fluid element to equal any net input of mass into said element. This ensures that an increase in pressure cannot happen unless the operator allows fluid to enter the system at a specified direction, order and dimension.

The rate of change of momentum may be considered to be an outcome of the allowed forces acting on the fluid particle as programmed into the system by the operator. The forces acting on the fluid particle can be surface or body force:

Surface forces: Pressure forces

Viscous forces

Body forces: Gravity forces

Centrifugal force

Coriolis force

Electromagnetic force

It is obviously vital that the operator enters such force parameters so the system can begin to function as would be expected under physical experimentation.

The derivation of the energy equation from the 1st law of thermodynamics ensures that heat energy is accounted for when assessing the total energy of a fluid particle. Heat energy must be allowed to flow through the system for accurate modelling (Versteeg and Malalasekera, 1995).

The model that was constructed was made as simply as possible allowing faster computations. Modelling consists of building a mesh of the design and incorporating as much detail as allowed into the design. Once the boundary limits and interior framework are set the operator may begin setting the fluid flow conditions. The advantage of using this technique is that the model design once created may be relatively easily changed.

This is of great use when carrying out a project such as this where physical modelling was found to be very costly and time consuming.

It was decided that the whole model should be analysed using CFD but constructed in two-dimensions only. The first CFD model was based on the incomplete SML and those are the diagrams that will be investigated. If more time could have been allowed then the model would have been investigated further and related to work presented further in this chapter.

It is possible using this technique to model the velocity of the fluid flow. This is extremely useful when looking at areas that potentially cause turbulence in a model. The pressure changes in the system can be assessed as can be seen in Figure 3.6 below. Particle deposition or particle tracking can also be analysed with CFD.

The results from the model in figure 3.6 indicate that there are significant pressure drops as the fluid moves from the bifurcation through to shells 1, 2 and 3. This would suggest that at these points in the model any drug particles in the system might deposit as the fluid properties change.

3.4.2 CFD model

Figure 3.6. CFD diagram of pressure changes in the 2DSML. The inlet velocity was set at 1.28ms^{-1}.

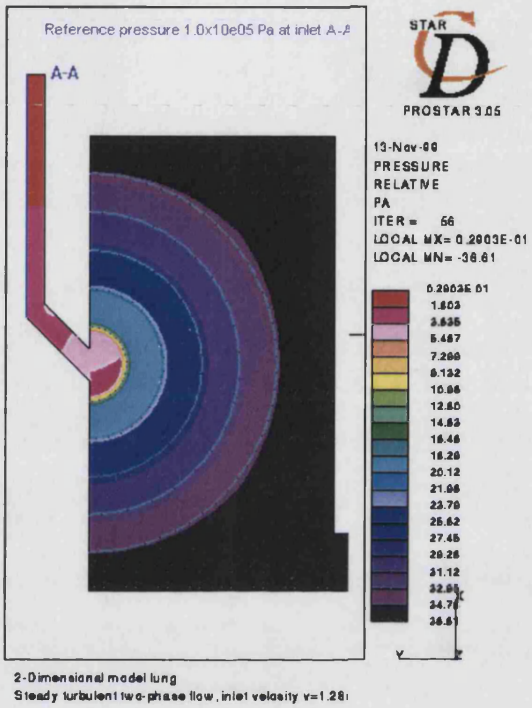

3.4.3 Results and Discussion

CFD has many limitations but it is a very useful tool when investigating design and implementing changes to those designs. The technique cannot be used alone without physical experimental measurements taking place but with careful validation procedures it may be possible to use the tool more routinely. It is essential that the system operator understands fully the CFD software and its limitations and the design to be analysed.

3.4.4 Current relevant CFD uses

Many stages of the lung and simplified impactor stage geometries have been studied using CFD. Airstream effects in parts of the lung and canine whole lung systems have been investigated.

Li and Edwards, 1997 have made throat geometry assessments. They used simplified (USP) throat geometries comprising a 90^0 bend and a more anatomically correct throat model. Both geometries were considered in three-dimensions. Particle deposition was estimated by making the internal surfaces of the model 'wet', this instruction is possible when using the technique.

It was seen that the anatomic throat more closely resembled an empirical formula developed earlier, which was based on *in vivo* comparisons. The reliability of this method was not sufficiently evaluated in the text of the reference. However, over 80% deposition was seen of 10μm particle in the throat and approximately 40% deposition of 1μm particles was seen thus, it is reasonable to accept the comparative study in the interest of throat deposition only. A USP throat was used as the inlet port to the SML and the 2DSML in a two-dimensional capacity.

The wide variation of predicted deposition between three-dimensional and two-dimensional models reported should be expected as any surface roughness or changes and variation of geometry will introduce turbulence and thus affect deposition. It was clear the particle deposition seen for the studied simplified (USP) throat was less than in a

more 'correct' anatomical throat, 10μm at approximately 10% and 1μm particle deposition at around 10% also.

As a DPI was used as the model aerosol in this study it was necessary to ascertain the deaggregation forces acting on the drug and carrier particles. If particle were in a more turbulent environment the direction and thus velocity of such forces will be less predictable and deposition possibly enhanced.

When investigating the effects of lung geometry on airflow it is necessary to look at small changes throughout the lung. The easiest points of interest to look at are probably bifurcation regions. It is relatively easy to set up CFD models of bifurcating tubes of set diameters and branches at realistic angles. Carinal ridges at the point of bifurcation will have effects and influences on the airflow through the region. Martonen *et al.,* (1994) looked at the effects of carinal ridges in generations 6 to 7 of the Weibel model. For each ridge shape, parabolic, blunt, saddled and asymmetric at high flow rates (qualified at 60 l min^{-1}) a higher incidence of turbulence was found than seen at sedentary (7 l min^{-1}) and light activity (20 l min^{-1}) breathing patterns.

Ignoring the effects of the carinal ridge it was seen that plug flows in the parent branch result in less skewed daughter branch flow profiles than when the parent branch displays parabolic of fully developed flow. In the investigations made on the 2DSML it was assumed that the flow was fully developed throughout.

Geometry features as presented here will affect turbulence, airflow and aerosol deposition. The assessment made was simplified but indicates further and more detailed examples must be investigated.

A physiologically realistic bifurcation model has been characterised by Balásházy *et al.*, 1996. Based on the Weibel lung model at generations 3 and 4 (56mm □ 45mm at an angle of 35^0) the model assumes the airways are smooth and round.

The airflow was seen to become turbulent after entry into the daughter branches at the boundary opposite airflow entry. The amount of turbulence in reality is likely to be much higher as geometry features are present in the airways. Boundary conditions are extremely simplistic and symmetrical.

The 'realistic' bifurcation does not model the airflow and deposition sufficiently. It is however a good basis for improving CFD models and introduces the ideas of actual geometry and the proposed effects on CFD models.

A double branching bifurcation model has been used to assess the deposition and dispersion of an aerosol bolus (Lee *et al.*, 2000). The model although improving on the techniques employed by Balásházy *et al.*, was till found lacking but proved far better agreement with physiological models described. Increased complexity has obviously become possible as technology advances; the techniques of investigating bifurcational disturbances in airflow require further refinement.

The SML and 2DSML contain only one bifurcation representing the transition between the larynx and bronchi. The bifurcations as presented above refer to generations deeper in the lung. It is likely that the SML as an over-simplification of the situation will collect particles in this region of higher MMAD than would be the case in reality. Anatomically correct models would include the geometries that make turbulence a feature of the airflow in the respiratory tract and allow smaller particles to deposit.

A significant improvement in the modelling of the lung was made when a realistic CFD model of the canine bronchial tree was constructed from a cast having undergone tomographic scans (Perzl *et al.*, 1996). The data gained from this method were of very high quality but limitations of the technology resulted in the geometry data having to be reduced so the computation could be performed within reasonable time restrictions. The model was of course very realistic and the authors propose it may be used for studying particle deposition.

Any simulations carried out would have to be verified by experimental means. Animal studies are essential for many drug evaluations but when concerned with particle deposition in the human respiratory tract airway geometries the canine and human respiratory structures are different and this must be taken into consideration. If drug deposited in the lung is to have a local or systemic effect it is vital to understand where deposition will occur in a human subject as drug action depends on receptors, areas of smooth muscle or entry into alveolar regions must be targeted. It is unlikely that canine

models will provide good correlation but the CFD model is of great use in understanding the complex geometries present.

It is clear from the literature that using numerical and CFD models to study the lung is valuable and becoming more realistic as technology improves. The importance of physiologically correct, three-dimensional models and the inclusion of realistic flow patterns were noted by Ferron and Edwards, (1996) for accurate CFD modelling.

Considering particle flow and deposition in the lung system requires taking into consideration the pitfalls present in CFD modelling techniques and applying further appropriate theoretical situations. The behaviour of a commercial aerosol in the lung system put further constraints of shape, hygroscopic growth, coagulation of particles and mass changes as particle deposition takes place in the system.

The constant variation of lung morphology as breathing occurs and the transition from conducting airways to regions where gaseous exchange takes place pose further questions and challenges for the mathematical and computational modellers.

Particle deposition even when considering situations will not be realistic if the airways modelled are smooth straight tubes as presented by Gradoń and Podgórsky, (1996). It is of vital importance that oversimplification does not greatly affect the accuracy of the results (Finlay *et al.,* 1996). It was demonstrated (Zhang *et al.,* 1996) that even in simple bifurcations flow patterns were complicated. It is drawn to the attention that the working

relationship between operator, model and software must be very good and never reduce the merits of each factor. If a CFD solution is physically investigates and qualified then it can be held as valid.

The most advanced CFD model of the respiratory tract to date has been designed and developed to generation 4 (Clayborough *et al.*, 2001). The model clearly shows the degree of asymmetry present in the lung system. It was demonstrated, using a laminar flow, due to the constriction of the airways around generation 4 air velocity increases. It is expected that after this area the flow velocity will fall as the number and surface area of the airways increase. The authors hope to develop the model further and use the technology to incorporate aerosol devices into the system but due to the complex nature of the project it is expected to take quite some time.

3.5 Analytical Model

3.5.1 Introduction

An analytical model was designed by Daniel Clark, a final year MEng. student at the University of Bath to predict airflow characteristics at specified points through the 2DSML. This model was designed and constructed under personal direction as an alternative to using CFD it was a quick easy to understand and modify technique that requires no computer work. The model can be modified when experimental determinations provide evidence to give a more realistic representation of the physical model. The modelled factors were:

- Reynolds number (Re)
- Flow regime (either laminar or turbulent)
- Velocity (v/ms^{-1})
- Loss in total pressure, relative to atmospheric conditions ($\Delta P_0/Nm^{-2}$)
- Loss in static pressure, relative to atmospheric conditions ($\Delta P/Nm^{-2}$)
- Total pressure (P_0/Nm^{-2})
- Static pressure (P/Nm^{-2})

Figure 3.7 contains a line drawing of the positions of the points (stations) in the 2DSML. The model is arranged on a spreadsheet and the user simply types in the relevant conditions: flow rate and atmospheric temperature and pressure (Clark, 2001)

Figure 3.7. Positions of sampling points (stations) through the 2DSML.

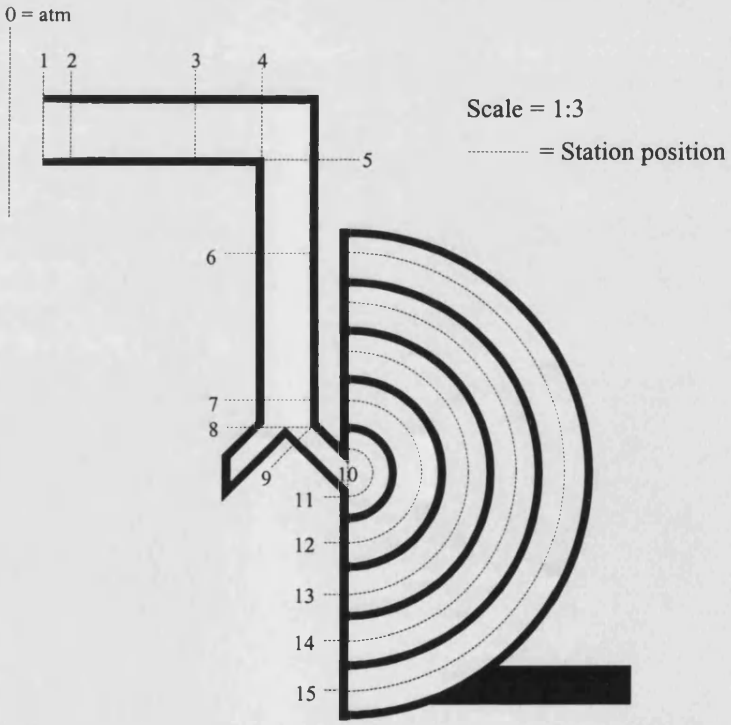

3.5.2 Basic Assumptions

To ensure the model is user friendly and quick to use several assumptions have been made.

1. Compressibility is insignificant and so is ignored. The estimated velocity at which compressibility effects become apparent was 100 ms^{-1}. It was shown that the maximum velocity achieved in the 2DSML was less than 14 ms^{-1}.
2. Air temperature was constant throughout the model.
3. Flow was steady; any fluctuations in pump performance were ignored.
4. Airflow velocity changes were considered to be instant.
5. Modelled airflow was considered to be one-dimensional.
6. Airflow was considered to be evenly distributed around each hole and shell.
7. Jet effects throughout the model were ignored.
8. Flow at the bifurcation region was assumed to follow in the direction of shells only.
9. All surfaces were considered to be 'fluid dynamically smooth'.

The assumptions made are indeed simplistic but for the purposes of the work in the time frame allowed it proposed a suitable mathematical model of the 2DSML. In particular it is unlikely that there will be insignificant jet effects and they will be most apparent in the lower regions of the shells, as the position of the pump will probably influence the direction of flow. This of course leads to an uneven distribution of flow through each hole and subsequently each shell.

The analytical model was used to compare experimental data collected using the 2DSML; an account of this work will be given below.

3.6 Pressure Testing

3.6.1 Introduction

The purpose of constructing the analytical model was to relate it to physical experimental data collection in the 2DSML and assess its suitability. It would be of great value as an insight into the flow characteristics in the two-dimensional model but it is ultimately the three-dimensional flow characteristics we are concerned with. Daniel's work was at all times directed by the author and reflects work previously investigated

3.6.2 Methods

At corresponding positions to the sampling points (stations) of the analytical model holes of a suitable size were drilled into the Perspex cover of the 2DSML. Figure 3.8 shows a photograph of the 2DSML as set up for pressure testing experimentation.

Figure 3.8. Photograph of the 2DSML with hypodermic tubing connected to its pressure tapings.

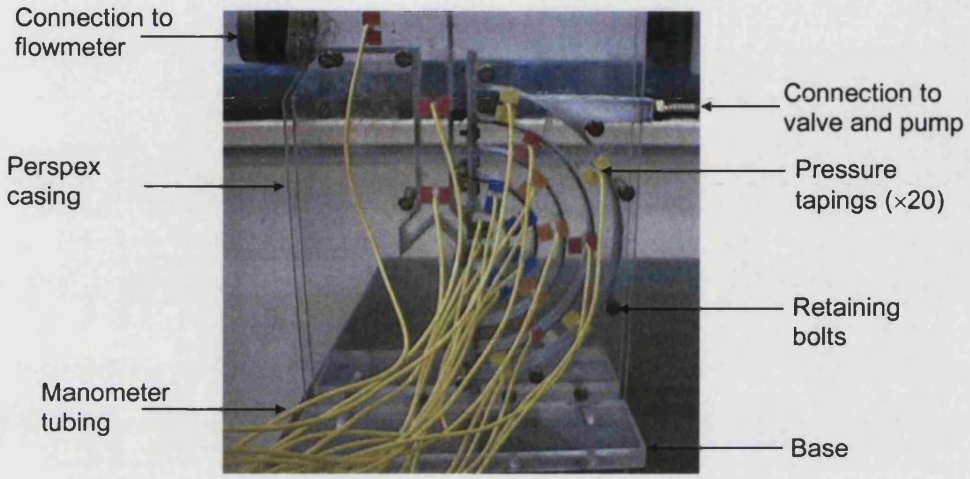

The Perspex sheets were fitted onto the model with a layer of silicone grease between and securely bolted together. The yellow tubing (1.6 mm ext. diam., 1.0 mm int. diam.) was connected to the Perspex sheet using fitted pieces of metal hypodermic tubing for rigidity securely glued into the Perspex sheet and at the other ends to a manometer. Figure 3.9 contains a photograph of the experimental set-up.

The procedure for pressure testing in the 2DSML was as follows:

A vacuum pump (GAST, Model 1423 101Q Q626X. Benton Harbour M.I. USA.) was used to generate the airflow. The inlet of the pump was connected to a regulating valve that was used to vary the flow rate. The system had an operational range of 0-70 $lmin^{-1}$.

The pump system was connected to the 2DSML using suitable flexible tubing; airtight seals were formed using jubilee clips.

Figure 3.9. Photograph of the 2DSML pressure testing experimental set-up.

Using a flow meter (SCR2, Glass precision Ltd., UK.) The airflow at the inlet was determined. The flow meter was calibrated prior to the experiments using a Chell™ CPD 100 digital flow meter. The experimental work was carried out using flow rates of 10, 30, 45, 60 and 70 l min^{-1}.

At each determined flow rate manometer readings were taken. When low flow rates were being investigated it was necessary to tilt the manometer to achieve a suitably sensitivity for the readings. The angles used were measured using protractor and spirit level, the readings were adjusted for angles during calculation.

The results of the work are presented according to grouped data around each shell, this enables and insight into the pressure drops occurring between shells and so averages any positional differences in airflow intensity around each shell. Figure 3.10 shows a diagram of the positions of the pressure tapings followed by figure 3.11 a chart of the grouped tapings for processing of the results.

3.6.3 Pressure Tapings and Zone Grouping

Figure 3.10. Diagram of the position of pressure tapings in the 2DSML.

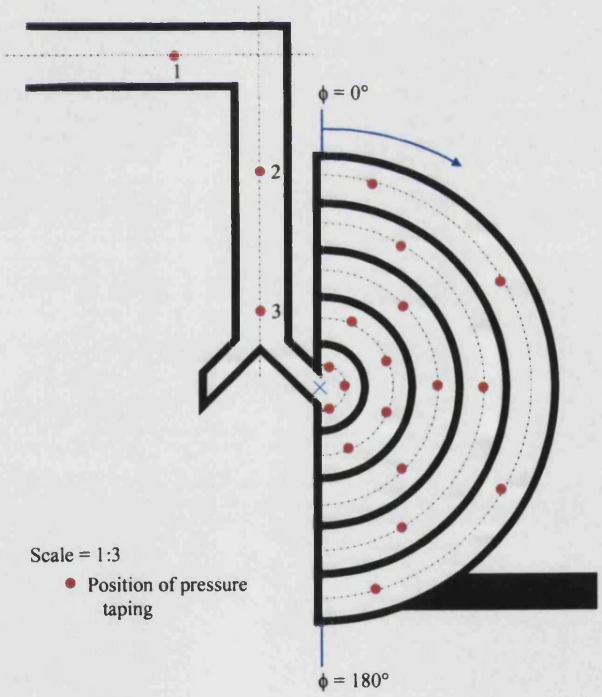

Figure 3.11. Chart detailing the position and grouping methods used for data analysis, the stated angle measurements were the variation of the point from vertical as detailed in figure 3.10 above.

Tapping No.	Region	Corresponding zone	ϕ / °
1	Throat 1	1	NA
2	Throat 2	2	NA
3	Throat 3	3	NA
4	Bifurcation-Shell 1	4	90
5	Bifurcation-Shell 1	4	20
6	Bifurcation-Shell 1	4	160
7	Shell 1-Shell 2	5	25
8	Shell 1-Shell 2	5	70
9	Shell 1-Shell 2	5	110
10	Shell 1-Shell 2	5	155
11	Shell 2-Shell 3	6	45
12	Shell 2-Shell 3	6	90
13	Shell 2-Shell 3	6	135
14	Shell 3-Shell 4	7	30
15	Shell 3-Shell 4	7	90
16	Shell 3-Shell 4	7	150
17	Shell 4-Shell 5	8	15
18	Shell 4-Shell 5	8	60
19	Shell 4-Shell 5	8	120
20	Shell 4-Shell 5	8	165

3.7 Results and discussion of Analytical and Experimental Pressure Testing

The results are presented graphically and contain data for both analytical and experimental 2DSML models. The graphs are presented to indicate the relationship between static pressure loss relative to atmospheric conditions (ΔP) and the corresponding zone of interest.

Figure 3.12. Graph showing static pressure changes in the analytical and experimental 2DSML at 10 l min^{-1}.

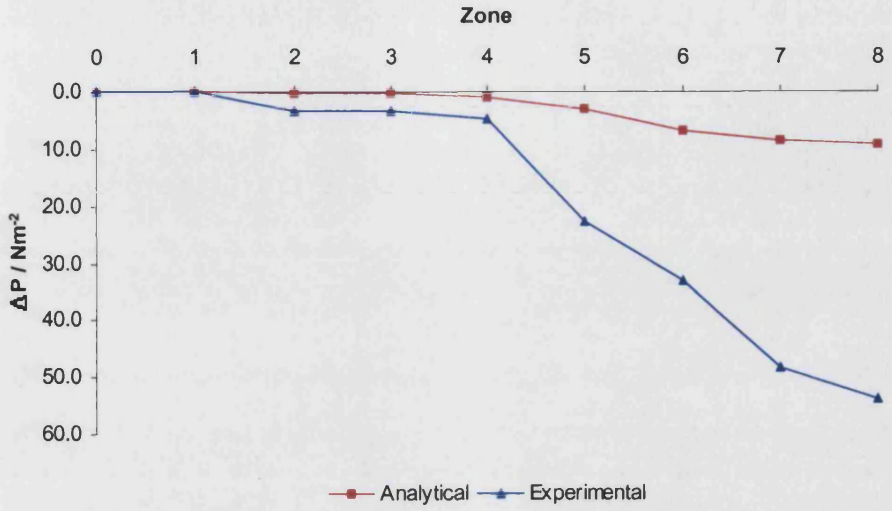

Figure 3.13. Graph showing static pressure changes in the analytical and experimental 2DSML at 30 l min^{-1}.

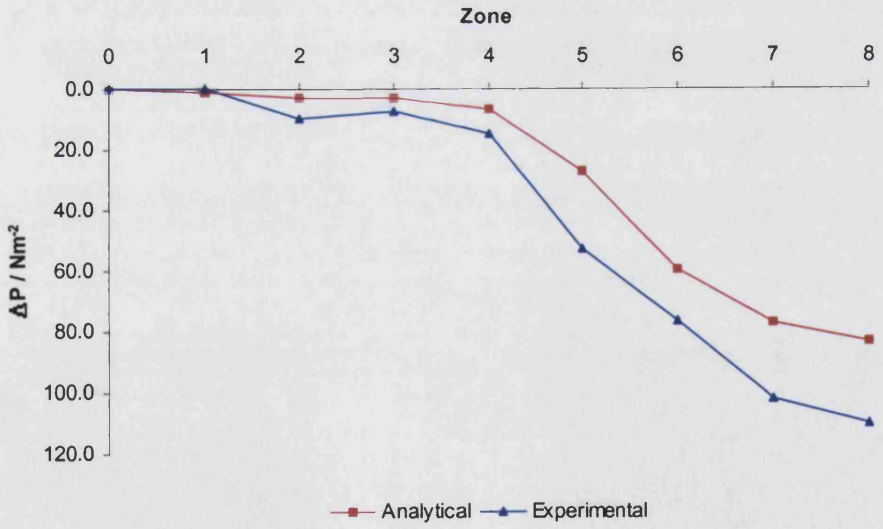

Figure 3.14. Graph showing static pressure changes in the analytical and experimental 2DSML at 45 l min^{-1}.

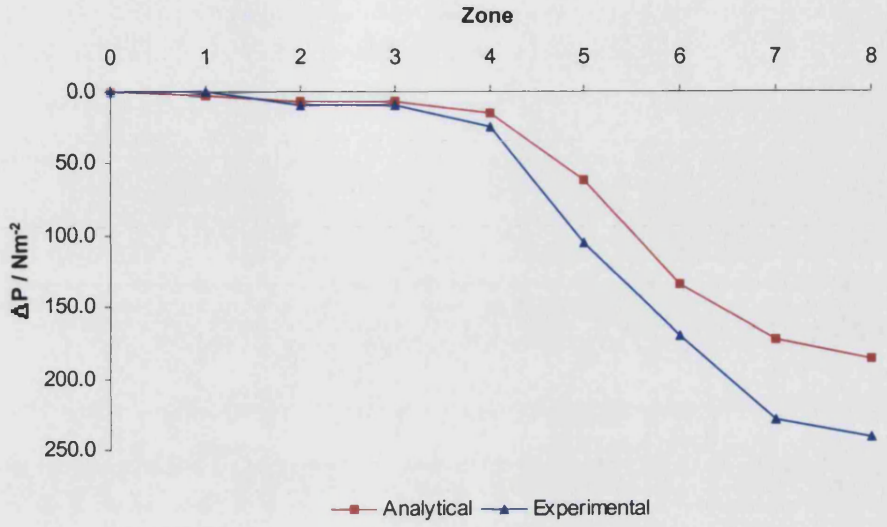

Figure 3.15. Graph showing static pressure changes in the analytical and experimental 2DSML at 60 l min^{-1}.

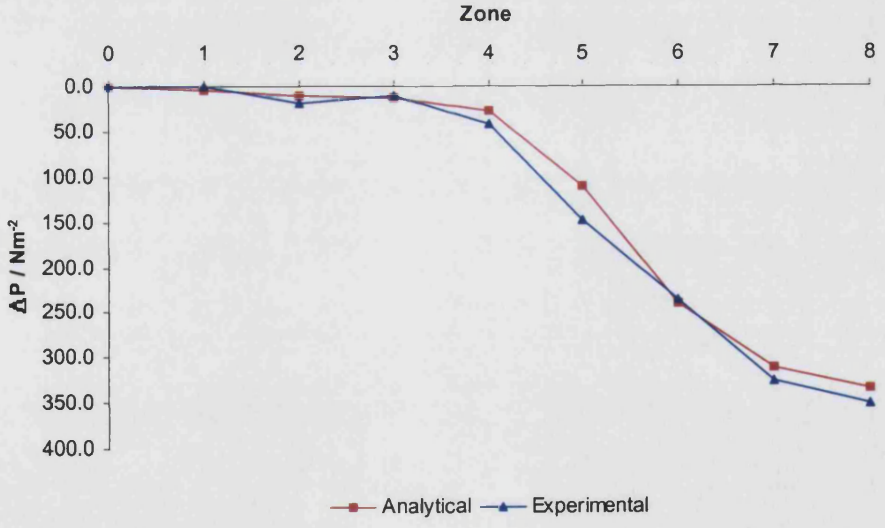

Figure 3.16. Graph showing static pressure changes in the analytical and experimental 2DSML at 70 l min^{-1}.

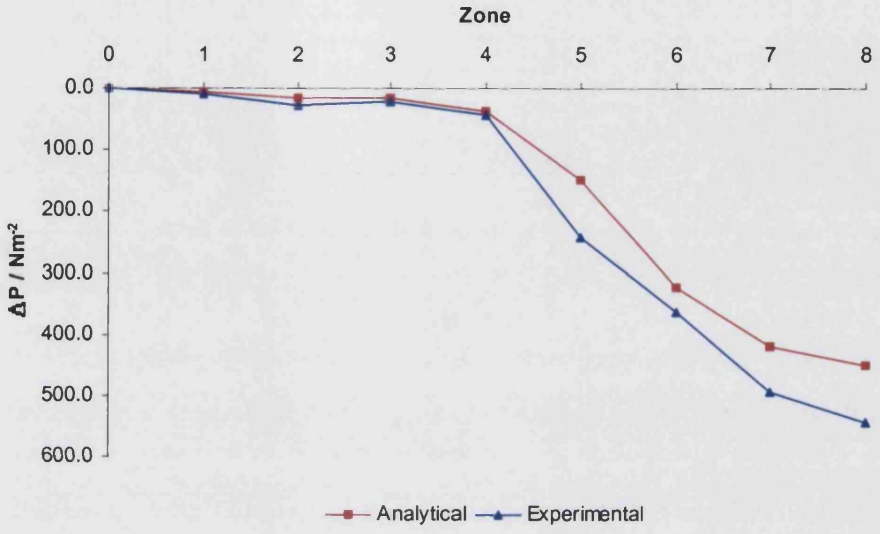

3.8 Discussion

The pressure as would be expected decreases as a function of distance from the inlet (Throat) through the model. Agreement between the analytical and experimental work becomes better at higher flow rates where experimental errors are not as large. it was seen that the static pressure varied around the shell zone possibly due to the positioning of the outlet, if it were more central then the variation may have been less.

The geometric constraints of the model causes the drop in pressure it can be seen that the differences are greater in all instances after zone 4 (shells). It can be said that for higher flow rates the analytical model is a suitable tool for the investigation of flow within the 2DSML. The design of an analytical model for assessing the flows in the three-

dimensional physical model would have to be far more complex however, the approach can be said to be appropriate.

3.9 Flow Visualisation

3.9.1 Introduction

Using water as the fluid in question the 2DSML was set up to investigate the direction of flow in the model. Using a dye tracer it was possible to track streak lines in the fluid and assess areas of particular interest such as possible impaction points (back of Throat, Shell1 and Shell 2).

To make the experiments as reliable as possible calculations were made to change the fluid from air to water and pass water through the model at comparable Reynolds numbers to that of the air at specified flow rates (equation 27).

$$Re = \frac{\rho v d}{\eta} \qquad (27)$$

Where

ρ = fluid density (kgm^{-3}),

v = fluid velocity (ms^{-1}),

η = fluid viscosity ($kgm^{-1}s^{-1}$)

d = characteristic length scale (m).

Flow rates of 10, 15 and 30 l min^{-1} were investigated using this technique. In order to observe the motion of the water, the fluid was marked with a coloured dye. Observing the motion of the dye allowed conclusions to be drawn relating to the direction of the flow. There are three main conditions that a tracer used for such purpose should meet; neutral buoyancy, high stability against mixing and good visibility.

It was possible to inject dye into the 2DSML either as a streak in effect a prolonged injection of dye matching the flow of the fluid through the device or as a cloud where a fixed 'dose' of dye was injected all at once.

Investigations were made into:

- Flow rate: Q = 10 $lmin^{-1}$, Q = 15 $lmin^{-1}$, Q = 30 $lmin^{-1}$
- Point of dye injection: Throat, or Shell 1
- Point of interest: Throat, bifurcation, shell 1, shell 2, shells 1-5
- Trace type: Streak, cloud

Figure 3.17. Adjusted flow of water (Q_W) for correct representation of Reynolds number when air flow (Q_A) was used.

Q_a / $lmin^{-1}$	Q_w / $lmin^{-1}$
10	0.66
15	1
30	2

3.9.2 Methods

The experimental set-up for the flow visualisation study is shown in figure 3.18. As in the airflow experiments, the 2DSML was encased between two transparent Perspex plates. A watertight seal was made by attaching lengths of flexible silicon tubing to the edges of the 2DSML. Bolts were then used to securely clamp the model in place.

Figure 3.18. Experimental set-up of the 2DSML flow visualisation studies.

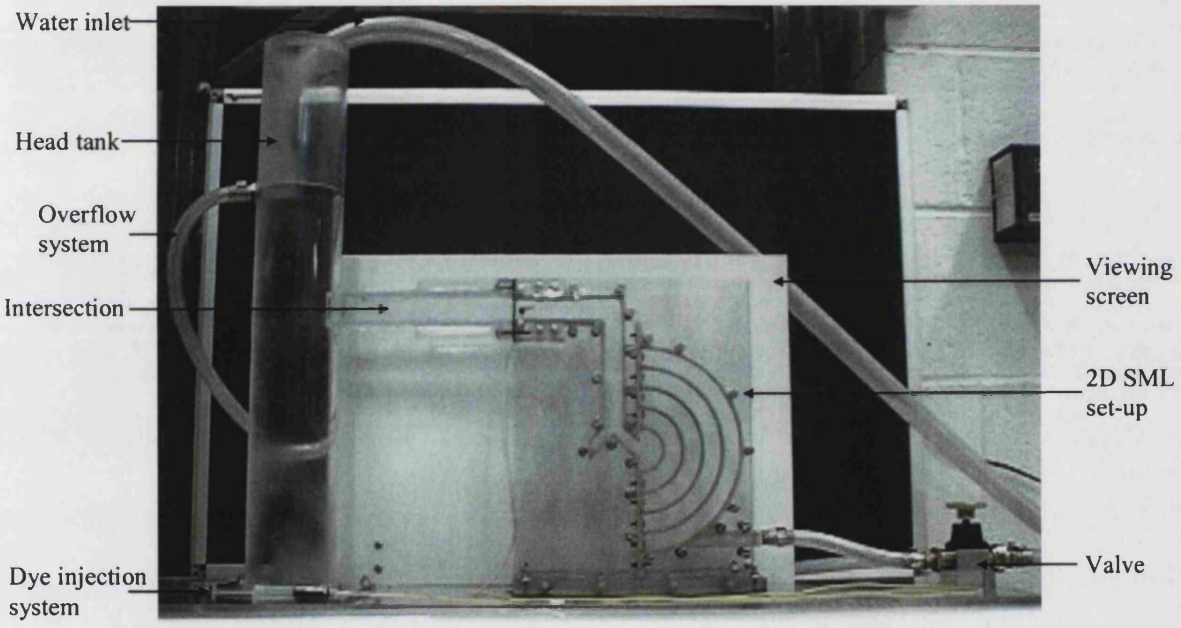

3.9.3 Flow Visualisation Results and Discussion

The series of experiments described here although not quantitative allow the viewer to see the pattern of flow dispersion through the 2DSML. Once the flow properties of the 2DSML are understood clearly it may be possible to investigate the flow in the three-

dimensional model. These experiments give some insight into the flow properties of the 2DSML and SML.

Results are presented as a series of stills taken from digital films made of the flow visualisation experiments. Experimental work showing streak traces show variations in flow characteristics as the flow rate was changed. Data for cloud injection into the model are shown as a function of time at a flow rate of 2 l min^{-1}.

Figure 3.19. Streak lines indicating direction of flow at a. 0.66 l min^{-1}, b. 1.00 l min^{-1} and c. 2.00 l min^{-1}.

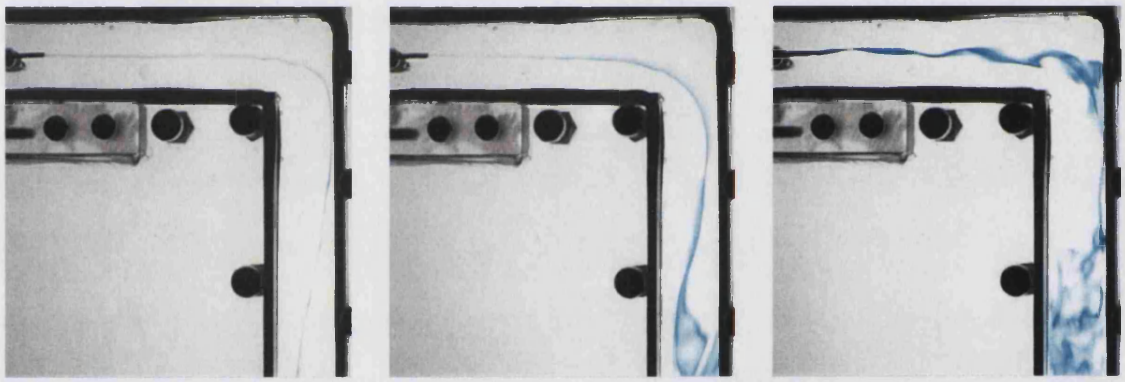

a. b. c.

Discussion:

At the highest flow rate of 2.00 l min^{-1} it can be seen that the streak line becomes 'broken' and variable with the flow. In each of the cases it is reasonable to assume that the flow carries the streak and it hits the back of the throat before it can make the 90^0 bend.

Figure 3.20. Flow visualisation of a 'cloud' moving through the 2DSML at time intervals (t) from t = 0 point of injection to t = 1.25s dispersion of the cloud in shell 3.

t = 0.0s t = 0.25s t = 0.50s

t = 0.75s t = 1.00s t = 1.25s

Discussion:

It is evident at t = 0.50s that the 'cloud' of dye begins to mix in shell 1. The area develops into a region of turbulence as the time sequence moves on. Throughout the sequence it can be seen that jets are indeed formed from the holes in shells 1, 2 and to a lesser degree 3. As theory suggests it is likely that impaction occurs in shell 1 and the data seen here supports that.

Figure 3.21. Streak lines indicating the direction of flow in shell 1 at flow rates of a. 0.66 l min^{-1}, b. 1.00 l min^{-1} and c. 2.00 l min^{-1}.

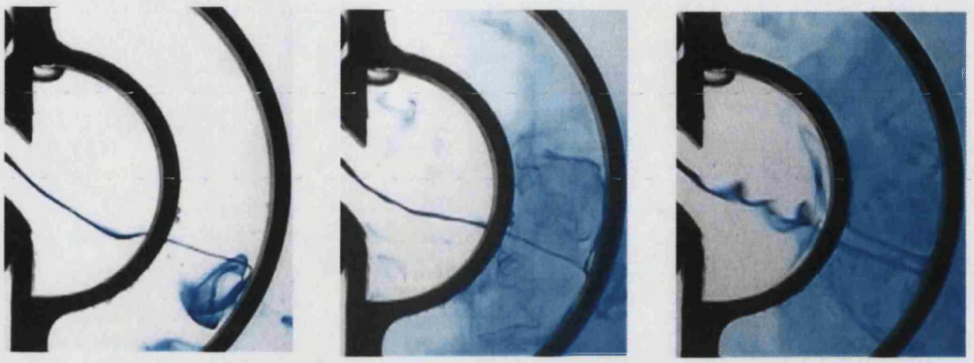

a. b. c.

Discussion:

The dye tracer here reinforces what we have seen in the data displayed in Figure 3.19. The dye at lower flow rates finds it way through Shell1 to hit Shell 2. At the higher flow rate (c.) it is clear that the streak line hits shell 1 and mixing of the dye in the region occurs. It is proposed that (c.) represents evidence for jet impaction onto the surface of Shell1.

Possible jet impaction can also be observed on the surface of Shell 2 in (c.). It is noted however that this effect is less than seen in Shell 1.

3.9.4 General Comments

There are limitations and errors that occur in this type of experiment. The introduction of foreign matter into the flow by the method used will disrupt the body of flow. If the dye

were injected at a distance then it would become too diffused in the flow to be able to give a good guideline to the flow properties. It is not sufficient to view the data as determining turbulence in the flow, the model has manufacturing faults and external disturbances will play a part in influencing what we may perceive to be turbulent flow.

The experimental design and procedure were fitting for this work and provided an excellent insight into the mechanics and direction of the flow as functions of flow rate and time.

Chapter 4 Calibration of the Shell Model Lung

4.1 Introduction

The design of the Shell Model Lung was intended to provide a model that demonstrates the particle deposition characteristics as seen in a human lung. The positioning, number and diameter of the holes in each shell allows the passage of air through the model. Particles are carried with the air until forces dictate their deposition at points throughout the model.

The SML was designed with the 'non-ideal' separation of an aerosol cloud as seen in the human lung in mind, therefore it was not envisaged that the model would or indeed should only collect particles by the impaction method.

It was first thought that the model could be calibrated using polystyrene latex particles however it was found that the method was not sufficiently accurate in that any evaporation would leave residue and any impurities in the water for dilution would results in the aerosol being less than monodisperse (Berglund and Liu, 1973).

4.2 Creating monodisperse particles

Evaporation/Condensation Aerosol Generators produce an aerosol that is of a good monodisperse order (g.s.d. <1.15). The advantage of this equipment is that the operator may set the particle size. The size range is from about 0.1 to 8 microns, for many applications this range is too narrow. The aerosol material used may be non-volatile oils such as Di-Octyl Phthalate (DOP) or Di-Ethylhexyl Sebacate (DEHS) or a solid such as Methylene Blue. It has been shown that a solution of Methylene Blue: Liquid Solution (1:2000) (Liquid solution 50:50 ethanol: water) produces spherical dry particles of Methylene Blue after aerosolisation using a VOAG (Berglund and Liu, 1973). A variety of methods could be used to cover a wide range of particle sizes (Marple *et al.*, 1991).

4.3 Vibrating Orifice Aerosol Generator

4.3.1 Description

The equipment used to calibrate the SML was the Vibrating Orifice Aerosol Generator (VOAG). The generator is based on the fact that liquid jets are unstable and break-up. If a liquid jet is produced it will naturally break-up into droplets of varying size. If the breaking point of these droplets is carefully controlled then the droplets produced will be theoretically uniform. To prevent these monodisperse droplets from coalescing and coagulating the droplets must be dispersed and diluted, the VOAG performs all these operations. Constant airflow during drying should result in spherical particles (Asking and Olsson, 1997).

Altering the diameter of the orifice allows a wide size range of droplets to be produced by the generator. There is a range of orifices available from 10μm to 100μm. The size of the droplets may be finely tuned by varying the concentration of the liquid jet (a non-volatile solute in a volatile solvent). Theoretically using a VOAG with a non-volatile solvent it should be possible to calculate the particle size of solute produced. The VOAG is extremely difficult to operate and many factors can affect differences in resulting particle size therefore it is always necessary to size the particles using a reliable method.

It is also essential that dispersion air is used to prevent not only coalescing of the particles but also to reduce electrostatic effects. Using a radioactive source may also reduce these effects.

The method of calibration selected was governed by the time remaining for the study. Unfortunately due to these time constraints the work could not be carried out at the University. An attempt was made to produce some monodisperse particles using the vibrating orifice aerosol generator (VOAG) but it was felt that this would take up too much valuable time. The instrumentation is particularly delicate and difficult to master so Dr Ian Marshall and his team carried out calibration of the SML at AEA (Culham). A description of the instrumentation and methods follow.

Figure 4.1 Schematic diagram of the break-up of a liquid jet as occurs when creating monodisperse particles in the VOAG.

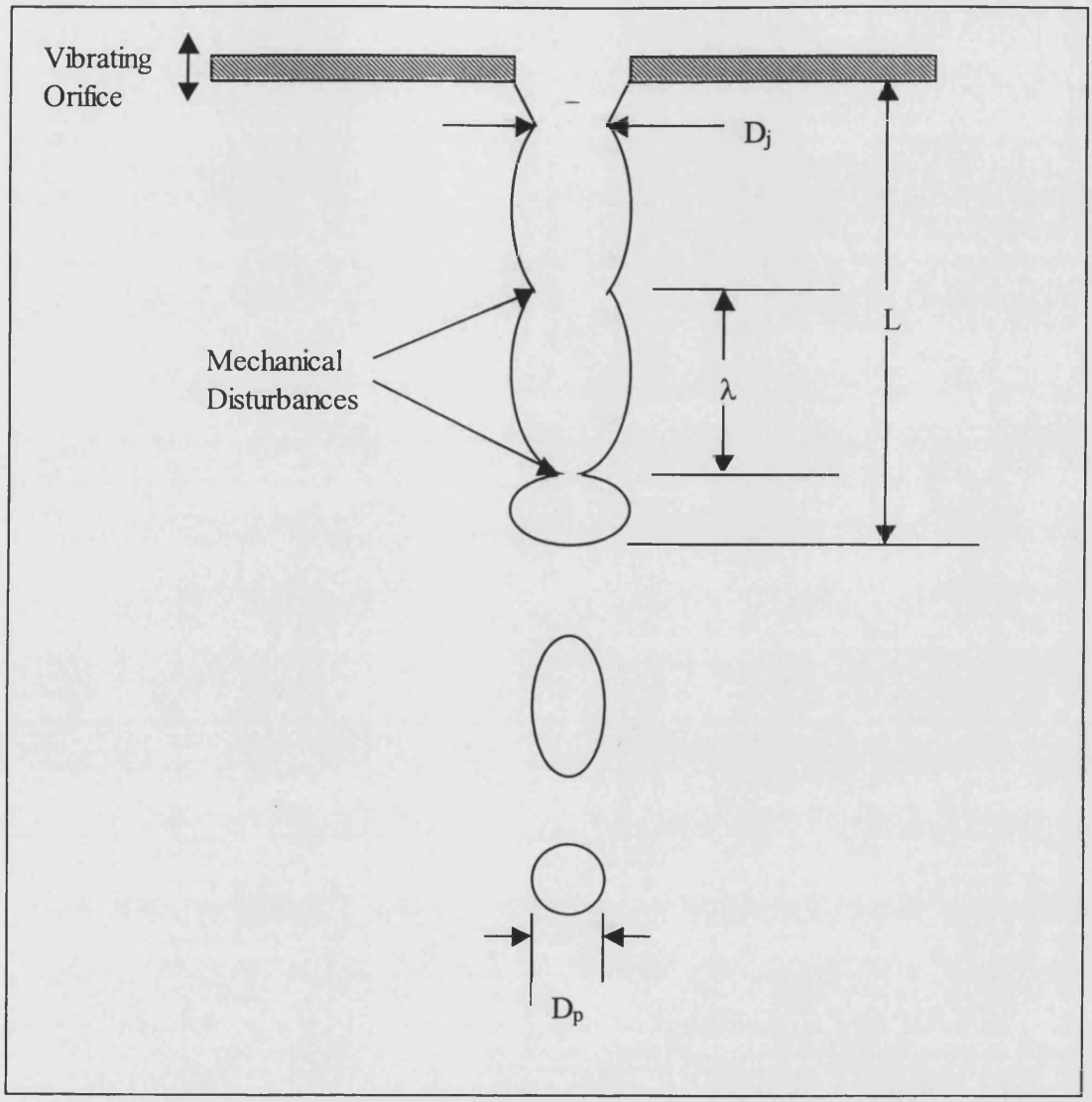

4.3.2 Governing equations

The theory of cylinder break-up has been derived (VOAG operating manual). The consideration of surface energy has contributed to the derivation of a minimum wavelength (distance between disturbances) for a disturbance to be unstable on a liquid cylinder of infinite length.

$$\lambda_{min} = \pi D_j \qquad (28)$$

D_j = liquid cylinder (Jet) diameter (m)

For an inviscid, incompressible jet the optimum wavelength was derived as:

$$\lambda_{opt} = 4.508\ D_j \qquad (29)$$

It was determined experimentally that varying λ within the following limits could produce uniform droplets:

$$3.5\ D_j < \lambda < 7\ D_j \qquad (30)$$

As energy is conserved a minimum liquid velocity required to form a liquid jet from a capillary tube was derived.

$$V_j, min = (8\sigma / \rho^{D}_{j})^{1/2} \qquad (31)$$

σ = surface tension N m^{-1}

ρ = density of the liquid (g cm^{-3})

Consequently uniform droplets may only be generated when maintaining both:

$$V_j > V_j, \min \qquad (32)$$

and

$$3.5\, D_j < (V_j / f)\,,\, 7D_j \qquad (33)$$

f = frequency of crystal vibration (λ / V_j) (Hz)

Since one droplet is produced after each cycle of disturbance, the droplet volume is given by Q / f, and the droplet diameter by:

$$D_d = (6Q/\pi f)^{1/3} \qquad (34)$$

Q= liquid flow rate ($cm^3\ min^{-1}$)

The droplet diameter can theoretically be calculated precisely using the above equation. When the liquid solution is forced through the orifice and the volatile solvent are allowed to evaporate from the droplets, non-volatile particles of the solute are obtained. The particle diameter is given by:

$$D_p = C^{1/3}\, D_d \qquad (35)$$

C = volumetric concentration of the solute in the solution (v/v)

D_d = initial droplet diameter calculated from equation 19 (m)

An error in the calculation will occur if impurities are present in the solvent, this may be estimated but the inherent errors in the VOAG and during its use means that each aerosol produced will be different even when another batch of the same liquid is run through the generator using the same settings. It is unfortunately necessary that each time an aerosol is produced it must be analysed by a specialist aerosol particle sizer (APS TSI inc. 33b s/n 196 in this calibration exercise). This was one of the many reasons for the calibration work being carried out by AEA, the equipment and expertise in using these system was far superior to any work that could have been achieved at the University laboratories. The use of an APS would be essential to this type of calibration. The APS gives an accurate result quickly and efficiently.

When producing particles using a VOAG it is essential that the surrounding environment is very clean and dust free. This factor was overcome to some extent at AEA by covering the orifice set-up so it didn't get blocked as easily or frequently. Dust and fibre particles can block the orifice. Once the orifice becomes blocked it must be carefully cleaned in a detergent solution and then rinsed in the solvent. It is easy to see using a light microscope for example that the orifice is clear of debris.

4.3.3 Instrumentation set-up at AEA

The set-up of the VOAG at AEA was modified to give an optimum output and least possible variation in particle diameter. The orifice may also become blocked if the solvent is not free of contaminants therefore it is essential that the liquid feed be thoroughly filtered before use. The VOAG at AEA included a pump from a HPLC machine to drive the liquid through the orifice. The pumps are dampened and had a much smoother action than the pump supplied with the VOAG. This in effect ensures that the liquid flow rate (Q) was kept constant according to equation 19 the diameter of the droplet produced had a lower GSD which means the aerosol produced was more reliably closer to being monodisperse.

4.4 Equipment

Figure 4.2 Analytical equipment used during the calibration of the SML

	Type	Certification
Spectrophotometry	Pye Unicam PU8600 S/N 342527	ATI Unicam 200226 19/05/00
Aerodynamic Sizing	TSI APS 33b S/N 196	Biral S5230 23/06/00
Balance	Sartorius B3100P S/N 40010153	SMK Balance Services 06850 07/12/99
Flow Meter	Hastings H-10KMS/ENALL-50K S/N 11486/6394	Chell 007100 15/06/00
Temperature	Digitron 2751-K S/N 083/23	DERA UKAS (013) 200005137 26/06/00

4.5 AEA Method

Particles of Methylene blue were produced at the VOAG orifice. Particles of approximately 10μm, 7μm, 5μm and 4μm were generated to cover the expected range of deposition in the SML. The VOAG was set up at the top of a rig of approximately 3 metres in height. Once the particles had been produced they were dispersed and diluted using air and collected into a drying column. The drying column extended from the orifice to the sampling level. As the particles were released from the column they were completely dry. This is essential if the APS is to give a reliable result. The particles are drawn through the APS and if they are not completely dry their diameter will change as they travel through the sizing apparatus due to evaporation and give a result that is variable and inaccurate.

During the drying stage it is usually advised that a radiation source is used to reduce the electrostatic properties of the particles unfortunately the radiation source wasn't available at the time of the calibration procedure. At this point the particles were sized using the APS.

The vacuum pump was set at a flow rate of 30 l min^{-1} through the SML using the Hastings flow meter and adjusted for temperature as read from the Digitron thermometer, according to a calibrated scheme. At the exit point of the column a short piece of tubing was used to connect the column to the SML throat. The sampling time varied between 2 and 10 minutes depending upon the size of the particles and therefore the production rate. After each experiment the SML was washed as in section 5.4.5 using Methanol, the

washings were weighed and the concentration of Methylene Blue detected using the spectrophotometer. The mass of Methylene Blue was then calculated. For each experiment the mass percentage collected on each stage and the collection efficiency for each stage were calculated and plotted against the recorded particle MMAD.

4.6 Results

The first part of the results shows the mass percentage deposition in each stage according to particle MMAD. This gives an indication of how each shell behaves in relation to the rest of the model when an aerosol of known aerodynamic diameter deposits. The presentation of these graphs is similar to the presentation of the graphs in chapter 5 where the percentage of 'Drug Recovered' from a commercial inhaler is plotted as the y-axis. The relationship between aerodynamic diameter and deposition in the SML will be investigated according to these results. The mass percentage graphs do not indicate deposition by impaction or any other mechanism.

The collection efficiency for each stage will be presented in the second part of these results. Collection efficiency is an indication of the collection properties of the stage. If the line passes through 50% we can say that the stage will collect particles by impaction.

Figure 4.3 Particle diameters generated during run 1 and run 2

Aerodynamic Diameter μm		
Run 1	**Run 2**	**Mean**
11.6	11.6	11.6
7.6	7.1	7.3
5.0	4.9	4.9
4.0	4.0	4.0

Generation of the particles by a VOAG are not sufficiently accurate to be able to quote the values to 2 decimal places therefore the raw data were rounded up to 1 decimal place. The mean diameters are quoted to 2 decimal places where appropriate. The particles are completely dry when entering the APS they are stable and so do not change in size therefore the quoted diameters are of a good accuracy.

The results are presented as graphs where appropriate discussions will indicate actual values. Graphs show actual data collected as scatter points and the mean value as a line through those points. Unfortunately the economic restrictions on this project allowed only one repeat calibration in each size range.

4.6.1 Mass percentage/particle MMAD for each stage

Figure 4.4. Graph showing mass percentage of Methylene Blue collected in the Throat.

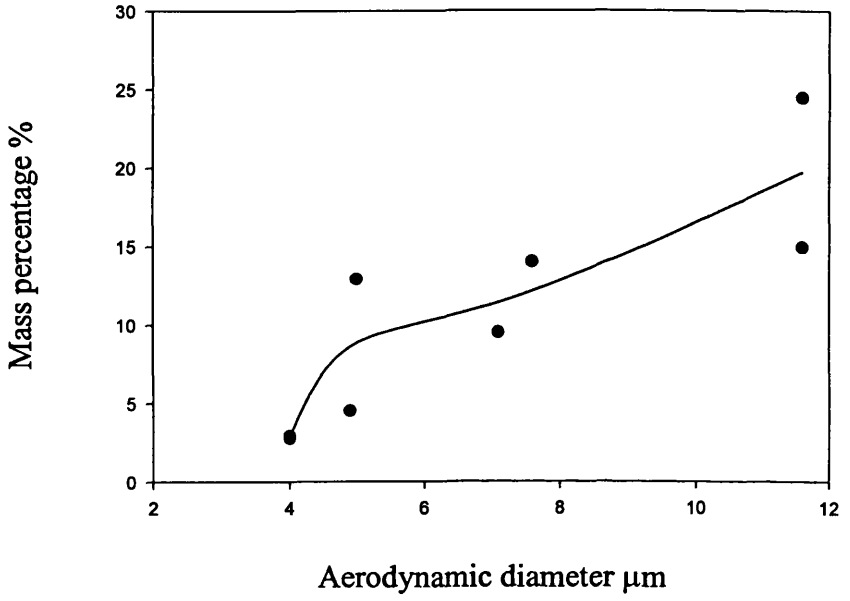

Figure 4.5. Graph showing mass percentage of Methylene Blue collected in the Bifurcation.

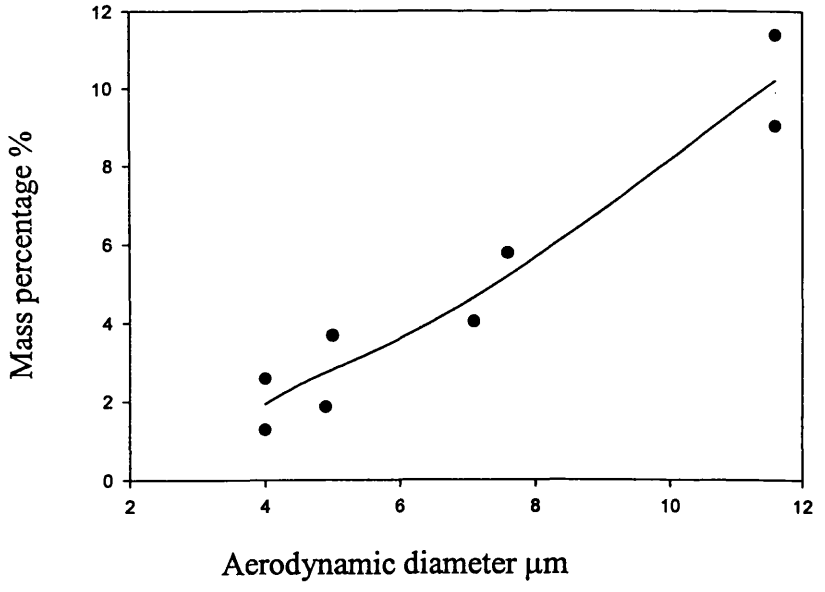

Figure 4.6. Graph showing mass percentage of Methylene Blue collected in the Throat and Bifurcation (Figures 4.4 and 4.5 combined).

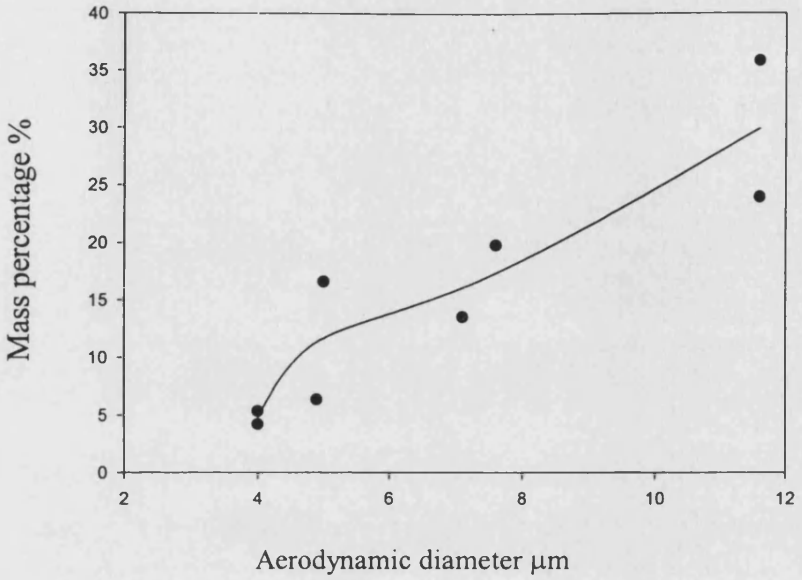

Figure 4.7. Graph showing mass percentage of Methylene Blue collected in Shell 1 and Shell 2.

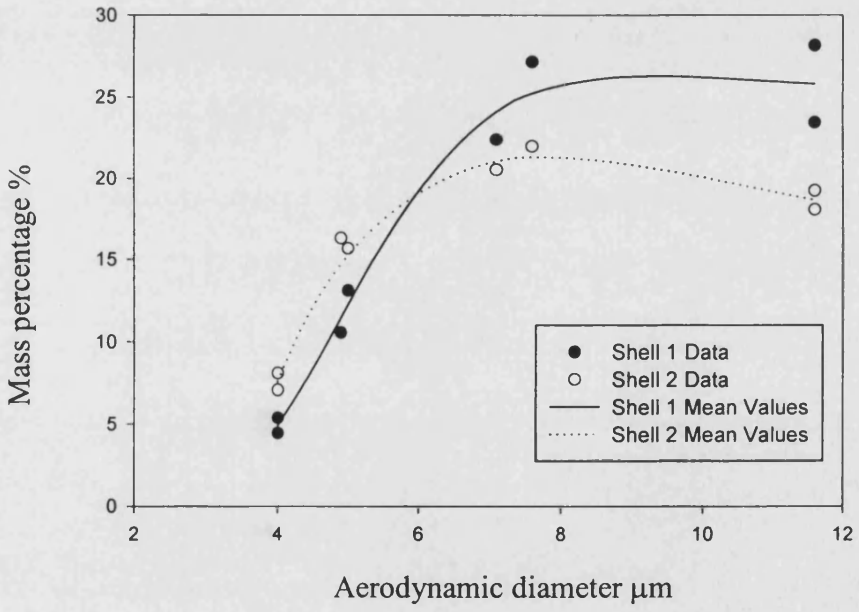

Figure 4.8. Graph showing mass percentage of Methylene Blue collected in Shell 3, Shell 4 and Shell 5

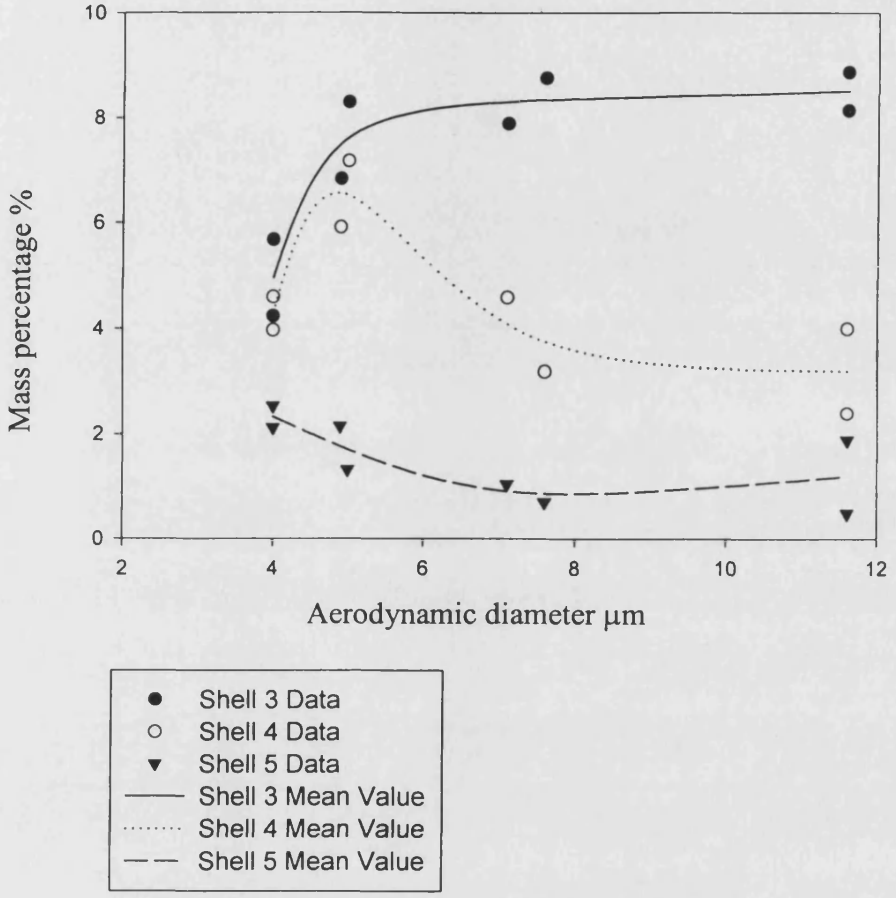

Figure 4.9 Graph showing mass percentage of Methylene Blue collected in the back plate.

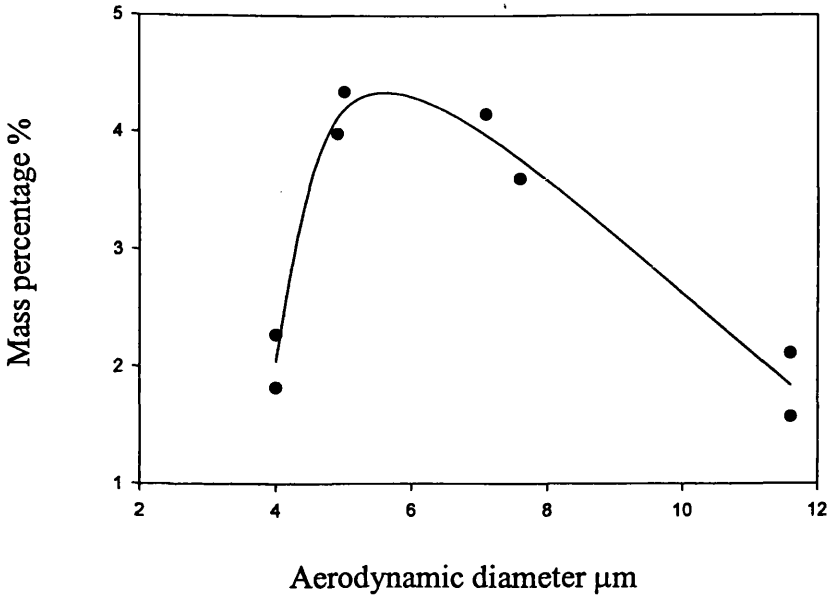

Figure 4.10 Graph showing mass percentage of Methylene Blue collected in the Filter.

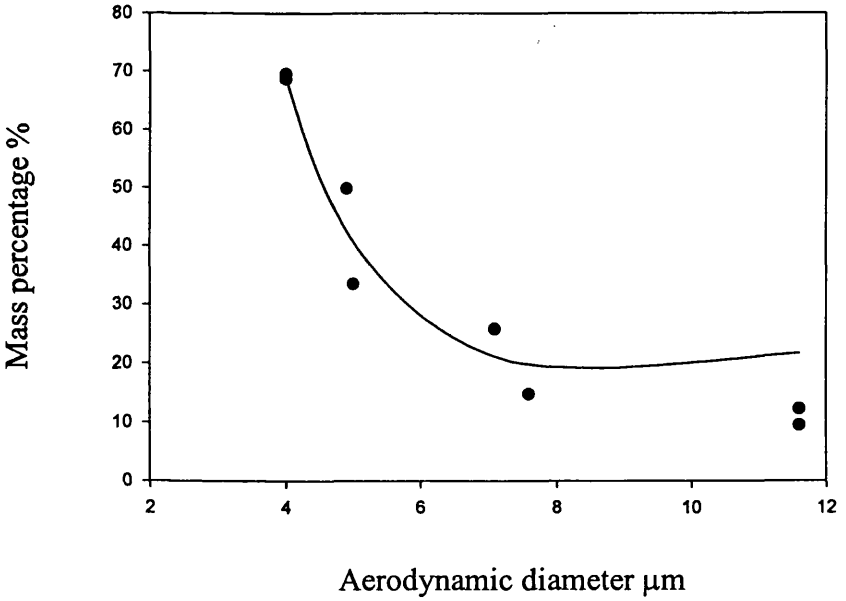

4.6.2 Collection efficiency/ particle MMAD for each stage

Collection efficiency was plotted against the aerodynamic diameter of the monodisperse particles generated and then tested in the SML. As discussed in section 1.6 the collection efficiency defines if impaction occurs and how the cut point curve fits the ideal cut point curve. If the graph passes through the 50% then it can be said that impaction occurs. The variation of the graph from ideal means particles that are undersize get collected and particles oversize will escape collection. Graphs show actual data collected as scatter points and the mean value as a line through those points.

Figure 4.11 Graph showing, collection efficiency in the Throat for monodisperse Methylene Blue particles.

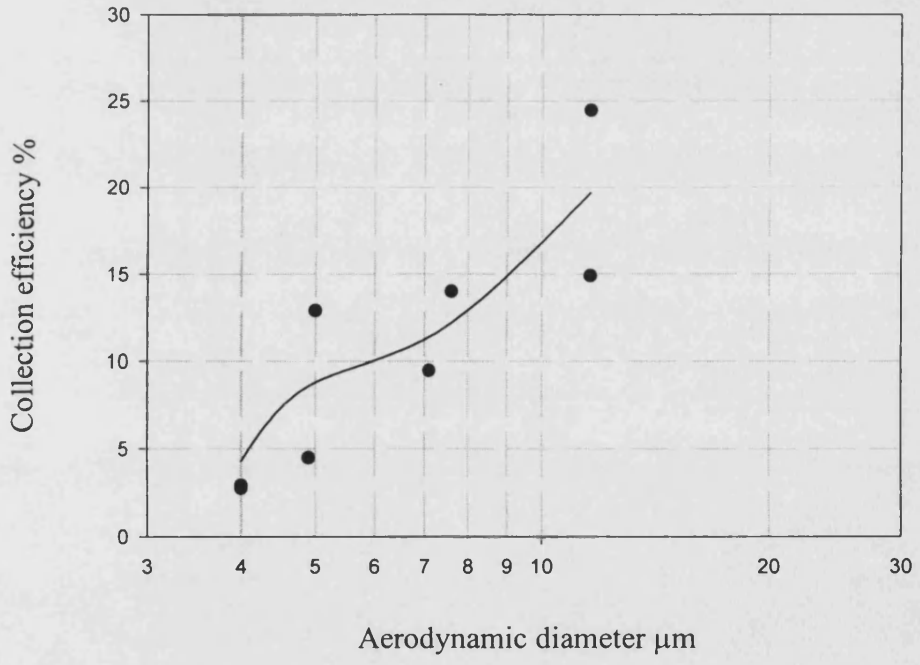

Figure 4.12 Graph showing, collection efficiency in the Bifurcation for monodisperse Methylene Blue particles.

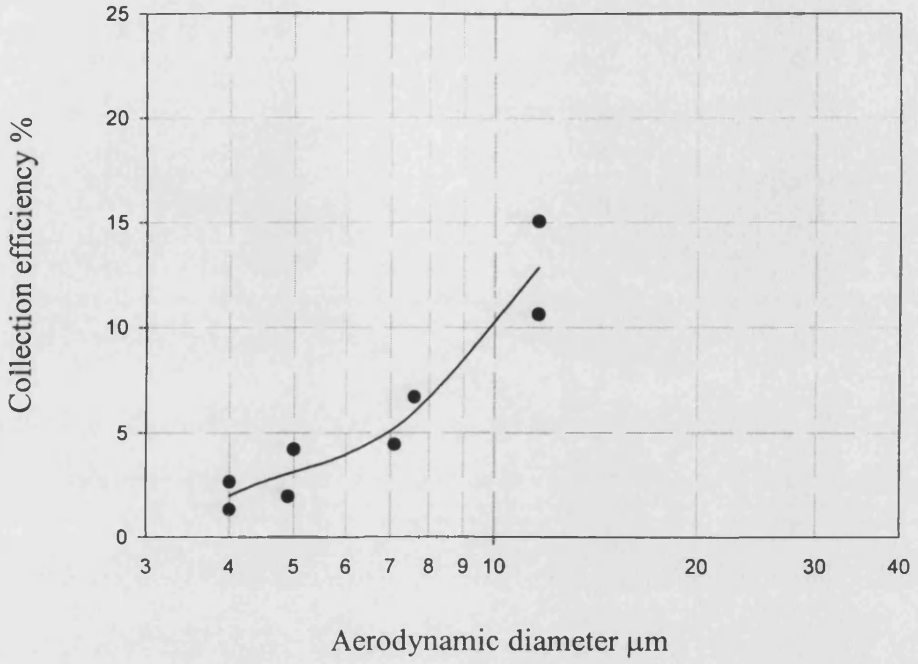

Even though the graphs presented in figures 4.11 and 4.12 above do not go through 50% it was calculated that the 50% cut point in the throat would be approximately 19μm. The following graph figure 4.13 presents the data for the throat and bifurcation together. The data was simply added together to give the collection efficiency for both regions. Throughout the results presented the throat and bifurcation were washed together and displayed as one stage.

Figure 4.13 Graph showing, collection efficiency in the Throat and Bifurcation for monodisperse Methylene Blue particles. (Data added together)

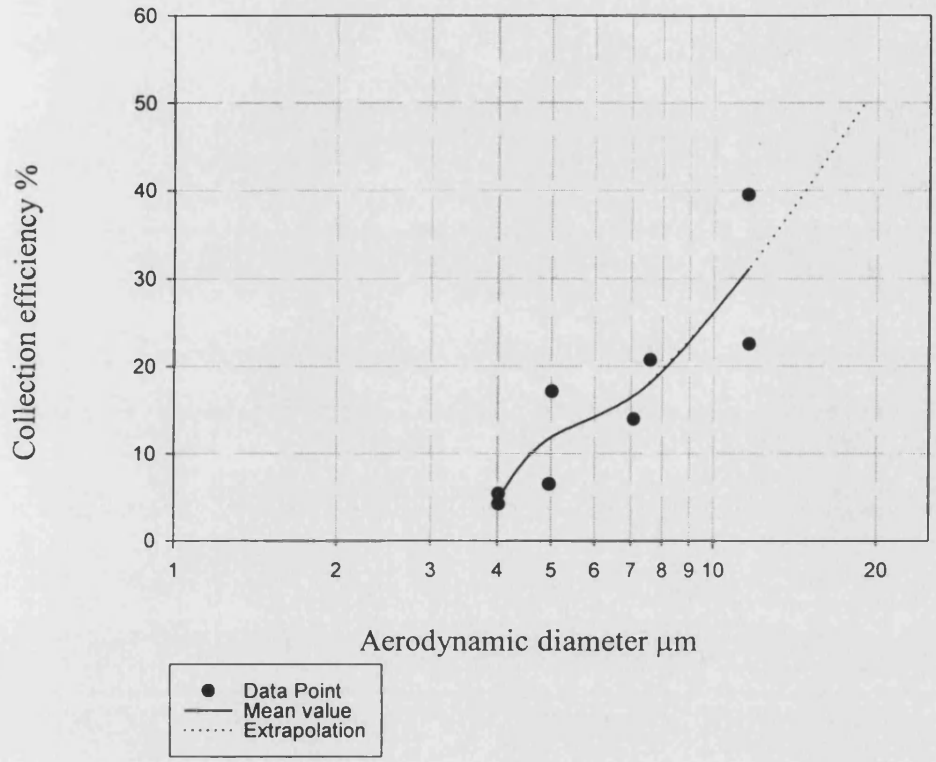

Further calibration must be performed before any such extrapolation can be said to be valid. The summed data when extrapolated shows a (theoretical) 50% cut point at 19μm. The cutpoint at the throat when testing a commercial inhaler depends very much upon the ballistic qualities of the aerosol cloud exiting the inhaler mouthpiece.

Figure 4.14 Graph showing, collection efficiency in the Shells for monodisperse Methylene Blue particles.

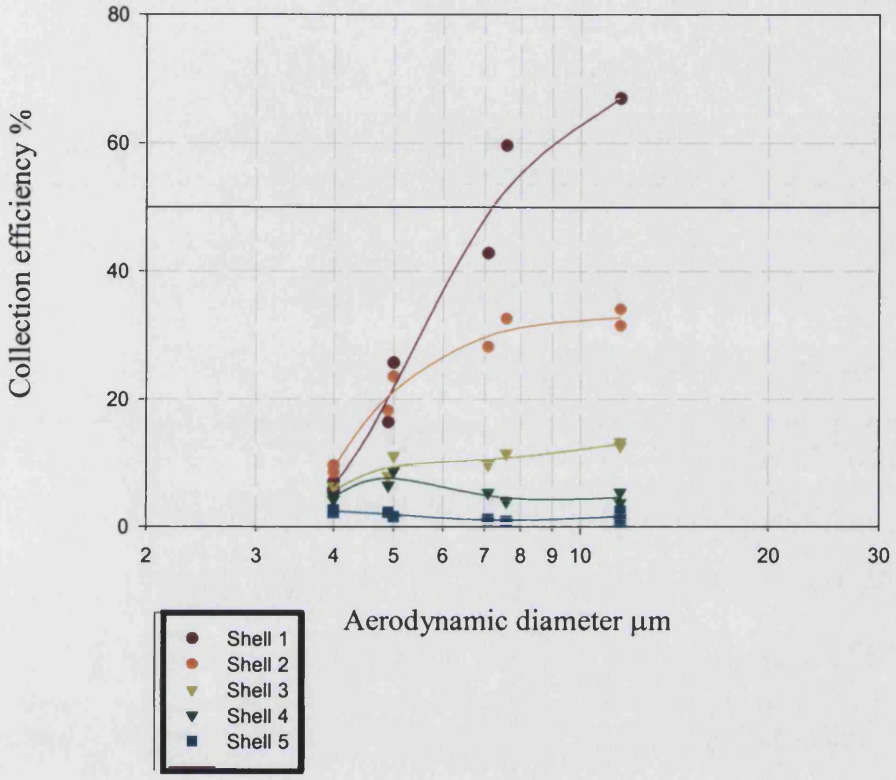

Discussion:

The collection efficiency curve for Shell 1 passes through the 50% value indicating that impaction is occurring. For a sharp cut off Hinds (1999) states that the Reynolds number should be between 500 and 3000 from equation (24) the calculated Reynolds number was found to be 3511. The theoretical value for the cut point was found to be 7.75µm. The experimentally determined cut point was 7.2µm. A number of factors contribute to this discrepancy. The shell acts as the collection site and as it contains holes much larger than the particles seen at this stage it is possible that they simply follow the airstream through the holes in the shell. Most of the particles collected on the back plate result from air

mixing as the jet from the bifurcation reaches Shell1. Due to the design of the model this is inevitable and further design modifications will be discussed in section 6.6.

The collection efficiency curves for Shell 2, Shell 3, Shell 4 and Shell 5 do not pass through the 50% value. It is clear that the shells are collecting particles but as this analysis only defines impaction the criteria is not met. The collection of particles may be taking place due to gravitational settling or diffusion.

Figure 4.15 Graph showing, collection efficiency for the Back Plate for monodisperse Methylene Blue particles.

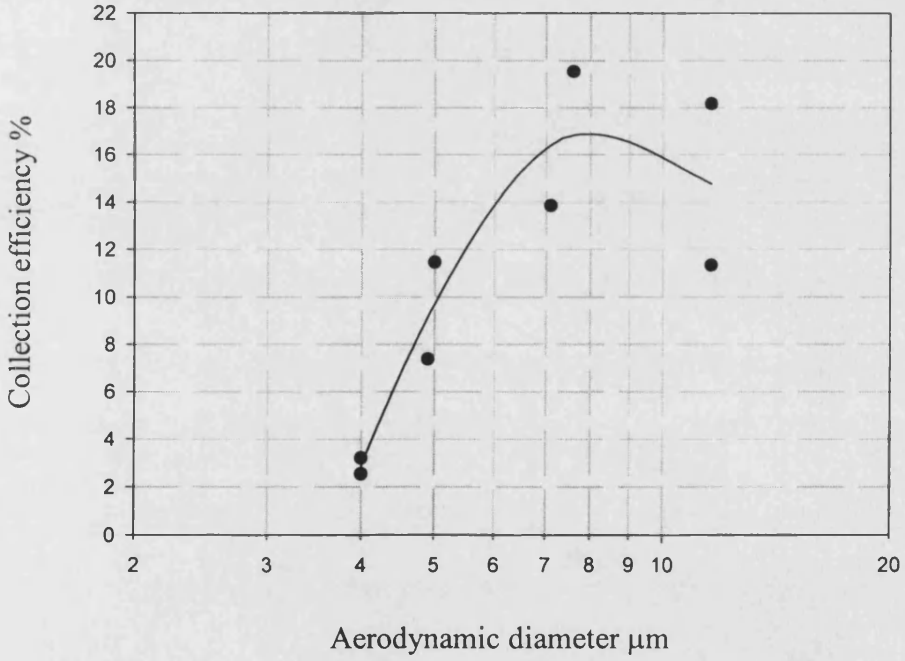

As previously discussed collection on the back plate is dependent on the air mixing or turbulence created from the air jet exiting the Bifurcation. Peak collection efficiency occurs at around 8μm when the flow rate is at 30 l min^{-1}. It would be expected that this value would increase at higher flow rates as the airflow becomes more turbulent in the shells.

4.7 General Discussion

The experimentally determined cutpoint at shell 1 (7.2μm) was found to be in good agreement with the calculated value (7.7μm and 10.2μm) (section 2.3.13 and 2.3.14). There are a number of possible reasons for the discrepancy:

- Geometric factors
    - Impaction onto a curved surface
    - Angle of flow from bifurcation
    - Direction of flow through the model
- Calculated Re could be less than actual Re
    - Discrepancies in model geometries
    - 'Roughness' inside bifurcation may increase turbulence
- High Re may result in errors
    - High turbulence and mixing may prevent impaction
    - Re>3000 therefore cutpoint dependent on Re (Marple *et al* 1998)

Although the model was not intended to collect particle by impaction it has been shown that this method of particle deposition does occur but only in Shell1.

It would have been interesting to calibrate the model at various flow rates. DPIs require greater inspiratory effort by the patient and current impactors were not designed to operate at such high flow rates (around 60 l min^{-1}). The Andersen cascade impactor has been modified to operate at 60 l min^{-1} (Nichols *et al.*, 1998) to give as good a range of cut points as the regular ACI by inserting a stage above stage 0 and removing stage 7. A low flow rate would be desirable to simulate the respiratory effort seen in infants, children and the severely respiratory impaired patient. A low flow rate version of the Marple-Miller impactor was devised (Olson *et al.*, 1998) to operate at 4.9 l min^{-1} or 12 l min^{-1}. It was found to be of a sufficiently high standard and met the objectives set out for the original impactor.

It is desirable for *in vitro* devices to be capable of performing well at several different flow rates so that the whole range of aerosol generating devices may be tested. In particular there are problems when sizing nebulised aerosols using impactors or impingers at their regular flow rates for particle sizing (Dennis, 1998 and Stapleton and Finlay, 1998). Using a 'breathing pattern' when calibration the SML would allow the device to be used for nebuliser testing. It may then be possible for the model to be used to assess environmental pollution.

The calibration has shown that the calculations used to determine the theoretical cut point were appropriate. Further calibration would be of great benefit however, economic and time constraints upon this work left little scope for improving the situation.

Chapter 5 Data collection and Results

5.1 Materials

This chapter describes the materials and methods used to characterise aerosol clouds. A summary of aerosol devices used and their contents is followed by a description of the analytical methods. The general methods for using both the Shell Model Lung and the Andersen Cascade Impactor are described here.

5.1.1 Formulations

Figure 5.1 Table of commercial products used

Product	Type	Drug	Batch / Expiry	Supplier
Ventolin	CFC MDI	Salbutamol	BN: M62 EXP: 05/2001	Allen & Hanburys Ltd Greenford, UB6 0HB.
Airomir	HFA MDI	Salbutamol	BN: 97102C EXP: 09/99	3M, 3M Healthcare Ltd, Loughborough, LE11 1EP.
Airomir	HFA MDI	Salbutamol	BN: 9BD028A EXP: 04/2002	3M, 3M Healthcare Ltd, Loughborough, LE11 1EP.
Ventolin Evohaler	HFA MDI	Salbutamol	BN: 10483695 EXP: 05/2000	Allen & Hanburys Ltd Greenford, UB6 0HB.
Bricanyl	CFC MDI	Terbutaline	BN: ZG 347 EXP: 07/2001	Astra Pharmaceuticals Ltd, Kings Langley Hertfordshire, WD4 8DH
Bricanyl	Turbuhaler	Terbutaline	BN: 351037F EXP: 05/2002	Astra Pharmaceuticals Ltd, Kings Langley Hertfordshire WD4 8DH.
Ventolin	Diskhaler	Salbutamol	BN: DO13788 EXP: 10/2003	Allen & Hanburys Ltd Greenford, UB6 0HB.

Each formulation was primed before use (5shots to waste) and weighed before, during and after each actuation.

5.1.2 Solvents

- Distilled water
- Methanol (washing and during VOAG) Supplier: BDH Laboratory Supplies, Poole, BH15 1TD.

5.1.3 Equipment

Compressor: Novair Compressor 88862 Type MK 3.500.80.35 Intrasurgical Ltd. Crane House, Gould Road, Twickenham, Middlesex TW2 6RS.

Pump: GAST, Model 1423 101Q Q626X. Benton Harbour M.I. USA.

Flow Meter: SCR2, Glass precision Ltd., UK.

Digital Flow Meter: Chell™ CPD 100 digital flow meter (Vectura Lab Meter 4 Serial Number: 00646 00001).

Filter paper: Gelman Sciences Type A/E Glass 76mm Lot: 80933. 600 South Wagner Road Ann Arbour Street Michigan 48106 USA.

5.2 Analytical techniques

5.2.1 Fluorimetry

Figure 5.2 Mechanisms of Fluorescence

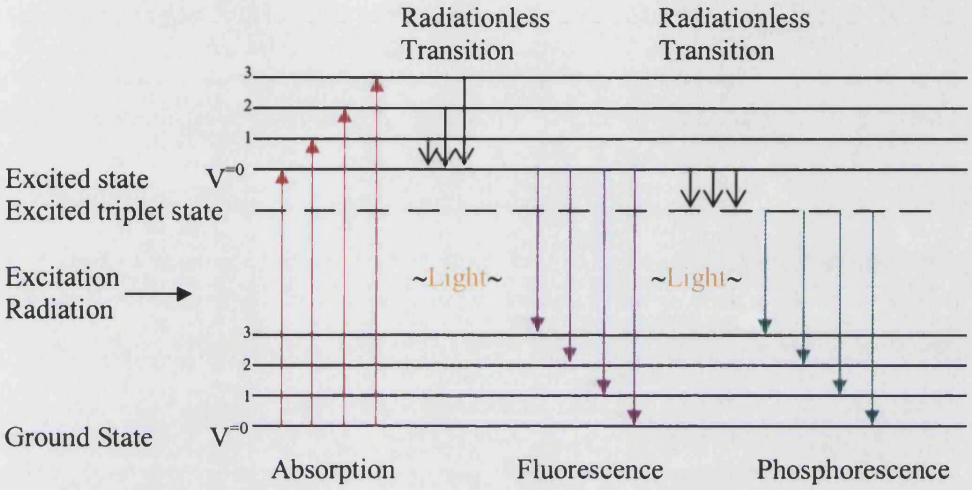

An organic molecule will absorb radiation of certain wavelengths to jump to an excited state. Some of the absorbed energy is lost on vibrational relaxation (radiationless transition to the lowest vibrational level take place in the excited state). The molecule eventually returns to the ground state and emits energy which; is termed "fluorescence". If radiationless transition to the triplet state takes place, the molecule emits optical energy when returning to the ground state. The optical energy emitted is termed "phosphorescence".

Phosphorescence persists for 10^{-4} seconds and fluorescence usually for 10^{-8} to 10^{-9} seconds.

The ratio of the optical energy absorbed by a substance to the total fluorescence energy emitted from the substance is called "quantum efficiency". Generally if a sample has high quantum efficiency it will have a high fluorescence emission.

For a dilute sample, the intensity of fluorescence is expressed by the following formula:

$$F = KI_0 c l \varepsilon \varphi \qquad (36)$$

F= intensity of fluorescence

K= instrumental constant

I_0= intensity of excitation radiation

c = concentration of substance

l = optical path length of cell

ε= absoptivity of substance

φ= quantum efficiency of substance

Analysis by fluorescence has advantages over absorption methods. If a sample has a transmittance of 99% and the blank has a transmittance of 100%, an error factor, which is unavoidable in absorbance measurement, must be considered in both cases. The error factor is 0.1%, therefore,

Transmittance of blank solution = $100.0 \pm 0.1\%$

Transmittance of sample = $99.0 \pm 0.1\%$

Difference = 1.0 ± 0.2% (value depending upon sample concentration)

In this example an error as high as ±20% is involved in the analysis of samples with low absorbance, as is the case for salbutamol.

In fluorescence analysis, differences from the zero level generally correspond to sample concentration, as follows,

Output signal level in sample measurement = 100 ±0.1

Value corresponding to blank = 0 ± 0.2

Difference = 100 ± 0.2 (proportional to sample concentration)

The examples show that fluorescence analysis is based upon principles that assure low error percentages even in the case of low concentrations. At very low concentrations error values are enhanced but it can still be said that fluorescence allows measurements of concentrations a factor of 10^{-3} below those measurable by the absorption method.

The analytical data obtained from an absorption spectrophotometer is the absorption spectra only however, in a fluorescence spectrophotometer an excitation and emission spectra are obtained.

There are some disadvantages associated with the use of fluorimetry; the intensities are reduced 1 to 2% as the sample temperature rises by 1°C. Certain samples are chemically affected by excitation light. Rayleigh scattering may appear at the same wavelength as

the excitation light, caused by electromagnetic radiation emitted from the particles' electrons. The electrons are in an intense alternating field caused by the electric and magnetic components of the radiation. Raman scattering appears at longer wavelengths, it occurs if one or more of the normal modes of vibration of a molecule involves changes in the polarizability. The scattered radiation contains this vibrational frequency superimposed upon the frequency of the incident radiation. Both forms of scattering appear on the spectra as peaks.

Samples of high concentrations are associated with various error factors:

- Excitation light is absorbed at the cell inlet, which prevents the excitation light reaching the cell centre.
- Molecules may interact causing "concentration extinction"
- The fluorescence may be reabsorbed if the excitation and emission wavelengths overlap

It is very important that the cell is not contaminated. It is possible that the sample may adhere to the wall of the cell and if not washed properly the cell will retain the sample.

To reduce the errors involved with fluorimetry, samples must be of a low concentration (typically 0.01 to 5.00 $\mu g\ ml^{-1}$). Each time the fluorimeter is switched on it must be calibrated, due to a small drift in the relative intensity value, unfortunately inherent in the equipment. The instrument was zeroed before each analysis this may further reduce any error.

5.3 Calibration work

Spectrofluorimeter conditions

Equipment: Hitachi, model F-2000 (251-0005) Fluorescence Spectrophotometer

Lamp: Hitachi Long –life Xenon lamp UXL-1157 583769

10mm quartz cell, Merck 307371401 Far U.V. silica – fluorescence.

The light source was allowed to stabilise for at least 20 minutes before the first sample was measured, after the instrument was calibrated the analysis of the samples could begin.

5.3.1 Salbutamol – instrument settings and appropriate results

Figure 5.3 Instrument settings for Salbutamol

Parameter		**Setting**
Wavelength	EX	273nm
	EM	309nm
Replicates		1
Initial delay		1s
Integration time		2s
Hi limit		800.0
Low limit		0.0
Unit label		$\mu g\ ml^{-1}$
Response		2s
Bandpass	EX	10nm
	EM	10nm
PM Voltage		400

Calibration of Salbutamol

Spectrofluorimetry was used as the method of analysis as it is more sensitive test than Ultra Violet (UV) analysis via High Performance Liquid Chromatography (HPLC) (as

discussed above) when analysing salbutamol. It is also a quicker less wasteful method than HPLC as no mobile phase or internal standard is necessary.

A calibration profile of salbutamol was undertaken to ensure experimental procedure was correct and a linear relationship between concentration and relative intensity of the signal occurred. Two stock solutions of around 50μg ml^{-1} were prepared, a series of dilutions were made to produce concentrations in the range of 0.5μg to 5μg. The instrument automatically produces a calibration curve and correlation coefficient to three decimal places. To check these values the data points were entered into Sigma Plot 4.0 (1997 SPSS Inc.) the graph package used throughout this work to check the linearity. As previously stated the spectrofluorimeter requires calibrating each time it is switched on, to ensure reproducibility it was necessary to achieve a calibration correlation coefficient of 0.999 read from the instrument. The instrument measures relative to the calibration curve. After the calibration procedure the instrument was blanked using the solvent then each unknown solution was tested and its relative intensity as calculated by the spectrofluorimeter was recorded. From this the percentage of drug delivered into the device was calculated.

Figure 5.4 Typical values when assaying Salbutamol using the method outlined above

Stock	Gradient		Intercept		r^2
	Mean Value	St Dev	Mean Value	St Dev	
Stock 1	58.05	0.212	9.525	0.672	0.9998
Stock 2	57.30	0.566	9.125	0.403	0.9997

5.3.2 Terbutaline – instrument settings and appropriate results

Figure 5.5 Instrument settings for Terbutaline

Parameter		Setting
Wavelength	EX	273nm
	EM	311nm
Replicates		1
Initial delay		1s
Integration time		2s
Hi limit		800.0
Low limit		0.0
Unit label		$\mu g\ ml^{-1}$
Response		2s
Bandpass	EX	10nm
	EM	10nm
PM Voltage		400

Figure 5.6 Typical values when assaying Salbutamol using the method outlined above

Stock	Gradient		Intercept		r^2
	Mean Value	St Dev	Mean Value	St Dev	
Stock 1	24.44	0.49	5.55	0.52	0.9997
Stock 2	25.02	0.33	4.45	0.66	0.9998

5.4 Statistical analyses

Throughout this work statistical comparisons were made between commercial inhalers and the properties of the SML. During the calibration work described above values of linearity were found in order to be confident of results collected. The sections below summarise the statistical models used (Weiss, 1995)

5.4.1 Standard deviation

Variations from the mean in a group of data are described by the standard deviation. It is calculated by:

$$s = \sqrt{\frac{n\sum x^2 - \left(\sum x\right)^2}{n(n-1)}} \qquad (37)$$

where:

s = standard deviation

n = sample size

The standard deviation of samples was found using Minitab 12.1.

5.4.2 Coefficient of determination (r^2)

The coefficient of determination describes for the purpose of the calibration work the accuracy of the standard solutions. r^2 describes how 'straight' a calibration curve was. After running the standard solutions on the fluorimeter the instrument drew a graph of

intensity against concentration. A 'calibration' function of the instrument then calculated the value of the coefficient of determination. The instrumental determination was used in each case after it was ensured (also using Minitab 12.1) to be at least 0.999.

5.4.3 Analysis of variance (ANOVA)

This statistical method can compare thee means of more than two sets of data. One-way ANOVA compares the means of populations with respect to one factor. Two-way ANOVA similarly compares the means with respect to two factors. Many values are calculated using this method, probably the most useful is the P value and to a lesser extent the F statistic. The method was carried out using Minitab 12.1

The P value is the probability of the populations being similar therefore the close the P value is to 0 the less likely the data are related.

The F statistic describes the variation between the sample means. Large F values show the population means are not equal

5.5 Experimental procedure – Shell Model Lung

5.5.1 Assembly of the incomplete SML

Filter: A filter was inserted into a filter holder on the inside of the cylinder over the outlet.

Bifurcation: The bifurcation was carefully screwed into the back plate, it was necessary to take care with this procedure as the metal can deform.

Shell 1: The bifurcation side of the model was rested on the bench and shell 1 was screwed into position into the back plate, the holes aligned in one orientation only which is clearly marked on each shell and on the back plate.

Shell 2: As above.

Shell 3: As above.

Cylinder: A filter was placed over the outlet hole in the interior of the cylinder the filter holder was firmly screwed into position keeping the filter in place. The cylinder was placed over the shells and screwed into the back plate.

Throat: Once the model was repositioned on its base a tight seal was made when the throat was pushed firmly onto the opening of the bifurcation.

Mouthpiece: A mouthpiece was then fitted to the inlet of the throat. It was ensured that for each type of device tested, a mouthpiece with a good tight fit was used.

5.5.2 Assembly of the SML

Filter: A filter was inserted into a filter holder (Pari) situated after the outlet pipe.

Bifurcation: The bifurcation was carefully screwed into the back plate, it was necessary to take care with this procedure as the metal can deform.

Shell 1: The bifurcation side of the model was rested on the bench and shell 1 was screwed into position into the back plate, the holes align in one orientation only which is clearly marked on each shell and on the back plate.

Shell 2: As above.

Shell 3: As above.

Shell 4: As above.

Shell 5: As above.

Throat: Once the model was repositioned on its base a tight seal was made when the throat was pushed firmly onto the opening of the bifurcation.

Mouthpiece: A mouthpiece was then fitted to the inlet of the throat. It was ensured that for each type of device tested, a mouthpiece with a good tight fit was used.

5.5.3 Settling time

Once the SML was assembled as described above a vacuum pump and timer device were fitted to the outlet pipe of the model. At this stage the flow rate was tested at the throat using a calibrated float type flow meter. A timer was set to the required time and the model was ready for aerosol delivery.

Each inhaler was delivered into the device according to the manufacturers instructions. Once the required amount of drug had been delivered into the SML a period of ten minutes was timed to allow any settling to take place then the device was dismantled. Ten minutes was found to be sufficient according to the Stokes settling rate (Hinds, 1999):

$$v = g\, a^2\, (\rho_1 - \rho_2)/18\eta \qquad (38)$$

Where:

v = rate of sedimentation ($m\ s^{-1}$)

a = particle radius (m)

ρ_1 = particle density ($kg\ m^{-3}$)

ρ_2 = density of the medium ($kg\ m^{-3}$)

g = gravitational constant ($m\ s^{-2}$)

η = viscosity of the dispersion medium ($N\ s\ m^{-2}$)

$$v = \frac{9.807 \times [(10 \times 10^{-6})^2] \times (10^3 - 1.205)}{18 \times (1.822 \times 10^{-5})} \qquad (39)$$

$$v = 3.0 \times 10^{-3}\ m\ s^{-1} \qquad (40)$$

This is equivalent to $3mm\ s^{-1}$, therefore in 10 minutes a particle 10μm in diameter would fall 1.8m over nine times the total height of the device. A particle of 1μm would

therefore fall 1.8cm in 10 minutes. The maximum distance between shells is 2cm for particles of 1μm 10 minutes was thought sufficient time to allow particle settling. Deposition on the model was analysed as follows.

5.5.4 Washing procedure – incomplete SML

Distilled water was used as the solvent for all washings for each inhaler device unless otherwise stated.

1. The cylinder was unscrewed and the filter holder removed. The interior of the cylinder was washed into a 100ml volumetric flask.
2. The filter was removed from the filter holder and placed into a beaker containing the solvent this was then sonicated for 2 minutes the filter and solvent washings were collected into a 100ml volumetric flask
3. The mouthpiece and device were both washed into a 250ml volumetric flask, if the inhaler device was not detachable then the mouthpiece was washed into a 100ml volumetric flask.
4. The throat was detached and washed then the bifurcation was unscrewed and washed both washings were collected into one 250ml volumetric flask
5. Shell 3 was unscrewed and placed into a large funnel and washed into a 100ml volumetric flask.
6. Shell 2 was unscrewed and placed into a smaller funnel and washed into a 100ml volumetric flask.

7. Shell 1 was unscrewed and placed into the smaller funnel and washed into a 100ml volumetric flask.
8. The back plate was then washed through the large funnel into a 50ml volumetric flask

5.5.5 Washing procedure - SML

Distilled water was used as the solvent for all washings for each inhaler device unless otherwise stated.

1. The filter was removed from the filter holder and placed into a beaker containing the solvent this was then sonicated for 2 minutes the filter and solvent were then washed into a 100ml volumetric flask
2. The mouthpiece and device were both washed into a 250ml volumetric flask, if the inhaler device was not detachable then the mouthpiece was washed into a 100ml volumetric flask.
3. The throat was detached and washed then the bifurcation was unscrewed and washed both were collected into one 250ml volumetric flask.
4. Shell 5 was unscrewed and washed into a 100ml volumetric flask.
5. Shell 4 was unscrewed and placed into the large funnel; the washing procedure was done with great care as the small holes in this shell caused the spray to misdirect on occasions. This shell was washed into a 50ml volumetric flask.
6. Shell 3 was unscrewed and placed into a large funnel and washed into a 100ml volumetric flask.

7. Shell 2 was unscrewed and placed into a small funnel and washed into a 100ml volumetric flask.
8. Shell 1 was unscrewed and placed into a small funnel and washed into a 100ml volumetric flask.
9. The back plate was then washed through a large funnel into a 50ml volumetric flask

After the washing procedure each stage of the model was rinsed in Methanol to ensure it was clean grease free and was then left to dry. The model was ready to reassemble once it was completely dry. Results chapter (5) illustrates the work done in the characterisation of various inhaler devices during this study. Where any methods were changed or slightly altered from that shown above they are clearly stated. As the model is a novel device it was sometimes necessary and interesting to investigate these alterations.

5.6 Experimental procedure - Andersen Cascade Impactor

5.6.1 Physical description

The Mark II ACI contains 8 stages it separates an aerosol cloud into discreet size fractions. Stages 0 and 1 both have 96 orifices arranged radially around the stage. These stages have collection plates containing holes of 22.2mm diameter in their centre to allow airflow through the centre. Stages 2 to 6 all have 400 orifices arranged in a circular pattern around each stage. Stage 7 contains 201 orifices again arranged radially around the stage. The collection plates of stages 2 to 7 have no holes in them. The collection plates sit on small props on the top of the stage directly below. This allows the air to flow around the collection plates and contributes to the separation mechanism (Graseby – Andersen Inc., 1985). The collection plates were at all times handled using tweezers.

5.6.2 Assembly

Filter: A filter was placed in the filter holder and an o-ring was positioned to hold the filter directly over the area of flow

Stage 7: A collection plate was placed on the filter holder and Stage 7 positioned above this.

Stages 6 to 0: These collection plates and stages were assembled as for Stage 7

Adapter: The adapter was fitted above Stage 0 and the closing springs were attached at the indented points.

Throat: A USP throat as specified was push-fitted onto the adapter.

Mouthpiece: A mouthpiece was then fitted to the inlet of the throat. It was ensured that for each type of device tested, a mouthpiece with a good tight fit was used.

5.6.3 Washing procedure

All washings for each inhaler device were done using distilled water as the solvent unless otherwise stated

1. The mouthpiece and device were both washed into a 250ml volumetric flask, if the inhaler device was not detachable then the mouthpiece was washed into a 100ml volumetric flask.
2. The throat was detached and washed then the adapter was removed from the impactor and washed both washings were collected into a 250ml volumetric flask.
3. Stage 0 was removed and washed its collection plate was the removed and washed, all washings were collected into a 100ml volumetric flask.
4. Stages 1 to 7 were washed according to the procedure outlined above in point 3.
5. The filter was removed from the filter holder and placed into a beaker containing the solvent this was then sonicated for 2 minutes the filter and solvent washings were collected into a 100ml volumetric flask.

After washing the impactor each component was rinsed with methanol to ensure it was clean and grease free. The ACI was then left to dry before reassembling.

5.7 Results

Throughout the work aerosol performance in the SML is described as the % Drug Recovered:

$$\% \text{ Drug Recovered} = \frac{\text{Mass of drug detected in stage(s) / } \mu m}{\text{Total mass of drug detected / } \mu m} \times 100 \qquad (41)$$

This equation was applied for each stage or interval as required. Aerosol performance in an ACI is described either as above for each stage or as the 'Fine Particle Fraction' FPF. It is convention to describe the FPF as the drug collected in stage 2 to filter, expressed as a fraction or mass of the dose as collected in the device (excluding the actuator and mouthpiece). Commercially available inhalers were used throughout the work as they are widely available and well characterised by both the manufacturer and in most cases by other researchers. The purpose of the results presented here is to compare the properties of the SML with the ACI when analysed under similar laboratory conditions.

In the majority of the work presented here metered dose inhalers were used to assess the SML. MDI's are widely prescribed, as they are relatively inexpensive and suitable for the majority of patients. The drug is formulated as a solution or suspension. The formulation may also contain solvents, cosolvents and propellants. Significant co-ordination problems for patient groups such as the elderly and children make this dosage form less acceptable. It is important that each actuation is well co-ordinated with the patients breathing or the dose may not be inhaled fully or even at all. It was shown that

in an *in vitro* model (Gradon, 2000) perfectly synchronised actuation and inspiration leads to better 'tracheal' penetration by particles (<100μm).

For improved patient co-ordination Easi Brethe™ devices may be used, these self-actuate when the patient's inspiratory effort is at an optimum point. The devices were found to improve particle deposition after the model trachea in Gradon's *in vitro* device (Gradon, 2000) in comparison with MDI's. It is though this would be due to better co-ordination, as the device is not reliant on patient thought and action just patient breathing. The Easi Brethe™ device was not investigated.

The propellants traditionally used in MDI's were chlorofluorocarbons (CFC's); these chemicals are responsible for the depletion of the ozone layer. More than 100 countries that signed the Montreal Protocol have banned the production of CFC's. The new propellants used in MDI's are hydrofluoroalkanes (HFA's) (Hickey, 1992). Some problems including loss of internal pressure, leakage of the propellant, poor solvency properties and patents on new technologies (Howlett, 1998) are obstacles, these have been overcome by the development or the first HFA inhaler Airomir™ (Leach, 1996) a formulation containing salbutamol.

5.8 Initial 'incomplete' model

5.8.1 Airomir at 30 l min^{-1}

A comparison of intra-batch variability of Airomir™ was undertaken. The incomplete SML was used to test six cans. The cans of Airomir™ were taken from the same batch and tested at 30 l min^{-1} and 60 l min^{-1}. In each case 10 actuations were used to load the incomplete SML. The experiment was carried out as described in section 5.4.1 and 5.4.4.

Figure 5.7 Percentage drug recovered in the incomplete SML tested at 30 l min^{-1} using Airomir (n=9, errors are s.d.)

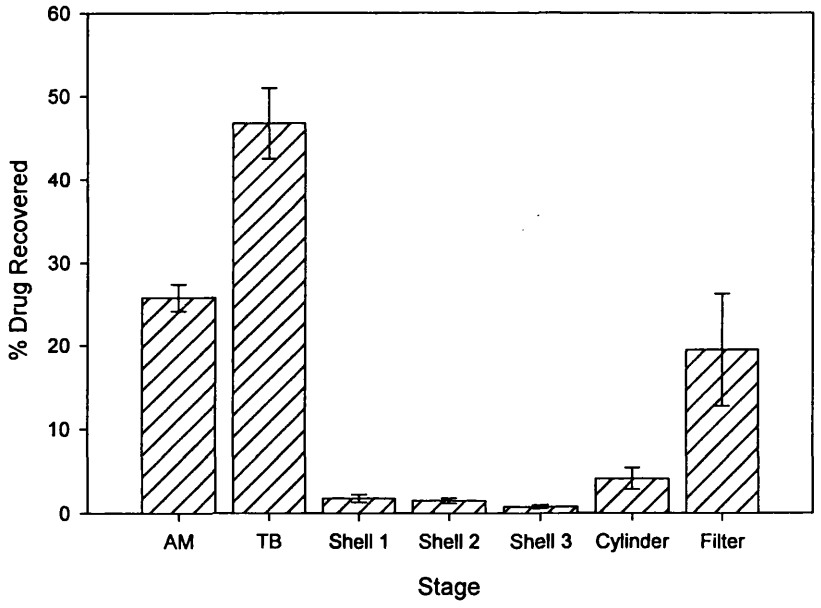

Figure 5.8 Percentage drug recovered in the shells and cylinder incomplete SML tested at 30 l min^{-1} using Airomir (n=9, errors are s.d.)

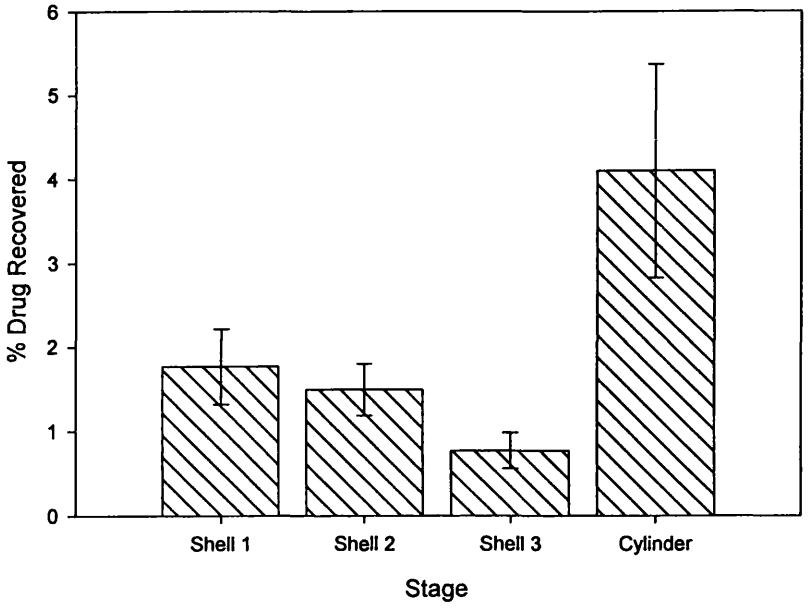

Figure 5.9 Percentage drug recovered in the incomplete SML tested at 30 l min^{-1} using Airomir™ (n=9, errors are s.d.)

Stage	% Drug Recovered	s.d.
AM	25.7	1.6
TB	46.7	4.2
Shell 1	1.8	0.4
Shell 2	1.5	0.3
Shell 3	0.8	0.2
Cylinder	4.1	1.3
Filter	19.4	6.7

Discussion:

Over 72% of the recovered drug was retained in the actuator mouthpiece and throat. The total amount of drug recovered in the shells and cylinder (figure 5.7) was 8.2%. Unfortunately 19.4% of the recovered drug was found in the filter. The problem here seems to be that a great deal of drug is being carried through the entire model without much aerosol cloud separation in the shells.

To improve the performance of the model it was decided to run the vacuum pump at 60 l min^{-1}. This increase in flow should have the effect of increasing the momentum of each particle in the aerosol cloud. Assuming that deposition by impaction takes place in some stages of the model, deposition should increase, favourably altering the deposition profile.

5.8.2 Airomir at 60 l min^{-1}

Figure 5.10 Percentage drug recovered in the incomplete SML tested at 60 l min^{-1} using Airomir (n=6, errors are s.d.)

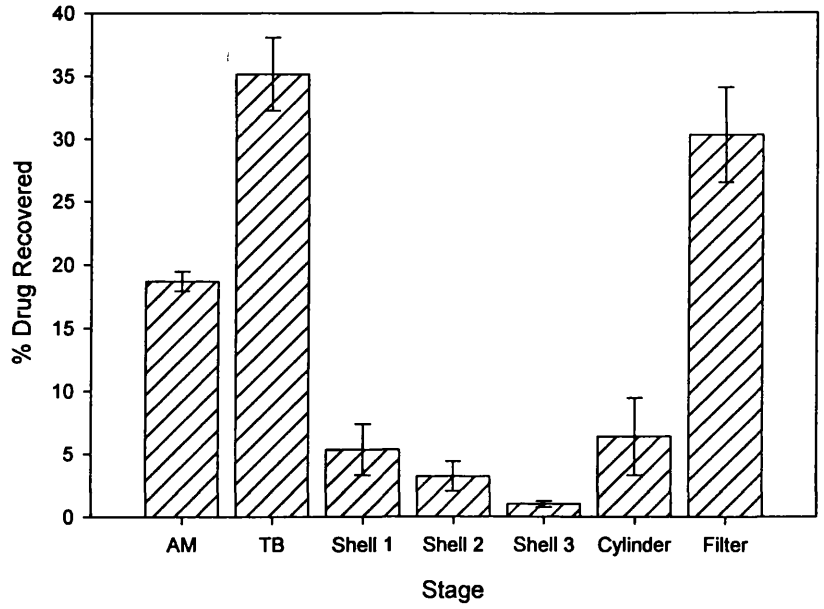

Figure 5.11 Percentage drug Recovered in the shells and cylinder of the incomplete SML tested at 60 l min^{-1} using Airomir (n=6, errors are s.d.)

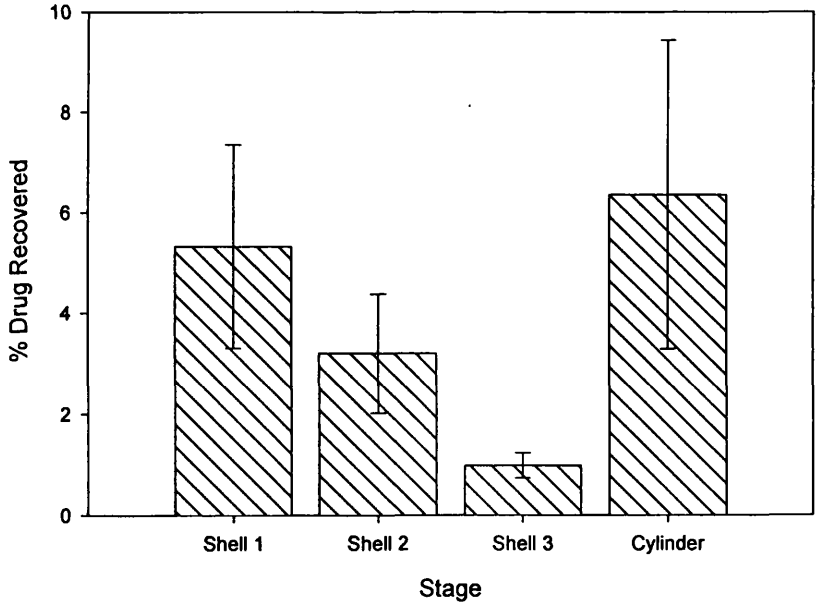

Figure 5.12 Percentage drug recovered in the incomplete SML tested at 60 l min^{-1} using Airomir™ (n=6, errors are s.d.)

Stage	% Drug Recovered	s.d.
AM	18.7	0.8
TB	35.2	2.9
Shell 1	5.3	2.0
Shell 2	3.2	1.2
Shell 3	1.0	0.2
Cylinder	6.4	3.1
Filter	30.3	3.8

Discussion:

Over 50% of the recovered drug was left in the actuator, mouthpiece and throat. This is an improvement on the situation at 30 l min^{-1}. The aerosol cloud was deposited in the shells and cylinder region more effectively at this flow rate. The total % drug recovered in the shells and cylinder was 15.9%. However, the increase flow rate seems to have made a marked difference to the quantity of drug pulled through the model and deposited onto the filter. The problems encountered at the previous flow rate have become worse as have the errors associated with drug deposition. Although the drug collected in the shells and cylinder has increased the drug collected by the filter should have decreased if all the shells were acting as an impaction collecting system. The drug particles seem to have been pulled directly through the model without having the chance to deposit by other mechanisms as a result of the higher flow rate. An assessment of the performance of a Ventolin™ MDI was then made at the higher flow rate to compare the findings with the investigation discussed here.

5.8.3 Ventolin at 60 l min^{-1}

An experiment was carried out to assess the qualities of Ventolin™ in the incomplete SML. The procedure outlined in section 5.4.1 and 5.4.4 was followed.

Figure 5.13 Percentage drug recovered for each Stage of the incomplete SML at 60 l min^{-1} (n=5 and errors are s.d.)

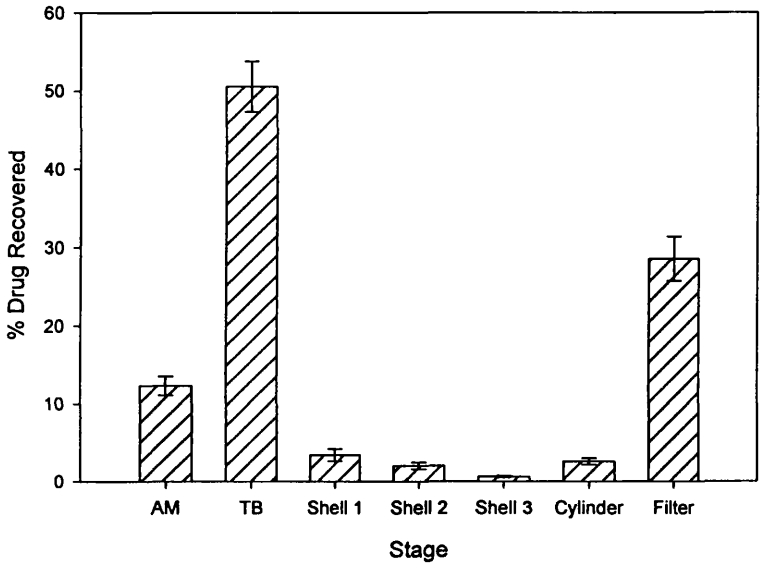

Figure 5.14 Percentage drug recovered in the shells and cylinder of the incomplete SML tested at 60 l min^{-1} using Ventolin™ (n=5, errors are s.d.)

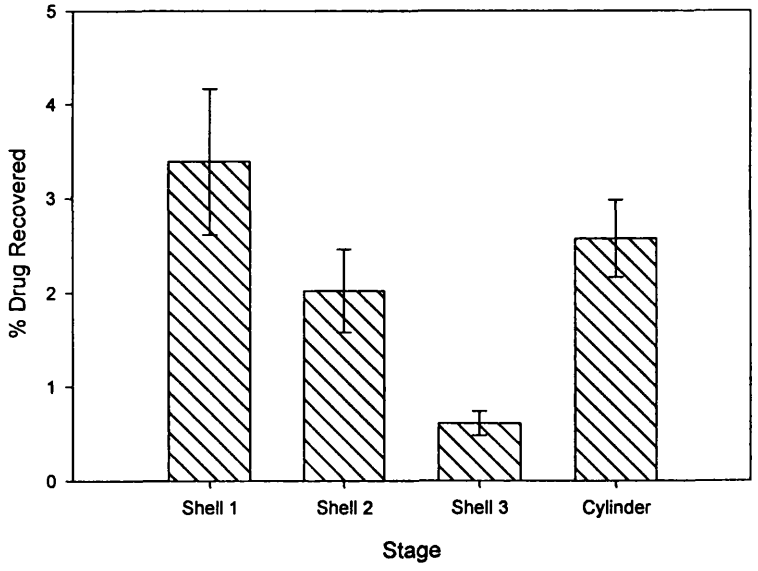

Figure 5.15 Percentage drug recovered in the incomplete SML tested at 60 l min^{-1} using Ventolin™ (n=5, errors are s.d.)

Stage	% Drug Recovered	s.d.
AM	12.3	1.2
TB	50.6	3.2
Shell 1	3.4	0.8
Shell 2	2.0	0.4
Shell 3	0.6	0.1
Cylinder	2.6	0.4
Filter	28.5	2.8

Discussion:

Less drug has reached the shells with the Ventolin™ formulation than the Airomir™ MDI. This implies that the formulation contains coarser particles that have been deposited by impaction (in the throat).

The total % drug recovered in the shells and cylinder was 8.6%. A large percentage of drug was also being recovered from the filter with this formulation.

The large deposition of drug in the filter seen here gave an ideal opportunity to investigate if distilled water or methanol would be a better solvent using this formulation at this flow rate.

5.8.4 Suitability of solvents

The experiment was carried out as in section 5.4.1 and 5.4.4 apart from when the washing procedure was undertaken the solvents used were, distilled water only, distilled water for the metal parts and methanol for the filter and methanol only. This investigation was undertaken to establish whether methanol would be a more suitable solvent for washing the SML to remove deposited salbutamol and if the benefits would outweigh the expense and waste management problems associated with methanol.

Figure 5.16 Percentage drug recovered in the outer stages of the incomplete SML tested at 60 l min^{-1} using Ventolin™ (lot: M62 exp: 05-2001) when washed using;

1. Distilled water only,
2. Distilled water for the metal parts and methanol for the filter and
3. Methanol only

(n =3 for each solvent combination errors are s.d.).

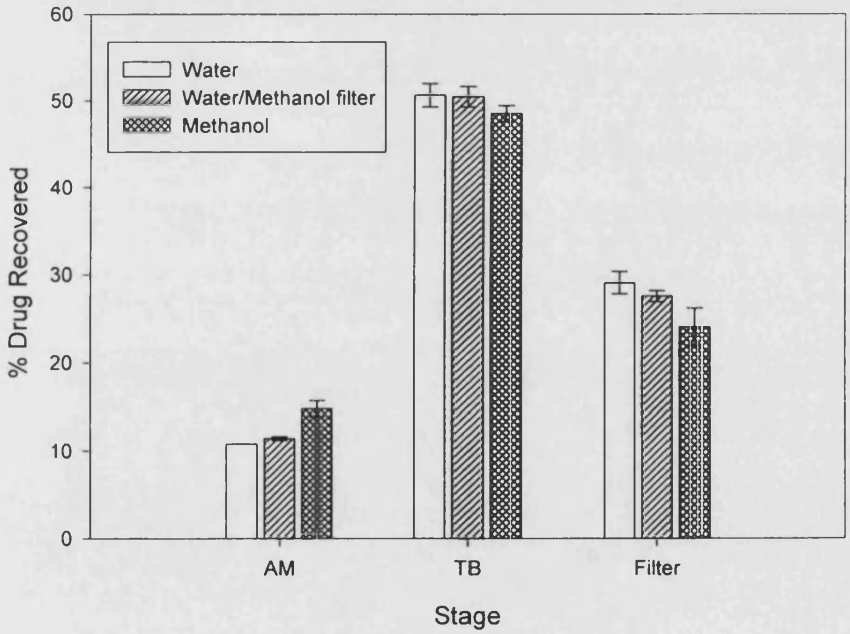

Figure 5.17 Percentage drug recovered in the shells and cylinder of the incomplete SML tested at 60 l min^{-1} using Ventolin (lot: M62 exp: 05-2001) when washed using;

1. Distilled water only
2. Distilled water for the metal parts and methanol for the filter
3. Methanol only

(n =3 for each solvent combination errors are s.d.).

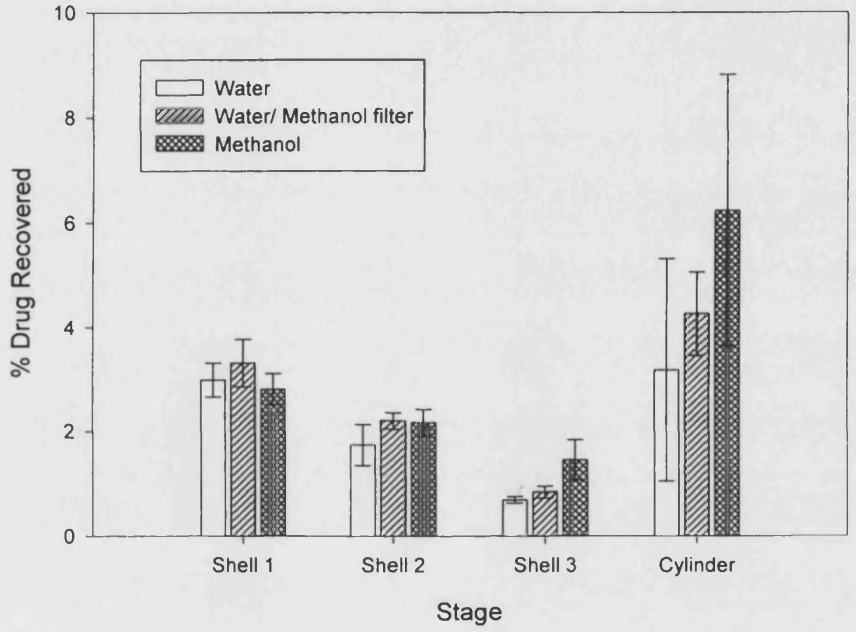

Figure 5.18 Percentage drug recovered in the incomplete SML tested at 60 l min^{-1} using Ventolin™ (n=3 for each solvent, errors are s.d.)

	% Drug Recovered for stated Solvent					
Stage	1.Water	s.d.	2. Water/Methanol	s.d.	3. Methanol	s.d.
AM	10.8	0.0	11.4	0.2	14.8	0.9
TB	50.6	1.3	50.5	1.2	48.5	0.9
Shell 1	3.0	0.3	3.3	0.5	2.8	0.3
Shell 2	1.7	0.4	2.2	0.2	2.2	0.3
Shell 3	0.7	0.1	0.8	0.1	1.4	0.4
Cylinder	4.1	2.1	4.3	0.8	6.2	2.6
Filter	29.1	1.3	27.6	0.6	24.0	2.1

Discussion:

The filter was chosen as the experimental focus of this investigation as the model was manufactured from aluminium and the filter was glass fibre (the mouthpiece was made of silastic rubber but did not retain as high a percentage dose as the filter).

Using one way Analysis of Variance the stages displaying significantly different (specified significance level 0.05) % drug recovered data were:

AM: (P <0.001) the complexity of the actuator design probably retains a small amount of the drug. Methanol has a lower surface tension than water (22.6mN m^{-1} vs. 72.7mM m^{-1} both at 20^0C) so the solvent may be able to rinse around the obstacles in the actuator more effectively.

Shell 3: (P = 0.017) the % drug recovered from shell 3 was very small so the effect is less meaningful however, it may be due again to the lower surface tension of methanol and its ability to recover any drug deposited around the entrance or exit of a hole in shell 3.

Filter: (P = 0.015) when the filter was washed in methanol it appears that the recovered

drug has decreased when in fact the case is that the total drug recovered from the model by weight increased so the % drug recovered from the filter is less than in the previous cases. It was decided that the cost of using methanol was too high to use the solvent routinely.

At this stage of experimentation the SML was completed and so the following results are for the completed 5 Shell Model Lung. A brief report of experimentation comparing the use of an MDI alone and an MDI used with a spacer device (Volumatic™) may be found in Appendix B, Ms J Au-Yung performed the work (under personal direction at all times) for her B. Pharm. final year project

5.9 SML MDI Formulations comparisons

5.9.1 At 30 l min^{-1}

Using the SML MDI formulations of Ventolin™, Ventolin Evohaler ™ and Airomir ™ were assessed in the SML. The experiment was carried out as stated in section 5.4.2 and 5.4.5. Comparisons were made to investigate the formulations' performance in the SML under similar laboratory conditions.

Figure 5.19 Percentage drug recovered for each formulation in the outer stages of the SML flow rate at 30 l min^{-1} (n=3 in each case errors are s.d.)

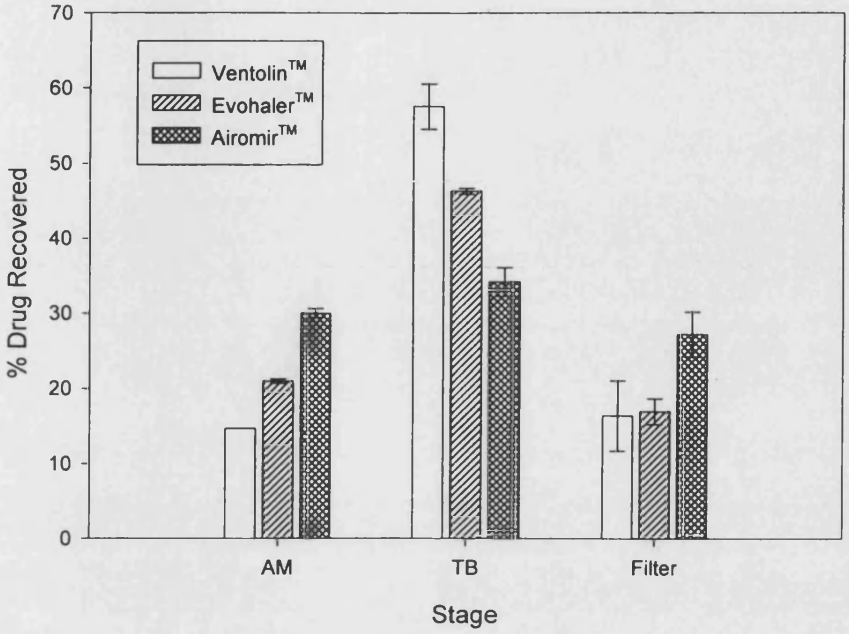

Figure 5.20 Percentage drug recovered for each formulation in the inner stages of the SML flow rate at 30 l min^{-1} (n=3 in each case errors are s.d.)

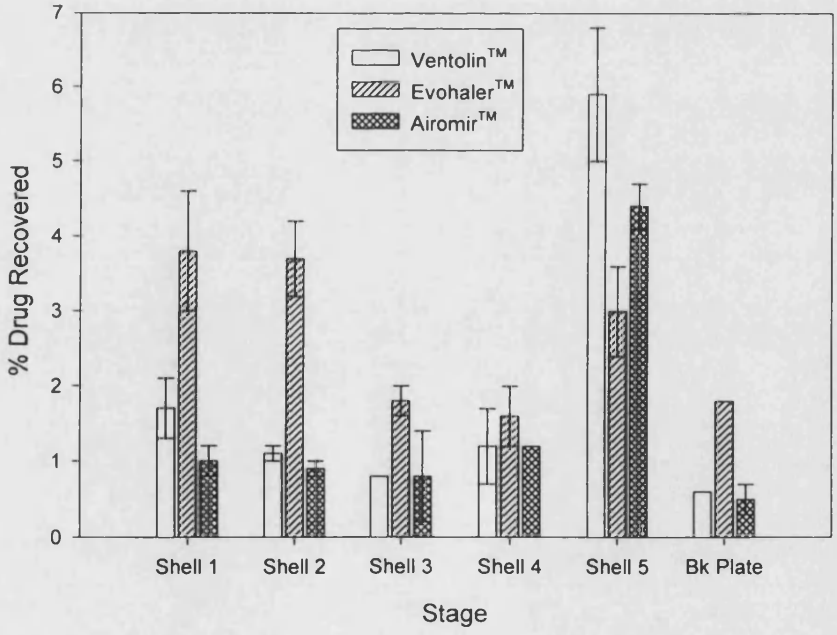

Figure 5.21 Percentage drug recovered in the SML tested at 30 l min^{-1} using Ventolin™ Evohaler™ and Airomir™ (n=3 for each formulation, errors are s.d.)

	% Drug Recovered					
	Ventolin		Evohaler		Airomir	
Stage	Mean	s.d.	Mean	s.d.	Mean	s.d.
AM	14.7	0.0	21.0	0.3	30.0	0.6
TB	57.5	3.0	46.3	0.4	34.2	1.9
Shell 1	1.7	0.4	3.8	0.8	1.0	0.2
Shell 2	1.1	0.1	3.7	0.5	0.9	0.1
Shell 3	0.8	0.0	1.8	0.2	0.8	0.6
Shell 4	1.2	0.5	1.6	0.4	1.2	0.0
Shell 5	5.9	0.9	3.0	0.6	4.4	0.3
Bk Plate	0.6	0.0	1.8	0.0	0.5	0.2
Filter	16.4	4.7	17.0	1.7	27.2	3.0

Discussion:

Ventolin™ deposited over 70% of the recovered drug in the actuator, mouthpiece and throat regions. The percentage drug deposited in the shells (including back plate as this is considered to be part of the 'inner structure' even though the collected drug was low) was 11.3%. The filter collected 16.4% an improvement on the situation seen in the incomplete SML at 60 l min^{-1}. It is possible that the more compact nature of the model, the extra shells and most certainly the lower flow rate has affected the fluid dynamics through the device and so a difference should have been expected anyway.

Evohaler™ also deposits 67% of its recovered drug in the actuator mouthpiece and throat region. The total drug collected in the shells (including the back plate) was 15.7% and 17% of the recovered drug was found in the filter.

Airomir™ had the least recovered drug in the actuator, mouthpiece and throat regions at 64.2%. The total drug collected in the shells (including back plate) was 8.8%. The percentage of drug recovered on the filter was 27.2%. The filter collection was very high and comparable to the filter deposition seen in the incomplete SML when tested at 60 l min^{-1}.

The deposition profiles of all three formulations are very interesting. The general pattern of deposition seen in the shells for Ventolin™ and Airomir™ are quite similar. Evohaler™ however, appears to deposit more evenly throughout the shells. The rise in deposition over the five shells and the high deposition of drug in the filter for Airomir suggests that this formulation contains the finest particles of the three tested here.

5.9.2 At 60 l min^{-1}

Using the SML MDI formulations of Ventolin™, Ventolin Evohaler ™ and Airomir ™ were assessed in the SML. The experiment was carried out as stated in section 5.4.2 and 5.4.5

Figure 5.22 Percentage drug recovered for each formulation in the outer stages of the SML flow rate at 60 l min^{-1} (n=3 in each case errors are s.d.)

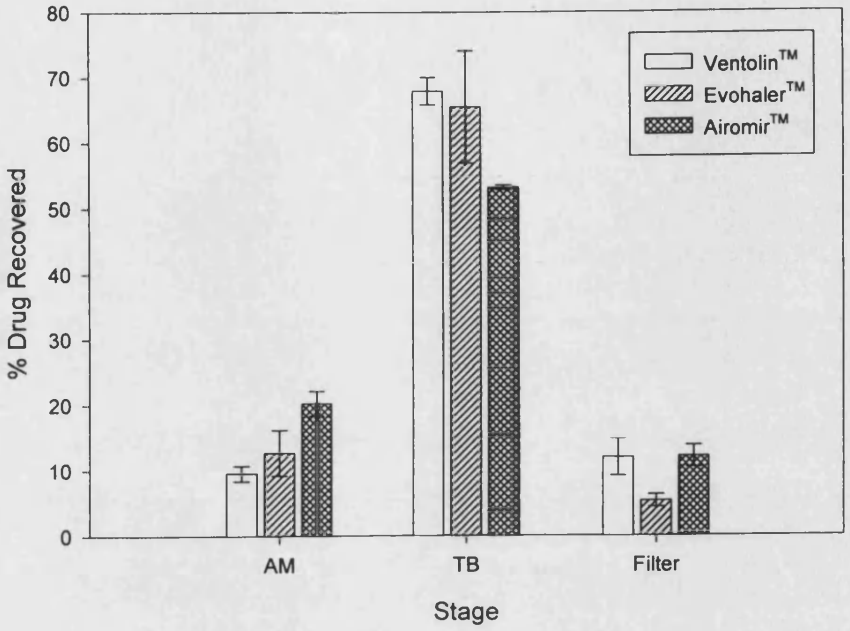

Figure 5.23 Percentage drug recovered for each formulation in the inner stages of the SML flow rate at 60 l min^{-1} (n=3 in each case errors are s.d.)

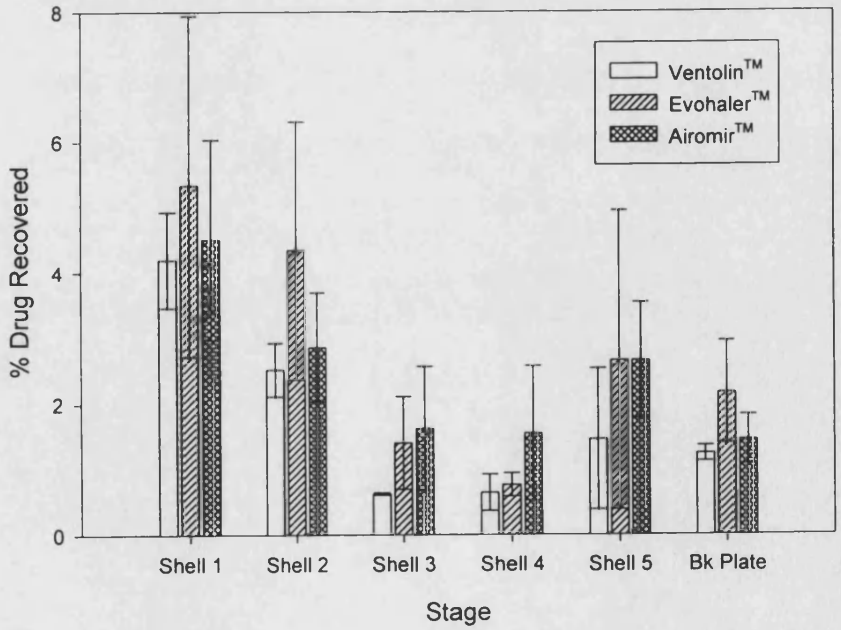

Figure 5.24 Percentage drug recovered in the SML tested at 60 l min^{-1} using Ventolin™ Evohaler™ and Airomir™ (n=3 for each formulation, errors are s.d.)

	% Drug Recovered					
	Ventolin		Evohaler		Airomir	
Stage	Mean	s.d.	Mean	s.d.	Mean	s.d.
AM	9.5	1.2	12.6	3.5	20.2	1.9
TB	67.9	2.1	65.4	8.6	53.1	0.4
Shell 1	4.2	0.7	5.3	2.6	4.5	1.5
Shell 2	2.5	0.4	4.3	2.0	2.9	0.8
Shell 3	0.6	0.0	1.4	0.7	1.6	1.0
Shell 4	0.6	0.3	0.8	0.2	1.5	1.0
Shell 5	1.5	1.1	2.7	2.3	2.7	0.9
Bk Plate	1.2	0.1	2.2	0.8	1.5	0.4
Filter	11.9	2.8	5.3	1.0	12.0	1.7

Discussion:

Ventolin™ drug deposition in the actuator, mouthpiece and throat regions was 77.4% of the recovered dose. The percentage drug recovered in the shells (including the back plate) was 10.6% a decrease at the higher flow rate. The drug recovered from the filter was 11.9% at 60 l min^{-1} at 30 l min^{-1} it was 16.4%.

The Evohaler™ percentage deposition in the actuator, mouthpiece and throat regions was 78%. The deposition seen in the shells (including the back plate) was 16.7% a slight increase at the higher flow rate. The percentage drug recovered in the filter was only 5.3%.

Airomir™ had a similar percentage drug recovery in the actuator, mouthpiece and throat region as the other two formulations at 73.3%. The drug recovery in the shells (including

the back plate) almost doubled at the higher flow rate to 14.7% (from 8.8%). The filter percentage drug recovery more than halved in value from 27.2% to 12% at 60 l min^{-1}.

The errors associated with the results here are in part due to the fact that as flow rate increases turbulent flow becomes more prominent and makes particle deposition less predictable. The errors used are the standard deviation which although should generally not be used for such a small sample, it gives an idea of the repeatability of the experimental procedure.

It can be seen that the profiles in the shells of the three formulations has altered, it appears that the pattern of deposition has shifted towards the inner shells (shell 1 and 2). The filter deposition has decreased and the deposition in the throat and bifurcation region has increased for each formulation.

5.10 Andersen Cascade Impactor MDI Formulation comparisons

These experiments were performed to assess the difference between the formulations. It is possible as discussed to analyse the formulations using the ACI and gain valuable data about the formulation properties.

5.10.1 Ventolin™

Using the ACI MDI formulations of Ventolin™, Ventolin Evohaler ™ and Airomir ™ were assessed. The experiment was carried out as stated in sections 5.5.2 and 5.5.3.

Figure 5.25. Percentage drug recovered for Ventolin™ in the inner stages of the ACI, flow rate at 28.3 l min^{-1} (n=6)

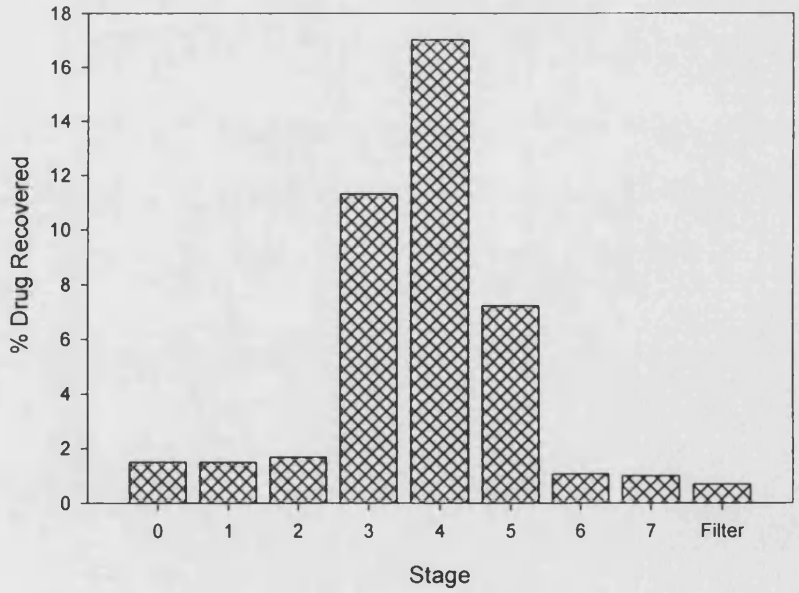

Figure 5.26 Complete Ventolin™ ACI data (28.3 l min^{-1}, n=6)

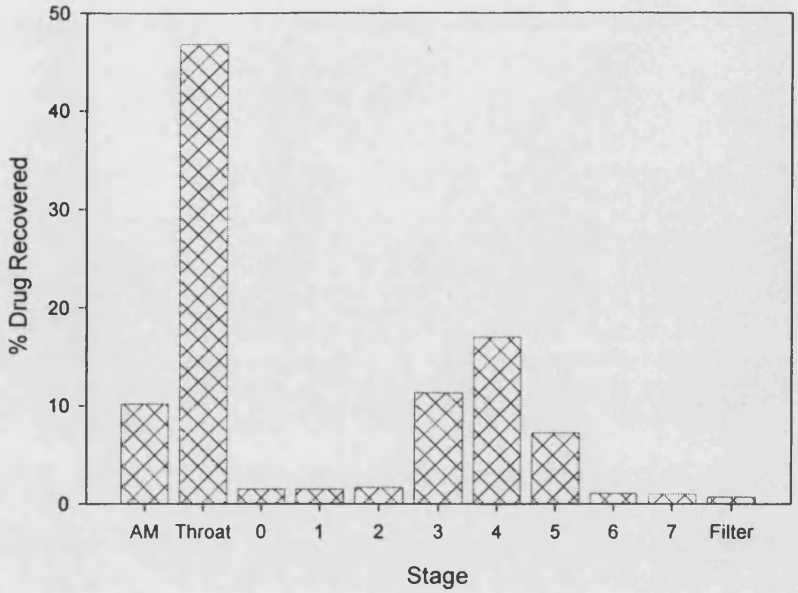

The data represents 6 sets of experiments all performed on one Ventolin™ formulation. Five shots were fired to waste and then ten shots were used during each experiment. Using a spreadsheet designed to give aerosol cloud data from an Andersen cascade impactor (courtesy of Dr. D A Lewis, Vectura Limited, University of Bath Campus, Bath, BA2 7AY). The following results were obtained.

Figure 5.27 ACI data describing the aerosol cloud.

Shot Nos.	MMAD (μm)	GSD
6-15	2.6	1.4
16-25	2.7	1.5
26-35	2.6	1.4
36-45	3.3	1.6
46-55	2.8	1.8
56-65	2.8	1.8

The mean MMAD was found to be 2.8μm however, it can be seen that perhaps the MMAD found from shot numbers 36-45 is a little high. Excluding the high value gives a mean MMAD of 2.7μm(± 0.1). It was found that the FPF for Ventolin™ was 42.1μg (± 8.6).

Product information for Ventolin™ (GlaxoWellcome Inc., March 2000) states the formulation contains a suspension of Salbutamol drug particles 95% ≤10μm. This study has found the mean value of the drug particles < 10μm was 43%. It is probable that the product information is quoting the initial size of the Salbutamol particles put into the device. On exit from the device particles can agglomerate thus increasing the mean aerodynamic diameter.

Data presented by Lewis (Management Forum, 1998) is in good agreement with this study. The study found Ventolin™ to have an MMAD of 2.5μm (± 0.1) (n=6) and FPF of 41.6μm (± 6).

The data collected appears to be similar to other studies performed on Ventolin™ and so it is viewed as reliable. The data presented suggests that Ventolin™ MDI to be a stable formulation giving reproducible results.

5.10.2 Evohaler™

Figure 5.28 Percentage drug recovered for Evohaler™ in the inner stages of the ACI, flow rate at 28.3 l min^{-1} (n=3)

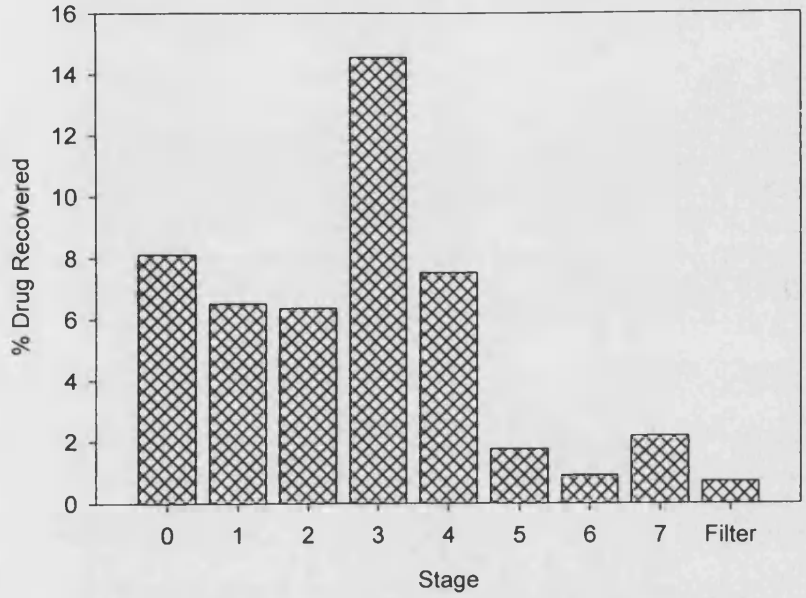

Figure 5.29. Complete Evohaler™ ACI data (28.3 l min^{-1}, n=3)

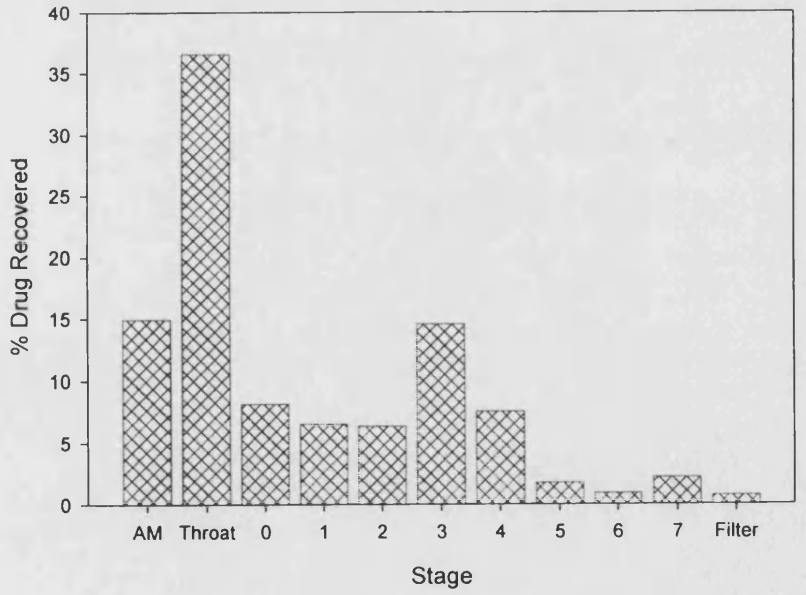

The data represents 3 sets of experiments all performed on one Evohaler™ formulation. Five shots were fired to waste and then ten shots were used during each experiment. The following results were obtained.

Figure 5.30 ACI data describing the aerosol cloud.

Shot Nos.	MMAD (μm)	GSD
6-15	4.1	2.2
16-25	4.6	2.2
26-35	4.4	2.3

The mean MMAD was found to be 4.3μm. This is higher than the MMAD found for Ventolin™ and is a possible explanation for the different behaviour of each formulation in the SML as seen in section 5.8. The FPF was found to be 38.3μm (±3.6).

Product literature states that 10 – 20% of the inhaled dose reaches the lower airways (http:/uk.gsk.com/products/assets/uk_Ventolin_Evohaler.pdf). Unfortunately 'lower airway' is not defined so we cannot make a relevant comparison with the manufacturers data.

The study carried out by Lewis (Management Forum, 1998) stated that Evohaler™ had an MMAD of 3.2μm (±0.2) and a FPF of 33μg (±3). The study presented here shows a higher MMAD than was found Lewis 1999, the FPF is in better agreement.

5.10.3 Airomir™

Figure 5.31 Percentage drug recovered for Airomir™ in the inner stages of the ACI, flow rate at 28.3 l min^{-1} (n=6)

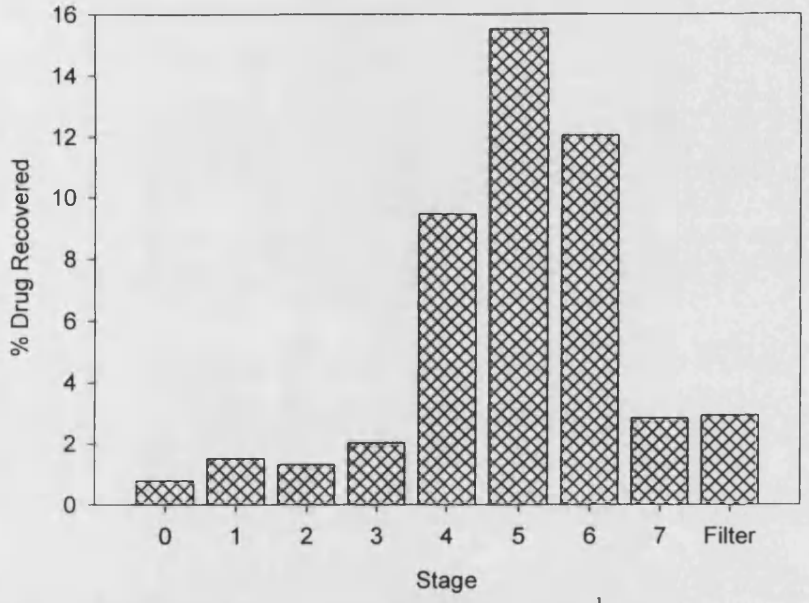

Figure 5.32 Complete Airomir™ ACI data (28.3 l min^{-1}, n=6)

The data represents 6 sets of experiments all performed on one Airomir™ formulation.

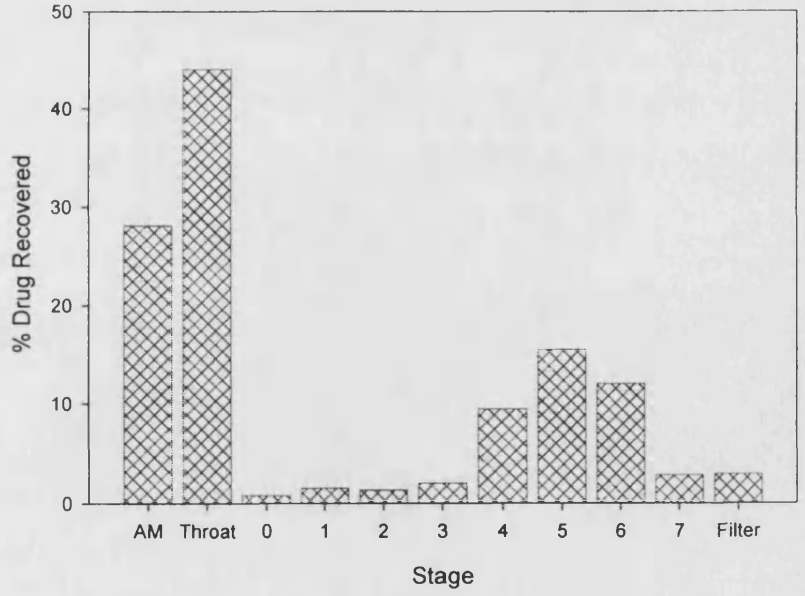

Five shots were fired to waste and then ten shots were used during each experiment. The following results were obtained.

Figure 5.33 ACI data describing the aerosol cloud.

Shot Nos.	MMAD (μm)	GSD
6-15	1.6	1.7
16-25	1.5	1.7
26-35	1.2	1.9
36-45	1.1	2.5
46-55	1.7	1.9
56-65	1.7	2.4

The mean MMAD was found to be 1.5μm, indicating a very fine aerosol cloud. The mean FPF was found to be 44.6μg (±12.7).

Airomir™ is a solution formulation; its valve is smaller than conventional CFC formulations (25μl). Product development data suggest it is a stable formulation (Tansey, 1995).

Estimating MMAD from product data (Leach, 1996) gives a higher result than the study here, 2.4μm. The product literature does suggest that the manufacturers are aware of some erratic dosing emissions from the can throughout its life. This however does not account for the very low MMAD results reported here. The errors were found to be large and further reproducibility problems were identified when the can was weighed after each actuation. Lewis found the MMAD of Airomir™ to be 2.6μm (±0.1) and the FPF 44μg (±4) (n=3).

The study reported here does not estimate the MMAD of Airomir™ MDI to be similar to the studies performed previously. The analytical problems associated with Airomir are thought to be due to formulation issues it is possible that the particles will be dry when they enter the body of the impactor and bouncing off the plates may contribute to the large errors seen. To reduce this factor it may be worth coating the plates of the impactor with a suitable component making them 'sticky' and so reducing the possibility of dry particle bounce and / or re-entrainment.

5.10.4 Bricanyl™

Figure 5.34 Percentage drug recovered for Bricanyl™ in the inner stages of the ACI, flow rate at 28.3 l min^{-1} (n=3)

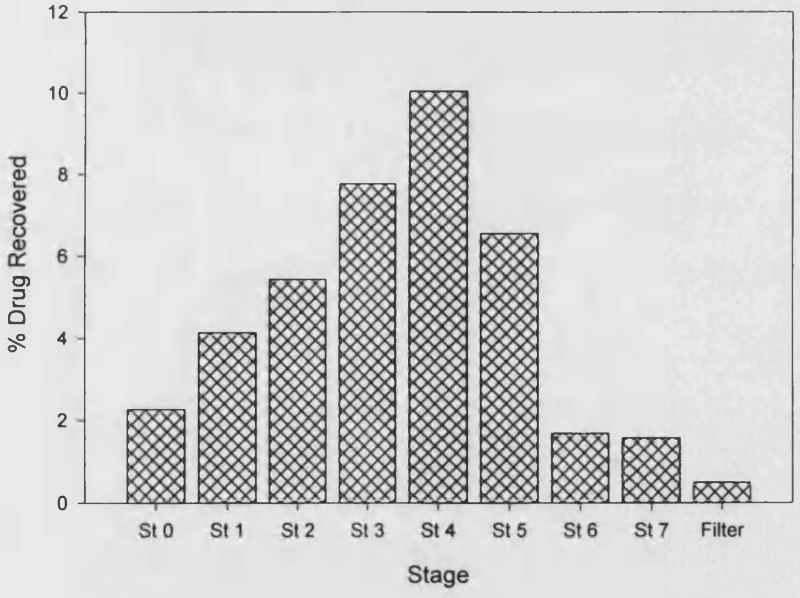

Figure 5.35 Complete Bricanyl™ ACI data (28.3 l min^{-1}, n=3).

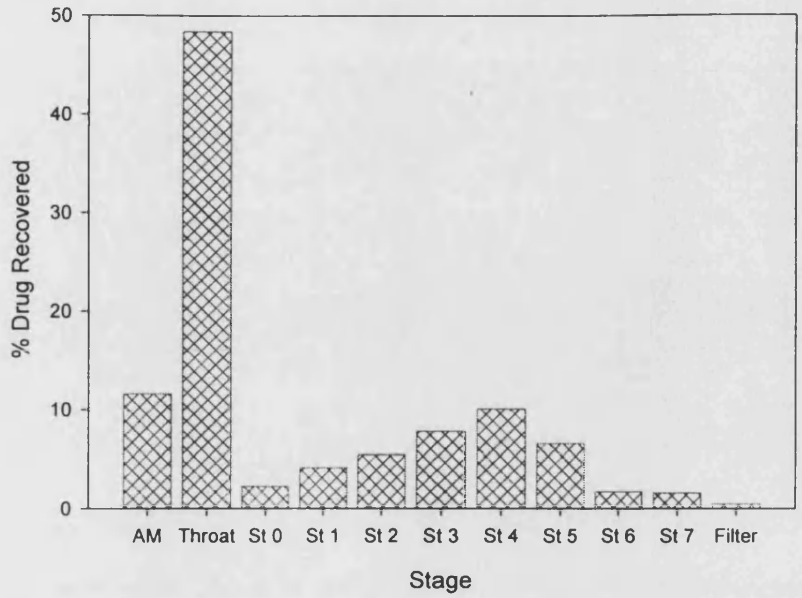

Five shots were fired to waste and then four shots were used during each experiment.

The following results were obtained.

Figure 5.36 ACI data describing the aerosol cloud.

Shot Nos.	MMAD (μm)	GSD
6-9	3.2	2.0
10-13	3.3	2.0
14-17	2.5	2.5

The mean MMAD for Bricanyl was found to be 3.0μm and mean GSD was 2.2.

5.10.5 General discussion

Evohaler™ appears to be deposited more in the inner shells (shells 1 and 2) of the SML than Ventolin™. The Ventolin™ formulation having a lower MMAD and GSD contains fine particles in a smaller size range thus, reaching further into the SML and displaying more of a 'peak' at shell 5. The higher GSD of Evohaler™ indicates that the aerosol cloud contains fine particles in a wide size range i.e. more polydisperse, this may explain the deposition distribution in the SML being wider than for either Ventolin™ of Airomir™.

The GSD for Airomir™ was variable and in general the errors associated with this formulation are greater than with Ventolin™ or Evohaler™. The small MMAD explains the higher drug recovery of this formulation in the filter of the SML at 30 l min^{-1}.
The Bricanyl™ MDI studied had a similar GSD to the Evohaler™ formulation however, the MMAD was found to be 3.0μm, slightly higher than that seen for Ventolin™.

5.11 SML Bifurcation re-manufacture

Details of the reasons for changing the manufactured component are outlined in section 2.3.10. The SML for routine experimentation was run at 30 l min^{-1} this is an equivalent value to the flow rate used in the ACI (28.3 l min^{-1}). The experiment was carried out as stated in sections 5.4.2 and 5.4.5. The flow rate used was 30 l min^{-1} and the formulations were Ventolin™ Bricanyl™ MDI. Figures 5.37 and 5.38 show the old bifurcation in the first instance and the new bifurcation in the last.

Figure 5.37 Percentage drug recovered in each of the outer stages of the SML using either the new or the old bifurcation using Ventolin™ or Bricanyl™ MDI.

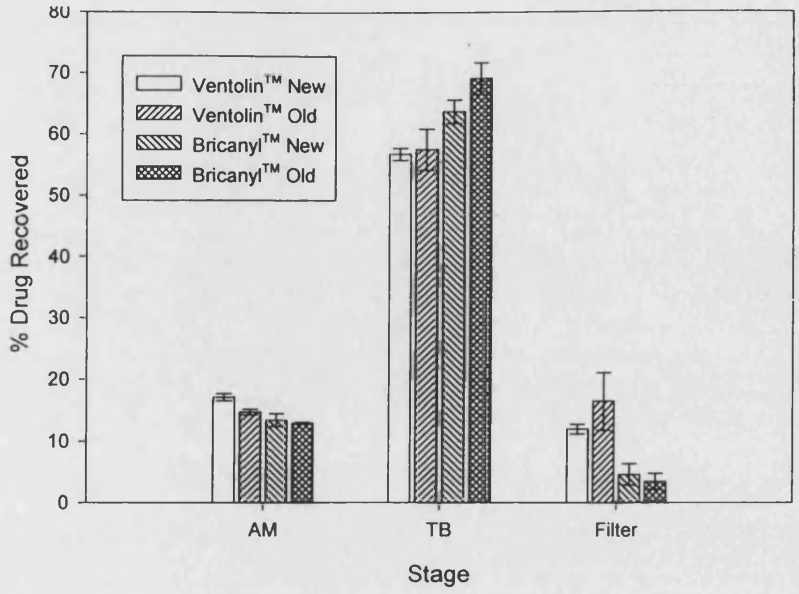

Figure 5.38 Percentage drug recovered in the shells of the SML using either the new or the old bifurcation using either Ventolin™ or a Bricanyl™ MDI.

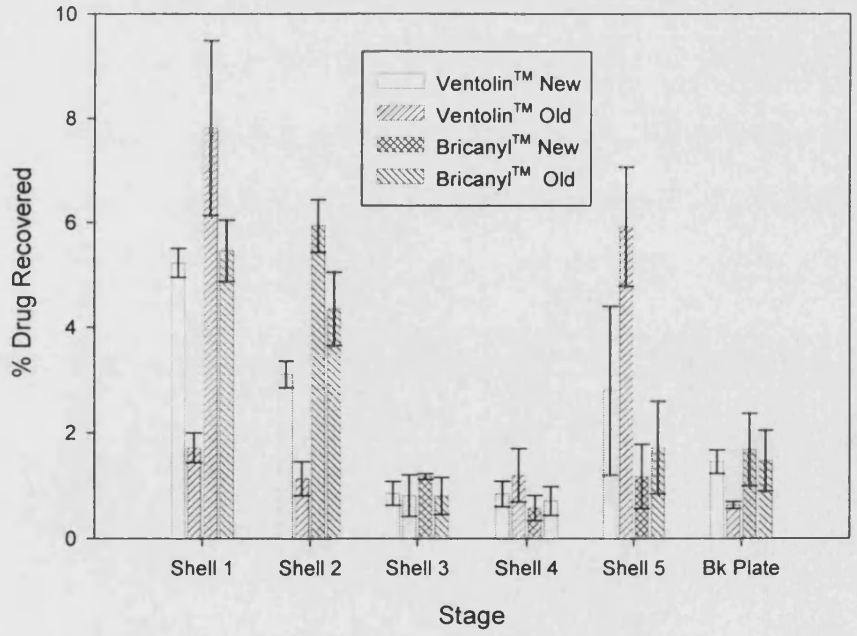

Figure 5.39 Percentage drug recovered in the SML tested at 30 l min^{-1} using either the New or Old Bifurcation in position. Ventolin™ and Bricanyl™ were the MDI formulations used (n=3 for each data set, errors are s.d.).

	% Drug Recovered							
	Ventolin™ New Bifurcation		Ventolin™ Old Bifurcation		Bricanyl™ New Bifurcation		Bricanyl™ Old Bifurcation	
Stage	Mean	s.d.	Mean	s.d.	Mean	s.d.	Mean	s.d.
AM	17.1	0.6	14.7	0.5	13.4	1.0	12.9	0.2
TB	56.7	1.0	57.5	3.4	63.7	1.9	69.1	2.6
Shell 1	5.2	0.3	1.7	0.3	7.8	1.7	5.5	0.6
Shell 2	3.1	0.3	1.1	0.3	5.9	0.5	4.4	0.7
Shell 3	0.8	0.2	0.8	0.4	1.2	0.1	0.8	0.4
Shell 4	0.8	0.2	1.2	0.5	0.6	0.2	0.7	0.3
Shell 5	2.8	1.6	5.9	1.1	1.2	0.6	1.7	0.9
Bk Plate	1.5	0.2	0.6	0.1	1.7	0.7	1.5	0.6
Filter	11.9	0.8	16.4	4.7	4.6	1.7	3.4	1.3

Discussion:

Data was analysed using one way Analysis of Variance (Minitab).

Ventolin™:

The new bifurcation affected deposition of drug in the actuator and mouthpiece ($P<0.001$). Throat and bifurcation deposition was not affected significantly. It is clear from figure 4.38 that the entire deposition pattern seen in the shells is affected, the 'peak' of deposition has moved towards the inner shells (shells 1 and 2) when the new bifurcation was used. $P< 0.001$ for shell 1 and $P= 0.001$ for shell 2. Shells 3 and 4 display no significant change in the % drug recovered value. This may be due to the fact that very little drug is deposited in these shells anyway. Deposition in shell 5 decreased ($P= 0.051$) with the new bifurcation however; more drug was deposited in the shells as a

whole and less in the filter. The total % drug deposition in the shells (including the back plate) was 11.4% with the old bifurcation; the new bifurcation improves the situation to 14.3% ($P< 0.050$).

Bricanyl™:

The new bifurcation does not significantly affect deposition in the actuator and mouthpiece as seen in Ventolin™. Throat and bifurcation deposition was significantly increased with the new bifurcation in place ($P< 0.050$). Shell 1 ($P=0.084$) was increased but not greatly deposition in shell 2 was significantly increased ($P<0.050$). The slight changes seen in other parts of the model are not significant changes but are observed and noted. Total shell drug recovery increased from 14.5% to 18.4% a significant increase ($P < 0.050$).

Patient data as reported by Borgström and Newman, (1993) is a little lower than the value for total lung deposition seen in SML data (with new bifurcation fitted). It was reported that at a mean flow rate of 33.8 l min^{-1} is 8 subjects a mean total lung deposition of 16.7% was recorded.

The nature of aerosol testing involves many errors the alteration of the bifurcation was deemed a success and was used routinely from this point onwards as part of the SML.

5.12 Dry Powder Inhaler Studies

DPI's are devices delivering a formulation of drug with an excipient such as lactose which acts as carrier for the drug particles. The devices deliver a unit dose of the drug.

The formulation may be stored in various ways, for example in a blister, capsule or unit fill device. The devices are generally well used by patients because they are automatically actuated the contents are delivered as the patient inhales. Problems with DPI's include irritation of the patients' throat by the powder, inability of the patients' inhalation force to partly or fully remove the whole dose and settling out of the powder and drug within the device or packaging unit. Even though the model was designed for use with metered dose inhalers it is preferable for any device to be used for all pharmaceutical aerosol devices.

The model was coated with a 10% v/v solution of glycerol in methanol to provide a 'wet' surface for the dry powder to deposit thus reducing the possibility of the particles bouncing off a dry surface. For the purpose of comparison the DPI formulations used were analysed using an ACI, the plates were coated as above. The ACI was run at 28.3 l min^{-1} it is appreciated that this flow rate is not suitable for testing DPIs but for the purposes of comparison it was deemed necessary and suitable. The formulations used were Bricanyl™ Turbuhaler and Ventolin™ Diskhaler. The purpose of these experiments was not to make a direct comparison of the formulations and devices but to assess the qualities of the SML when using DPIs. The experiments were carried out as described in section 5.4.2 and 5.4.5.

5.12.1 SML / ACI Bricanyl™ Turbuhaler™

The results for Bricanyl™ Turbuhaler™ do not include data for actuator retention of drug because the formulation is a self contained system that cannot be dismantled. The first component to be washed was therefore the mouthpiece (M).

Figure 5.40 Percentage drug recovered for Bricanyl™ Turbuhaler™ in the outer stages of the SML flow rate 30 l min^{-1} (n=6 errors are s.d.)

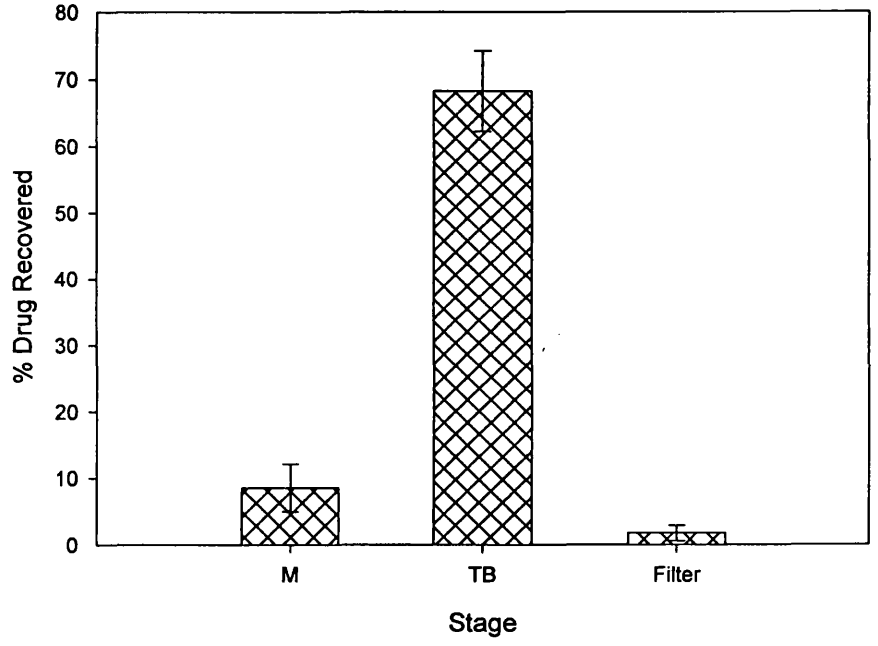

Figure 5.41 Percentage drug recovered for Bricanyl™ Turbuhaler™ in the inner stages of the SML flow rate 30 l min^{-1} (n=6 errors are s.d.)

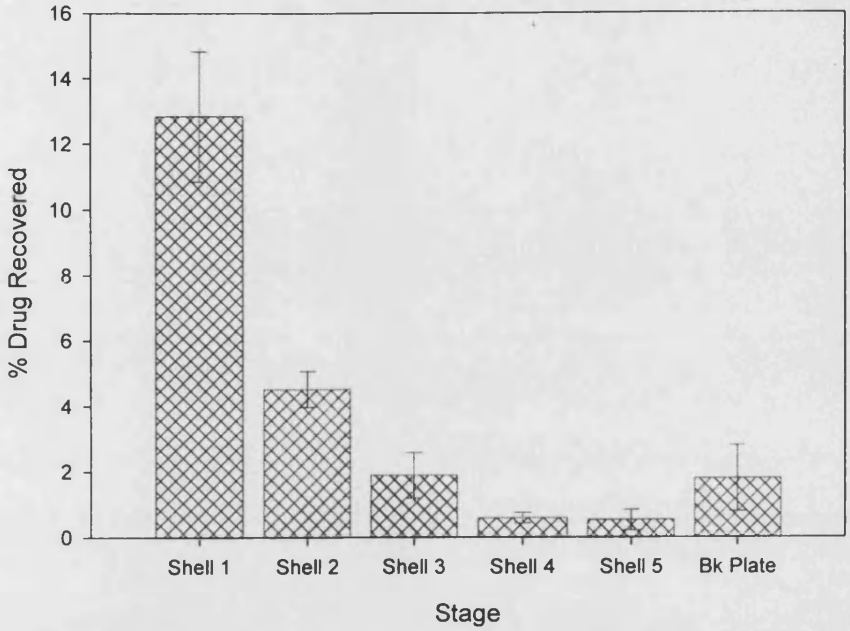

Figure 5.42 Percentage drug recovered for Bricanyl™ Turbuhaler™ in the ACI, flow rate at 28.3 l min^{-1} (n=5)

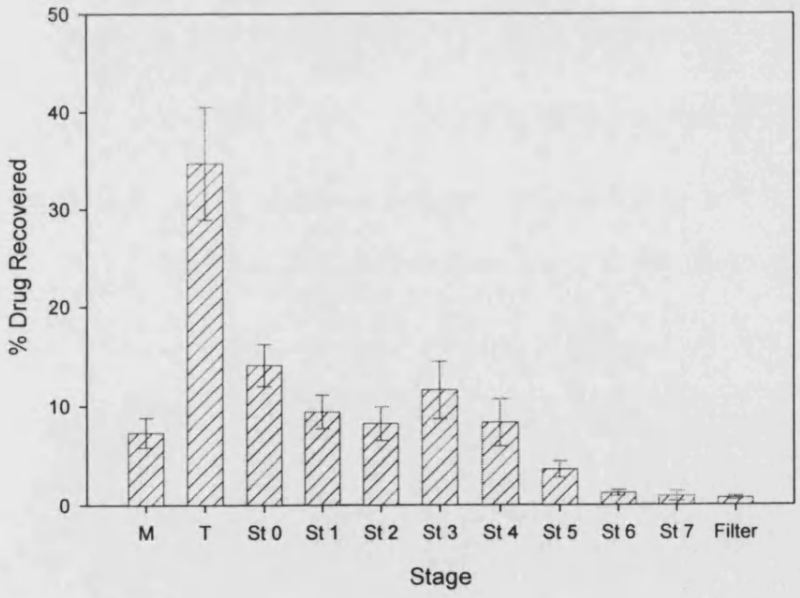

The data represents 5 sets of experiments all performed on one Bricanyl™ Turbuhaler™ formulation. Two shots were used during each experiment. The following results were obtained.

Figure 5.43 ACI data describing the aerosol cloud.

Shot Nos.	MMAD (μm)	GSD
1-2	5.4	2.0
5-6	5.2	2.3
7-8	5.1	2.1
9-10	5.1	2.1
11-12	5.0	2.0

Discussion:

The MMAD for the formulation was 5.1μm according to this comparative study. The aerosol cloud produced by the Turbuhaler appears to be of a good quality as the mean GSD was found to be 2.1. The distribution of the drug in the SML indicates that the MMAD will be higher than that seen in MDIs. The total shell recovery for the formulation was 22.1%. Generally the SML gives a good representation of the formulations characteristics.

Radiolabelled Terbutaline delivered via Turbuhaler™ was found to deposit in the lungs of 8 subjects at a mean value of 21.4%. This value was found to fit well with similar studies performed using gamma scintigraphy (Borgström and Newman, 1993). The study was performed using two-dimensional imaging but for total lung content provides a useful source of data and is in good agreement with SML data. The flow rates used were different, patient mean data for inhalation follow rate was calculated to be 57.8 l min^{-1}.

Data from a study on radiolabelled Terbutaline administered to patients via a Turbuhaler® (Conway *et al,* 2000) compares favourably with this experimental data. The study used a peak inhalation rate of 62 l min^{-1}, this experiment was performed under flow conditions of 30 l min^{-1} it is therefore expected that lung deposition in the Conway study will be higher than that reported here. When adjusting for no actuator recovery, the data from Conway's study was gathered non-destructively, the comparison is detailed in figure 5.44. The specific data of deposition per shell does not compare well with the SML however the problems with the novel device will be addressed in Chapter 6.
A pharmacokinetic method of ascertaining Terbutaline deposition and effect in asthmatic patients was reported by Borgström *et al.,* (2000). Peak inhalation rate was not stated however it is understood that the mean forced expiratory volume was 85% of normal. Mean Lung deposition when using a Turbuhaler 0.25mg dose of Terbutaline is reported in figure 5.44 Both patient studies used here cannot be directly compared with the SML as the methods of collecting the data are different, the dosing regimes cannot be replicated and in the Conway study a Turbuhaler 0.5mg device was used.

Generally the SML gives a good representation of the formulation characteristics. It can be seen that the SML is at least collecting particles in similar quantities as real patient data suggest.

Figure 5.44 Comparative data for Terbutaline delivered via a Turbuhaler® device, γ indicates the Conway study, Pk indicates the Borgström study and SML indicates the study above.

	% Deposition		
Stage	γ	**Pk**	**SML**
Mouthpiece and Throat regions	62		76.8
Lung / Shells	37.5	20.8	23.2

When the Borgström study looked at lung deposition with a 0.5mg terbutaline dose it was found that the percentage deposition decreased to 16.9%. Possibly at the higher dose more drug clearance occurred in the lung so less drug was detected.

5.12.2 SML / ACI Ventolin™ Diskhaler™

Figure 5.45 Percentage drug recovered for Ventolin™ Diskhaler™ in the outer stages of the SML flow rate 30 l min^{-1} (n=5 errors are s.d.)

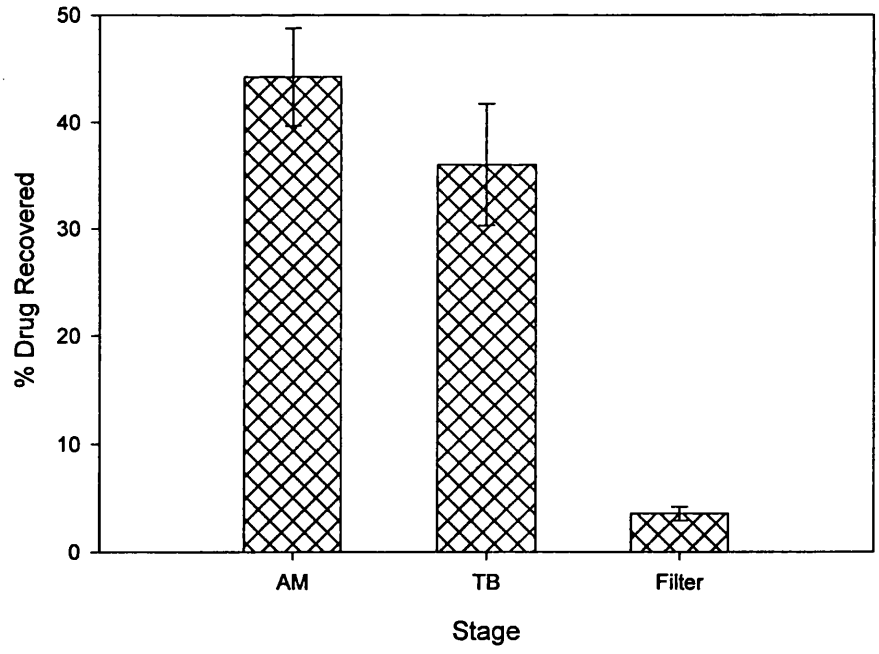

Figure 5.46 Percentage drug recovered for Ventolin™ Diskhaler™ in the inner stages of the SML flow rate 30 l min^{-1} (n=5 errors are s.d.)

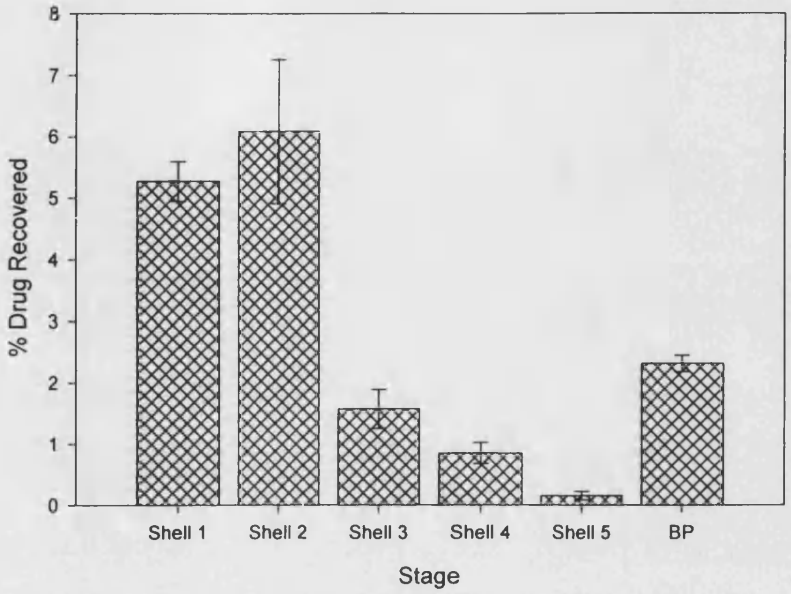

Figure 5.47 Percentage drug recovered for Ventolin™ Diskhaler™ in the ACI, flow rate at 28.3 l min^{-1} (n=5)

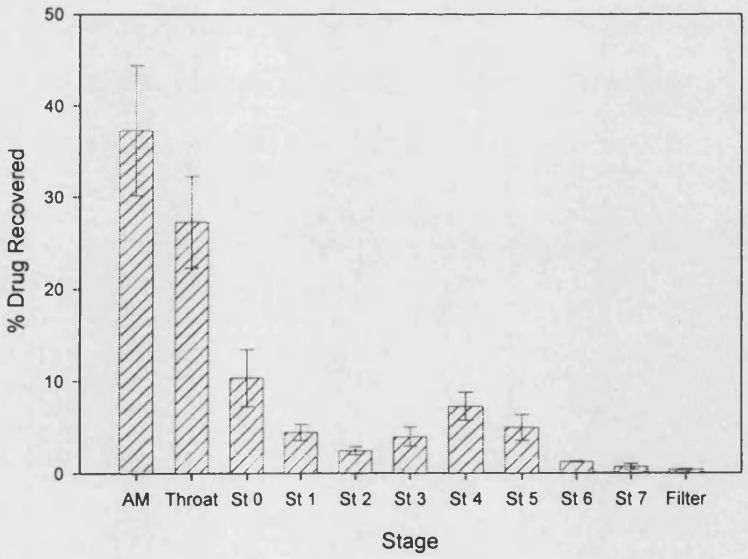

The data represents 5 sets of experiments all performed on the Ventolin™ Diskhaler™ formulation. Five actuations were used during each experiment. The following results were obtained.

Figure 5.48 ACI data describing the aerosol cloud.

Shot Nos.	MMAD (μm)	GSD
1-5	4.7	2.8
6-10	4.8	2.9
11-15	5.5	3.1
16-20	4.1	2.5
21-25	4.3	3.7

Discussion:

The MMAD as found in this comparative study was 4.7μm and the mean GSD was 3.0. The aerosol cloud is finer but more polydisperse than in the previous example. This may explain the more even spread of distribution between the shells. It was likely in both cases that the errors associated with this experimentation were heavily influencing the outcome. The total shell recovery (including the back plate) for the Ventolin™ Diskhaler™ was found to be 16.2%. A particular problem encountered with this formulation appears to be the amount of drug retained in the actuator. From a patient perspective if this region isn't cleaned on a regular basis drug delivery may be reduced as deposits of the formulation build up.

5.13 Ventolin MDI performance at various flow rates

An investigation was undertaken to assess the effects of flow rate on the model with the new bifurcation in position. A Ventolin™ MDI was used at flow rates of 10, 30 and 55 l min^{-1}, the maximum flow rate achievable. The external filter impeded the flow rate so 60 l min^{-1} as previously achieved in the incomplete SML could not be reached.

Figure 5.49 Percentage drug recovered for each outer Stage of the SML at 10 l min^{-1}, 30 l min^{-1} and 55 l min^{-1} (n=3 and errors are s.d.)

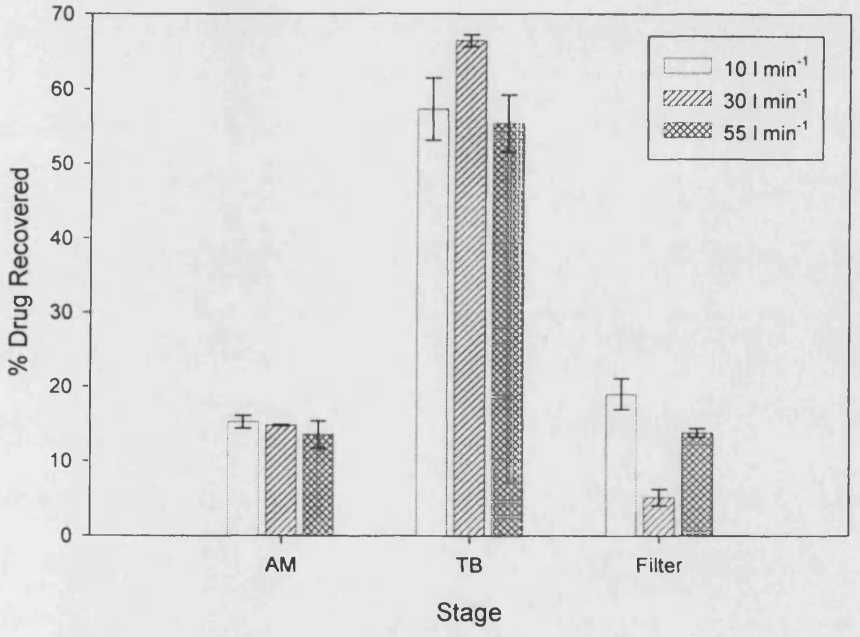

Figure 5.50 Percentage drug recovered for each inner Stage of the SML at 10 l min^{-1}, 30 l min^{-1} and 55 l min^{-1} (n=3 and errors are s.d.)

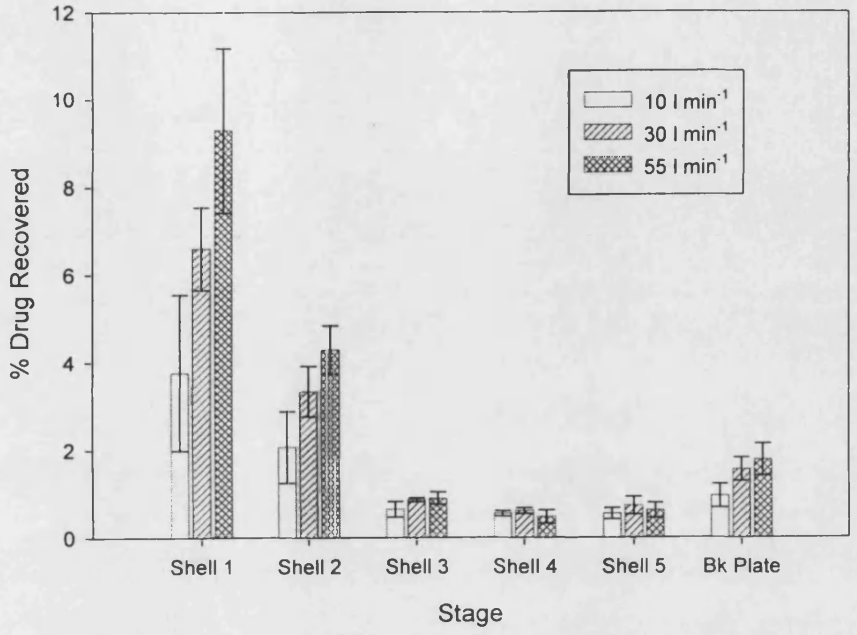

Figure 5.51 Data for each flow rate using a Ventolin™ MDI in the SML

	% Drug Recovered					
Stage	Mean at 10 l min^{-1}	s.d.	Mean at 30 l min^{-1}	s.d.	Mean at 55 l min^{-1}	s.d.
AM	15.2	0.8	14.8	0.1	13.5	1.8
TB	57.3	4.2	66.4	0.8	55.4	3.8
Shell 1	3.8	1.8	6.6	0.9	9.3	1.9
Shell 2	2.1	0.8	3.3	0.6	4.3	0.5
Shell 3	0.6	0.2	0.9	0.0	0.9	0.1
Shell 4	0.6	0.1	0.6	0.1	0.5	0.2
Shell 5	0.5	0.1	0.7	0.2	0.6	0.2
Bk Plate	1.0	0.3	1.6	0.3	1.8	0.4
Filter	19.0	2.1	5.1	1.1	13.8	0.6

Discussion:

Although we can theoretically attribute cut points to shell 1 at these flow rates. The fluid dynamics throughout the model significantly alters deposition throughout. The pattern of deposition cannot be predicted as the model does not behave as an impactor and we have evidence for impaction only in shell 1 at 30 l min^{-1}. Total shell deposition (including back plate deposition) increases from 8.6% at 10 l min^{-1} to 13.7% at 30 l min^{-1} to 17.4% at 55 l min^{-1}. Filter deposition is a point of interest in that it decreases form 19% at 10 l min^{-1} to 5.1% at 30 l min^{-1} and then increases to 13.8% at 55 l min^{-1}. Section 5.10 (bifurcation remanufacture) shows a filter deposition of 11.6% at 30 l min^{-1} so this is in part experimental error. The general trend of the deposition pattern does seem to shift towards the inner shells (shells 1 and 2) as previously seen in the incomplete SML section 5.7.

5.14 General Discussion

It is drawn to the attention of the reader that the SML losses in some cases are up to 20% of the drug administered. It is thought this occurs due to the small area of filter available for particle collection and therefore the airflow through it was high resulting in possible losses through the filter. It was seen during experimental work that the filter if not adequately supported by a mesh would break. Suggestions for further improvement of the filter mechanism and model performance in general follow in section 6.6.4.

Chapter 6 Conclusion and Further Work

A novel aerosol testing device, the Shell Model Lung, has been designed, manufactured, calibrated and investigated. The device demonstrates that *in vitro* devices could be made more realistic. The SML at this stage provides a good starting point for further development of a model collecting particles by deposition methods other than impaction as occurs in the human lung.

6.1 Calibration of the SML

Calculated predicted cut-points at shell 1 are in fairly good agreement with calibration data. The results show that shell 1 collects aerosol particles by impaction at 30 l min^{-1}. It was not intended that each stage of the model should collect particles by impaction as outlined in section 1.9. The model appears to be collecting particles less than 10μm in the shells and filter this should be lower and proposed methods of improving the performance of the model are suggested below.

During calibration of the model only Shell 1 demonstrated a collection efficiency curve passing through the 50% point. The curve is steep and therefore it can be said that this shell collects particles by impaction. Focusing on the initial aims of this project this point seems irrelevant for the remaining shells as impaction is not the main method of particle deposition further into the human lung. A cut-point of 7.2μm at shell 1 means that it is likely any aerosol particles reaching past that point would be less than 10μm. A

theoretical cut point of 5.4μm at 60 l min^{-1} would be suitable for the work if the errors involved at the higher flow rate could be reduced. Data supports the use of the SML over 10 to 60 l min^{-1}. The 2DSML has been investigated over 10 to 95 l min^{-1} (see section 3.7). Due to economic constraints the SML was only calibrated at 30 l min^{-1}, the most relevant for the purposes required here.

6.2 Success and additional requirements

It has been demonstrated that the SML collects particles by impaction and other mechanisms. The SML was designed to collect particles by various methods as occurs in the respiratory tract. Flow regimes in the lung are such that it is expected that particles will impact in generations 1 to 4. As further branching occurs, moving through the generations, the flow velocity decreases and particle deposition is more dependent upon gravitational settling and diffusion. The model is robust and not complicated to operate. The run times are comparable to using an ACI in the laboratory. Other devices such as the TSI have much shorter run times but the data collected is rather limited.

Results from the flow visualisation experiments (section 3.9.3) demonstrate that even at low flow rates streak lines introduced into the flow hit the back of the throat. It is reasonable to assume a MDI aerosol cloud will at a sampling flow rate of 30 l min^{-1} in air (2 l min^{-1} in water) will cause further turbulence in the initial throat section and at the 90° bend.

The flow visualisation of a cloud in shell 1 and 2 demonstrates how an aerosol 'bolus' would disperse (figure 3.20). It appears that the top corner in particular allows recirculation of the cloud. The angle of the bifurcation and the direction of the flow dictate the direction the cloud exits the bifurcation. The void spaces and resulting recirculation allow greater mixing of the particles making deposition more likely.

Results shown in figure 5.44 demonstrate that the SML collects particles in a comparable ratio to those seen in γ - scintigraphy and pharmacokinetic studies. Although the SML results are not 'matching' the patient data seen here it is envisaged that the model could with slight modifications become a comparable analytical tool.

The SML contains five shells a suitable number of collection stages, it is possible that a pre-filter could be incorporated however as the model was designed to be more realistic it is unlikely this would be of any benefit. A USP throat was used as the entry port in all the experimental work reported here and a suitable filter was used at all times.

Recovery of drug from the SML was variable and the initial incomplete model gave fewer errors during analysis. Reasons and suggestions for improving this will be discussed below. Generally the errors seen could be said to result from the fact that collection mechanisms in the model were not as defined as in other particle collection devices. This is unfortunately inherent in the model although if some of the further design ideas were to be incorporated as described below the situation may be improved.

It was thought when using the more volatile formulations the errors involved could be attributed to particle bounce. Coating the SML during the DPI studies proved an effective way of minimising errors so this may also be suitable when using 'drier' MDI formulations.

The model could be acceptable for quality control purposes depending upon reliable validation of the model. This would have to include work incorporating γ scintigraphy to demonstrate the application of the model to real data. It may not be as applicable to in-process quality assurance procedures involving for example stage removal for quick particle size checking. The SML was designed as a 'flow-through' device it is probable that the nature of the fluid dynamics would alter significantly on removal of a shell or shells. This was not investigated although may provide scope for further work on both the 3D and 2D models.

6.3 Effects of model re-design

It was observed that during the initial experiments on the 'incomplete' SML a generally higher recovered dose was collected than when the 5 Shell model was used. It was thought that the airflow effects contributed to the loss of particles through the filter (see section 6.6.4 below).

Re-manufacturing the bifurcation has improved the collection performance of the Shells. It would have been interesting to calibrate the model using every combination of model component.

6.4 Properties of commercial inhalers

Throughout this work it has been evident that commercial MDI's and DPI's are rather variable in their performance. Even when using standard methods and applying controlled conditions it was often the case that experimental errors involved were so large that many results were disregarded. Looking at data presented here and from other sources as seen in chapter 5 it is clear that experiments involving aerosols should always be performed under controlled conditions using designated equipment to be sure that comparisons can be drawn.

As dosing devices inhalers are commercially successful as they are, in most cases, more acceptable to the patient, reducing systemic delivery of drugs and therefore unwanted side effects. The reliable analysis of the systems proves difficult in that patient variability (physiologically) is large, patients use of the devices correctly has to be taught by a healthcare professional and the drug delivery device has moving parts, seals and is made of materials which may confer an electrostatic charge on the particles. Formulations contained in such devices vary considerably offering the patient changes in appearance of the packaging, 'feel' of dosing when actuating related to the valve volume and taste.

6.5 Comparison of 2DSML data with 3DSML findings of deposition affected by flow rate

Further investigation into the similarities between the 2DSML and the 3D model is required however, it is evident that changes in static pressure over the 2DSML as the flow rate increases (section 3.7) means that flow rate in the 3DSML has an effect on particle deposition. CFD would be of benefit here to calculate the changes in airflow through the model and following on from that give predictions of particle deposition patterns.

6.6 Further design proposals for improving the performance of the model

The following sections describe work the author would suggest for future investigation of the SML.

6.6.1 General design / manufacturing improvements

It is thought the basic structure of the model is sound and although improvements of performance will be suggested further design will be discussed here.

Throughout the use of the model it has been found to wear in critical areas. The majority of the fittings are made using screws. As the model is made of aluminium the screws used have worn threads in the screw holes. A particular problem was encountered in the bifurcation to back plate fitting. The screws had worn the aluminium back plate so much

that a close fit could no longer be achieved. New holes were drilled into the two components and new larger threaded screws were supplied by the Department of Pharmacy workshop.

The design of the model would have to be reassessed in the light of these in-progress findings. This problem may be overcome by introducing a method of pushing the fittings into the back plate instead of using the present method. Design suggestions include:

- Incorporating a clip mechanism. Once each shell was positioned correctly a clip secured to the back plate would fit firmly over the holding edge of the shell.
- Introducing a 'stack and hold' feature of the shells. The shell could be push-fitted into the back plate ensuring a tight seal.

It has been suggested that for routine testing a simplified method should be acceptable (Van Oort and Truman, 1998). If the model was quick to use and analyse time wouldn't be taken up by routine laboratory procedures and data collection could be more complete.

6.6.2 Design of a new final shell and enclosing case

The original design for the 5th shell could be manufactured with the intended number of holes (figure 2.5) this would of course increase the cost of the model but, for research purposes it is thought this would be a suitable investment.

When the incomplete SML was used it was clear that in comparison deposition in shells 2 and 3 was higher than when shells 4 and 5 were added to complete the model. The reason for this is believed to be the position and size of the outlet pipe. When the outlet was connected to the cylinder it was further away from the shells and the increasing air velocity associated with it did not interfere with the fluid dynamics of the air passing through shells 1, 2 and 3. For this reason the fifth shell would be encased in a final collection vessel similar to the cylinder design of the incomplete SML as described in section 2.3.9.

It would be interesting to design into the model a feature allowing it to be more closely correlated to the human lung. This would reduce the analytical practicality of the model but may give an insight into its potential for modelling lung efficiency more closely rather than aerosol deposition. The proposed design would consist of a packing material similar to a sponge or other porous material. The material could be soft or rigid depending on the use required. If breathing patterns were to be investigated then foam could be used. Each shell could house material of a specific pore diameter or the whole model could be reconstructed using graduated pore sized material.

6.6.3 Introduction of an anatomical throat

The effect of inlet dimensions on the collection properties of aerosol testing devices influences deposition in the device itself (Fults *et al.,* 1991). The shape and size of the inlet will have an effect on the evaporation of the droplets, turbulence and therefore inertial deposition (impaction).

A possibility for improving the correlation between *in vitro* and *in vivo* models may be to attach a biological throat (Velasquez and Gabrio, 1998) to the model. A USP throat collected approximately 80% less of drug per dose than a 'biological' replica throat (Gabrio B.J. *et al.*, 1999). An 'anatomical throat replica' developed by Astra Draco (Olsson B., *et al.*, 1996) retained 50 to 80% of the dose delivered via a dry powder inhaler compared with 10 to 20% using a glass bulb (TSI) throat.

Adding a oral throat cast (Srichana *et al.*, 1999) reportedly reduced the cut point in a TSI from 6.3μm to 5.2μm. When using an MDI 42% of the delivered dose was retained by the glass bulb throat whereas the anatomical throat collected 77% of the dose. It can be said that an anatomical throat affects the amount of drug collected further in the device. It was demonstrated that even when using the 'anatomical throat replica' *in vitro* results of fine particle fraction were almost 50% more than *in vivo* lung deposition data (collected using the charcoal block method).

It is thought that the geometry of the throat replicas introduces more turbulence into the system. The casts were made after studying MRI scans of human throats. Throat geometry changes when an actuator is held in the mouth and the tongue is pushed back towards the throat (Fan and Cheng, 2000), the constriction that is produced may account for the over prediction in potentially respirable particles. However the introduction of anatomically correct throat models is though to be crucial to the correct modelling of aerosol deposition in the lung (Van Oort and Truman, 1998).

6.6.4 Flow Issues

There are problems with stage losses at the filter in the SML. This could be overcome if the area of the flow was increased. If the flow used was very high then the filter actually broke on a number of occasions allowing particles to escape. If the proposals made above (packing material included) were put into practice then it is likely that all the particles would be captured within the model. Another problem with the position of the outlet in shell 5 is that it is probably causing an increase in velocity that encroaches shell 4 thus not allowing particle deposition by sedimentation. It has been shown that particles are likely to deposit in the lower regions of each shell (figure 3.20) and this is the area we are concerned with.

A simple modification to shell 5 could improve the drug loss through the filter. It is thought that airflow over a larger surface area would reduce the effect seen as described above. A diagram of a proposed redesign of shell 5 is shown in figure 6.1 below. The filter would be placed on a mesh support to provide a continuity of geometry. If the filter collects all the particles under 4.2μm as calibration data suggests are collected here we could draw more conclusions about the inhalers studied such as potentially classifying filter collection as the fine particle fraction of the aerosol cloud.

Figure 6.1 Proposed redesigned outlet pipe.

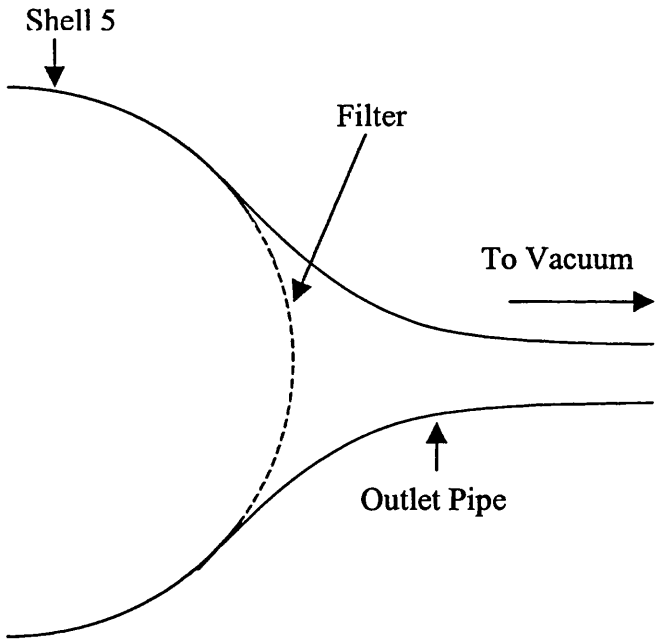

The diagram is not to scale however if the filter diameter were 100mm in diameter this would provide a larger surface area for particle collection than is used presently and the velocity of the airflow through the filter would be greatly reduced.

An interesting experiment could be performed by introducing air into the model at the throat position instead of using a vacuum pump at the exit. Using the modified outlet as described above and introducing a modified Andersen (USP) throat (Figure 6.2) a flow could be introduced at the entry port allowing an even more marked reduction in velocity through the model.

Figure 6.2 Schematic diagram of the proposed Modified Andersen (USP) throat

a. Side view (diagram not to scale)

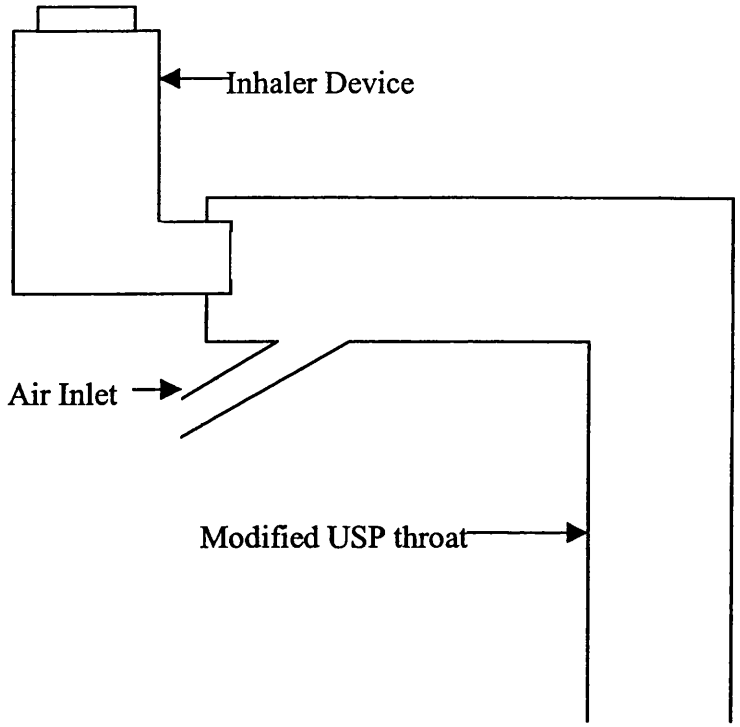

b. End view (diagram not to scale)

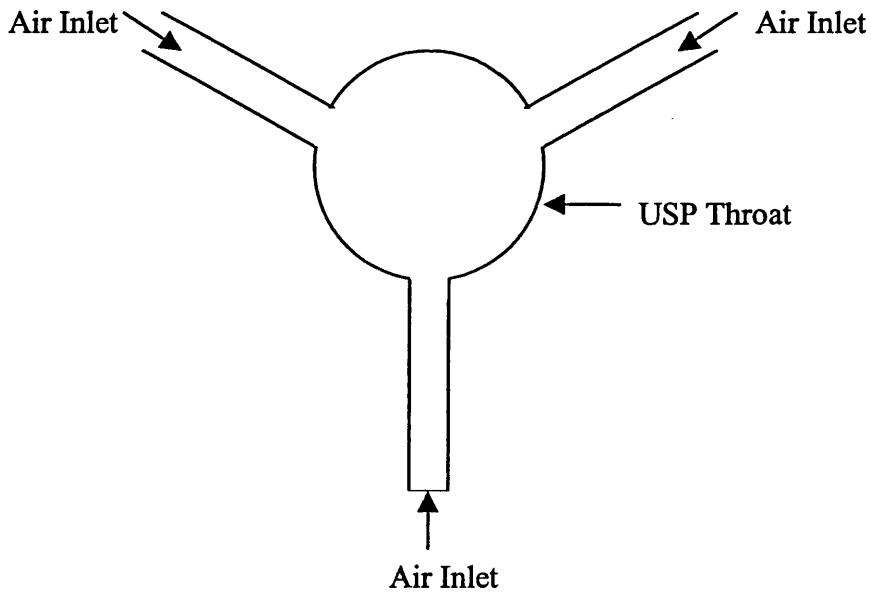

Airflow could be pumped into the model at an appropriate flow rate and timed accordingly. It may also be possible to introduce humidified air to model the humidity in the human lung. The characteristics of the aerosol particles could then be investigated under such conditions. It has been demonstrated that for nebulisers humidity has a significant effect on the size of the droplets produced (Finlay *et al.*, 1997). It would be beneficial to the study of this device to incorporate a system of humidification to investigate hygroscopic growth of particles. Airborne particles in particular are subject to growth under humid conditions (Hitzenberger *et al.*, 1997) for the SML to have uses outside the pharmaceutical field in aerosol research it would be of benefit to include such mechanisms for potential use in environmental science.

It would have been useful to be able to use a breathing device during these studies. Using a realistic breathing pattern for the investigation of aerosols would have suitably enhanced the characteristics of the SML as an *in vitro* device. A piston set-up as used in the Electronic lung™ could have been employed (Brindley *et al.*, 1994). It has been suggested for the analysis of nebulised aerosols (Dennis, 1998) in particular this would be of value as the patient inhales the aerosol throughout a period of time rather than a simple actuation. Nebulisers are devices intended for use over a period of time for patients who find it difficult or impossible to use other methods of drug delivery to the lung. They supply a constant stream of medication to the patient. The aerosol produced by a nebuliser contains water vapour. As the water evaporates the temperature of the aerosol can fall to around 10°C in a few minutes (Dennis, 1998). There are two types

commercially available, air blast and ultrasonic nebulisers. A new type of nebuliser is under investigation (Stangl *et al.*, 2000). The 'vibrating membrane nebuliser' aims to reduce the drug loss seen within the walls and filtering mechanisms of traditional nebulisers. Although they are not as widely used as MDIs or DPIs they are very effective in treating patients with chronically diseased airways.

6.6.5 Coating

It may be advantageous to coat the throat surface of the shells even when using MDIs. Coating impaction surfaces improves particle deposition when one actuation of an MDI was presented to an impactor (Ross *et al.*, 1996) but the case was reversed when up to 10 actuations were used. Coating plates and collection cups of and ACI and MMI has been shown to be beneficial when using single actuations (Nasr *et al.*, 1997). As the surfaces of the larger shells provide a larger deposition area than a regular impactor it may be advantageous to investigate this further. Routine coating of the inlet is advisable when using DPIs (Van Oort and Truman, 1998) therefore for comparative purposes it is probably wise to use the same techniques for MDIs.

Coating a USP throat was shown to increase throat deposition by over 50% when using an MDI (Shrubb, 1998). It is thought that particularly when using MDIs that produce drier particles coating the throat would be advantageous in reducing errors associated with particle bounce.

Modifying the coating of a material to imitate the lung during a period of hypersecretion as occurs during an asthma attack would be an advantage (Pattern, 2000). The immune system reacts intensely during an asthmatic episode so it would help investigators to observe the fact.

6.6.6 Evidence based redesign

The general SML design has proved to be valuable and has given a useful analytical tool. The model does not provide a direct correlation between *in vitro* and *in vivo* data. It is therefore necessary to improve the model to an acceptable level. It is unfortunately beyond the time and economic scale of this research project to investigate the possibilities of CFD based redesign. The use of CFD during this project has helped the understanding of fluid flow in the 2DSML and provided possible explanations for the high regions of deposition. The problems associated with turbulance and three-dimensional manufacturing techniques have been highlighted.

The best feature of CFD has not been exploited during the work presented here. A CFD mesh may when previously set up be modified and altered as necessary. This technique could be used to investigate the effects of altering the size and number of holes in each shell. The computations involved in gathering data are complicated and take many hours or even days in some cases. The CFD time available to this project was unfortunately not sufficient to perform these alterations.

If the data could have been produced it would have been interesting to look at the redesign of each shell in turn and investigate the deposition properties associated with the cases described in figure 6.3. It is anticipated that this would involve in one instance halving the number of holes present in each shell and in another halve the airway diameter. It would be of interest to also rearrange the holes in the shell made possible using this advanced computational technique.

Figure 6.3 Table of hypothetical CFD data inputs for evidence based redesign.

Shell	Mean Hole Diameter / mm	Number of Holes (N)
Shell 1	5.43	**3**
Shell 2	3.02	**21**
Shell 3	1.82	**149**
Shell 4	0.99	**1239**
Shell 1	**2.7**	7
Shell 2	**1.5**	43
Shell 3	**0.9**	298
Shell 4	**0.5**	2478

Another possibility would then be to introduce a 'breathing' pattern into the CFD model to investigate the flow throughout an inhalation and exhalation phase.

Testing and experimentally determining the flow pattern through the model using a 'breathing' pattern would be easier using the 2DSML. Analytical and experimental work as described in sections 3.5 and 3.6 would be possible.

Modelling generations of the airways deep in the lung is important when considering the delivery of drugs for systemic purposes or particles posing a hazard to health. Unlike the upper respirator tract acinar airways are in a constant rhythmic motion. This enables convective mixing of air in the alveoli necessary of course for respiration to occur. Wall

expansions can therefore result in recirculation effects if the expansion is large enough and the airflow low enough (Tsuda *et al.*, 1996). It was suggested that the acinar model based on theoretical and experimental data as supported by complex finding in rabbit lung excision and experimentation was valid.

The rhythmic alveolar model was physically investigated using a large scale silicone copy (Tippe and Tsuda, 1999). The alveolar flow was found to be largely dependent upon volume changes and low flow rates as had been suggested (Tsuda *et al.*, 1996). Low Reynolds numbers do not therefore indicate in such complex geometric situations that the flow is simple and laminar.

6.6.7 Suggestions to create a larger deposition surface

Creating a larger surface area for particles to deposit would improve collection throughout the model. Between the shells 'packing' material could be included. It is thought glass beads of varying diameters could be introduced to create a filtering mechanism through the device with large beads in shell 1 and smaller beads between shell 4 and 5. A similar effect could be achieved with foam cut appropriately to fit between the shells this would have the advantage over glass beads by being one defined piece of material creating a packing surface that would not change with each use. Glass beads would have the same amount of space between them but would create geometrically diverse patterns (representing the airways) on each packing.

6.6.8 Gamma Scintigraphy Studies

It is thought that it would be possible to image radionuclide in the SML. SPECT imaging provides spatial data and although this cannot be used to validate lung models (Fleming *et al.*, 1996) it should be possible to make some correlation with the SML. The internal structure of the SML is very similar to the hemispherical model used for data interpretation therefore instead of trying to relate data per generation of a lung model it should be possible to directly see any similarities.

6.6.9 2DSML for aerosol testing

If the casing of the 2DSML was changed to aluminium it is likely that to assess the accuracy of the 2DSML analytical and experimental model it could be used for aerosol testing and undergo calibration testing. Using aluminium as the casing would prevent any undesirable electrostatic effects interfering with results. The model may after modification be more suitable for testing small doses than the three-dimensional model as there would be less surface area to wash and results may be more accurate.

6.9 Final Summary

It has been demonstrated that the SML collects particles by impaction and other mechanisms. The model does not replicate the impactors or impingers currently on the market. Further investigation and modifications should allow the model to be used for an *in vitro* respiratory model. The use of the SML in conjunction with the available testing methods would allow greater flexibility in the laboratory qualification of new formulations and active compounds.

Appendix A - Percentage Drug recovery for sections 5.8 to 5.13 inclusive

Data referring to: 5.7.1 Airomir™ at 30l min^{-1}

	Can / experiment number										
Stage	3.1	3.2	3.3	3.4	3.5	4.3	4.4	4.5	4.6	Mean	St Dev
AM	29.44	26.60	24.46	25.05	24.97	26.60	24.46	25.05	24.97	25.73	1.61
TB	56.36	43.43	43.68	48.93	46.05	43.43	43.68	48.93	46.05	46.73	4.24
Shell 1	2.90	1.46	1.51	1.75	1.77	1.46	1.51	1.75	1.77	1.77	0.45
Shell 2	2.23	1.24	1.40	1.35	1.59	1.24	1.40	1.35	1.59	1.49	0.31
Shell 3	1.33	0.72	0.69	0.66	0.72	0.72	0.69	0.66	0.72	0.77	0.21
Cylinder	5.36	5.97	3.36	3.26	3.15	5.97	3.36	3.26	3.15	4.10	1.27
Filter	2.37	20.57	24.89	18.99	21.75	20.57	24.89	18.99	21.75	19.42	6.75

Data referring to 5.7.2 Airomir™ at 60 l min^{-1}

	Can / experiment number							
Stage	4.1	4.2	4.7	5.1	5.2	5.3	Mean	St Dev
AM	18.91	19.96	18.59	18.99	17.96	17.84	18.71	0.77
TB	34.48	35.43	31.41	40.38	34.53	34.68	35.15	2.91
Shell 1	3.48	3.26	3.84	7.93	6.80	6.64	5.32	2.03
Shell 2	2.24	2.18	2.07	4.79	4.07	3.84	3.20	1.18
Shell 3	1.28	1.29	0.87	0.94	0.85	0.67	0.98	0.25
Cylinder	9.87	7.94	9.48	3.71	3.76	3.37	6.36	3.07
Filter	29.75	29.94	33.75	23.27	32.03	32.96	30.28	3.79

Data referring to: 5.7.3 Ventolin™ at 60 l min^{-1}

	Can / experiment number					
Stage	1.1	1.2	1.3	1.4	Mean	St.Dev.
AM	10.87	12.26	13.78	12.29	12.30	1.19
TB	54.02	49.73	52.10	46.51	50.59	3.24
Shell 1	3.67	2.58	2.98	4.34	3.39	0.78
Shell 2	2.09	1.66	1.71	2.61	2.02	0.44
Shell 3	0.61	0.53	0.51	0.79	0.61	0.13
Cylinder	2.96	2.02	2.54	2.78	2.58	0.41
Filter	25.78	31.23	26.38	30.67	28.52	2.83

Data referring to: 5.7.4 Suitability of solvents using Water, Water for the metal parts of the model and methanol for the filter (W/M) and Methanol for all parts.

	Experimental conditions										
Stage	Water	W/M	Methanol	Water	W/M	Methanol	Water	W/M	Methanol	Mean total	St.Dev.total
A+MP	10.80	11.53	15.61	10.83	11.48	13.78	10.78	11.13	15.01	12.33	1.93
T+BIF	49.95	49.21	48.26	49.77	50.62	49.51	52.17	51.53	47.78	49.87	1.42
Shell 1	2.64	3.84	2.93	3.03	3.04	2.47	3.29	3.07	3.03	3.04	0.39
Shell 2	1.95	2.37	2.44	1.27	2.11	1.96	1.96	2.09	2.07	2.03	0.33
Shell 3	0.73	0.93	1.90	0.63	0.87	1.26	0.74	0.72	1.20	1.00	0.40
Cylinder	4.11	4.31	4.40	4.69	5.04	5.09	3.46	3.44	9.20	4.86	1.73
Filter	29.82	27.79	24.46	29.79	26.84	25.94	27.60	28.02	21.72	26.89	2.58

Data referring to: 5.8.1 MDI formulation comparisons at 30 l min^{-1}

Ventolin™:

	Experiment No.				
Stage	1	2	3	Mean	St Dev
AM	15.23	14.44	14.45	14.70	0.01
T+Bif	60.49	53.83	58.12	57.48	3.03
Shell 1	1.87	1.39	1.89	1.71	0.36
Shell 2	1.49	1.04	0.87	1.13	0.12
Shell 3	1.26	0.60	0.57	0.81	0.02
Shell 4	1.61	0.63	1.33	1.19	0.49
Shell 5	4.85	5.81	7.12	5.93	0.93
Bk Plate	0.55	0.65	0.68	0.63	0.02
Filter	12.64	21.62	14.98	16.41	4.70

Evohaler™:

	Can / experiment No.				
Stage	1	2	3	Mean	St Dev
AM	22.52	20.03	20.51	21.02	0.33
T+Bif	46.16	46.70	46.18	46.35	0.37
Shell 1	3.54	3.27	4.44	3.75	0.83
Shell 2	3.55	3.38	4.05	3.66	0.47
Shell 3	1.60	1.76	2.05	1.80	0.21
Shell 4	1.72	1.87	1.32	1.64	0.39
Shell 5	2.71	2.70	3.61	3.00	0.64
Bk Plate	1.74	1.80	1.76	1.77	0.03
Filter	16.46	18.49	16.08	17.01	1.71

Airomir™:

	Experiment No				
Stage	1	2	3	Mean	St Dev
AM	27.88	30.53	31.45	29.95	0.65
T+Bif	36.76	31.62	34.26	34.21	1.87
Shell 1	1.27	0.96	0.66	0.96	0.21
Shell 2	1.18	0.78	0.66	0.87	0.09
Shell 3	0.49	0.47	1.36	0.77	0.62
Shell 4	1.35	1.07	1.03	1.15	0.03
Shell 5	4.38	4.12	4.58	4.36	0.32
Bk Plate	0.71	0.50	0.28	0.50	0.15
Filter	25.99	29.96	25.73	27.22	2.99

Data referring to: 5.8.2 MDI formulation comparisons at 60l min^{-1}

Ventolin™:

	Experiment No.				
Stage	1	2	3	Mean	St Dev
AM	8.60	9.09	10.85	9.51	1.18
T+Bif	69.34	68.83	65.47	67.88	2.10
Shell 1	4.82	3.39	4.34	4.19	0.73
Shell 2	2.96	2.15	2.45	2.52	0.41
Shell 3	0.62	0.60	0.65	0.62	0.02
Shell 4	0.95	0.59	0.39	0.64	0.28
Shell 5	2.60	1.34	0.45	1.46	1.08
Bk Plate	1.33	1.30	1.11	1.24	0.12
Filter	8.79	12.70	14.30	11.93	2.84

Evohaler™:

	Experiment No.				
Stage	1	2	3	Mean	St Dev
AM	9.53	11.94	16.39	12.62	3.48
T+Bif	70.77	70.05	55.45	65.42	8.64
Shell 1	3.24	4.50	8.25	5.33	2.61
Shell 2	2.86	3.59	6.57	4.34	1.97
Shell 3	0.94	1.05	2.22	1.40	0.71
Shell 4	0.92	0.57	0.80	0.76	0.18
Shell 5	5.23	1.86	0.89	2.66	2.28
Bk Plate	1.58	1.86	3.05	2.17	0.78
Filter	4.93	4.57	6.38	5.29	0.95

Airomir™:

	Experiment No.				
Stage	1	2	3	Mean	St Dev
AM	19.22	18.94	22.39	20.19	1.91
T+Bif	52.70	53.33	53.34	53.12	0.36
Shell 1	5.83	2.84	4.85	4.50	1.53
Shell 2	3.52	1.92	3.14	2.86	0.83
Shell 3	0.67	3.65	0.56	1.62	1.75
Shell 4	0.51	3.85	0.28	1.55	2.00
Shell 5	1.84	3.59	2.54	2.66	0.88
Bk Plate	1.74	1.02	1.59	1.45	0.38
Filter	13.97	10.86	11.32	12.05	1.68

Data referring to: 5.9.1 ACI data for Ventolin™ MDI formulation

	Shot Numbers						
	5-15	16-25	26-35	36-45	46-55	56-65	Mean
AM	10.77	9.58	9.99	11.66	9.71	9.34	10.18
Throat	53.46	52.14	50.88	41.53	41.63	41.46	46.85
0	0.13	0.70	0.53	2.84	2.23	2.56	1.50
1	0.18	0.41	0.39	3.02	2.25	2.69	1.49
2	0.70	0.85	0.65	3.00	2.56	2.34	1.68
3	7.66	8.82	9.07	14.59	14.36	13.41	11.32
4	16.58	17.23	17.95	15.40	17.32	17.65	17.02
5	8.46	8.71	8.78	5.06	5.57	6.73	7.22
6	0.90	0.82	0.72	1.00	1.40	1.54	1.06
7	0.35	0.34	0.30	1.39	2.03	1.60	1.00
Filter	0.82	0.40	0.76	0.50	0.93	0.69	0.68

Data referring to: 5.9.2 ACI data for Airomir™ MDI formulation

	Shot Numbers						
	6-15	16-25	26-35	36-45	46-55	56-65	Mean
AM	28.72	27.50	29.44	28.07	28.72	26.29	28.12
Throat	48.83	39.90	43.90	47.28	41.14	42.97	44.00
0	0.34	0.62	1.31	1.02	0.62	0.77	0.78
1	0.48	1.15	1.25	1.89	1.91	2.44	1.52
2	0.43	0.99	0.88	1.40	1.53	2.61	1.31
3	0.65	1.28	1.35	1.15	2.41	5.30	2.02
4	3.39	10.93	4.52	2.32	14.53	21.09	9.47
5	14.18	20.25	11.71	8.25	20.45	18.25	15.52
6	1.36	11.07	25.76	22.69	6.51	4.90	12.05
7	1.03	1.67	3.25	6.91	1.77	2.32	2.83
Filter	0.59	1.71	3.08	2.42	3.06	6.70	2.93

Data referring to: 5.9.3 ACI data for Evohaler™ MDI formulation

	Shot Numbers			
	6-15	16-25	26-35	Mean
AM	17.1	13.3	14.3	14.9
Throat	39.4	32.5	37.8	36.6
0	6.6	9.5	8.2	8.1
1	5.1	7.5	6.9	6.5
2	5.2	8.1	5.8	6.4
3	13.1	16.3	14.2	14.6
4	8.2	7.2	7.1	7.5
5	2.1	1.4	1.7	1.7
6	0.8	1.0	0.9	0.9
7	1.9	2.4	2.2	2.2
Filter	0.6	0.7	0.8	0.7

Data referring to: 5.9.4 ACI data for Bricanyl™ MDI formulation

	Shot Numbers			
	6-15	16-25	26-35	Mean
AM	7.49	10.19	17.21	11.63
Throat	47.90	46.18	51.18	48.42
0	1.62	2.53	2.66	2.27
1	4.74	4.66	3.01	4.14
2	9.09	5.26	1.95	5.43
3	6.75	12.50	4.06	7.77
4	11.79	10.66	7.69	10.04
5	6.99	4.61	8.05	6.55
6	2.74	2.06	0.27	1.69
7	0.50	0.77	3.44	1.57
Filter	0.41	0.57	0.48	0.49

Data referring to: 5.10 Bifurcation re-manufacture

Old Bifurcation Ventolin™:

	Experiment			
	1	2	3	Mean
AM	15.23	14.44	14.45	14.70
Throat	60.49	53.83	58.12	57.48
0	1.87	1.39	1.89	1.71
1	1.49	1.04	0.87	1.13
2	1.26	0.60	0.57	0.81
3	1.61	0.63	1.33	1.19
4	4.85	5.81	7.12	5.93
5	0.55	0.65	0.68	0.63
6	12.64	21.62	14.98	16.41
7	15.23	14.44	14.45	14.70
Filter	60.49	53.83	58.12	57.48

New bifurcation Ventolin™:

	Experiment			
	1	2	3	Mean
AM	17.08	17.65	16.47	17.07
Throat	57.72	55.71	56.71	56.71
0	4.94	5.48	5.26	5.23
1	2.87	3.07	3.38	3.10
2	0.87	0.61	1.06	0.85
3	0.87	0.59	1.06	0.84
4	1.85	4.66	1.90	2.80
5	1.56	1.19	1.60	1.45
6	12.25	11.04	12.55	11.94
7	17.08	17.65	16.47	17.07
Filter	57.72	55.71	56.71	56.71

Old bifurcation Bricanyl™:

	Experiment			
	1	2	3	Mean
AM	12.82	13.07	12.77	12.89
Throat	66.49	69.25	71.69	69.14
0	5.37	6.09	4.92	5.46
1	4.93	4.56	3.58	4.36
2	1.19	0.69	0.52	0.80
3	0.93	0.79	0.40	0.71
4	1.36	1.08	2.72	1.72
5	1.95	1.64	0.83	1.48
6	4.94	2.84	2.56	3.45
7	12.82	13.07	12.77	12.89
Filter	66.49	69.25	71.69	69.14

New bifurcation Bricanyl™:

	Experiment			
	1	2	3	Mean
AM	14.32	12.30	13.60	13.40
Throat	61.52	65.13	64.42	63.69
0	5.93	9.14	8.37	7.81
1	5.44	6.44	5.93	5.94
2	1.21	1.19	1.11	1.17
3	0.85	0.49	0.39	0.58
4	1.88	0.83	0.82	1.17
5	2.30	0.94	1.81	1.68
6	6.57	3.54	3.55	4.55
7	14.32	12.30	13.60	13.40
Filter	61.52	65.13	64.42	63.69

Data referring to: 5.11.1

SML Bricanyl™ Turbuhaler™

	Experiment No.							
Stage	**1**	**2**	**3**	**4**	**5**	**6**	**Mean**	**St Dev**
AM	8.67	11.16	9.16	13.31	5.16	3.82	8.55	3.57
T+Bif	64.93	63.89	72.54	60.32	75.19	72.60	68.25	5.97
Shell 1	15.84	13.50	10.10	12.51	11.41	13.63	12.83	1.99
Shell 2	4.56	4.73	3.75	5.32	4.09	4.62	4.51	0.54
Shell 3	1.72	2.07	1.22	3.17	1.64	1.45	1.88	0.69
Shell 4	0.68	0.58	0.83	0.61	0.34	0.49	0.59	0.16
Shell 5	1.08	0.24	0.69	0.48	0.39	0.29	0.53	0.31
Bk Plate	1.44	2.47	0.62	3.31	0.93	1.98	1.79	1.00
Filter	1.08	1.35	1.10	0.97	0.85	1.12	1.08	0.17

ACI Bricanyl™ Turbuhaler™

	Experiment No.						
Stage	**1**	**2**	**3**	**4**	**5**	**Mean**	**St. Dev**
AM	28.72	27.50	29.44	28.07	28.72	26.29	28.12
Throat	48.83	39.90	43.90	47.28	41.14	42.97	44.00
0	0.34	0.62	1.31	1.02	0.62	0.77	0.78
1	0.48	1.15	1.25	1.89	1.91	2.44	1.52
2	0.43	0.99	0.88	1.40	1.53	2.61	1.31
3	0.65	1.28	1.35	1.15	2.41	5.30	2.02
4	3.39	10.93	4.52	2.32	14.53	21.09	9.47
5	14.18	20.25	11.71	8.25	20.45	18.25	15.52
6	1.36	11.07	25.76	22.69	6.51	4.90	12.05
7	1.03	1.67	3.25	6.91	1.77	2.32	2.83
Filter	0.59	1.71	3.08	2.42	3.06	6.70	2.93

Data referring to: 5.11.2

SML Ventolin™ Diskhaler™:

	Experiment No.							
Stage	**1**	**2**	**3**	**4**	**5**	**6**	**Mean**	**St Dev**
AM	40.07	68.14	50.94	35.80	48.54	45.73	48.20	9.45
T+Bif	38.72	19.91	31.47	44.77	33.46	31.71	33.34	8.32
Shell 1	5.68	3.33	5.17	5.03	4.93	5.52	4.94	0.84
Shell 2	6.80	3.51	5.01	5.24	5.55	7.78	5.65	1.48
Shell 3	1.69	0.79	1.26	1.38	1.44	2.06	1.44	0.43
Shell 4	1.07	0.56	0.67	0.79	0.73	0.98	0.80	0.19
Shell 5	0.03	0.00	0.16	0.20	0.19	0.18	0.13	0.09
Bk Plate	2.29	1.07	2.11	2.29	2.43	2.44	2.10	0.52
Filter	3.64	2.70	3.21	4.49	2.72	3.59	3.39	0.68

ACI Ventolin™ Diskhaler™

	Experiment No.						
Stage	**1**	**2**	**3**	**4**	**5**	**Mean**	**St. Dev**
AM	35.58	33.86	31.01	36.40	49.45	37.26	7.12
Throat	28.91	26.57	27.94	33.25	19.48	27.23	5.00
0	9.64	11.41	14.91	6.63	9.08	10.33	3.08
1	4.91	5.52	4.61	3.47	3.59	4.42	0.88
2	2.70	2.54	2.66	2.52	1.60	2.40	0.46
3	4.61	4.75	2.73	4.65	2.86	3.92	1.03
4	6.41	7.45	9.50	7.33	5.43	7.23	1.51
5	5.23	5.79	3.89	3.15	6.61	4.94	1.41
6	1.13	1.26	1.20	1.29	1.18	1.21	0.07
7	0.46	0.44	1.09	0.93	0.45	0.67	0.31
Filter	0.41	0.40	0.46	0.37	0.28	0.38	0.07

Data referring to: 5.12

Ventolin™ MDI @ 10 l min^{-1}

	Experiment No.				
Stage	**1**	**2**	**3**	**Mean**	**St Dev**
AM	14.27	15.54	15.83	15.21	0.83
T+Bif	53.89	55.99	61.97	57.28	4.19
Shell 1	5.64	3.56	2.11	3.77	1.77
Shell 2	2.96	1.89	1.36	2.07	0.82
Shell 3	0.74	0.76	0.45	0.65	0.18
Shell 4	0.58	0.48	0.60	0.55	0.06
Shell 5	0.69	0.51	0.45	0.55	0.13
Bk Plate	1.21	0.98	0.68	0.96	0.27
Filter	20.01	20.31	16.55	18.96	2.09

Ventolin™ MDI @ 30 l min^{-1}

	Experiment No.				
Stage	**1**	**2**	**3**	**Mean**	**St Dev**
AM	14.88	14.76	14.69	14.78	0.09
T+Bif	65.52	66.88	66.86	66.42	0.78
Shell 1	7.41	6.83	5.56	6.60	0.94
Shell 2	3.81	3.52	2.70	3.34	0.57
Shell 3	0.92	0.86	0.82	0.87	0.05
Shell 4	0.60	0.54	0.68	0.61	0.07
Shell 5	0.59	0.64	0.96	0.73	0.20
Bk Plate	1.37	1.86	1.44	1.56	0.27
Filter	4.90	4.10	6.29	5.10	1.11

Ventolin™ MDI @ 55 l min^{-1}

	Experiment No.				
Stage	**1**	**2**	**3**	**Mean**	**St Dev**
AM	12.99	15.54	12.01	13.51	1.82
T+Bif	52.55	53.84	59.70	55.36	3.81
Shell 1	11.44	8.49	7.95	9.30	1.88
Shell 2	4.75	4.42	3.68	4.28	0.55
Shell 3	0.88	1.05	0.77	0.90	0.14
Shell 4	0.40	0.65	0.38	0.47	0.15
Shell 5	0.57	0.82	0.49	0.62	0.17
Bk Plate	2.03	1.95	1.36	1.78	0.37
Filter	14.39	13.24	13.66	13.76	0.58

Appendix B

Study on the SML using Ventolin™ MDI with or without a spacer device (Volumatic™)

Introduction

The SML was used to analyse the deposition profile of a Ventolin™ MDI when used with a Volumatic™ spacer device and used alone. Spacers are devices designed to 'hold' the aerosol cloud reducing the velocity and momentum of the particles and preventing impaction of the drug particles on the back of the throat. Spacers are particularly useful for the elderly, children and patients who experience difficulty coordinating actuation of a MDI with breathing.

Methods

The SML was assembled as described in section 5.4.2. The model was used to test Ventolin™ without or with the Volumatic™ spacer device. The flow rate was set to 30 l min^{-1} and the timer was set to 10 seconds ten actuations were made during each experiment. Three MDIs were used during the experiment however as Ventolin™ is a relatively reproducible formulation the intra-batch differences were ignored and a new can began after 5 experiments. Each new can was primed by actuating 5 shots to waste. A series of 14 experiments were carried out n=7 with the spacer in position and n=7 when no spacer was used.

Ventolin: Lot: 10467848 Exp: 10/01

Volumatic® spacer device: Lot: 10c417119

The SML was washed according to section 5.4.5 the spacer was washed and analysed last. The spacer was washed using the same solvent for analysis. After washing for analysis the spacer was rinsed using clean tap water then methanol and left to dry naturally on the bench. To prevent accidental adding of an electrostatic charge the spacer was not dried using a towel or an air stream.

Results and Discussion

The graph shown in figure A2.1 clearly displays the difference the spacer device makes to the deposition of drug in the throat region. When the spacer was not used over 40% of the drug deposited in the throat region. When the spacer device was used this went down to 2%. The spacer device retained 36% of the drug. The remaining drug in the spacer device although we cannot say if it is in fact of the correct size range, which would have impacted on the throat, is of the correct proportion.

Figure B1. Graph showing percentage drug recovered for each stage of the SML and Volumatic spacer device when using Ventolin™.

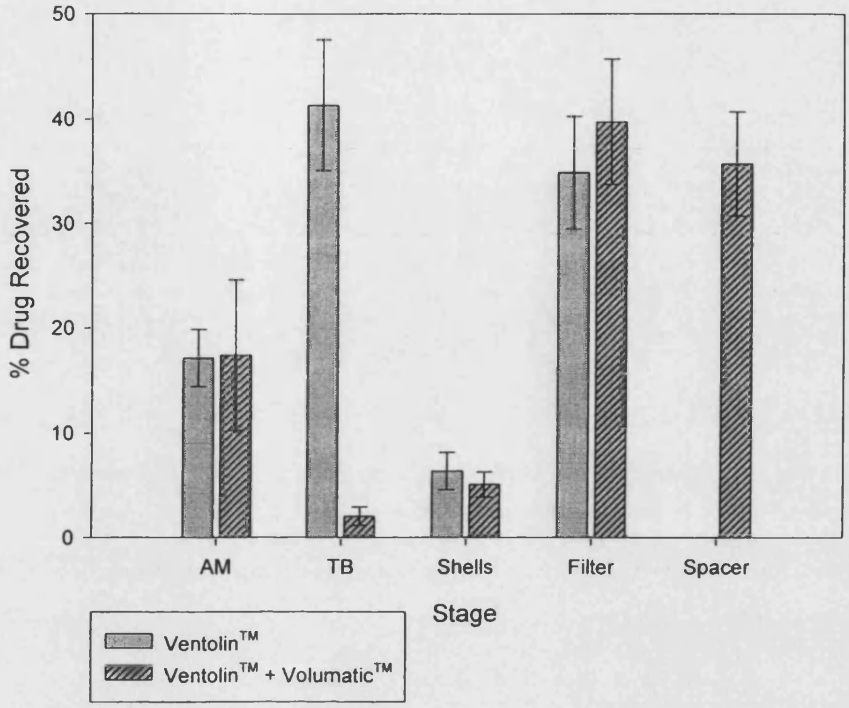

The results were analysed using one-way Analysis of Variance and it was found that the only significant difference seen when using the MDI alone or when using the spacer and the MDI together was in the Throat and bifurcation ($P< 0.05$). Although the mean value of drug deposited in the filter increased when the spacer device was used the difference was not found to be significant ($P=0.626$). A similar result for deposition in the mouth and throat was found *in vivo* ($p < 0.05$, 2-tailed student t-test) when analysing the pulmonary deposition of radiolabelled Fluticasone delivered using an MDI (Berridge *et al* 2000).

Unfortunately the total drug recovered in the first three experiments was below 800μg however even though these results cannot be considered to be reliable it is clear that the distinction between spacer and no spacer use is valid.

A comparison of the studies using spacers is summarised in Figure AX. The results of these studies display deposition in the oropharynx, lung and retention in the spacer where appropriate.

Figure B2 Comparison of spacer studies performed for MDI use.

Study	Device(s)	Oropharynx Deposition (%)	Lung Deposition (%)	Spacer Deposition (%)
Newman (1984)	MDI	80.9	8.7	
	MDI + Spacer	16.5	20.9	56
Hassanally (1987)	MDI	76.2	10.6	
	MDI + Spacer	1.5	21.2	55.7
Kim (1987)	MDI	33 – 71	29-67	
	MDI+Volumatic™ Spacer	<6	38	8-18
Mattys (1988)	MDI	64	26	
	MDI + Spacer	9.5	34	
Newman (1991)	MDI	78.2	12.8	
	MDI + Spacer	9.8	23.8	

The difference seen in the studies performed and summarised in Figure AX and the study presented here may be attributed to electrostatic effects.

Conclusion

It has been demonstrated that the use of a Volumatic™ spacer device with a Ventolin™ MDI reduces drug deposition in the throat and bifurcation of the SML. The evidence collected here does not demonstrate that an increase in lung deposition occurs with spacer

use. This study was performed when the first bifurcation was in use so it would be of value for the series of experiments to be repeated with the improved bifurcation in position.

Appendix C

SML diagrams from solid modelling package courtesy of Jeff Ward

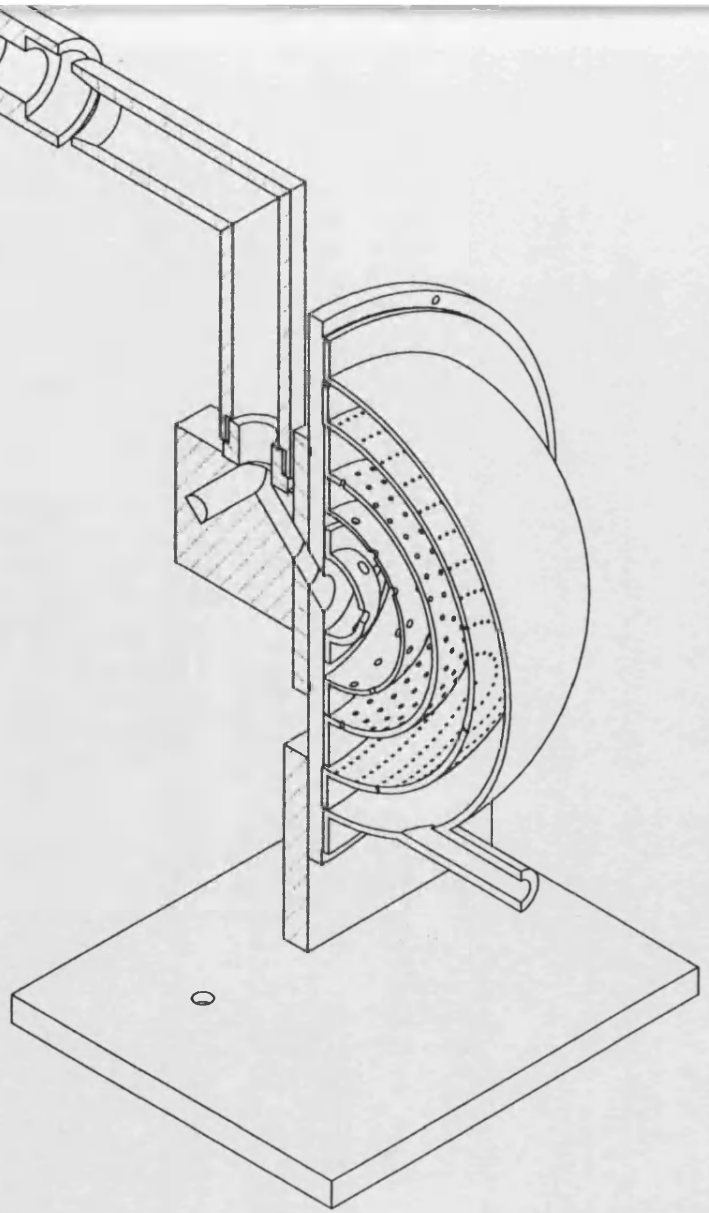

CUSTOMER:		TITLE:-	Cutaway General Arrangement
APPROVED:			
CHECKED:		USED ON:-	SERIAL No
DRAWN:	Jeff Ward	DRG No:-	RH-016 REV:
DATE:	5 Sep 2001	SCALE	SIZE: A3 Sheet 3 of 3

205

WITHOUT THE COMPANYS' PERMISSION | X.X ±0.2 X.XX ±0.1 | TOLERANCE ±0.25 | UNLESS OTHERWISE STATED | 3rd ANGLE PROJECTION

REV	DESCRIPTION	DATE	ACTIONED

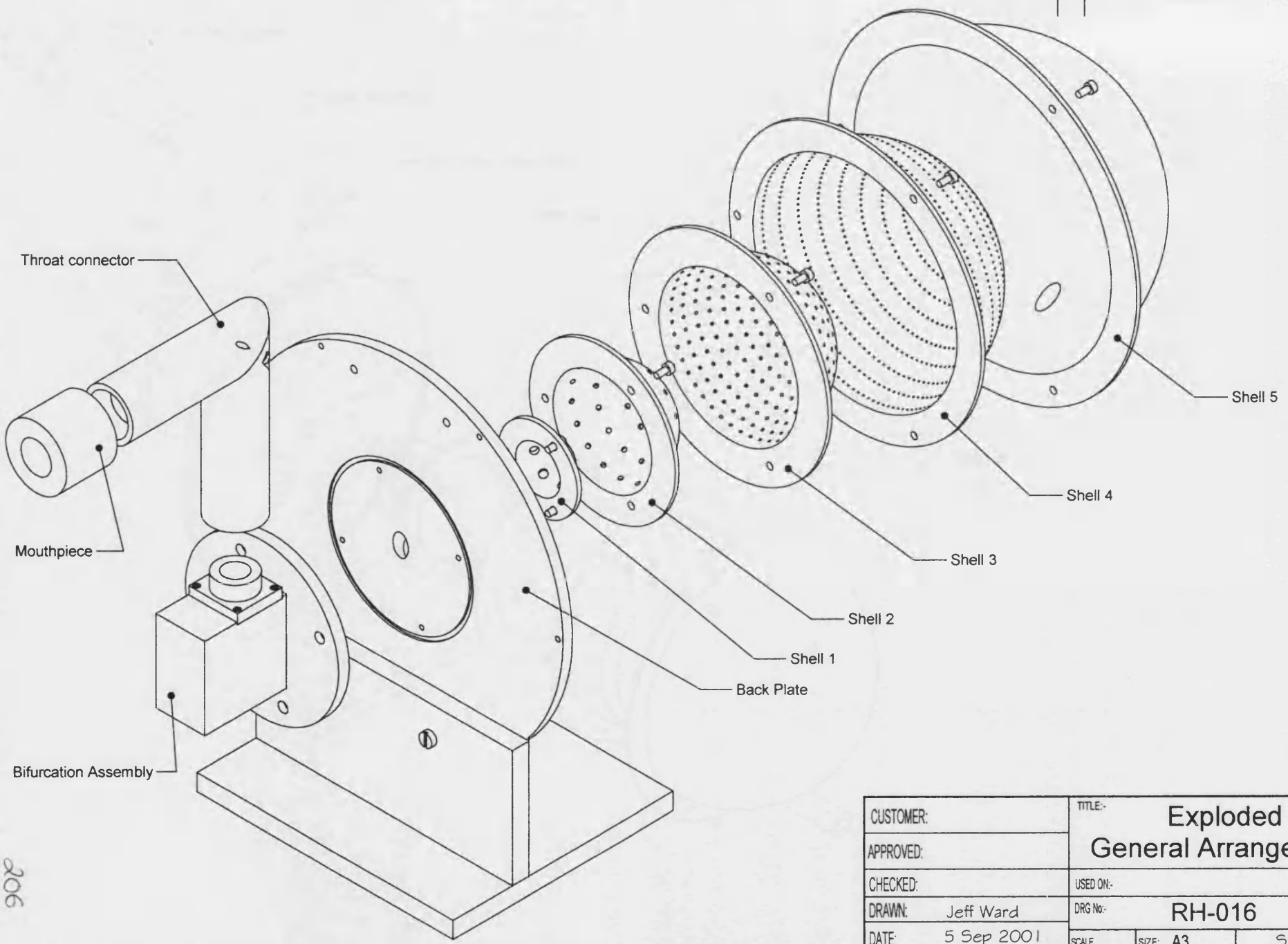

206

CUSTOMER:		TITLE:- Exploded General Arrangement	
APPROVED:			
CHECKED:		USED ON:-	SERIAL No
DRAWN:	Jeff Ward	DRG No:- RH-016	REV:
DATE:	5 Sep 2001	SCALE	SIZE: A3 Sheet 2 of 3

WITHOUT THE COMPANYS' PERMISSION | X.X ±0.2 X.XX ±0.1 | TOLERANCE ±0.25 | UNLESS OTHERWISE STATED | 3rd ANGLE PROJECTION

RH-016

REV	DESCRIPTION	DATE	ACTIONED

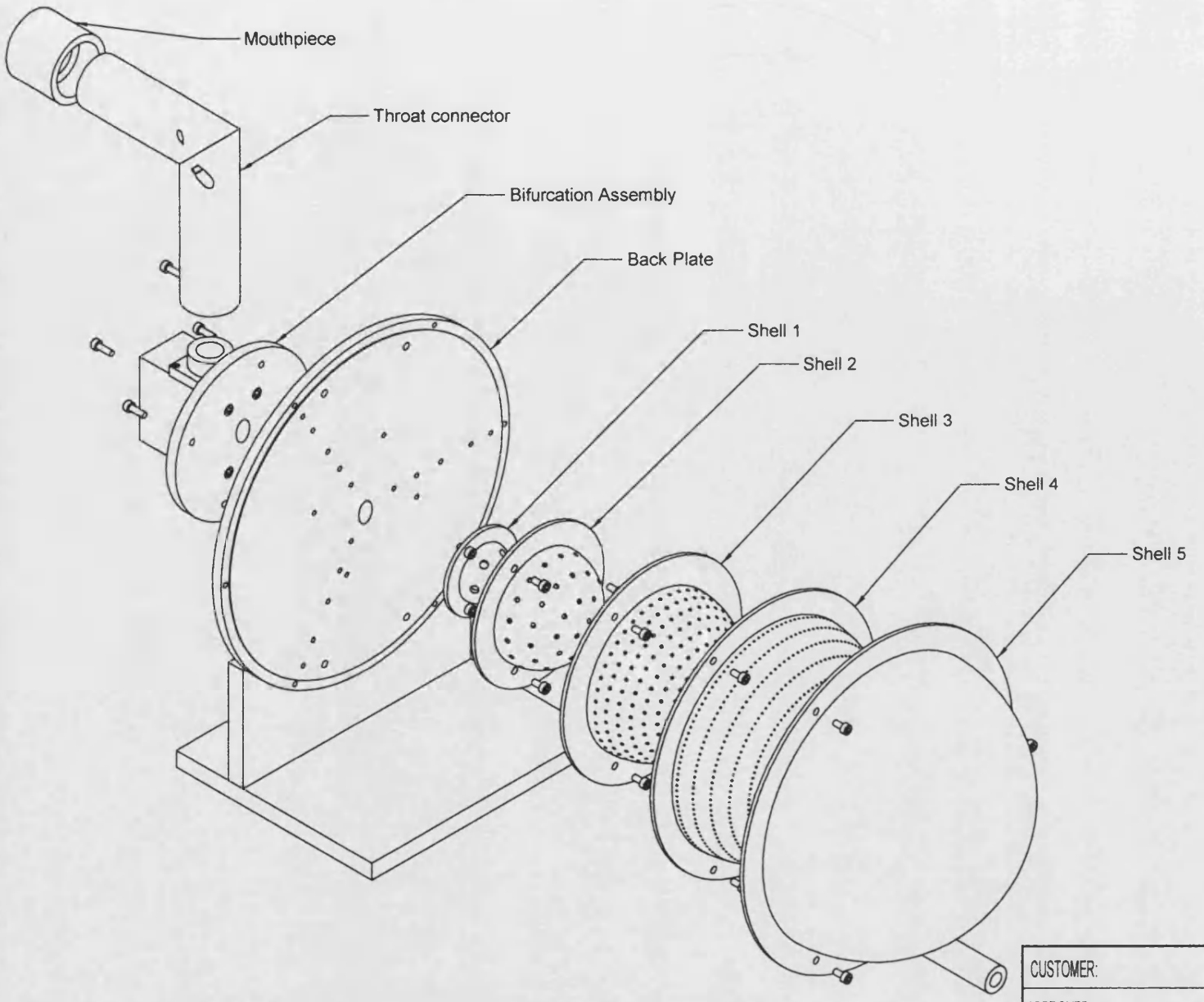

CUSTOMER:		TITLE:-	Exploded General Arrangement
APPROVED:			
CHECKED:		USED ON:-	SERIAL No
DRAWN:	Jeff Ward	DRG No:- RH-016	REV:
DATE:	5 Sep 2001	SCALE	SIZE: A3 Sheet 1 of 3

207

REV	DESCRIPTION	DATE	ACTIONED

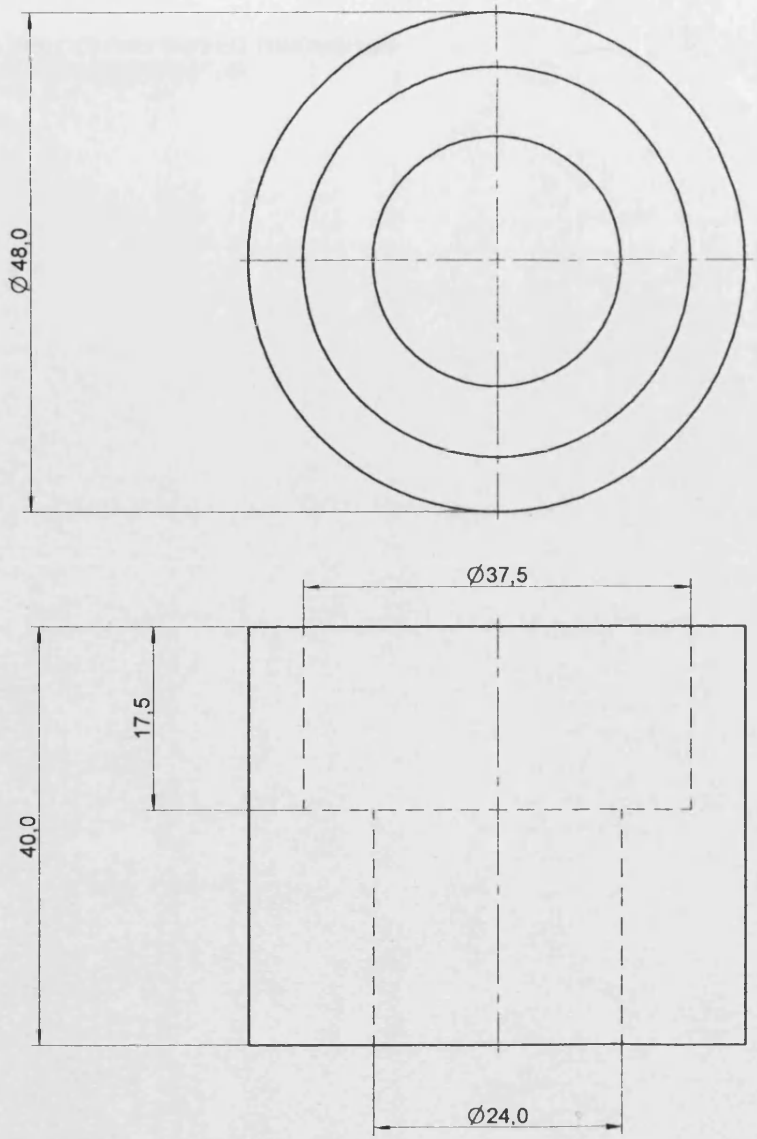

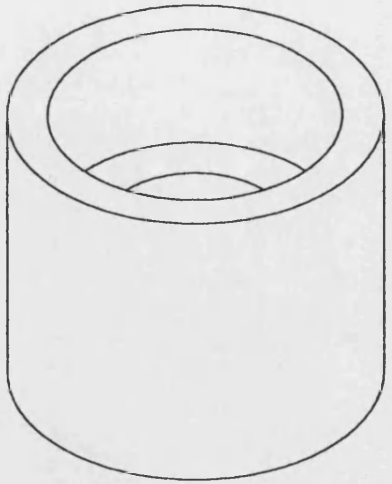

ISOMETRIC VIEW

MATERIAL: SOFT GREEN RUBBER

CUSTOMER:	TITLE:- Mouthpiece		
APPROVED:			
CHECKED:	USED ON:-	SERIAL No	
DRAWN: Jeff Ward	DRG No:- RH-010		REV:
DATE: 5 Sep 2001	SCALE	SIZE: A3	SHEET

A B C D E F G H

1 2 3 4 5 6 7 8 9 10

208

REV	DESCRIPTION	DATE	ACTIONED

2 HOLES DRILLED AND TAPPED THROUGH M4
IN CONJUNCTION WITH RH-009

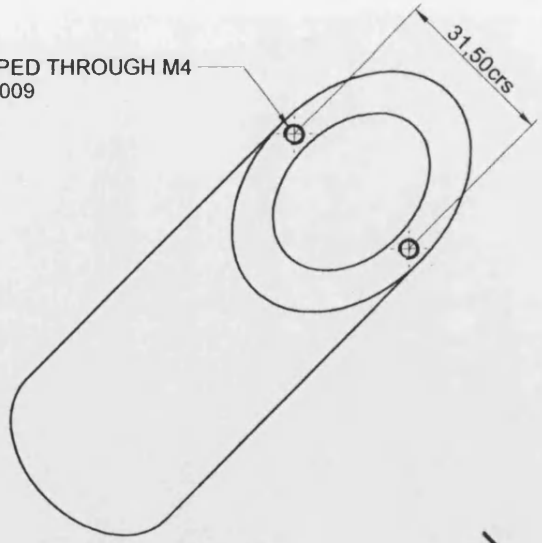

VIEW A

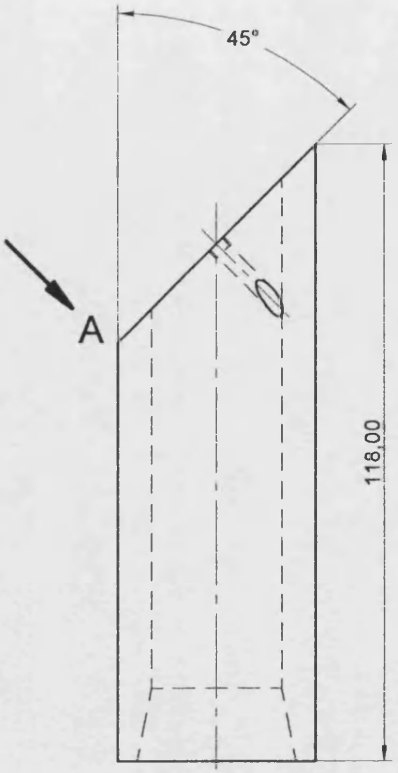

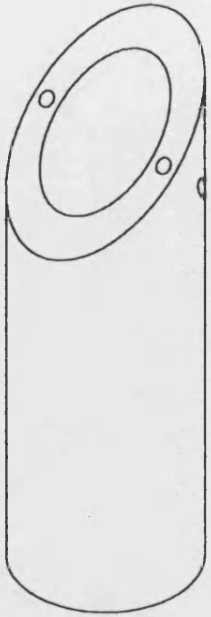

ISOMETRIC VIEW

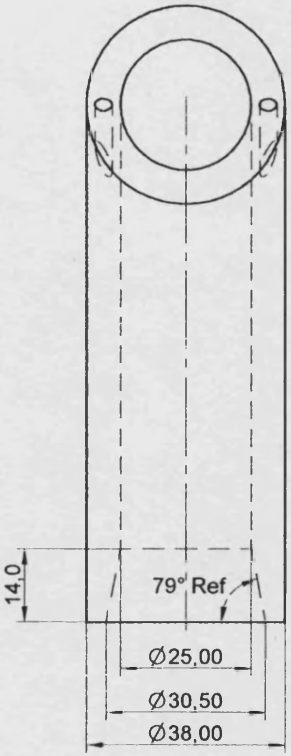

MATERIAL: ALUMINIUM ALLOY

CUSTOMER:		TITLE:- Throat (Inlet)	
APPROVED:			
CHECKED:		USED ON:-	SERIAL No
DRAWN:	Jeff Ward	DRG No:- RH-008	REV.
DATE:	5 Sep 2001	SCALE / SIZE: A3 / SHEET	

208

XXX ±0.1 ±0.25

REV	DESCRIPTION	DATE	ACTIONED

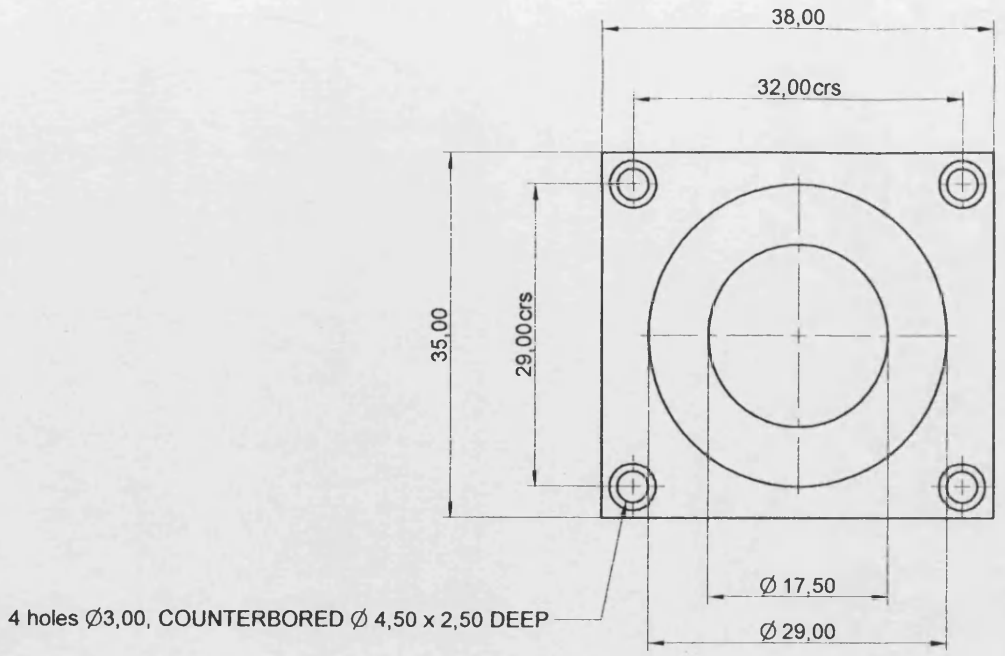

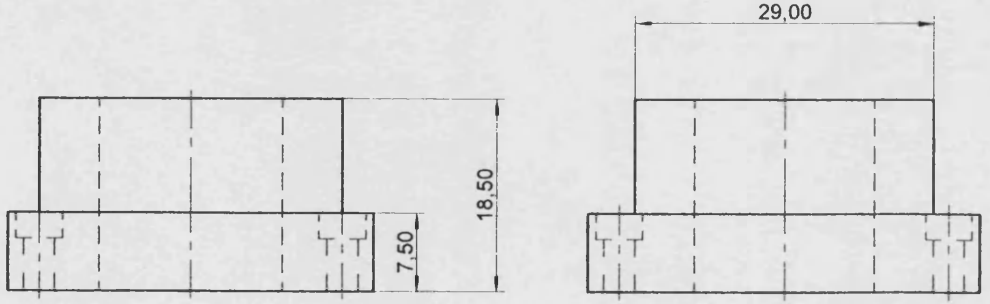

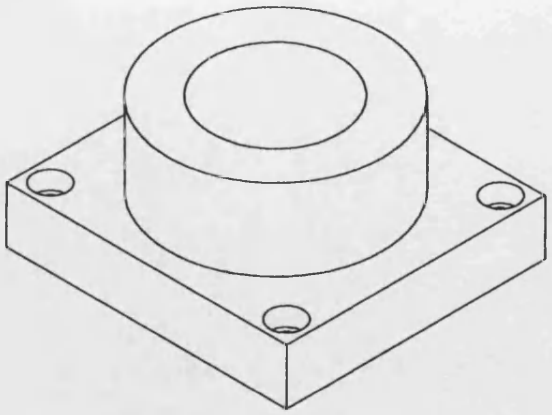

ISOMETRIC VIEWS

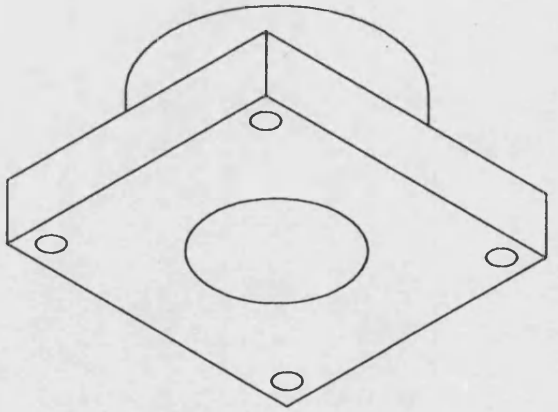

Material: Aluminium Alloy

CUSTOMER:	TITLE:- Bifurcation (Throat Connector)	
APPROVED:		
CHECKED:	USED ON:-	SERIAL No
DRAWN: Jeff Ward	DRG No:- RH-007	REV:
DATE: 5 Sep 2001	SCALE / SIZE: A3 / SHEET	

A B C D E F G H

1 2 3 4 5

210

REV	DESCRIPTION	DATE	ACTIONED

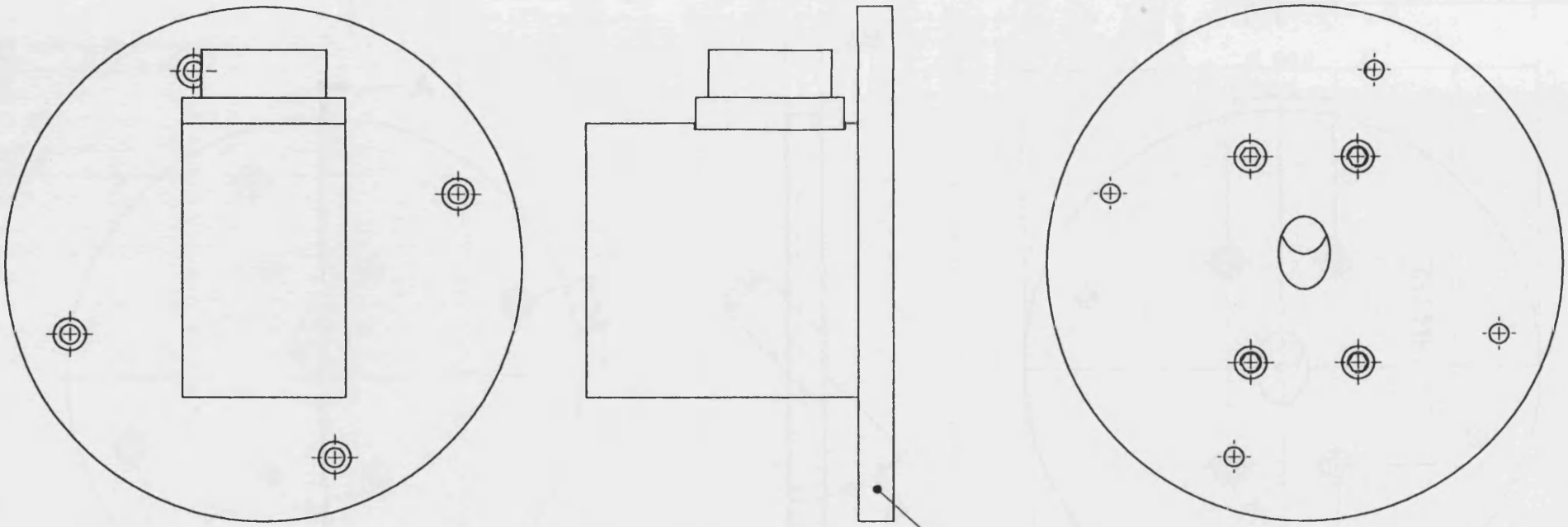

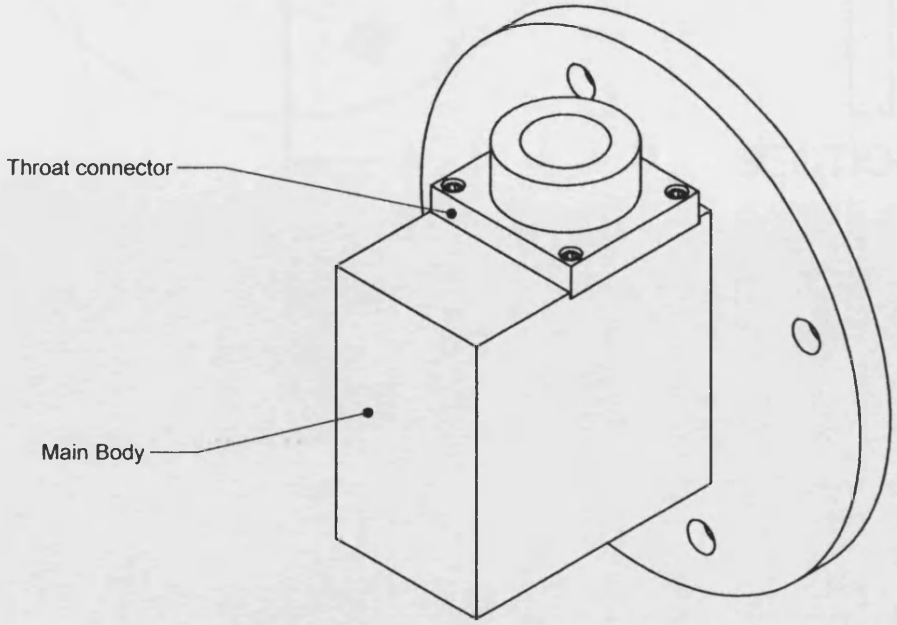

Back Plate Connector

CUSTOMER:	TITLE:- Bifurcation (complete)
APPROVED:	
CHECKED:	USED ON:- / SERIAL No
DRAWN: Jeff Ward	DRG No:- RH-004 / REV:
DATE: 5 Sep 2001	SCALE / SIZE: A3 / SHEET

112

X	±0.4	ANGULAR	UNLESS OTHERWISE STATED
X.X	±0.2	TOLERANCE	
X.XX	±0.1	±0.25	

3rd ANGLE PROJECTION

REMOVE SHARP EDGES

DWG NO. RH-006

REV	DESCRIPTION	DATE	ACTIONED

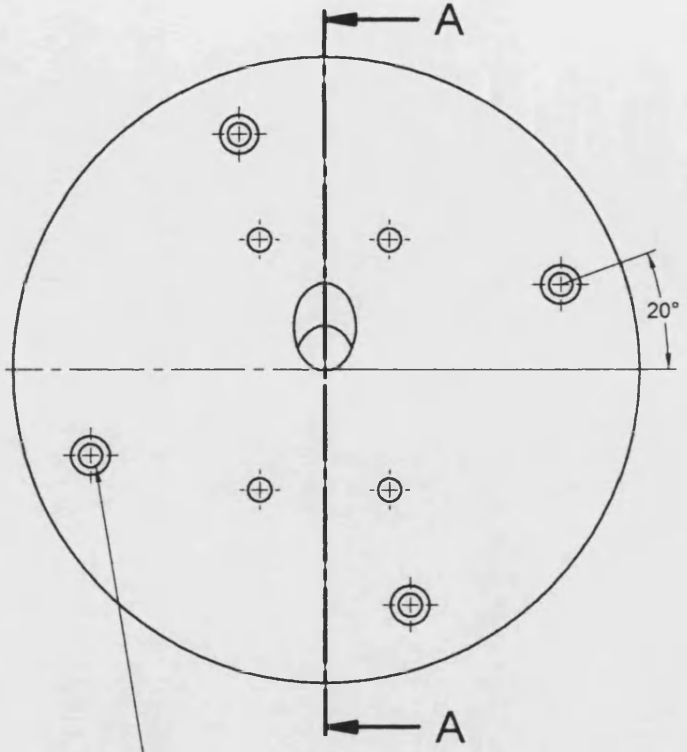

4 holes Ø4,5, COUNTERBORED 7,5 x 4,5 DEEP
EQUI-SPACED ON 96.00 PCD. OFFSET 20° AS SHOWN

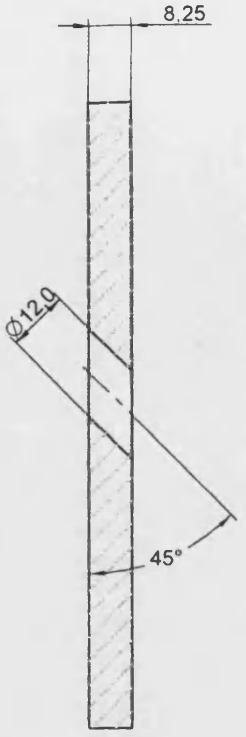

SECTION A-A

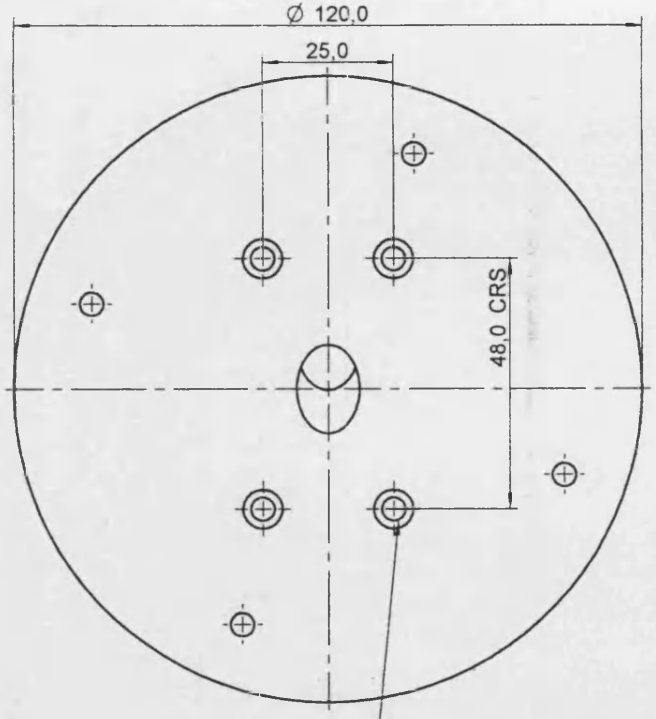

4 holes Ø4,5, COUNTERBORED Ø7,5 x 5,5

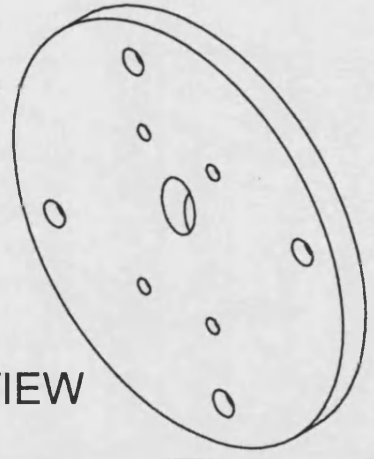

ISOMETRIC VIEW

CUSTOMER:		TITLE:-	Bifurcation (Back Plate connector)
APPROVED:			
CHECKED:		USED ON:-	SERIAL No
DRAWN:	Jeff Ward	DRG No:- RH-006	REV:
DATE:	5 Sep 2001	SCALE	SIZE: A3 SHEET

213

X	±0.4	ANGULAR	UNLESS OTHERWISE STATED
XX	±0.2	TOLERANCE	
XXX	±0.1	±0.25	

3rd ANGLE PROJECTION

REMOVE SHARP EDGES

DWG NO. RH-005

REV	DESCRIPTION	DATE	ACTIONED

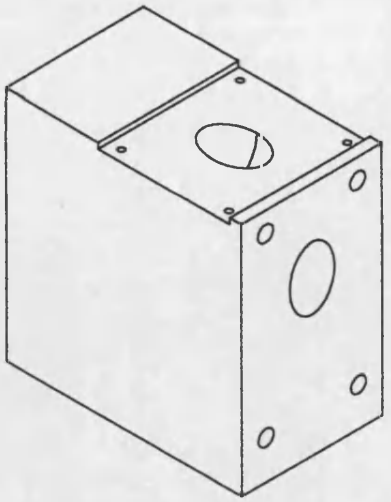

ISOMETRIC VIEW

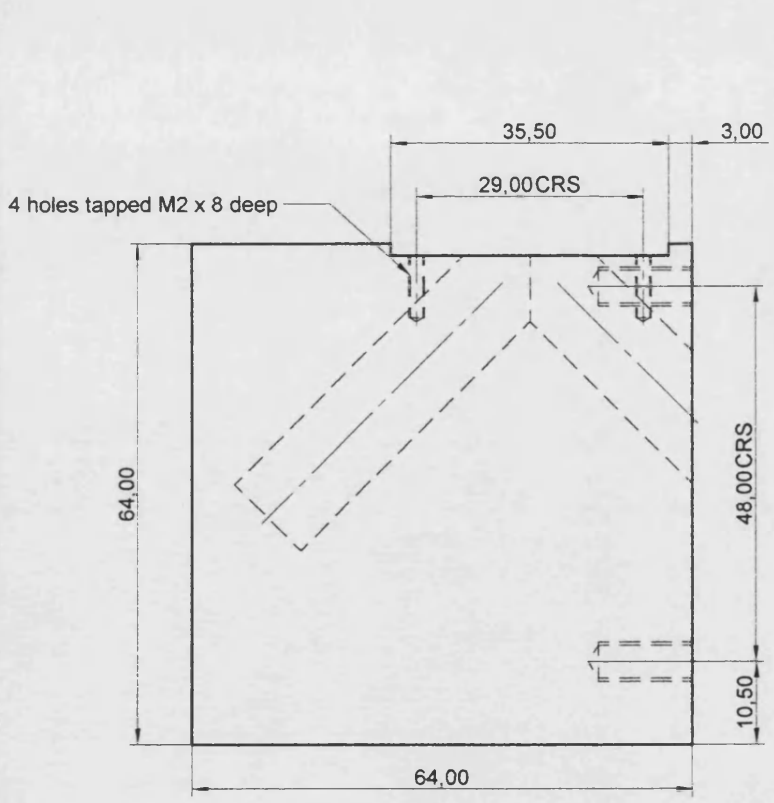

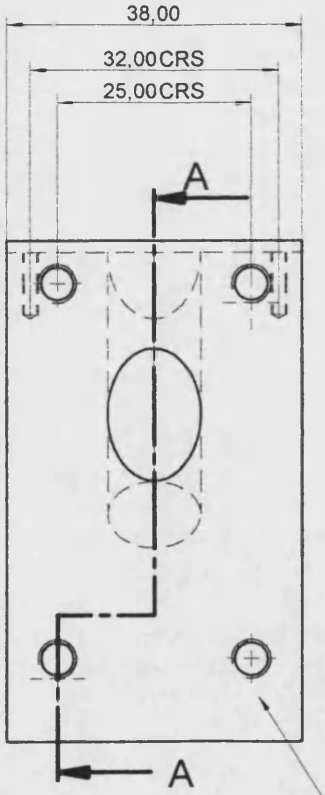

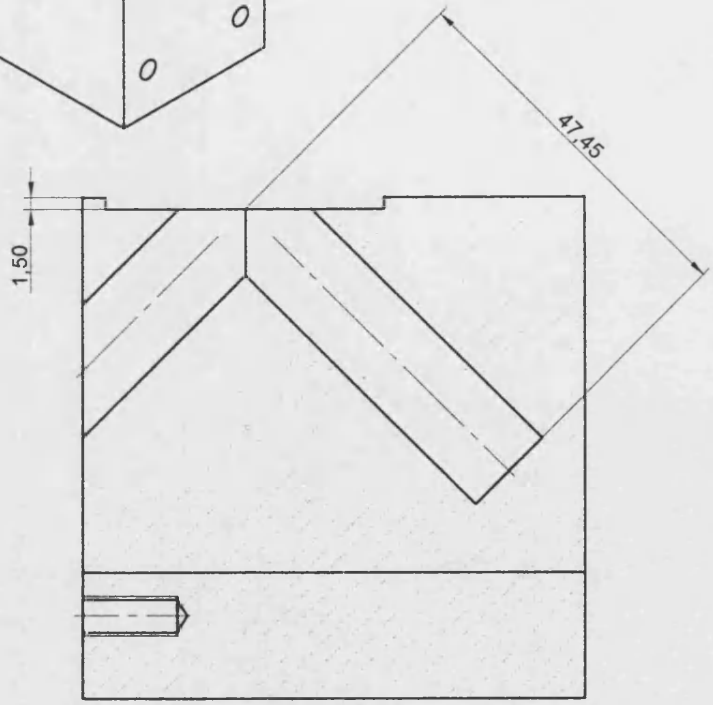

SECTION A-A

Material: Aluminium Alloy

NOTE
12 DIA HOLES TO BE BORED IN CONJUNCTION WITH COMPONENTS RH-001 AND RH-006

213

CUSTOMER:		TITLE:- Bifurcation (Main Body)	
APPROVED:			
CHECKED:		USED ON:-	SERIAL No
DRAWN:	Jeff Ward	DRG No:- RH-005	REV:
DATE:	5 Sep 2001	SCALE	SIZE: A3 SHEET

UNSPECIFIED TOLERANCES
X ±0.4 ANGULAR
X.X ±0.2 TOLERANCE
X.XX ±0.1 ±0.5

DIMENSIONS IN MILLIMETRES UNLESS OTHERWISE STATED

3rd ANGLE PROJECTION

DO NOT SCALE—IF IN DOUBT 'ASK'

DWG NO: RH-001 REV *

REVISIONS				
REV	DESCRIPTION	DATE	EC No	APPROVED
*	*	*	*	

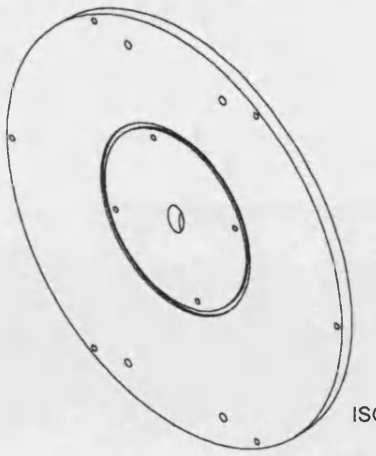

ISOMETRIC VIEW

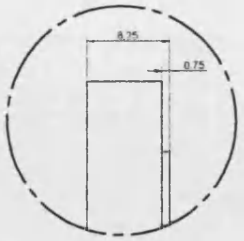

DETAIL B

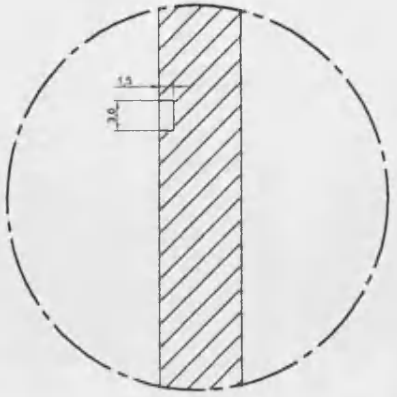

DETAIL C

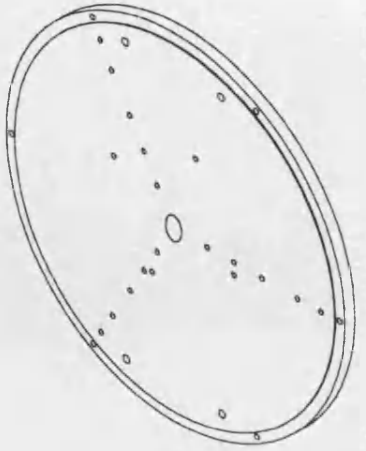

ISOMETRIC VIEW

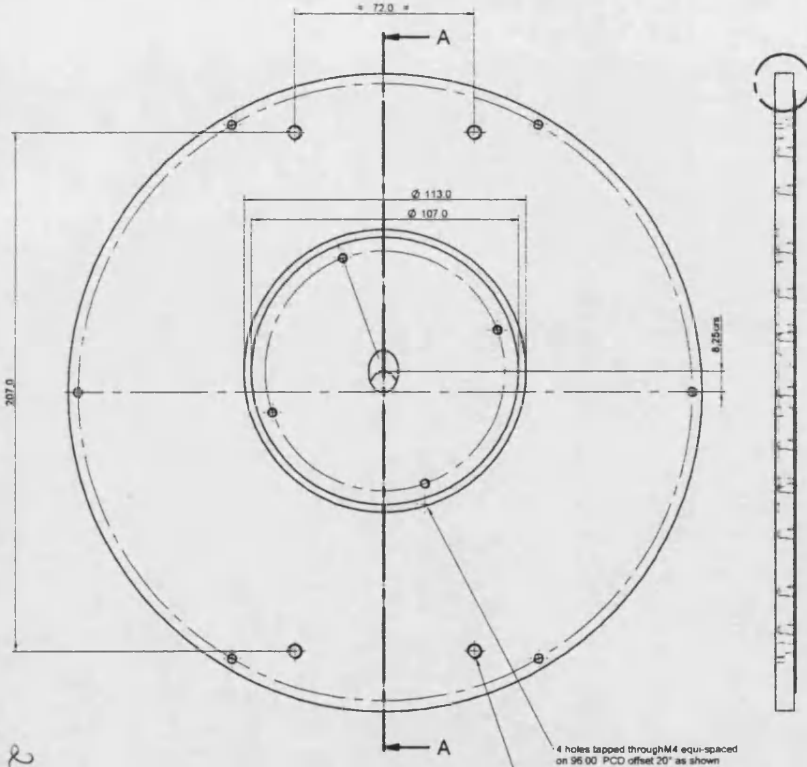

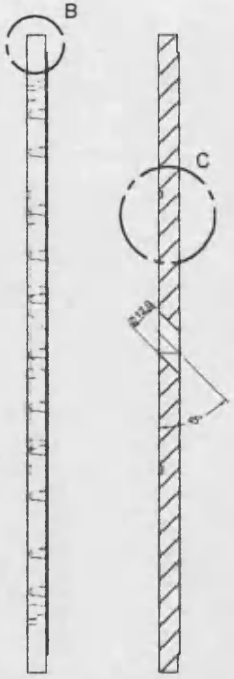

SECTION A-A

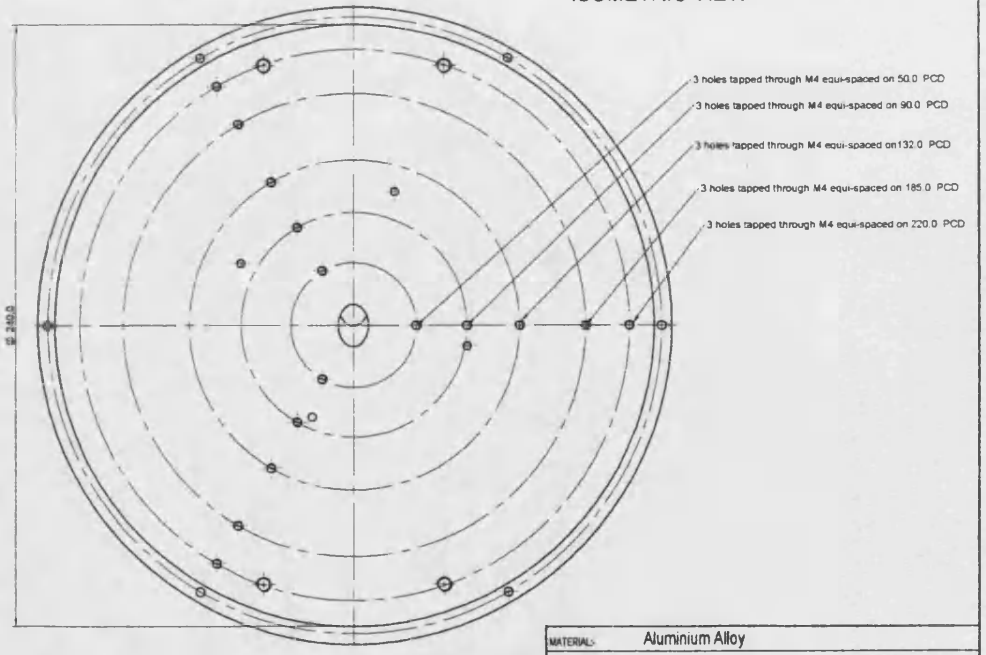

NOTE
12 Dia hole to be bored in conjunction with components RH-005 and RH-006

MATERIAL:	Aluminium Alloy		
FINISH:			
CUSTOMER:		TITLE:	Back Plate
APPROVED:			
CHECKED:		USED ON:	SERIAL No
DRAWN:	Jeff Ward	DWG NO:	RH-001 REV *
DATE:	5 Sept 2001	SCALE: NTS A3	SHEET 1 # 1

X	±0.4	ANGULAR
X.X	±0.2	TOLERANCE
X.XX	±0.1	±0.25

UNLESS OTHERWISE STATED

3rd ANGLE PROJECTION

REMOVE SHARP EDGES

DWG NO. RH-002

REV	DESCRIPTION	DATE	ACTIONED

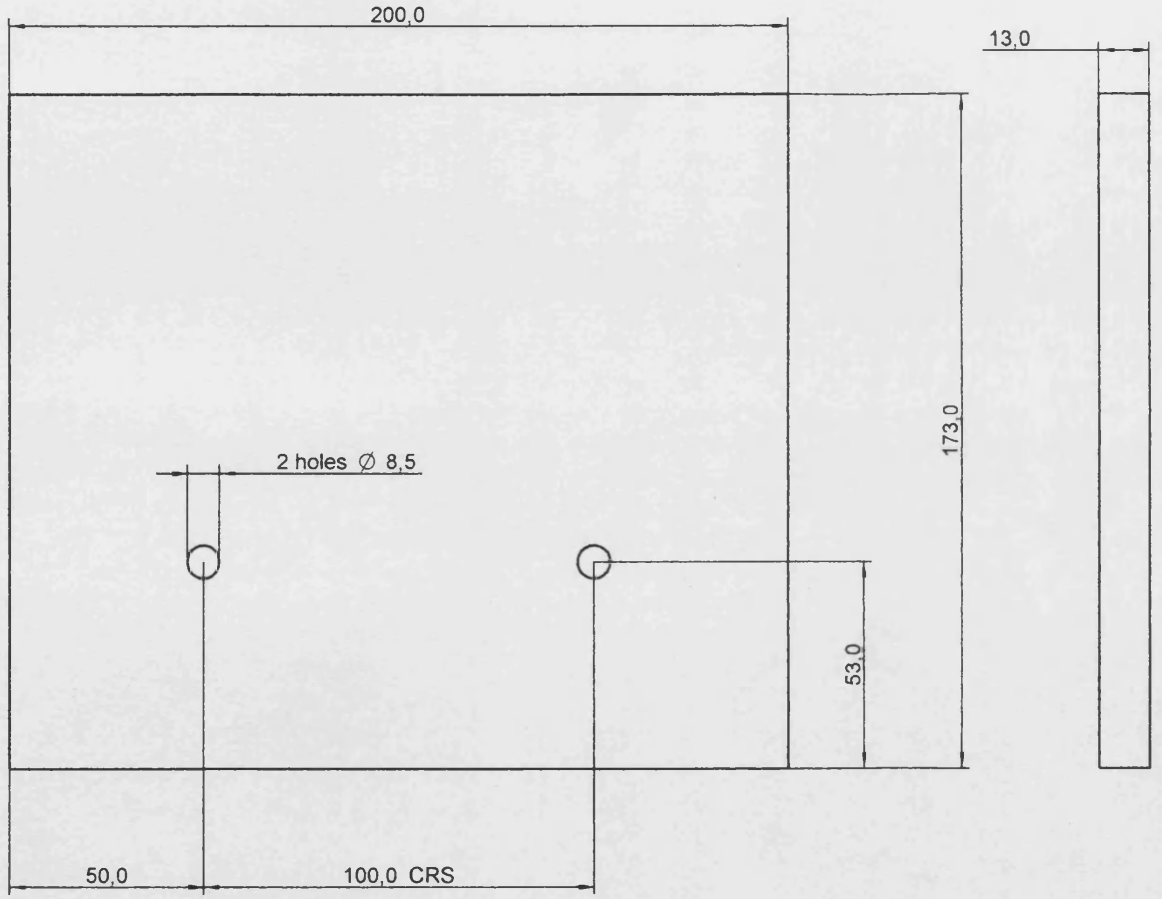

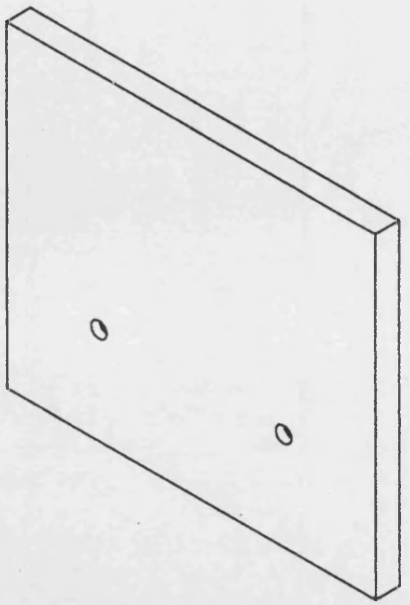

Isometric view

MATL: ALUMINIUM ALLOY

CUSTOMER:	TITLE:- Base Plate
APPROVED:	
CHECKED:	USED ON:- / SERIAL No
DRAWN: Jeff Ward	DRG No:- RH-002 / REV:
DATE: 5 Sep 2001	SCALE NTS / SIZE: A3 / SHEET

215

X ±0.4	ANGULAR TOLERANCE ±0.25	DIMENSIONS IN MILLIMETRES UNLESS OTHERWISE STATED	3rd ANGLE PROJECTION	REMOVE SHARP EDGES	DO NOT SCALE IF IN DOUBT 'ASK'
X.X ±0.2					DWG NO. RH-003
X.XX ±0.1					

REV	DESCRIPTION	DATE	ACTIONED

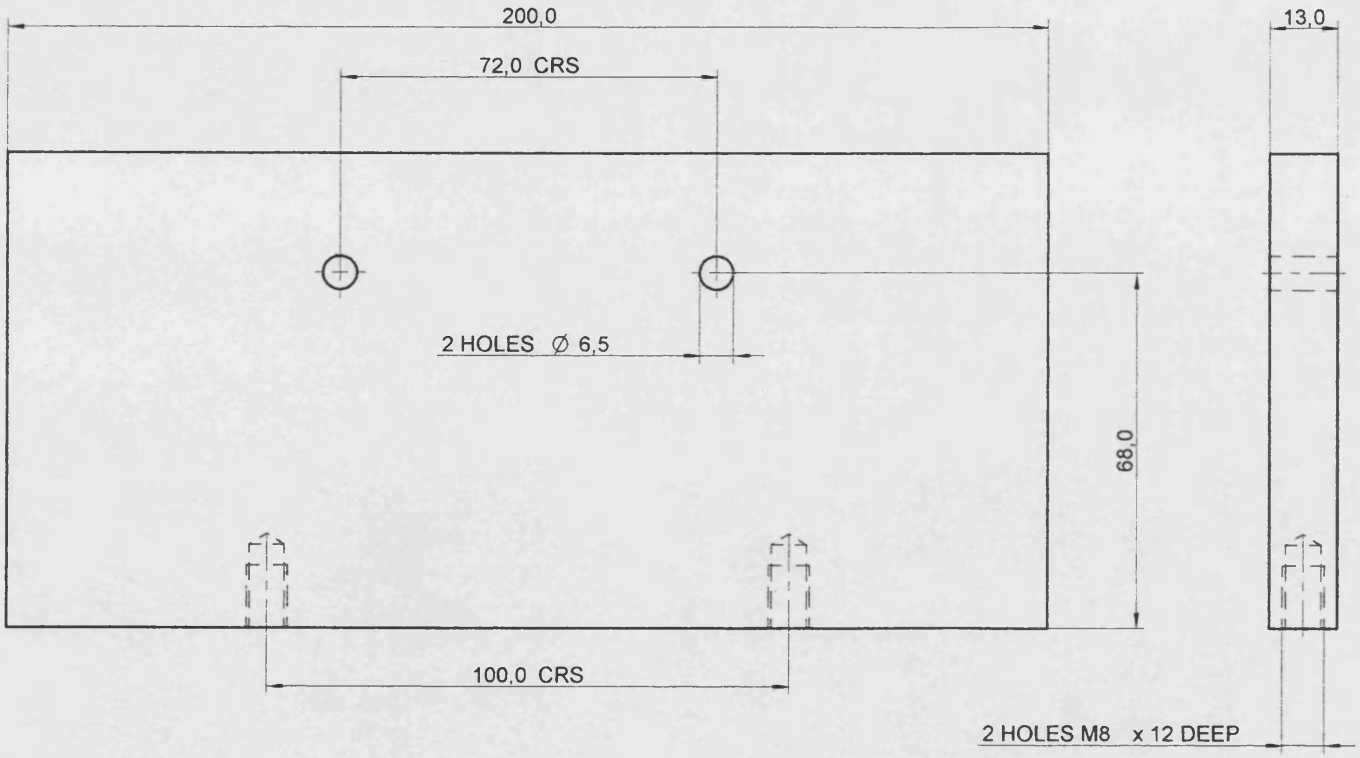

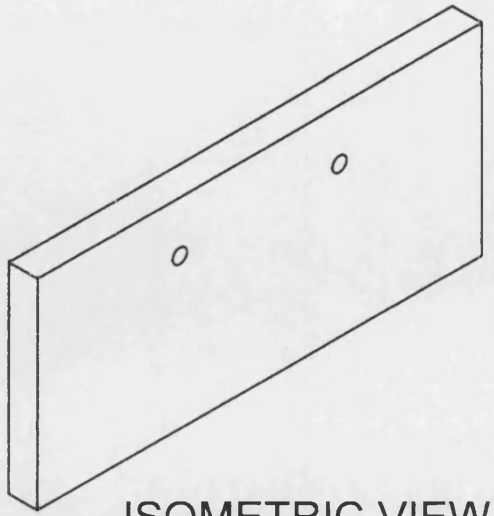

ISOMETRIC VIEW

MATERIAL ALUMINIUM ALLOY

CUSTOMER:		TITLE:- Vertical Support Plate	
APPROVED:			
CHECKED:		USED ON:-	SERIAL No
DRAWN: Jeff Ward		DRG No.- RH-003	REV:
DATE: 5 Sep 2001		SCALE	SIZE: A3 SHEET

216

REV	DESCRIPTION	DATE	ACTIONED

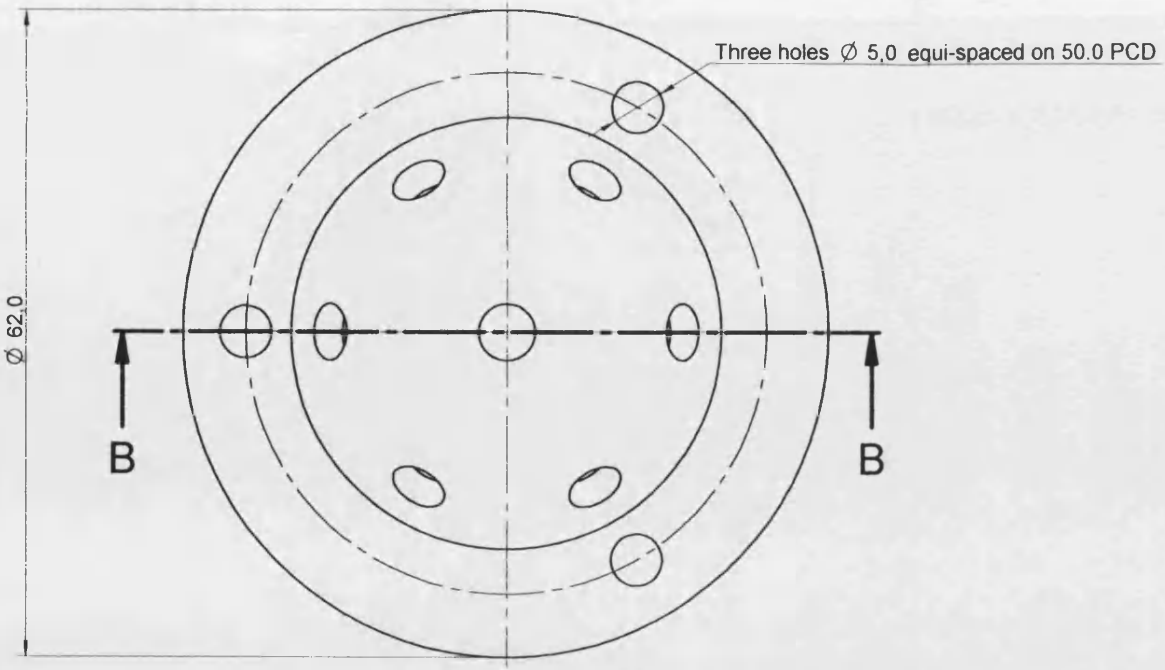

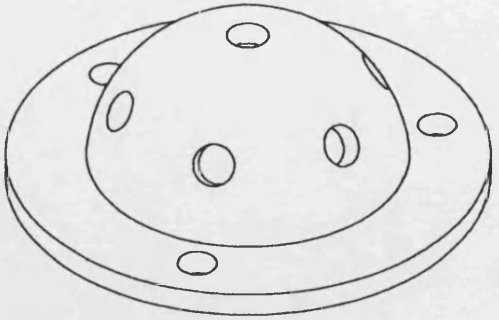

ISOMETRIC VIEW

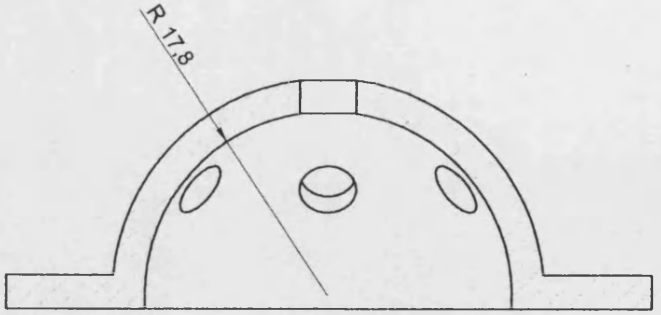

SECTION A-A

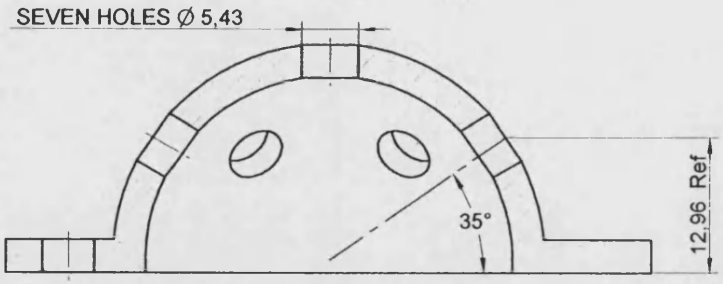

SECTION B-B

CUSTOMER:	TITLE:- Shell 1		
APPROVED:			
CHECKED:	USED ON:-	SERIAL No	
DRAWN: Jeff Ward	DRG No:- RH-011		REV:
DATE: 5 Sep 2001	SCALE	SIZE: A3	SHEET

217

X	±0.4	ANGULAR TOLERANCE	±0.25
X.X	±0.2		
X.XX	±0.1		

UNLESS OTHERWISE STATED | 3rd ANGLE PROJECTION | REMOVE SHARP EDGES | DWG NO. RH-012

REV	DESCRIPTION	DATE	ACTIONED

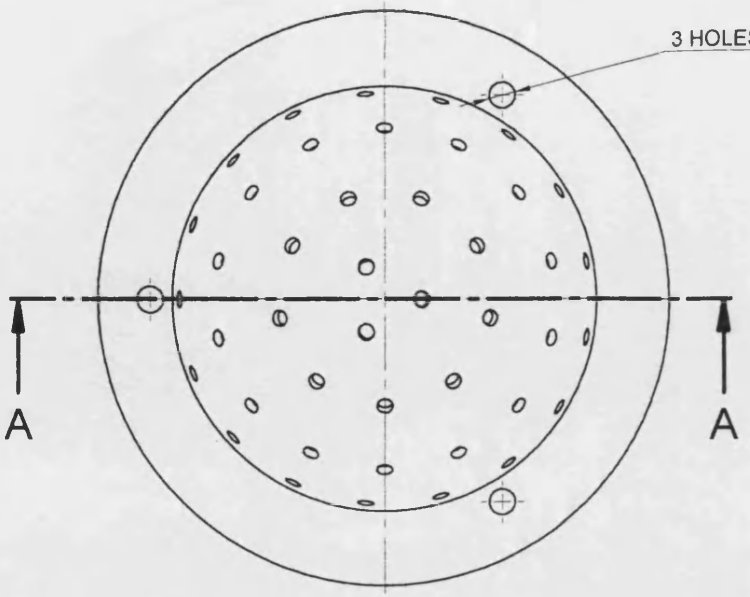

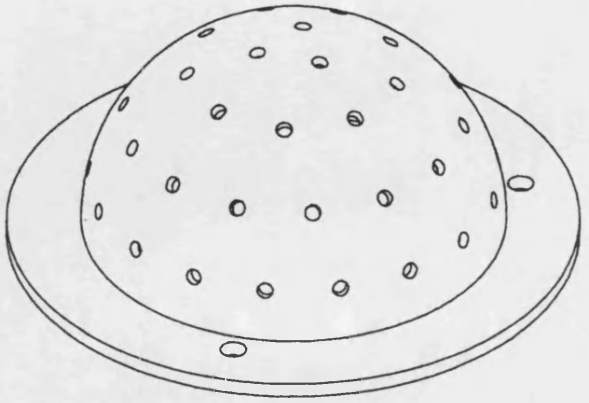

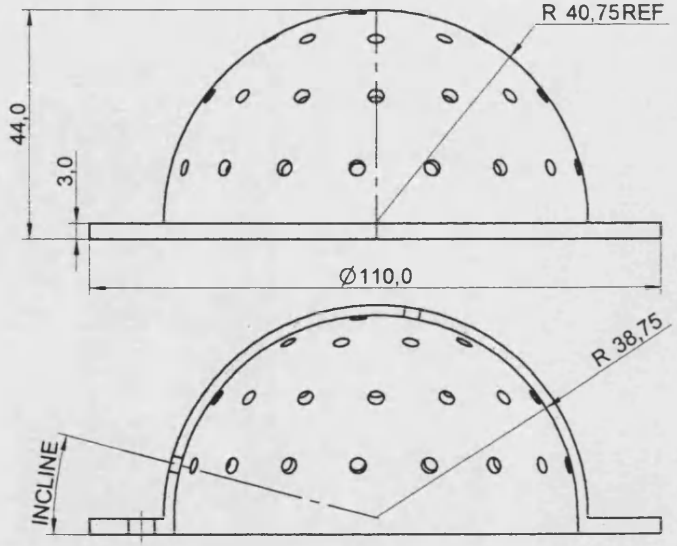

SECTION A-A

	INCLINE	HOLE DIA	NUMBER OF HOLES
Row 1	15°	3.02	17
Row 2	40°	3.02	14
Row 3	60°	3.02	9
Row 4	80°	3.02	3

MATL: ALUMINIUM ALLOY

CUSTOMER:	TITLE:- SHELL 2	
APPROVED:		
CHECKED:	USED ON:-	SERIAL No
DRAWN: Jeff Ward	DRG No:- RH-012	REV:
DATE: 5 Sep 2001	SCALE / SIZE: A3 / SHEET	

212

X	±0.4	ANGULAR	UNLESS OTHERWISE STATED
X.X	±0.2	TOLERANCE	
X.XX	±0.1	±0.25	

3rd ANGLE PROJECTION

REMOVE SHARP EDGES

DWG NO. RH-013

REV	DESCRIPTION	DATE	ACTIONED

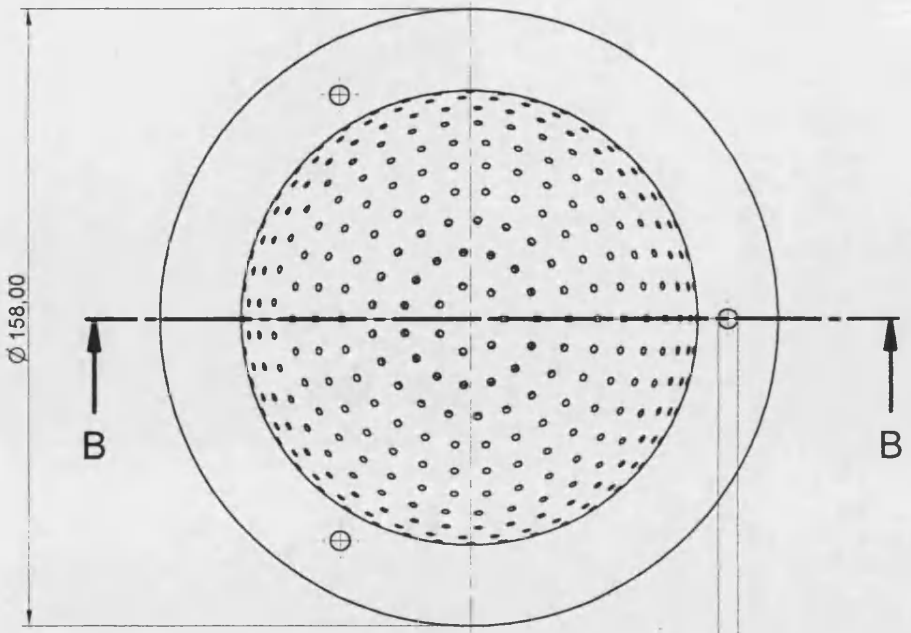

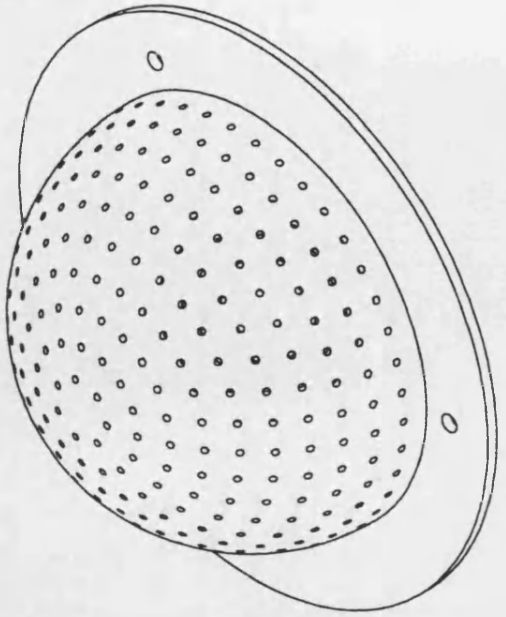

ISOMETRIC VIEW

	INCLINE	HOLE DIA	NUMBER OF HOLES
Row 1	10°	1.82	44
Row 2	18°	1.82	43
Row 3	26°	1.82	41
Row 4	34°	1.82	37
Row 5	42°	1.82	34
Row 6	50°	1.82	30
Row 7	58°	1.82	26
Row 8	66°	1.82	21
Row 9	74°	1.82	15
Row 10	82°	1.82	7

MATL: ALUMINIUM ALLOY

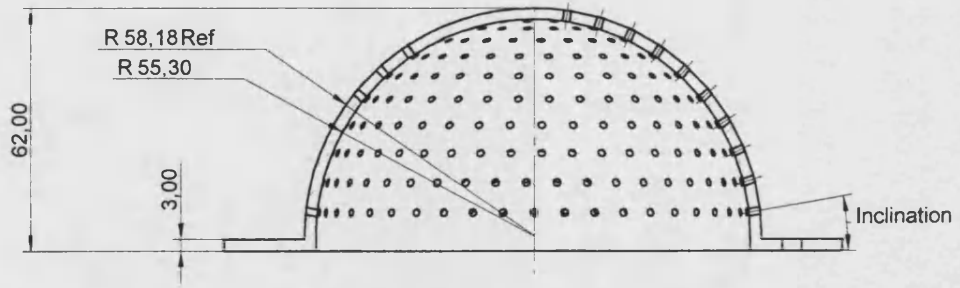

SECTION B-B

CUSTOMER:		TITLE:- SHELL 3	
APPROVED:			
CHECKED:		USED ON:-	SERIAL No
DRAWN:	Jeff Ward	DRG No:- RH-013	REV:
DATE:	5 Sep 2001	SCALE	SIZE: A3 SHEET

1 2 3 4 5 6 7 8 9 10

REV	DESCRIPTION	DATE	ACTIONED

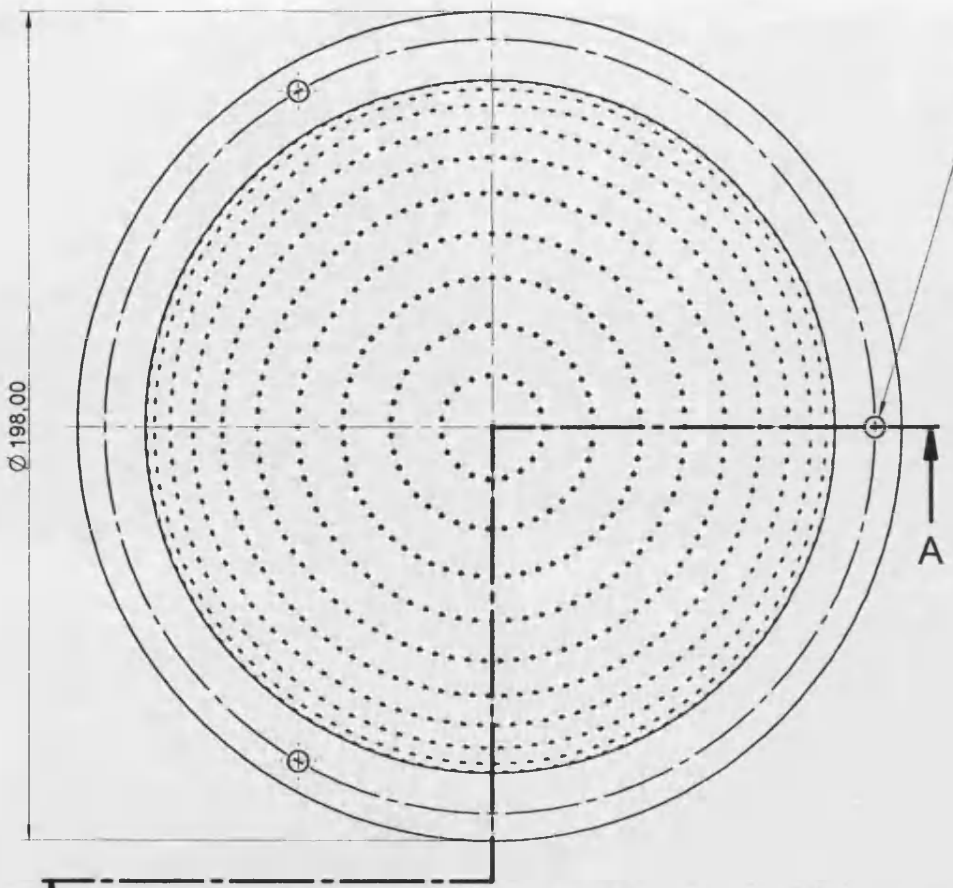

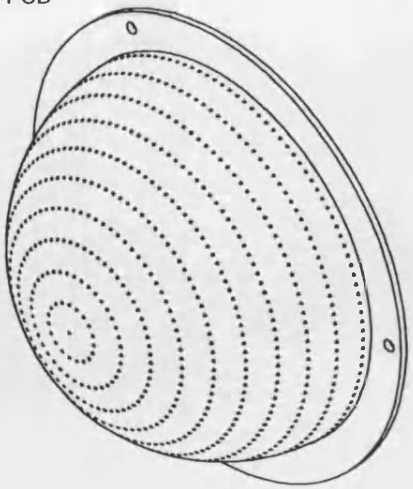

ISOMETRIC VIEW

Shell 4			
Number of row	Number of holes	Inclination	Δ α
1	127	5	2.833333
2	127	7.83333333	
3	126	10.6666667	
4	125	13.5	
5	123	16.3333333	
6	119	19.1666667	
7	118	22	
8	117	24.8333333	
9	115	27.6666667	
10	113	30.5	
11*	112	33.3333333	
12	110	36.1666667	
13	107	39	
14	103	41.8333333	
15	94	44.6666667	
16	90	47.5	
17	81	50.3333333	
18	80	53.1666667	
19	72	56	
20	67	58.8333333	
21	65	61.6666667	
22	60	64.5	
23	48	67.3333333	
24	45	70.1666667	
25	39	73	
26	31	75.8333333	
27	25	78.6666667	
28	19	81.5	
29	12	84.3333333	
30	7	87.1666667	
31	1	90	
	2478		
Gaps =	30		
Hole dia =	0.99		
Flange dia	198		
Flange thickness	3		
Fixing hole dia	5		
Fixing hole number	3		
Fixing hole PCD	185		
Shell thickness	3.04		
Shell int dia	160		
Overall height	83		

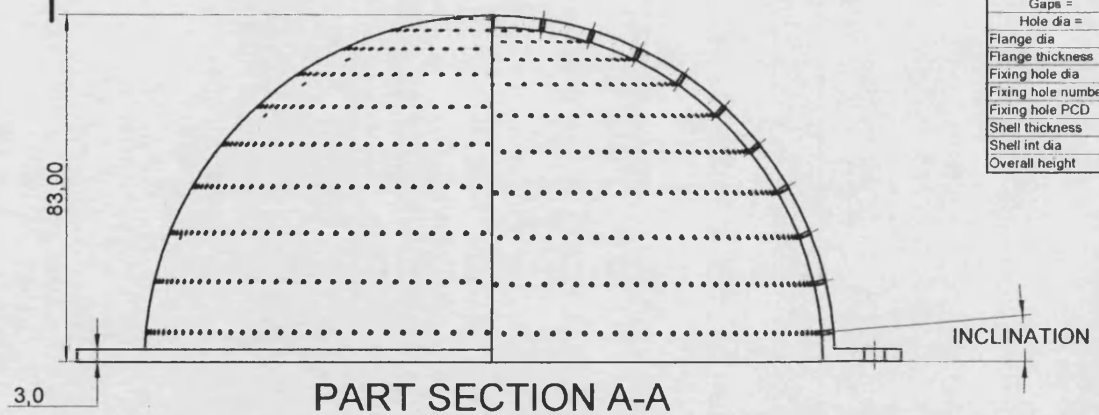

PART SECTION A-A

MATL: ALUMINIUM ALLOY

CUSTOMER:		TITLE:- Shell 4	
APPROVED:			
CHECKED:		USED ON:-	SERIAL No
DRAWN:	Jeff Ward	DRG No:- RH-014	REV:
DATE:	5 Sep 2001	SCALE	SIZE: A3 SHEET

220

UNSPECIFIED TOLERANCES
X ±0.4 ANGULAR
X.X ±0.2 TOLERANCE
X.XX ±0.1 ±0.25

DIMENSIONS IN MILLIMETRES UNLESS OTHERWISE STATED

3rd ANGLE PROJECTION

REMOVE SHARP EDGES

DO NOT SCALE IF IN DOUBT 'ASK'

DWG NO. RH-015 REV

REV	DESCRIPTION	DATE	ACTIONED

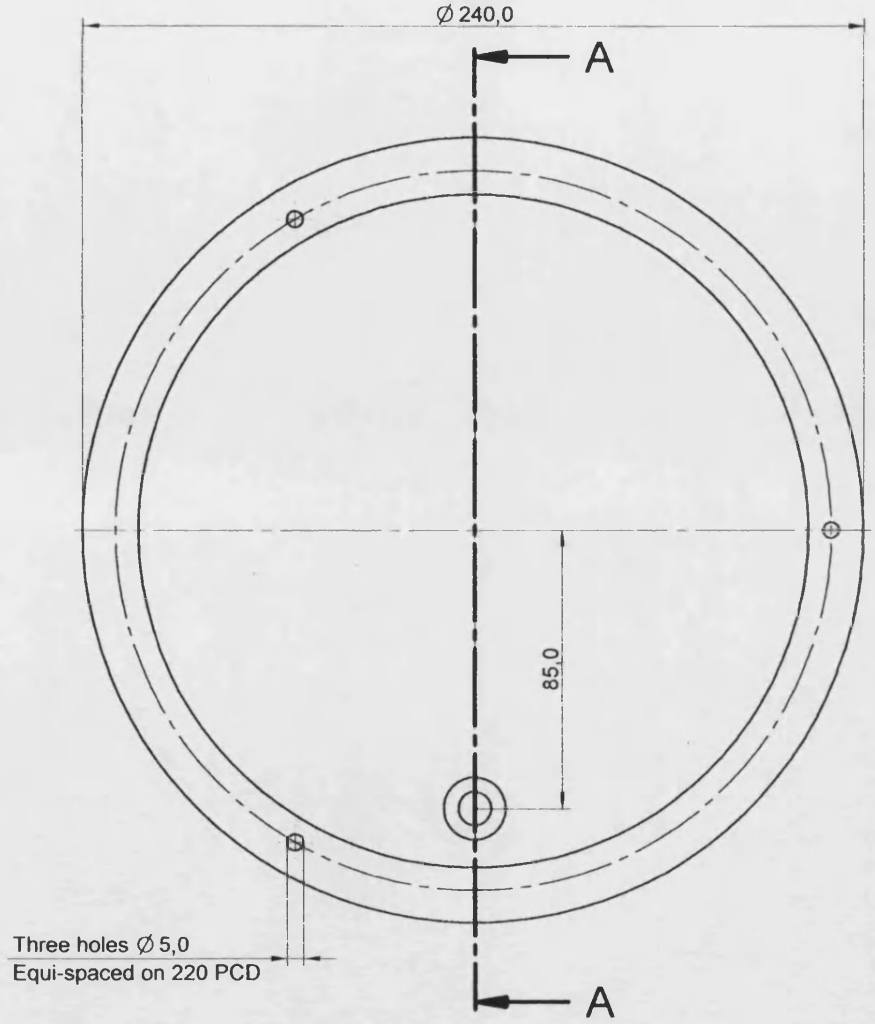

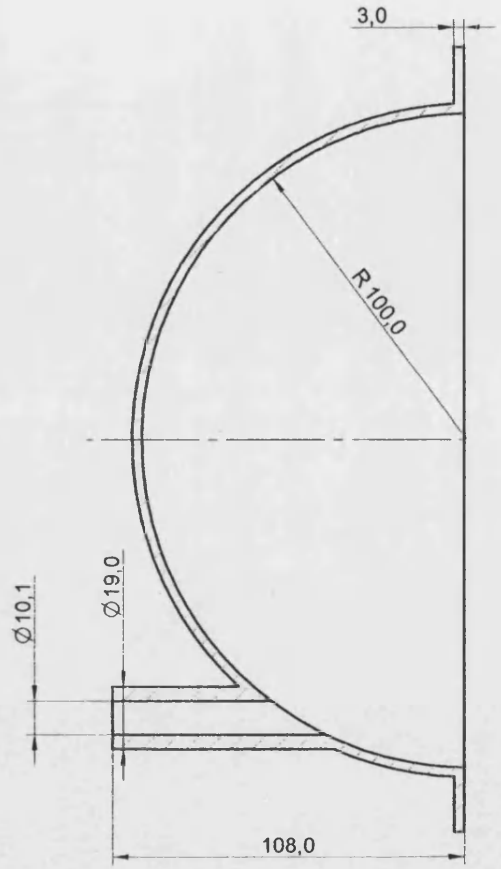

SECTION A-A

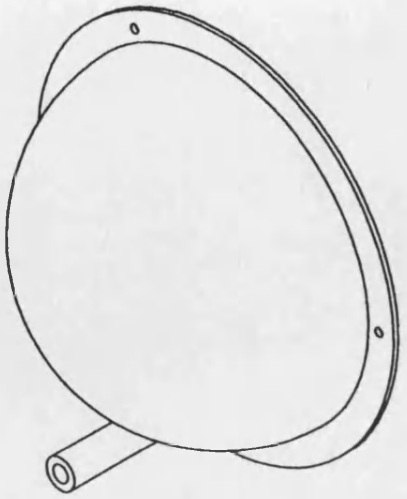

Isometric Views

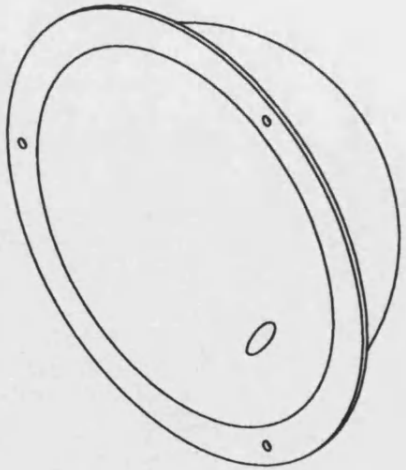

MATL: ALUMINIUM ALLOY

CUSTOMER:	TITLE:- SHELL 5
APPROVED:	
CHECKED:	USED ON:- SERIAL No
DRAWN: Jeff Ward	DRG No:- RH-015 REV.
DATE: 5 Sep 2001	SCALE SIZE: A3 SHEET

1838

References

Agnew, J.E., Lopez-Vidriero, M.T., Pavia, D. and Clarke, S.W. Functional small airways defence in symptomless cigarette smokers. *Thorax.* 41:524-530. 1986.

Andersen, A. A. *Development work on the Andersen Sampler.* Dugway Proving Ground Research Report 108, Dugway, Utah, November 13, 1956.

Asking, L. and Olsson, B. Calibration at different flow rates of a Multistage Liquid Impinger. *Aer. Sci. and Tech.* 27:39-49. 1997.

Balásházy, I., Heistracher, T. and Hofmann, W. Air flow and particle deposition paterns in bronchial airway bifurcations: The effect of different CFD models and bifurcation geometries. *J. Aer. Med.* Vol 9. No3. 287-301. 1996.

Berglund, R.N. and Liu B.Y.H., Generation of monodisperse aerosol standards. *Env. Sci. and Tech.* Vol.7. N° 2. 147-152. 1973.

Berridge, M.S., Lee Z. and Heald D.L. Pulmonary deposition and distribution as a function of spacer use. *RDD VII.* 553-555. 2000.

Biddiscombe, M.F., Melchor, R., Mak, V.H.F., Marriott, R.J., Taylor, A.J., Short, M.D. and Spiro, S.G. The lung deposition of salbutamol, directly labelled with

technecium-99m, delivered by pressurised metered dose and dry powder inhalers. *Int. J. Pharm.* 91:111-121. 1993.

Borgström, L., Bengtsson, T., Dermon, E. and Pauwels, R. Variability in lung deposition of inhaled drug, within and between asthmatic patients, with a pMDI and a dry powder inhaler, Turbuhaler®. *Int. J. Pharm.* 193. 227-230. 2000.

Borgström, L. and Newman, S., Total and regional lung deposition of Terbutaline sulphate inhaled via a pressurised MDI or via Turbuhaler®. *Int. J. Pharm.* Vol 97. 47-53. 1993.

Brindley, A., Reaville, K.J., Sumby, B.S. and Smith, I.J. The *in vitro* characteristics of inhalation devices using the Electronic Lung™. *RDD VI.* 143-151-1994.

British Pharmacopoeia. Her Majesty's Stationary Office, London, UK: 1993.

Byron, P., *Pharmaceutical Forum.* In-process revision, Aerosols USP <601> 23. 6. 5223. 1997.

Byron, P.R., Peart, J. and Staniforth, J.N. Aerosol electrostatics I: properties of fine powders before and after aerosolization by dry powder inhalers. *Pharm. Res.* Vol.14. No.6. 698-705.1997.

Cheng, Y-S., Fu, C.S., Snipes, M.B. and Mauderly, J.L. Use of human airway replica for standardized evaluation of inhaled drug delivery devices. *Drug Delivery to the Lung* 1997.

Clark, D.R.T., An investigation into the flow characteristics of a two-dimensional Shell Model Lung. *M. Eng. Final year project*, University of Bath. 2001.

Conway, J.H., Walker, P., Fleming, J.S., Bondesson, E., Borgström, L. and Holgate, S. Three-dimensional description of the deposition of inhaled Terbutaline sulphate administered via Turbuhaler®. *RDD VII* 607-609. 2000.

Dennis, J.H. A review of issues relating to nebulizer standards. *J. Aer. Med.* Vol. 11, Supp. 1. 1998.

Dolovich, M., Nahmias, C., Coates, G. Unleashing the PET: 3D imaging of the lung. *RDD VII* 215-230. 2000.

Eilbeck, J., Rowley, G., Carter, P.A. and Fletcher, E.J. Effect of contamination of pharmaceutical equipment on powder triboelectrification. *Int. J. Pharm.* Vol.195. 7-11. 2000.

Fan, B.J. and Cheng, Y.S. A MRI study of *in vivo* human oral airway and pulmonary aerosol delivery during inhaler administration. *RDD VII* 487-489. 2000.

Farr S.J., Warren S.J., Lloyd P., Okikawa J.K., Shuster J.a., Rowe A.M.m Rubsamen R.M., Taylor G. Comparison of *in vitro* and *in vivo* efficiencies of a novel unit-dose liquid aerosol generator and a pressurized metered dose inhaler. *Int. J. Pharm.* 198. 63-70. 2000.

Ferron, G.A. and Edwards, D.A. Numerical simulation of air and particle transport in the conducting airways. *J. Aer. Med.* Vol 9. No3. 303-316. 1996.

Finlay, W.H., Stapleton, K.W. and Yokota, J., On the use of Computational Fluid Dynamics for simulating flow and particle deposition in the human respiratory tract. *J. Aer Med.* Vol 9. No 3. 343-355. 1996.

Finlay, W.H. Stapleton, K.W. and Zuberbuhler, P. Errors in regional lung deposition predictions of nebulized salbutamol sulphate due to neglect or partial inclusion of hygroscopic effects. *Int. J. Pharm.* 149. 63-72. 1997.

Finlay, W.H., Hoskinson, M and Stapleton, K.W. Can models be trusted to subdivide lung deposition into alveolar and tracheobronchial fractions? *RDD VI.* 235-242. 1998.

Finlay, W.H. Inertial Sizing of aerosols inhaled during paediatric tidal breathing from an MDI with attached holding chamber. *RDD VI.* 333-335. 1998.

Fleming, J.S., Hashish, A.H., Conway, J.H., Nassim, M.A., Holgate, S.T., Halson, P., Moore, E., Bailey, A.G. and Martonen, T.B., Assessment of inhaled aerosol in the respiratory tract of man using three-dimensional multimodality imaging and mathematical modelling. *J. Aer. Med.* Vol.9. No.3. 317-327. 1996.

Fleming, J.S., Nassim, M., Hashish, A.H., Bailey, A.G., Conway, J., Holgate, S., Halson, P., Moore, E. and Martonen, T.B. Description of pulmonary deposition of radiolabelled aerosol by airway generation using a conceptual three-dimensional model of lung morphology. *J. Aer. Med.* 8:4. 1995.

Fults, K, Cyr, T.D and Hickey, A.J. The influence of sampling chamber dimensions on aerosol particle size measurements by cascade impactor and twin impinger. *J. Pharm and Pharmacol.* 43. 726-728.1991.

Gabrio, B.J., Stein, S.W. and Velasquez, D.J. A new method to evaluate plume characteristics of hydrofluoroalkanes and chlorofluorocarbon metered dose inhalers. *Int. J. Pharm.* 186. 3-12. 1999.

GlaxoWellcome Inc. Product information, Ventolin® (Albuterol USP), Research Triangle Park, NC 27709. March 2000.

Gradón, L. and Podgórski, A. Deposition of inhaled particles: Discussion of present modelling techniques. *J. Aer. Med.* Vol.9. No.3. 343-355. 1996.

Gradón, L., Oropharyngeal cast as a filter of inhaled particles. *J. Aer. Sci.* Vol.31. Supp. 1.S136-137. 2000.

Graseby-Anderson, Inc. *Operating manual for 1 ACFM non viable ambient particle sizing sampler*, Smyrna, Georgia, 1985.

Haefeli-Bleuer, B. and Weibel, E.R. Morphometry of the human pulmonary acinus. *Anat. Rec.* 220. 401-414. 1988.

Hickey, A.J. *Pharmaceutical inhalation aerosol technology*. 270 Madison Avenue, New York, NY: Marcel Dekker Inc., 1992.

Hinds, W.C. *Aerosol Technology: properties, behaviour and measurement of airborne particles.* 2nd edition., New York., Chichester., Wiley. 1999.

HITACHI, Ltd. *Instruction manual for Model F-2000 Fluorescence Spectrophotometer*, Japan, 1988.

Hitzenberger, R., Berner, A., Dusek, U. and Alabashi, R. Humidity dependent growth of size segregated aerosol samples. *Aer. Sci. and Tech.* 27. no.2. 116-130. 1997.

Hofmann, W. Modelling techniques for inhaled particle deposition: The state of the art. *J. Aer. Med.* Vol.9. No.3. 369-388. 1996.

Howlett, D.J. MDI technology: can it meet the challenges of CFC replacement and increasing regulatory demand. *RDD VI.* 123-131. 1998.

Holzner, P.M. and Müller, B.W. Particle size determinations of metered dose inhalers with inertial separation methods: Apparatus A and B (BP), Four stage impinger and Andersen Mark II Cascade Impactor. *Int. J. Pharm.* 116. 11-18. 1995.

Huang, C-H. and Tsai, C-J. Effect of gravity on particle collection efficiency of inertial impactors. *Aer. Sci.* 32. 375-387. 2001.

John, W. A simple derivation of the cutpoint of an impactor. *J. Aer. Sci.* Vol. 30. 1317-1320. 1999.

Johnson, K.A., Preparation of peptide and protein powders for inhalation. *Adv. Drug Del. Rev.* 26. 3-15. 1997.

Kaehu, M., Kuikka, J., Kauppinen, T., Bergström, K. and Vidgren, M. Pulmonary deposition of lactose carriers used in inhalation powders. *Int. J. Pharm.* 196. 95-103. 2000.

Kim, C.S., Brown, L.K., Lewars, G.G. and Sackner, M.A. Deposition of aerosol particles and flow resistance in mathematical and experimental airway models. *Journal of Applied Physiology, Respiratory, Environmental and Exercise Physiology.* Vol.55. No.11. 154-163. 1983.

Laube, B.L., Jashnani, R. and Dalby, R.N. Predicting *in vivo* lung deposition of cromolyn sodium from *in vitro* estimates. *J. Aer. Med.* Vol. 11. Supp.1. S 35-S 42. 1998.

Leach, C. Enhanced drug delivery through reformulation metered dose inhalers with HFA propellants – drug deposition and its effects on preclinical and clinical programs. *RDD V.* 133-144. 1996.

Lee, J.W., Lee, D.Y and Kim, W.S. Dispersion of an aerosol bolus in a double bifurcation. *J. Aer. Sci.* Vol 31, No4, 491-505, 2000.

Lewis, D. Portable Inhalers *Management Forum.* 1998.

Li, W-I. and Edwards, D. Aerosol particle transport and deaggregation phenomena in the mouth and throat. *Adv. Drug Del. Rev.* Vol 26. 41-49. 1997.

Marple, V.A. and Willeke, K., Impactor Design. *Atmosph. Env.* Vol.10. 891-896. 1976.

Marple, V.A., Liu, B.Y.H. and Whitby, K.T. On the flow fields of inertial impactors. *J. Fluids Eng.* 394-400. Dec. 1974.

Marple, V.A., Rubrow, K.L. and Behm, S.M. A Microorifice Uniform Deposit Impactor (MOUDI): description calibration and use. *Aer. Sci. and Tech.* Vol.14. 434-446. 1991.

Marple, V.A., Olsson, B.A. and Miller, N.C. A low loss cascade impactor with stage collection cups: Calibration and pharmaceutical inhaler applications. *Aer. Sci. and Tech.* 22:124-138. 1995.

Marple, V.A., Olson, B.A. and Miller, N.C. The role of inertial particle collectors in evaluating pharmaceutical aerosol delivery systems. *J. Aer. Med.* Vol.11. Supp.1. S139-S153. 1998.

Marriott, C. Mucus and mucocilliary clearance in the respiratory tract. *Adv. Drug Del. Rev.* Vol. 5. 19-35. 1990.

Martonen, T.B., Kratz, I., Fultz, K. and Hickey, A.J. Use of analytically defined estimates of aerosol respirable fraction to predict lung deposition patterns. *Pharm. Res.* 9. No. 12. 1992.

Martonen, T.B. Mathematical models for the selective deposition of inhaled pharmaceuticals. *J. Pharm. Sci.* Vo.82. No.12 1191-1199.1993.

Martonen, T.B., Yang, Y. and Xue, Z.Q. Effects of carinal ridge shapes on lung airstreams. *Aer. Sci. and Tech.* Vol 21, 119-136, 1994.

Nasr, M. M., Ross, D. L. and Miller, N. C., Effect of drug load and plate coating on the particle size distribution of a commercial Albuterol metered-dose inhaler (MDI) determined using the Andersen and Marple-Miller cascade impactors. *Pharm. Res.* Vol.14. No. 10. 1437 – 1443. 1997.

Newhouse, M.T., The current laboratory determination of "Respirable Mass" is not clinically relevant. *J. Aer. Med.* Vol.11. S122-S132. 1998.

Newman, S.P. A comparison of lung deposition patterns between different asthma inhalers. *J. Aer. Med.* Vol.8. Supp.3. S 21- S 26. 1995.

Newman, S.P. How well do *in vitro* particle size measurements predict drug delivery? *J. Aer. Med.* Vol 11, Supp 1. S 97-S 104. 1998.

Newman, S.P., Hirst, P.H., Pitcairn, G.R. and Clark, A.R. Understanding regional lung deposition data in gamma scintigraphy. *RDD VI* 9-15. 1998.

Newman, S.P. and Wilding, I.R. Gamma scintigraphy: an *in vivo* technique for assessing the equivalence of inhaled products. *Int. J. Pharm.* 170:1-9. 1998.

Nichols, S. C., Brown, D.R. and Smurthwaite, M. New concept for the variable flow rate Andersen Cascade Impactor and calibration data. *J. Aer. Med.* Vol.11. Supp. 1 S 133-S 138. 1998.

Nichols, S. C. and Smurthwaite, M., The Andersen Cascade Impactor: calibration data, operation at various flow rates and modified for use with DPI's at various flow rates. *RDD. VI.* 393 – 396. 1998.

Olsson, B., Asking, L. and Johansson, M. Choosing a cascade impactor. *Resp. Drug Del. VI.* 133-138. 1998.

Olson, B.A., Marple, V.A, Mitchell, P. and Nagel, M.W. Development and calibration of a low-flow version of the Marple-Miller Impactor (MMI ™). *Aer. Sci. and Tech.* 29:307-314. 1998.

Olsson, B., Borgström, L., Asking, L. and Bondesson, E. Effect of inlet throat on the correlation between measured fine particle dose and lung deposition. *RDD V.* 273-281. 1996.

Parkins, D.A. and Lashmar, U.T. The Formulation of biopharmaceutical products. *PSTT* Vol. 3. No. 4. April. 2000.

Patton, J.S. Mechanisms of macromolecular absorption by the lungs. *Adv. Drug Del. Rev.* 19. 3-36. 1996.

Patton, J.S. Deep-lung delivery of therapeutic proteins. *Chemtech* 34-38. 1997.

Patton, J.S. Overview of the human lung system and why does the asthmatic lung think it is infested with worms? *RDD VII* 171-179. 2000.

Peart, J., Magyar, G. and Byron, P.B. Aerosol electrostatics – metered dose inhalers (MDIs): reformulation and device design issues. *RDD VI* 227-233. 1998.

Perring, S., Summers, Q., Fleming, J.S., Nassim, M.A. and Holgate, S.T. A new method of quantification of the pulmonary regional distribution of aerosols using combined CT and SPECT and its application to nedocromil sodium administered by metered dose inhaler. *British J. Radiology.* 67:46-53. 1994.

Perzl, M.A., Schulz, H., Paretzke, H.G., Englmeier, K.H. and Heyder, J. Reconstruction of the lung geometry for the simulation of aerosol transport. *J. Aer. Med.* Vol 9. No3. 409-418. 1996.

Phipps, P. R. and Gonda, I. Droplets produced by medical nebulisers: Some factors affecting the size and solute concentration. *Chest.* 1327-1332. 1997.

Pitcairn, G.R. and Newman, S.P. Tissue attenuation corrections in gamma scintigraphy. *J. Aer. Med.* Vol. 10 (3). 187-198. 1997.

Poinar, H.N., Strohman, R.D., Lee, C.Y. and Bastacky, S.J. Digital photogrammetric quantification of surface area and volume on scanning electron micrographs of frozen hydrated lung tissue. *Scanning.* Vol.18. 456-459. 1996.

Pykönen, J. and Jokiniemi, J. Computational Fluid Dynamics based sectional aerosol modelling schemes. *J. Aer. Sci.* Vol 31. No5. 531-550. 2000.

Rao, A. K. and Whitby, K. T. *J. Aer. Sci.* 9. 87-100. 1978.

Richards, J.C., Pitcairn, G.R., Sista, S., Mahashabde, S., Abramowitz, W. and Newman, S.P. A scintigraphic study to assess the deposition of flunisolide delivered by HFA and CFC metered dose inhalers. *RDD VI.* 405-406. 1998.

Ross, D.L., Nasr, M.M. and Miller, N.C. Effect of drug load and plate coating on the particle size distribution of a commercial Albuterol metered dose inhaler (MDI) determined using a Marple-Miller Cascade impactor. *AAPS.* 1996.

Srichana, T. Martin, G.P. and Marriott, C. A human oral-throat cast integrated with a twin-stage impinger for evaluation of dry powder inhalers. *J. Pharm. Pharmacol.* 52. 771-778. 2000.

Shrubb, I. Influence of throat coating and flow rate on USP throat deposition. *RDD VI.* 413-416. 1998.

Stangl, R, Luangkhot, R., Liening-Ewert, R. and Jahn, D. Characterising the first prototype of a vibrating membrane nebuliser. *RDD VII.* 455-458. 2000.

Stapleton, K.W. and Finlay, W.H. Errors characterising nebulized particle size distributions with cascade impactors. *J. Aer. Med.* Vol. 11. Supp. 1. S 80 - S 83. 1998.

Steed, K.P., Hooper, G., Brickwell, J. and Newman, S.P. The Oropharyngeal and lung deposition patterns of a fusafungine MDI spray delivered by HFA 134a propellant or by CFC 12 propellant. *Int. J. Pharm.* 123. 291-293. 1995.

Stein, S.E. Size distribution measurements of metered dose inhalers using Andersen Mark II cascade impactors. *Int. J. Pharm.* 186. 43-52. 1999.

Stein, S.W. and Olson, B.A. Variability in size distribution measurements obtained using multiple Andersen Mark II Cascade Impactors. *Pharm. Res.* Vol.14. No.12. 1718-1725. 1997.

Tansey, I. Technological development of Airomir (Salbutamol Sulphate in CFC-free system) MDI. *Br. J. Clin. Prac.* Vol 49.Suppl. 79. 13-17.1995

Thorsson, L., Newman, S.P. and Borgström, L. Lung deposition of Budesonide in asthmatics: a comparison of different formulations. *Int. J. Pharm.* 168. 119-127. 1998.

Tippe, A. and Tsuda, A. Recirculating flow in an expanding alveolar model: experimental evidence of flow-induced mixing of aerosols in the pulmonary acinus. *J Aer. Sci.* Vol 31, No8. 979-986, 1999.

TSI Inc. Vibrating Orifice Aerosol Generator Model 3450 Instruction Manual., St Paul, MN. USA. 1987.

Tsuda, A., Henry, F.S., Otani, Y., Haber, S. and Butler, J.P. Aerosol transport and deposition in the rhythmically expanding pulmonary acinus. *J. Aer. Med.* Vol 9. No 3. 389-408. 1996.

US Pharmacopoeia, 1995. Rockville, MD, USA

Van Oort, M. and Truman, K. What is a respirable dose? *J. Aer. Med.* Vol.11. Suppl.1. 589-596. 1998.

Velasquez, D.J. and Gabrio, B. Metered dose inhaler deposition in a model of the human respiratory system and a comparison with clinical deposition studies. *J. Aer. Med.* Vol.11. Suppl. 1. S 23- S 28. 1998.

Versteeg, H.K. and Malalasekera, W. *An introduction to computational fluid dynamics, the finite volume method.* Longman House, Burnt Mill, Harlow, Essex, CM20 2JE, England UK: Longman Scientific and Technical, 1995

Weibe, B.M. and Laurensen, H. Human lung volume alveolar surface area and capillary length. *Micro. Res. and Technique.* 32. 255-262. 1995.

Weibel, E. R. and Gomez, D. M. Architecture of the human Lung. *Science.* 137:577-585. 1962.

Weibel, E.R. Design of airways and blood vessels considered as branching trees. *The Lung,* Scientific Foundations. Ed. R.G. Crystal, J.B. West *et al* Raven Press, Ltd., New York USA © 1991.

Weiss, N.A. *Introductory Statistics*, Addison-Wesley Publishing Company, Inc. World Student Series, USA. 1995.

Wright, P. and Shrubb, I. Next Generation Impactor – European update. *RDD VI.* 479-481. 1998.

Yeh, H-C and Schum, G.M. Models of human lung airways and their application to inhaled particle deposition. *Bul. Math. Biol.* Vol.42. 461-480. 1980.

Zainudin, B.M.Z., Tolfree, S.E.J., Biddiscombe, M., Whitaker, M., Short, MD. and Spiro, S.G. An alternative to direct labelling of pressurised bronchodilator aerosol. *Int. J. Pharm.* Vol. 51. (1) 67-71. 1989.

Zhang, L., Asgharian, B and Anjilvel, S. Inertial and interceptional deposition of fibers in a bifurcating airway. *J. Aer. Med.* Vol.9. No.3. 419-430. 1996.

Zhou, Y and Cheng, Y.S., Particle deposition in first three generations of a human lung cast. *J. Aer. Sci.* Vol. 31. Supp 1. S140-S141. 2000.